

EXPERIMENTAL STUDY ON CHARACTERISTICS OF BRAIDED STREAMS

A THESIS

*Submitted in fulfilment of the
requirements for the award of the degree*

of

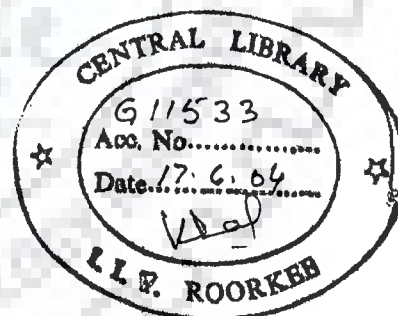
DOCTOR OF PHILOSOPHY

in

WATER RESOURCES DEVELOPMENT

By

MOHAMMAD ABDULLAH



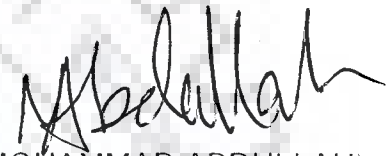
**WATER RESOURCES DEVELOPMENT TRAINING CENTRE
INDIAN INSTITUTE OF TECHNOLOGY ROORKEE
ROORKEE-247 667 (INDIA)**

DECEMBER, 2001

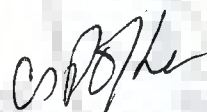
CANDIDATE'S DECLARATION

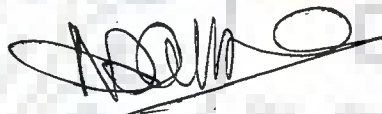
I hereby certify that the work which is being presented in the thesis entitled "EXPERIMENTAL STUDY ON CHARACTERISTICS OF BRAIDED STREAMS " in fulfillment of the requirement for the award of the Degree of Doctor of Philosophy and submitted in the Department of Water Resources Development Training Centre of the Indian Institute of Technology, Roorkee is an authentic record of my own work carried out during a period from January 1999 to December 2001 under the supervision of Dr. Nayan Sharma and Dr. C.S.P. Ojha.

The matter presented in this thesis has not been submitted by me for the award of any other degree of this or any other IIT / University.


(MOHAMMAD ABDULLAH)

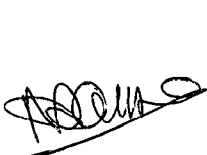
This is to certify that the above statement made by the candidate is correct to the best of my (our) knowledge.


(DR. C.S.P. OJHA)
ASSOCIATE PROFESSOR
CIVIL ENGINEERING DEPARTMENT
I.I.T., ROORKEE


(DR. NAYAN SHARMA)
PROFESSOR
W.R.D.T.C.
I.I.T., ROORKEE

DATE: 3RD DEC, 2001

The Ph.D. Viva-Voce examination of MOHAMMAD ABDULLAH, Research Scholar, has been held on 6th April, 2002




Signature of Supervisor (S)



Devidutta Das

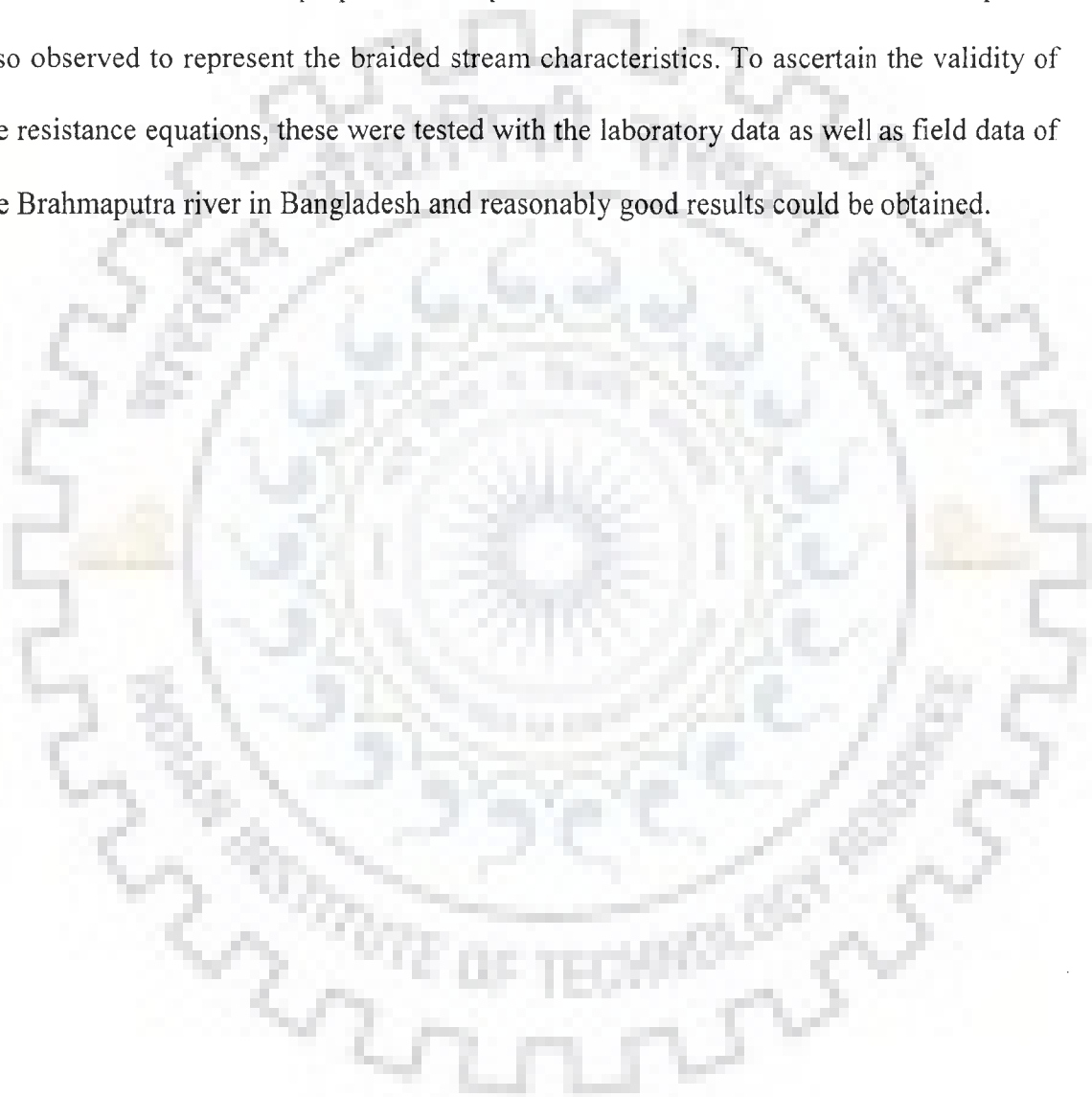
Signature of H.O.D



Signature of External Examiner



principle of maximum entropy were verified with the laboratory as well as field data of the Brahmaputra river and significant corroboration of the thresholds reported in the literature for wandering / braided stream could be discerned from the analysis. The study also indicates the role of composite braiding indices and presents performance evaluation in respect of many existing indices. A generalised resistance relationship based on the friction factor formula is proposed. The parameters of this resistance relationships are also observed to represent the braided stream characteristics. To ascertain the validity of the resistance equations, these were tested with the laboratory data as well as field data of the Brahmaputra river in Bangladesh and reasonably good results could be obtained.



ACKNOWLEDGEMENT

I have unfathomable gratitude for my supervisors **Dr. Nayan Sharma** and **Dr. C.S.P. Ojha**. The words prove to be insufficient to express my deep feelings for their high benevolence and un-hesitated guidance. They enlightened me throughout the experiment and Thesis period. Without their enthusiasm and determination the study would not have seen the light of the day.

I am very much grateful to Dr. Deva Dutta Das, Professor and Head, WRDTC, who has given each and every support for the construction of the experimental set-up (Laboratory Flume) and was source of inspiration during the entire experiments and thesis period. I express my heart felt thanks and gratitude to Prof. Gopal Chauhan, Ex. Director, WRDTC, Prof. G.C. Mishra, Prof. U.C. Chube, Prof. S.K.Tripathi, Dr. M.L. Kansal, Dr. Deepak Khare and all the faculty members of the WRDTC for their help and encouragement during the course of the study.

I also gratefully acknowledge the various authors and publications from where relevant references have been drawn in this thesis. I express my sincere thanks and compliments to Sri Radhey Shyam Sharma, Rtd. SLT of River Engineering Laboratory, who has assisted to construct the masonry flume at first. I must acknowledge the utmost co-operation and self-less help of Sri Beer Singh Chauhan, LT of R.E.Lab, Dr. Sunita Devi, Computer Programmer, Md. Sakir Ali, Sri Mukesh Kumar, Sri Atar Das of Computer Lab. Sri Brahma Chand, Sri Om Singh , Sri Yass Pal, Smt. Rekha, Smt. Kamla from Office, Sri. Vimal Chand, Sri. Ram Awadh, Md Aklak Ahmed, Md. Jabbar Hossain

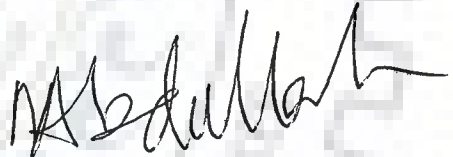
and all other staff of WRDTC. I am thankful to Mr. Ram Dular, Sri Hari Singh and Sri Anurag Kumar, Md. Ulfat Ali, who have extended their help throughout experimental work. I also acknowledge the help and co-operation of Dr. Pradeep Srivastava, Earth Science and Mr. M.P. Rajurkar, R/S, WRDTC.

I also express my respect and gratitude to the ICCR, Govt. of India and BTED, Govt. of Bangladesh for their sponsorship and G.O., respectively. I am grateful to Mr. Ramakar Jha, Scientist, NIH for checking carefully the thesis.

Finally, I must acknowledge the utmost co-operation and forbearance shown by my mother Mst. Amena Khatun, my wife Dr. Nuzhat Ara and my children Adnan, Sunan, Junan all throughout the study. I acknowledge my deepest feeling and heartiest gratitude to late. Md. Abdul Bari Biswas, Mir Mohammad Biswas, Dadi Kulsum Bibi, Joynal Biswas and Nani for their loving inspiration for my higher studies.

I must express my sense of gratitude to my In-laws, friends and relatives for their persistent encouragement.

December, 2001



(Mohammad Abdullah)

CONTENTS

DESCRIPTION	PAGE NO.
CANDIDATE'S DECLARATION	i
ABSTRACT	ii
ACKNOWLEDGEMENT	iv
CONTENTS	vi
NOTATIONS	ix
LIST OF FIGURES	xiii
LIST OF TABLES	xix
LIST OF PLATES	xxi
ABBREVIATIONS	xxiv
CHAPTER 1- INTRODUCTION	1
1.1 General	1
1.2 Objectives of the Study	5
1.3 Organisation of the Thesis	6
CHAPTER 2- REVIEW OF LITERATURE	7
2.1 General	7
2.2 Braided River Forms and Processes: Certain General Observations	8
2.3 Characteristics of Braided Channels and Braiding Indicators	14
2.3.1 General	14
2.3.2 Characteristics of Braided Channels	15
2.3.3 Adjustments to Stream Power	16
2.3.4 Existing Braiding Indicators	17
2.4 Resistance to Flow in Braided Stream	17
2.5 Extremal Hypotheses and Maximum Entropy Theory	24
2.5.1 Extremal Hypotheses	24
2.5.2 Maximum Entropy Theory	25
2.6 Scale Model Study	25
2.7 Concluding Remarks	26

CHAPTER 3- METHODOLOGY AND EXPERIMENTAL PROGRAMME	28
3.1 General	28
3.2 Identification of Study Reach	28
3.3 Experimental Set-up and Procedures	29
3.4 Experimental Programme for Phase-I	41
3.4.1 Planning of Present Experimental Work Programme Based on Experimental Study and Physical Observation of Past Investigators	41
3.4.2 Experimental Condition Phase-I	41
3.4.2.1 Non-sediment Feeding Condition for Present Study, Phase-1	41
3.4.2.2 Sediment Feeding Condition for the Present Study, Phase-1	41
3.5 Experimental Programme for Phase-II	45
3.5.1 Physical Model Studies for a Particular Stretch of the Brahmaputra River in Bangladesh	45
3.5.2 General Characteristics of the Brahmaputra River	45
3.5.3 Scale model Experiments	45
3.5.4 Physical Modelling Details	47
3.6 Design and Construction of Experimental Set-up	61
3.7 General Observations on the Laboratory Experiments	61
3.8 Variation of Sinuosity with Running Time and Slope of Channel	66
3.9 Summary	66
CHAPTER 4- BRAIDING INDICATORS	70
4.1 General	70
4.2 Existing Braiding Indicators	71
4.3 Discussion of Results	77
4.3.1 Existing Braiding Indicators	77
4.3.2 Proposed Braiding Index	85
4.3.3 Results Pertaining to Model Experiments	94
4.4 Concluding Remarks	104

LIST OF FIGURES

DESCRIPTION	PAGE NO.
Fig. 1.1: Principle River Types (Miall, 1977)	2
Fig. 3.1: Location Map of Study Reach as Well as Major Rivers of Bangladesh	30
Fig. 3.2: Brahmaputra River Stretch Under Study	31
Fig. 3.3: A Typical Longitudinal Profile of Study Reach of the Brahmaputra River for year 1997-98	32
Fig. 3.4a: Typical Cross-sections of Brahmaputra River at Doulatdia-ArichaBaruria (See A-A Section in Fig.3.2)	33
Fig. 3.4b: Typical Cross-sections of the Brahmaputra river at BangaBandhu-Jamuma Bridge, Bhuyapur (See B-B section in Fig.3.2)	34
Fig. 3.4c: Typical Cross-sections of the Brahmaputra river at Bahadurabad Ghat (See C-C section in Fig.3.2)	35
Fig. 3.5: Schematic Diagram of Experimental Set-up or Flume	36
Fig. 3.6: Longitudinal Elevation of Experimental Set-up or Flume with Necessary Accessories	37
Fig. 3.6a: Wooden Transition Channel	38
Fig. 3.6b: Sediment Feeder	37
Fig. 3.6c: Sediment Collector	37
Fig. 3.6d: Tail Gate	37
Fig. 3.7a: Cross-sections at J#7, J#7-1, J#8 and J#8-1 of the Brahmaputra River	49
Fig. 3.7b: Cross-sections at J#9, J#9-1, J#10 and J#10-1 of the Brahmaputra River	50
Fig. 3.7c: Cross-sections at J#11, J#11-1 and J#12 of the Brahmaputra River	51
Fig. 3.7d: Cross-sections at J#12-1, J#13 and J#13-1 of the Brahmaputra River	52
Fig. 3.8: Stage-discharge Curve at J#13-1 (Bahadurabad) Based on Both Field and Model Study Data	54
Fig. 3.9(a,b): Stage-discharge Curve for Observed Data as Well as Model Study Data of the Brahmaputra River at Sections J#7 and J#10	56

Fig. 3.10a:	Discharge Hydrograph of 1997-98 at Bahadurabad Ghat Transit	57
Fig. 3.10b:	Histogram of Applied Discharge for the Brahmaputra Model Study	57
Fig. 3.11(a,b&c):	Stage-discharge Curve for Observed Data as Well as Model Study Data of the Brahmaputra River at the Sections J#9, J#11 and J#12	58
Fig. 3.12:	Grain Size Analysis of Bed Material of the Brahmaputra River	59
Fig. 3.13a:	Grain Size Analysis of the Laboratory Channel Bed Materials	60
Fig. 3.13b:	Grain Size Analysis of Transported Materials in the Laboratory Channel	60
Fig. 3.14:	Longitudinal Profiles of Exp. Run No-43 at Different Running Time	62
Fig. 3.15a:	Sketches and Cross-sections Showing Progress in Development of Braid in the Experimental Run no. 43 at Different Running Time	64
Fig. 3.15b:	Sketches and Cross-sections Showing Progress in Development of Braid in the Experimental Run no. 43 at Different Running Time	65
Fig. 3.16a:	Showing Sinuosity Versus Running Time for Non-sediment Feeding Condition with Oblique Flow at an Angle 40^0	67
Fig. 3.16b:	Showing Sinuosity Versus Running Time for Sediment Feeding Condition with Oblique Flow at an Angle 40^0	67
Fig. 3.17a:	Showing Sinuosity Versus Running Time for Oblique Flow = 0^0 with Non-sediment Feeding Condition and Initial Sinuosity is 1.10	68
Fig. 3.17b:	Showing Sinuosity Versus Exp. Running Time for Oblique Flow = 0^0 and initial Sinuosity is 1.10 with Sediment Feeding Condition	68
Fig. 3.18:	Plot of Sinuosity against Slope of Channel for Laboratory Experimental Data of Sediment Feeding Condition	69
Fig. 4.1:	Demarcation of Braiding Zone Using S/F_r Vs D/B Diagram for Observed Data of the Brahmaputra River	78
Fig. 4.2:	Demarcation of Braiding Zone Using S/F_r Vs D/B for Laboratory Experimental Data	79
Fig. 4.3:	Demarcation of Braiding Zone Using S/F_r Vs D/B for the Field Data of Different Investigators	80
Fig. 4.4a:	Plot of Specific Energy (E) against Depth-to-Width Ratio (D/B) for 27 Cross-sections of the Brahmaputra River	81

Fig. 4.4b:	Plot of Velocity Head against Depth-to-Width Ratio (D/B) for 27 Cross-sections of the Brahmaputra River	81
Fig. 4.5a:	Plot of Specific Energy (E) against Depth-to-Width Ratio (D/B) for Laboratory Experimental Data	82
Fig.4.5b:	Plot of Velocity Head against Depth-to-Width Ratio (D/B) for Laboratory Experimental Data	82
Fig. 4.6a:	Plot of Specific Energy (E) against Depth-to-Width Ratio (D/B) for Field Data of Different Investigators	83
Fig. 4.6b:	Plot of Velocity Head against Depth-to-Width Ratio (D/B) for the Field Data of Different Investigators	83
Fig. 4.7a:	Variation of Braiding Index (Brice 1964, Mosley 1981) with Total Sinuosity (Richards 1982) for Laboratory Experimental Data	86
Fig. 4.7b:	Variation of Braided Channel Ratio (Friend and Sinha, 1993) with Total Sinuosity (Richards 1982) for Laboratory Experimental Data	86
Fig. 4.8a:	Variation of Composite Index I_1 with Width-to-Depth Ratio, B/D for Field Data of the Brahmaputra River (Exponent of $S=0.5$)	89
Fig. 4.8b:	Variation of Composite Index I_2 and Width-to-Depth Ratio, B/D for Field Data of the Brahmaputra River (Exponent of $C_s=0.5$)	89
Fig. 4.9a:	Hypothetical Topology Representing Extent of Braiding for Two Loops	90
Fig. 4.9b:	Hypothetical Topology Representing Extent of Braiding for Two Loops	91
Fig. 4.9c:	Hypothetical Topology Representing Extent of Braiding for Three Loops and Complex Braiding	92
Fig. 4.10:	Demarcation of Braiding Indicators Using S/F_r Vs D/B for Model Study	95
Fig. 4.11a:	Plot of Specific Energy (E) against Depth-to-Width Ratio (D/B) for the Data of Model Study	96
Fig. 4.11b:	Variation of Velocity Head with Depth-to-Width Ratio, (D/B) According to Richardson and Throne (2001) for Model Study	96
Fig. 4.12a:	Variation of Composite Index I_1 with Width-to-Depth Ratio, B/D for the Data of Model Study	97
Fig. 4.12b:	Variation of Composite Index I_2 with Width-to-Depth Ratio, B/D for the Data of Model Study	97

Fig. 4.13 a(i): Topologic Definition on Braided Streams for Model Study of the Brahmaputra River e.g. Initial Topologic Condition of Model Runs From 1 to 7	98
Fig. 4.13 a(ii): Topologic Definition on Braided Streams for Model Study of the Brahmaputra River e.g. Final Topologic Condition of Model Run-1	98
Fig. 4.13 b(i): Final Topologic Definitions of Braided Stream of Model Run-2	99
Fig. 4.13 b(ii): Final Topologic Definitions of Braided Stream of Model Run-3	99
Fig. 4.13 c(i): Final Topologic Definitions of Braided Stream of Model Run-4	100
Fig. 4.13 c(ii): Final Topologic Definitions of Braided Stream of Model Run-5	100
Fig. 4.13 d (i): Final Topologic Definitions of Braided Stream of Model Run-6	101
Fig. 4.13 d(ii): Final Topologic Definitions of Braided Stream of Model Run-7	101
Fig. 5.1a: Variation of Manning's 'n' with Proposed Dimensionless Term $X = ((0.15d_{50}/12R) + ((0.85*v*0.221)/R (gRS)^{0.5}))$ for Field Data	116
Fig. 5.1b: Agreement Between Calculated (Considering Total Cross-section) and Observed Discharges Based on eq.(5.18)	116
Fig. 5.2a: Variation of $(n\sqrt{g}/R^{1/6})$ with Proposed Dimensionless Term, $X = ((0.15d_{50}/12R) + ((0.85*v*0.221)/R (gRS)^{0.5}))$ for Field Data	117
Fig. 5.2b: Agreement Between Calculated (Considering Total Cross-section) and Observed Discharges Based on eq. (5.19)	117
Fig. 5.3a: Agreement Between Calculated and Observed Discharges Based on eq.(5.20a) for Laboratory Experimental Data	120
Fig. 5.3b: Agreement Between Calculated and Observed Discharges Based on eq.(5.20b) for Laboratory Experimental Data	120
Fig. 5.4: Agreement Between Observed and Calculated Discharges for Data of Model study Based on eq. (5.18)	121
Fig. 5.5a: Variation of Roughness 'n' (eq. 5.18) with Width-to-Depth Ratio, B/D For Field Data	122
Fig. 5.5b: Variation of $(n\sqrt{g}/R^{1/6})$ with Width-to-Depth Ratio, B/D for Field Data	122
Fig. 5.6a: Variation of Roughness 'n' Based on Proposed Term X (eq. 5.20a) with Width-to-Depth Ratio, B/D for Laboratory Experimental Data	123

Fig. 5.6b:	Variation of Dimensionless Term ($n\sqrt{g}/R^{1/6}$) Based on eq.5.20b with Width-to-Depth ratio, B/D for Laboratory Experimental Data	123
Fig. 6.1:	Random Walk Path of Flow Thalweg in Alluvial Rivers	130
Fig. 6.2(a,b,c,d,e,f):	To	
	Variation of Minimum Energy Dissipation Rate (MEDR) with Width-to-Depth Ratio (B/D) for Laboratory Experimental Data	136-145
Fig. 6.12:	Variation of Minimum Energy Dissipation Rate (MEDR) with Width-to-Depth Ratio (B/D) for Model Study Data of the Brahmaputra River	146
Fig. 6.13:	Variation of Minimum Energy Dissipation Rate (MEDR) with Width-to-Depth Ratio (B/D) for field data	147
Fig. 6.14(a,b,c,d,e,f):	To	
	Variation of Minimum Stream Power (MSP) with Width-to-Depth Ratio (B/D) for Laboratory Experimental Data	148-157
Fig. 6.24:	Variation of Minimum Stream Power (MSP) with Width-to-Depth Ratio (B/D) for Model Study of a particular Stretch of the Brahmaputra River	158
Fig. 6.25:	Variation of Minimum Stream Power (MSP) with Width-to-Depth Ratio (B/D) for Field Data	160
Fig. 6.26(a,b,c,d,e,f):	To	
	Variation of Maximum Friction Factor (MFF) with Width-to-Depth Ratio (B/D) for laboratory Experimental data	161-170

Fig.6.36:	Variation of Maximum Friction Factor (MFF) with Width to Depth Ratio (B/D) for Model Study of a Particular Stretch of the Brahmaputra River	171
Fig.6.37:	Variation of Maximum Friction Factor (MFF) with Width-to-Depth Ratio (B/D) for Field Data	172
Fig.6.38:	Plot of Channel Pattern Co-efficient (CPC) against Width-to-Depth Ratio (B/D) for Laboratory Experimental Data	174
Fig.6.39:	Variation of Channel Pattern Co-efficient (CPC) against Width-to-Depth Ratio (B/D) for Model Study of a Stretch in the Brahmaputra River	175
Fig.6.40:	Plots of Channel Pattern Coefficient (CPC) against Width-to-Depth Ratio (B/D) for Field Data of the Brahmaputra River	176
Fig.6.41:	Variation of Channel Pattern Coefficient (CPC) Based on Constant (Manning's) 'n' with Width-to-Depth Ratio (B/D) for Laboratory Experimental Data	177
Fig.6.42:	Variation of Channel Pattern Coefficient (CPC) Based on Constant (Manning's) 'n' with Width-to-Depth Ratio (B/D) for Model Study of a Stretch in the Brahmaputra River	178
Fig.6.43:	Variation of Channel Pattern Co-efficient (CPC) Based on Constant (Manning's) 'n' with Width-to-Depth Ratio (B/D) for the Field Data of the Brahmaputra River	179

LIST OF TABLES

DESCRIPTION	PAGE NO.
Table 3.1: Basis for Planning of Present Experimental Work	42
Table 3.2: Details of Experiments (Non-sediment Feeding Condition) for phase-I	43
Table 3.3: Details of Experiments (Sediment Feeding Condition) for phase-I	44
Table 3.4: Details of Physical Model Experiments (Experimental Program, Phase-II)	46
Table 4.1: Classification of River types (Miall, 1977)	74
Table 4.2: Different Types of Indices	75
Table 4.3: Relationship between Different Parameters of Best Fitting Equations For Demarcating the Channel Patterns	84
Table 4.4a: Analysis of Different Parameters of Composite Index-I ₁ and Composite Index-I ₂ for Field Data	88
Table 4.4b: Analysis of Different Parameters of Composite Index-I ₁ and Composite Index-I ₂ for Laboratory Experimental Data	88
Table 4.5: Values of Hypothetical Topological Indices viz α -Index, β -Index and γ -Index (Howard et al., 1970) for Understanding Braiding Phenomenon	93
Table 4.6: Values of α -Index, β -Index and γ -Index (Howard et al., 1970) for Seven Model Experimental Runs	102
Table 4.7: Ranges of Values of (Different Indicators) PFI, FGI, Cross-Slope, Braiding Index, Total Sinuosity, Composite Index-I ₁ and Composite Index -I ₂	103
Table 5.1: Value of 'n' as per Different Study Approaches for Field Data	113
Table 5.2: Average Percentage Error with Different Approaches for Field and Laboratory Data	114
Table 6.1a: Different Morphological Parameters (ξ_p , ξ_0 and S_{cr}) for Field Data of the Brahmaputra River	180

Table 6.1b:	Different Morphological Parameters (ξ_p , ξ_0 and S_{cr}) for Laboratory Experimental Data	181
Table 6.2a:	Ranges of Values of Different Morphological Parameters (ξ_p , ξ_0 and S_{cr}) for Present Study	182
Table 6.2b:	Ranges of Values of Different Morphological Parameters (ξ_p , ξ_0 and S_{cr}) of Different Rivers (Deng and Singh, 1999)	183
Table A2.1:	Data of Study Reach of the Brahmaputra river	216
Table A2.2:	Basic Data of Laboratory Experimental Run-43	217
Table A2.3:	Sample Data of Laboratory Experiments, Phase-I	228
Table A2.4:	Data of Model Study of the Brahmaputra River	240



LIST OF PLATES

DESCRIPTION	PAGE NO.
Plate 1.1a: Satellite Image Showing the Braided Pattern of the Brahmaputra River	3
Plate 1.1b: Satellite Image Near the Peak of Moonsoon Flood of the Brahmaputra River	3
Plate 3.1: Showing Levelling Procedure of Rails and Trolley at the Last Stage of Flume Construction	38
Plate 3.2: Wooden Transition Channel	38
Plate 3.3: Sediment Feeding System When Wooden Transition at an Angle 40°	40
Plate 3.4: Sediment Collector	40
Plate 3.5: Acoustic Doppler Velocimeter (ADV) in Using Condition	40
Plate 3.6a: Initial Planform of Experiment of Model Study for the Brahmaputra River	53
Plate 3.6b: Simulated Planform of Model Studies of the Brahmaputra River in Running Conditions	53
Plate A2.1a: Initial Condition of Run -1 Having Non-Sediment Feeding Condition and Oblique Flow (OF) at an Angle 40° , Channel Slope = 0.01	204
Plate A2.1b: Meandering Formation of Run - 1 after 2 Hours of Running Exp.	204
Plate A2.1c: Bar Development of Run - 1 After 20 Hours of Running Experiment	204
Plate A2.2a: Initial Condition of Run - 10 Having Non-Sediment Feeding Condition and Initial Sinuosity $P_c = 1.10$, OF = 0° , Slope (S) = 0.02	205
Plate A2.2b: Emerging of Bars of Run - 10 After 12 Hours of Running Exp.	205
Plate A2.2c: Braiding Condition With Multiple Channel of Run - 10 After 20 Hours of Running Experiment	205
Plate A2.3a: Meandering Condition of Run - 23 After 1 Hours Having Non Sediment Feeding Condition with Oblique Flow (OF) = 60° , S = 0.02	206
Plate A2.3b: Planform of Run - 23 after 8 Hours of Running Experiment	206
Plate A2.3c: Braiding Condition With Island of Run - 23 After 10 Hours	206

Plate A2.4a: Initial Condition of Run -26 Having Non-Sediment Feeding Condition and Oblique Flow (OF) at an Angle 20^0 , Slope (S) = 0.03 $p_c=0$	207
Plate A2.4b: Beginning of Meandering of Run - 26 After 2 Hours of Running Experiment	207
Plate A2.4c : Showing Bar or <i>Char</i> Formation After 20 Hours of Running Exp.	207
Plate A2.5a: Initial Condition of Run - 29 Having Non-sediment Feeding Condition With Initial Sinuosity $p_c=1.05$ and Oblique Flow = 0^0 , S = 0.03	208
Plate A2.5b: Meandering Planform of Run-29 after 1/2 Hours of Running Exp.	208
Plate A2.5c: Braiding Condition with Bars after 16 Hours of Running Exp.	208
Plate A2.6a: Initial Condition of Run - 30 Having Non-sediment Feeding Condition with Initial Sinuosity $p_c=1.10$ and Oblique Flow = 0^0 , S = 0.03	209
Plate A2.6b: Development of Bars after 8 Hours of Running Experiment	209
Plate A2.6c: Showing Bar or <i>Char</i> Formation after 16 Hours of Running	209
Plate A2.7a: Initial Condition of Run - 35 Having Sediment Feeding Condition with Initial Sinuosity $p_c=1.10$ and Oblique Flow = 0^0 , S = 0.01	210
Plate A2.7b: Multiple Channel with Bars of Run - 35 After 14 Hours Running	210
Plate A2.7c: Braiding Condition with Islands of Run-35 After 20 Hours of Running	210
Plate A2.8a: Initial Condition of Run - 35 Having Sediment Feeding Condition with Oblique Flow at an Angle 60^0 , $p_c=0.0$ and S = 0.03	211
Plate A2.8b: Meandering Condition Of Run - 43 After 1/2 Hours of Running	211
Plate A2.8c: Bars with Multi Channel Formation of Run-43 after 16 Hours	211
Plate A2.9a: Initial Condition of Run - 47 Having Sediment Feeding Condition with oblique flow at an Angle 40^0 , $p_c=0.0$ and S= 0.01	212
Plate A2.9b: Bar Formation of Run - 47 After 12 Hours of Running Exp.	212
Plate A2.9c: Braiding Condition with Multi Channel of Run - 47 After 20 Hours of Running Exp.	212
Plate A2.10a: Initial Condition of Run - 48 Having Sediment Feeding Condition with Oblique Flow at an Angle 60^0 , $p_c=0.0$ and S = 0.01	213
Plate A2.10b: Meandering Planform of Run - 48 After 1.5 Hours of Running	213
Plate A2.10c: Braid Bars with Multi Channel Formation of Run - 48 After 20 Hours of Running Exp.	213

Plate A2.11a: Initial Condition of Run - 51 Having Sediment Feeding Condition with Oblique flow at an Angle 20° , $p_c=0.0$ and $S = 0.02$	214
Plate A2.11b: Planform of Run - 51 After 12 Hours of Running Experiment	214
Plate A2.11c: Multi-Channel with Braid Bar: Formation of Run - 51 After 18 Hours of Running	214
Plate A2.12a: Initial Condition of Run - 59 Having Sediment Feeding Condition with Initial Sinuosity $p_c=1.05$ Oblique flow 0° and $S = 0.02$	215
Plate A2.12b: Meandering Planform of Run - 59 After 3 Hours of Running Exp.	215
Plate A2.12c: Multi-Channel Pattern of Run - 59 After 16 Hours of Running Exp.	215
Plate A3.1a: Middle Stage Construction of Experimental Set-up or Flume in River Engineering Laboratory, WRDTC	248
Plate A3.1b: Construction of Water Storage Tank Out Side the Building	248



ABBREVIATIONS

ASCE	: American Society of Civil Engineers
BWDB	: Bangladesh Water Development Board
BR	: Brahmaputra River
BRI	: Bed Relief Index
CPC	: Channel Pattern Coefficient
IB	: Initial Bend
MEDR	: Minimum Energy Dissipation Rate
MSP	: Minimum Stream Power
MUSP	: Minimum Unit Stream Power
MFF	: Maximum Friction Factor
MSTR	: Maximum Sediment Transport Rate
MDBJR	: Morphological Dynamics of the Brahmaputra-Jamuna River
OF	: Oblique Flow
SWMC	: Surface Water Modelling Centre
UPIRI	: Uttar Pradesh Irrigation Research Institute
WRDTC	: Water Resources Development Training Centre
TS	: Total Sinuosity
VE	: Vertical Exaggeration

INTRODUCTION

1.1 GENERAL

Alluvial river channels are 'self-formed' as they flow over the alluvial lands having sandy-silty-clay materials. Their morphology results from the entrainment, transportation and deposition of the unconsolidated sedimentary materials of the valley fill and flood plain deposits across which they flow (Richards, 1982). Alluvial channels are generally categorized as straight, meandering, anastomosing and braided patterns (Fig.1.1).

Braided streams are associated with high stream power and unstable braid bars formed of sediments, which are often unvegetated. Braiding is the division of a single channel into two or more anastomosing channel ways. Braided rivers may be envisaged as a series of channel segments, which divide and rejoin around bars in a regular or repeatable pattern as can be seen from the satellite image of the Brahmaputra river in Bangladesh vide Plate 1.1 (a,b). Generally, braiding is favoured by high-energy fluvial environments with steep valley gradients, large and variable discharges, dominant bed load transport, and non-cohesive banks lacking stabilisation by vegetation. Lane (1957) stated that a braided stream is characterised by 'having a number of alluvial channels with bars or islands between meeting and dividing again, and presenting from the air the intertwining effect of a braid'. Schumm (1963) expressed the braided channels as single

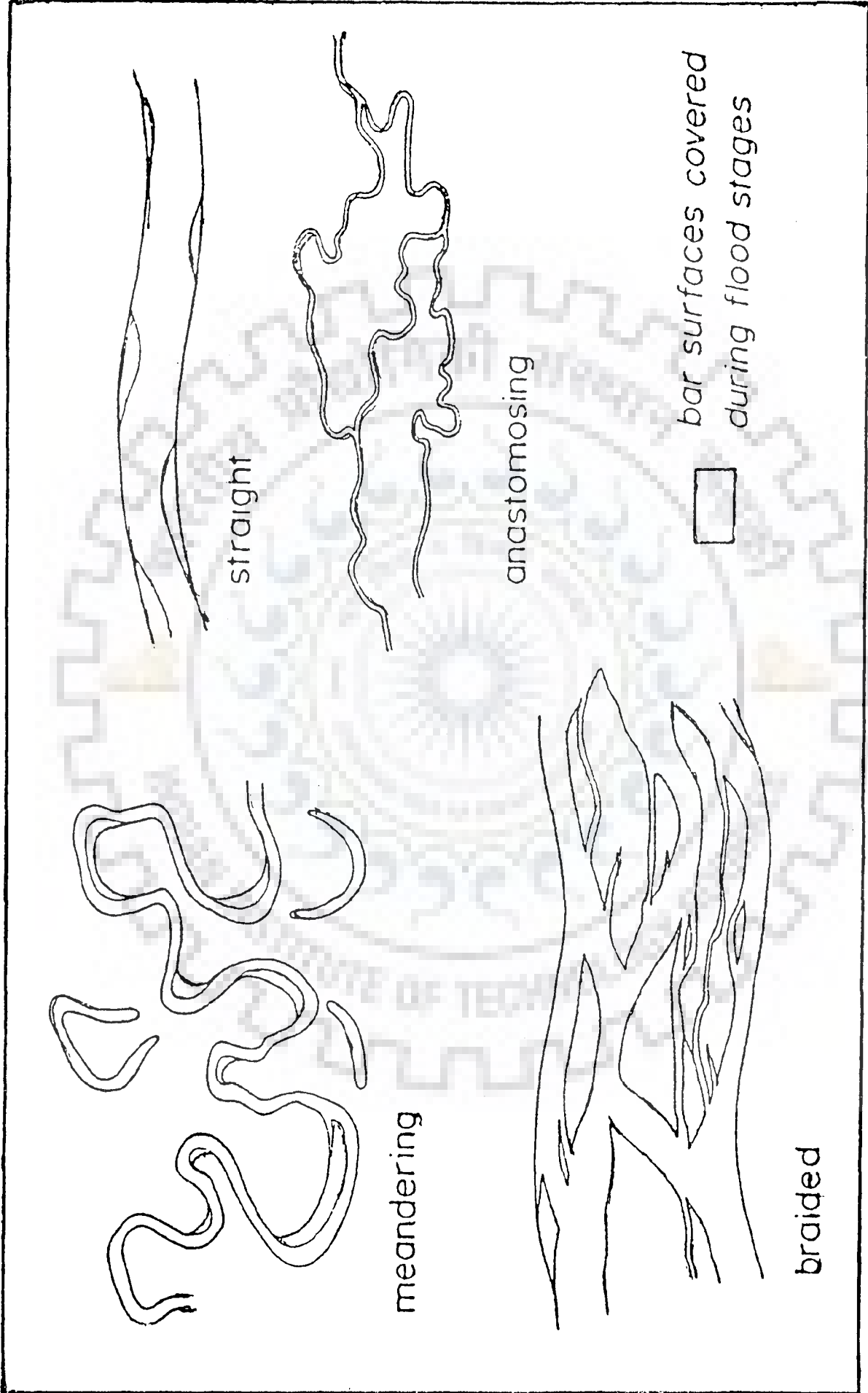


FIG. 1.1: PRINCIPAL RIVER TYPES (MIALL, 1977)



Plate 1.1 (a) Satellite image showing the braided pattern of the Brahmaputra River (7/2/1987)
(b) Satellite image near the peak of monsoon flood of the Brahmaputra River (17/8/1987)
(Best and Bristow, 1993; Images collected from ISPAN, FAP-19 Dhaka, Bangladesh)

bed load rivers which at low water have islands of sediment or relatively permanent vegetated islands in contrast to multiple channel (anastomosing and distributive) in which each branch may have its own individual pattern.

Earlier research (Leopold and Wolman, 1957; Lane, 1957; Brice, 1964; Coleman, 1969; Howard et al., 1970; Schumm and Khan, 1972; Parker, 1976; Miall, 1977; Hong and Davies, 1979; Mosley, 1981; Richards et al., 1982; Ashmore, 1991a; Friend and Sinha, 1993; Ashworth et al., 1992; Ashmore, 1996; Bristow and Best, 1993; Throne et al., 1993; Richardson and Thorne, 2001) on braided rivers has been towards the development of braiding indicators and understanding of the processes responsible for the occurrence of the braiding. In the last two decades, the use of energy conservation laws in the form of extremal hypotheses (Yang et al., 1981; Chang, 1980b; Yang and Song, 1979; Davies and Sutherland, 1980, 1983; Griffiths, 1984; White et al., 1982) and entropy theory (Singh and Fiorentino, 1992, Deng and Zhang, 1994; Deng and Singh, 1999) have found application in explaining the characteristics of braided streams.

Braiding may be influenced by a variety of parameters including flow rate, sediment load, shear stress, channel bed slope, sinuosity of the channel etc. Thus, the study of the influence of some of these parameters forms one of the objectives of the study.

A qualitative interpretation of the braided stream characteristics including the role of the above variables is also important. Towards this, the studies related to variations of braiding indicators merit attention.

To study the influence of different variables on braiding process, use of resistance relationships, extremal hypotheses and entropy theory are considered as these

show the aggregated effect of many of the variables. For example, a resistance relationship includes flow rates, channel slope, bed configurations in addition to the concentration of the sediment. Although, the role of each of these parameters may vary with respect to each other, it is interesting to mention here that for the river Brahmaputra, which also happens to be a highly braided stream, suitable resistance laws do not exist. For this reason, the modelling of flow resistance relationship for use in braided stream like the Brahmaputra river has been given an important consideration in the study. Like resistance, extremal hypotheses also involve flow, bed slope and in certain cases, the sediment concentration. The same holds true for maximum entropy. Considering the importance of these parameters in alluvial stream modelling, it is considered relevant to test these against the present experiments as well as the field data.

1.2 OBJECTIVES OF THE PRESENT STUDY

Keeping the above-mentioned points in mind, following objectives are decided for the present study.

1. To perform laboratory experiments to simulate braided conditions in the alluvial channels.
2. To analyse the experiments for understanding the role of braiding indicators in characterisation of braiding phenomenon.
3. To analyse the existing relationships for degree of braiding by using the extensive laboratory experimental data from the present work as well as field data of the Brahmaputra river in Bangladesh.
4. To analyse the field data regarding flow resistance in a stretch of the river Brahmaputra in Bangladesh. This includes the identification of an approach of modelling resistance relationship, which can be applied in the braided streams like the Brahmaputra.

5. To investigate the feasibility of using extremal hypotheses for understanding the braiding phenomenon.
6. To assess the performance of maximum entropy principle in analysis of braiding phenomenon and determine the channel pattern coefficient and stability criteria for laboratory channels and field data of alluvial braided rivers and compare these results with the reported values in the literature.
7. To assess some of the above objectives with regard of physical model based experiments for a stretch of the river Brahmaputra.

1.3 ORGANISATION OF THE THESIS

The study carried out is organised in the following way:

Chapter-1 describes introductory aspects of the topic studied in the thesis. Chapter-2 presents a comprehensive review of literature. Chapter-3 presents methodology and experimental work programme of the study. Chapter-4 describes the study and analysis of braiding indicators by using physical and laboratory data. Chapter-5 representing the evolution of resistance relationships of braided stream. Chapter-6 investigates the feasibility of using extremal hypotheses and entropy theory for understanding braiding phenomenon. Chapter-7 includes conclusions and scope for future work.

Furthermore, at the end of the thesis four Appendices are placed for the purpose of ready reference. These are (i) a short description of the Brahmaputra river in Bangladesh, (ii) plates and tables related to laboratory and field data, (iii) design and construction details of laboratory flume, and (iv) brief description of instruments used for experiments.

REVIEW OF LITERATURE

2.1 GENERAL

Braiding phenomenon is frequently observed in rivers. In Indian subcontinent the river Brahmaputra is famous for its braiding characteristics. Braiding carries differing importance to research workers of different disciplines. For the geomorphologists, braided fluvial systems are abundant within upland and proglacial settings and are agents of considerable erosion and sediment transport. For engineers, high rates of sediment transport, deposition and erosion combined with frequent channel shifting and rapid bank erosion may pose considerable design problems both to within channel structures, such as bridge piers and braid plain edge construction such as roads and railways. For the geologist, braided rivers form important agents of deposition that have been responsible for the accumulation of many sedimentary sequences that form valuable aquifers, hydrocarbon reservoirs and sites for heavy mineral accumulation (Bristow and Best, 1993). Considerable amount of literature is available on both single thread and multi-thread rivers. In the past, a lot of work has been done on braided rivers and their channel pattern forms by several researchers such as Jackson (Leopold and Wolman, 1957), Peal (Leopold and Wolman, 1957), Rubey (Leopold and Wolman, 1957), Leopold and Wolman (1957), Lane (1957), Callander (1969), Coleman (1969), Parker (1976), Mosley, 1982,88 (Bristow and Best, 1993), Thorne et al. (1993), Ashmore (1991), Ashworth et al. (1992), Ashworth (1996), Carson (1984), Miall (1977), Bridge et al.

(1986), Bristow (1987a, 1987b,1993) and Richardson & Thorne (2001) etc. and yet, when compared to the wealth of literature upon meandering systems, the braided rivers have been comparatively understudied. These relevant works particularly in the context of alluvial channel braiding and its channel form patterns, as reported in the literature are being reviewed here.

2.2 BRAIDED RIVER FORMS AND PROCESSES: CERTAIN GENERAL OBSERVATIONS

It has long been recognised that the division of the velocity field into multiple flow threads and the associated growth of mid channel bars are of fundamental importance to our understanding of braided rivers (Leopold and Wolman, 1957; Ashmore, 1991; Ashworth et al., 1992; Thorne et al, 1993; Ashworth, 1996). However, lack of data at the point of braid bar initiation and lack of knowledge concerning the fluvial and sediment processes responsible for braiding have limited the degree to which braiding in alluvial channels can be understood and explained (Bristow and Best, 1993). The division and joining of channels are essential features of braided rivers and, whilst the bars within these rivers have received attention from both geomorphologists and sedimentologists, the areas of flow convergence and divergence have not been incorporated into braided river depositional models. The flow dynamics and morphology of channel confluences have been studied by several researchers (Mosley, 1976,1982a; Best 1986,1988; Best and Roy, 1991; Roy and Roy, 1988) and attention has been focussed towards the abundant confluences within braided rivers (Ashmore 1982; Ashmore and Parker, 1983; Bristow and Best, 1993). However, the link between the

flow convergence and the downstream division of flow has been neglected, despite the fact this transition is the area which may be of fundamental importance to the development of braid bars (Ashmore, 1991; Ashworth et al., 1992). For over four decades, qualitative and geomorphic models have cited mid-channel bar initiation and growth due to stalling of bed load around the channel centerline as a primary process in braiding (Leopold and Wolman, 1957; Ashmore, 1991; Ashworth, 1996). However, Ashmore (1991) reported that central bar deposition seldom occurred in his flume experiments and he identified chute cut-off, chute-lobe and lobe dissection as further mechanisms of braid bar initiation and growth. Although some depositional models of braided rivers are beginning to recognise and incorporate confluence scour and fill (Cowan 1991; Bristow et al., 1993), areas of flow divergence are less well understood and mostly ignored in these models. Ferguson (1993) summarised these mechanisms and added avulsion as a possible fifth mechanism. While it is now accepted that there are multiple mechanisms for braid bar development, mid-channel bar formation, termed 'central bar deposition' by Ferguson (1993), is still recognised as major cause of channel division in many braided rivers. It is significant that the process of deposition of bed load at the center of the channel as pointed out by Ashworth (1996) is still little understood and remains a relevant topic for study. Carson (1984) and Thorne et al. (1993) worked on divergent flow with flow deceleration and sediment deposition. Cheetham (1979) described that distributary closure arises initially because at different flow stages there are changes in the location of maximum competence to transport bedload between the distributary and main channels. Bed shear stress has been shown to increase in shallow flows over bar tops where coarse bed armour may form.

The planform appearance of braided rivers can change radically with flow stage (Thorne et al., 1993). Bluck (1979) observed that disappearance and reformation of bars depend on flow stages. Similar observations have been reported by Smith (1974), Carson (1984), Gupta and Dutt (1989). However, Krigstrom (1962), Bridge et al. (1986), Coleman (1969) and Bristow (1987a) have explained that most braided rivers retain their bars at both high and low flow stage and they will experience a complex history of erosional and depositional modification related to change in stage.

Little data exist for the comparison of bar and channel morphology at different flow stages and this is an area in which controlled and correctly scaled flume models combined with field studies may contribute greatly to our understanding. Allen (1965) had given expression that braided streams have coarse sediments and structure dominated lens-shaped channel fills caused by abandonment of braid distributaries. Dury (1966a) defined different equilibrium state of braided rivers, i.e. temporal variation of channel form, continuity of sediment transport, efficiency of channel form and correlation of system properties.

Cause and effect of braid bars development is difficult to determine but Leopold and Wolman (1957) in their flume experiment reported that a bar of coarse sand diverts flow to cause bank erosion and positive feedback then accentuates bar development and widening. Miller (1958) noted that adjustment of width is the inverse of the behaviour at tributary junctions. If width varies downstream as the square root of discharge, then the sum of the widths of two equal distributaries is 1.41 times the width of the undivided parent channel.

Generally, high-energy streams may create braided channel patterns as a result of the instability of bedload transport in wide, shallow channels (Parker, 1976). Parker (1976) also has given an interpretation of the criterion for braiding and characteristics scales of meandering rivers. He took a parameter, e.g. ratio of sediment transport to water transport and concluded that if channel slope, S and B/D at formative discharges are low, meandering favoured but if sufficiently high, then braiding is favoured. Deep, narrow channels maintain double cell secondary circulation, which may lead to meander development and are indicative of resistance of banks. Wide and shallow streams (weak sandy banks) tend to be braided (Engelund and Skovgaard, 1973). Ackers and Charlton (1970b) and Nagabhushanaiah (1967) have both identified a straight-meandering threshold in flume channels where straight streams occurring at lower slopes and discharges. Intermediate power and width to depth ratios characterise meanders and high power streams in erodible sediments that develop wide, shallow cross-sections are likely to be braided. In fact, braid intensity increases above the braid threshold. Howard et al. (1970) demonstrated various topological indices which reveal that braided reaches show greater complexity (more bars and distributaries) in the highest energy environments. They introduced three indices namely α -index, β -index, and γ -index to measure the average number of channels in braided river. The continual spatial variation of channel pattern in response to varying energy conditions is needed to quantify pattern by a continuous variable, such as total sinuosity, in contrast to the use of qualitative discrete pattern definitions. This continuous system state variable (dependent) may then be related to two control variables (independent) measuring total stream power and sediment resistance. For a particular combination of control variables, the equilibrium total

sinuosity minimises an energy criterion (Chang, 1979). The origin of braided patterns in streams is poorly understood, but high regional slopes, variable discharges, and abundant sediment supply are important factors contributing to braiding. Ore (1964) recognised that braiding can arise by essentially two processes—by construction of longitudinal bars and bisection of transverse bars, depending on grain size and sorting of bed material. The underlying cause of braiding is not well understood but Fahnstock (1963) reviews some of the explanations which have been proposed, including easily eroded banks, rapid and extreme discharge fluctuations, high regional slopes, abundant sediment load, and local incompetence of streams.

Process-based explanations of mid channel bar initiation and growth, based on observation of flow patterns and sediment dynamics downstream of channel confluence have been proposed by Ashmore (1991) and Ashworth (1996) on the basis of measurements in the flumes and in the streams. In these models, stalling of bed material around the centerline of the channel and development of a bifurcation is driven by divergence of flow existing in the confluence coupled with downstream migration of flow patterns and sediment processes. This confluence-diffuence unit, referred to by Ashworth (1996) as a 'Y' pattern, is considered to be one of the basic building blocks of braided rivers. However, for the anabranches of a braided river to form a 'Y' pattern, it is first necessary for the anabranches to have already bifurcated some distance upstream. While the models of Ashmore (1991) and Ashworth (1996) may explain why bifurcation is likely to occur immediately downstream of an anabranch confluence, processes observed at a confluence-diffuence unit. However, this does not fully explain the initiation of braiding in a single channel.

While geomorphic approaches to the study of braiding have relied on observation and measurement in rivers and flumes, links between fluvial morphology and flow instability have also been investigated using the principles of fluid mechanics (Callander, 1969; Parker, 1976; Seminara and Tubino, 1989). It has long been argued that the occurrence of meanders in non-alluvial fluid system, such as oceans current and glacier meltwater stream, indicates that meandering tendency is inherent to any fluid shear flow, with sediment transport reacting to rather than driving the flow condition (Leopold and Wolman, 1957; Karcz, 1971; Gorycki, 1973). Parker (1976) argued that sediment transport is, in fact, essential for the occurrence of instability in flow, reconciling this with non-alluvial meanders by describing the necessity for a 'third effect' in addition to friction and potential. He went on to extend his argument to braiding, demonstrating that under appropriate condition, division of the flow into multiple threads was inevitable. Further, non-linear analysis of stability phenomena within flow and sediment transport processes using the approach pioneered by Parker has produced theoretical criteria for braid bar development within single channels (Colombini et al., 1987; Tubino, 1991). Callander (1969) described a linearised stability analysis of flow of water in a channel with a loose bed and straight banks.

If the results of analyses based on fluid mechanics are accepted, it follows that bifurcation of single channel results from inherent instability in the flow and that deposition of bed material load at the channel centre is driven by flow instability. That is, sedimentation plays an essential, but responsive, role in the bifurcation process. If braiding is, in fact, a flow-driven phenomenon, then there is only one cause of braiding; that is division of a single flow stream into two or more threads. Morphological

bifurcation of the channel can, indeed, subsequently develop by one of the five mechanisms described by Ferguson (1993).

Furthermore, many braided rivers do not aggrade. Leopold and Wolman (1957) have observed that braided patterns may also be close to quasi-equilibrium as possessed by rivers with meandering and other patterns. Basak (1992) studied the transition of open-channel and has given the design procedure from expansion to contraction of open channels.

The variation of resistance to flow and rate of transport of bed material with velocity are discussed by many researchers. Valentine et al. (2001) conducted experiments at a large laboratory scale to test rational regime theory and regime behaviour of straight boundary in a fixed floodplain. Rates of bank erosion were measured by them and constitute unique widening data for main channels under overbank flow conditions. These data may provide a basis for estimates of channel bank erosion in prototype channels and may throw some insight into the role of eroded sediment on the development of braiding condition.

2.3 CHARACTERISTICS OF BRAIDED CHANNELS AND BRAIDING INDICATORS

2.3.1 General

The channel pattern of a reach of an alluvial river reflects the flow dynamics within the channel and the associated channel process of sediment transport and energy expenditure. Adjustments of equilibrium channel pattern may occur over a widely varying time scale depending on the mobility of the channel-forming sediments and may

reflect the effects of any intervention by man for controlling water and sediment discharges that determine the fluvial process. Channel pattern forms a continuum in response to varying energy conditions, ranging from straight or meandering channels to multi-thread braided forms.

2.3.2 Characteristics of Braided Channels

Braided streams occur in high-energy environments of large and variable discharges, heavy sediment load, and steeper gradients with erodible banks. Braided streams are characterised by wide and shallow cross-sections with random bar formations creating flow divisions. Sediment transport takes place over the bar surface while incision in the lateral channels lowers the water surface to expose the bar, which then becomes dissected. The complex of islands is stabilised by vegetation in natural streams and experiences further high-stage sedimentation (Richards, 1982). The distributary channels formed by braiding are less hydraulically efficient than parent single channels. Braided reaches are characterised by steeper slopes for maintenance of stream power necessary for sediment transport. Braided reaches show greater complexity, that is, more bars and distributaries in the highest energy environments (Howard et al., 1970). This observation confirms that the braided channel pattern is optimal for the dissipation of energy in high energy streams since the enhanced total flow resistance of multi-thread channel results rapid energy loss (Richards, 1982). As per Smith (1970), general characteristics of braided stream deposits include abundant ripple and dune, cross stratification, thin lenticular shales, many intraclasts, thin sedimentary units indicating variable flow regimes, and numerous cut-and-fill structures.

2.3.3 Adjustments to Stream Power

Normally a natural channel accommodates flows approximately up to the mean annual flood before overbank flooding occurs. If the channel capacity is too small, overbank and bankfull flood events are more common. Thus, the threshold velocity or stream power of the perimeter sediment may be more frequently exceeded and sediment entrainment and perimeter erosion occur. The mean velocity over a period will be high in an initially small cross-section, and the excessive momentum of flow will be transmitted to the banks and bed by strong velocity shear at the perimeter. This causes erosion and channel enlargement until the frequency of exceedance of threshold velocities is lessened, the velocities associated with discharges of a given frequency are reduced and the channel is stabilised (Church, 1967). Establishment of an equilibrium section, therefore, reflects sediment properties as well as discharge magnitudes since adjustment of perimeter pre-supposes sufficient energy for entrainment. Energy of stream flow reflects the rate of conversion of its potential energy to kinetic energy and work, which depends on stream gradient and discharge. From the flume experiments by Wolman and Brash in 1961 (Sharma, 1995), it was evident that maximum channel changes occurred with the maximum rate of energy expenditure expressed in terms of $\rho g Q S_f$ where ρ is density, g is acceleration due to gravity, Q is discharge and S_f is energy gradient. This suggests that ultimate control of channel morphology be governed by the rate of loss of potential energy of the volume of stream flow generated at the frequency of channel forming events.

2.3.4 Existing Braiding Indicators

A number of indicators and hydraulic controls for channel pattern were proposed in the past as a measure of classifying streams in braiding category or as a measure of degree of braiding. Leopold and Wolman (1957) gave a functional relationship between bed slope and discharge to identify braided reaches. Lane (1957), Henderson (1961) and Antropovskiy (1972) developed similar functions relating slope with discharge to predict braids at higher slope and discharge. Smith (1970) formulated bed relief index to account for bar type and bed relief to implicitly characterise braids. Schumm and Khan (1972) plotted sinuosity as a function of experimental flume slope to provide the threshold when braiding begins. Brice (1964), Howard et al. (1970), and Rust (1978) have emphasized the role of sinuosity as well as braiding indicators in characterising the braided streams.

Many of the existing braid indicators do not adequately account for the hydraulic parameters and the underwater bars, both of which are seen to have a close relationship with the braiding process. Hence, it can be concluded that there is a need to formulate new braid indicators by incorporating the above indicators to have a more rational description of the braiding phenomenon. A variety of braiding indicators are described in Chapter-4, where the performance evaluation of the existing indicators is also done.

2.4 RESISTANCE TO FLOW IN BRAIDED STREAM

Resistance to flow encountered in braided river bed is a crucial parameter for discharge calculation. Rugosity coefficient varies from section to section of the braided river. It varies with time also. In alluvial river hydraulics, the resistance relationship has

been a subject of investigation by several research workers. Prandtl-Karman gave a relationship for rough boundaries (Garde and Ranga Raju, 2000). Manning's and Chezy's equations are commonly used resistance relationships (Garde and Ranga Raju, 2000), which are as given below:

$$Q = \frac{A}{n} R^{2/3} S^{1/2} \quad (2.1)$$

$$U = \sqrt{(2g/c_f)} \sqrt{(RS)} = C \sqrt{(RS)} \quad (2.2)$$

In eqs. (2.1) and (2.2), Q= discharge of water; R= hydraulic radius; S = slope of channel; n = Manning's rugosity coefficient; C = Chezy's coefficient and c_f = Local drag co-efficient.

Keulegan (1938) described a resistance relationship for rough boundary. Strickler in 1923 (Garde and Ranga Raju, 2000) evolved a useful relationship for 'n' using study of various streams of Switzerland. Lacey (1930) gave a resistance relationship, e.g. mean velocity formula for alluvial streams, which is valid for dominant discharge. Japanese formulae (Garde and Ranga Raju, 2000) are also used by Japanese Engineers as the basic equation for resistance. Tsubaki and Fuzuya (Garde and Ranga Raju, 2000), obtained an expression for k_s in the ripple and dune regime,

$$\log\left(\frac{k_s}{d}\right) = 3.48 (1 - 0.225 \tau_*^{-1/2}) \quad (2.3)$$

where k_s = equivalent roughness height; d = diameter of particle; and τ_* = dimensionless shear stress.

Ishihara, Iwagaki, and Sueishi (Garde and Ranga Raju, 2000) have derived resistance formulae on the basis laboratory experiments. Einstein (1950) developed the bedload function of sediment transportation in open channel flow. Einstein and

Barbarossa (1950, 52) studied the friction losses due to grain roughness, channel irregularities and other factors and gave following equations with division of hydraulic radius in two parts

$$\tau_0 = \tau_0' + \tau_0'' \quad (2.4a)$$

$$\gamma R S = \gamma R' S + \gamma R'' S \quad (2.4b)$$

$$R = R' + R'' \quad (2.4c)$$

where τ_0 = shear stress; τ_0' = shear stress due grain roughness; τ_0'' = shear stress due to bed undulation; R' = hydraulic radius due to grain roughness; and R'' = hydraulic radius due to form roughness.

Leopold and Wolman (1957) proposed an empirical relation between resistance parameter $1/\sqrt{f}$ and relative smoothness as

$$\frac{1}{\sqrt{f}} = \left(\frac{D}{d_{84}} \right)^{0.5} \quad (2.5)$$

in which d_{84} = grain size diameter of which 84% are finer; D = depth of flow; and f = Darcy-Weisbach friction factor.

Garde (1959) has suggested that a logarithmic velocity distribution law of the form

$$\frac{u}{u_*} = \frac{2.3}{k} \log \left(\frac{y}{k_s'} \right) \quad (2.6)$$

could be used in alluvial streams.

in which k = Karman constant; varies from 0.15 to 0.60; k_s' = length parameter i.e. distance from the bed at which above equation will give zero velocity; y = flow depth; and u_* = shear velocity.

Bharat Singh (1961) gave a formula for resistance relationship. Peter Ackers (1964) has given a resistance equation that appropriately may be written as

$$U = \alpha_2 D^{0.75} S_f^{0.50} \quad (2.7)$$

in which U = average velocity; $\alpha_2 = (7.13\sqrt{g/k^{0.5}})$, a resistance coefficient dependent on roughness; D = mean depth of flow; and S_f = slope of energy gradient.

Garde and Ranga Raju (1966) analysed data from flume studies, canals and natural streams and proposed an empirical equation for the mean velocity. Ranga Raju (1970), further identified the noticeable effect of sediment size on the relationship of Garde and Ranga Raju (1966). Engelund (1966,67) derived a resistance relationship, where he found that resistance of plane bed with motion is larger than that of a plane bed without motion of sediment. His method does not cover ripple regime. Alam and Kennedy (1969) divided the slope into two components like

$$S = S' + S'' \quad (2.8a)$$

and total friction

$$f = f' + f'' \quad (2.8b)$$

Here

$$f' = \frac{8gRS'}{U^2} \quad (2.8c)$$

$$f'' = \frac{8gRS''}{U^2} \quad (2.8d)$$

in which S' = slope due to grain resistance; and S'' = slope due to form resistance.

Ackers and White (1973) gave new sediment transport approach as given below.

$$\frac{U}{\sqrt{32g(s-1)d}} = \text{const} \tan t \times \log\left(\alpha_c \frac{D}{d}\right) \quad (2.9a)$$

which may be approximates to

$$\frac{U}{\sqrt{32g(s-1)d}} = \text{const} \tan t \times \log\left(\frac{10D}{d}\right) \quad (2.9b)$$

in which s = mass density of sediment relative to that of fluid; α_c = coefficient in rough-turbulent equation; and U = average velocity.

Kouwen and Unny (1973) studied the flexible roughness in open channels. Yen (1973) investigated the shape effects on resistance in flood-plain channels. Maddock (1973) described a role of sediment transport in alluvial channels.

Sugio (Garde and Ranga Raju, 2000) used river data from Japan and obtained the resistance equation for different flow regimes. Ilo (1975) gave equation for flow resistance in alluvial channels, which was applied both for laboratory and field data. Burkham et al. (1976) suggested a modified equation to resistance for turbulent flow in alluvial channels. Leopold et al. in 1964 (Burkham et al., 1976) gave an empirical equation to represent flow in channels. Chiu et al. (1976) developed resistance co-efficients formulae for simulation of hydraulic processes in open channels. Senturk (1978) proposed the general form of the equation for resistance to flow in sand bed channels. Knight and Macdonald (1979) presented a formula for shear velocity. Thompson and Camphell (1979) presented a resistance relationship by studying a large channel paved with boulders. Parker and Peterson (1980) gave a quantification of grain resistance of gravel bed streams. White et al. (1982) studied analytical approach to river regime and used sediment mobility parameter in their resistance analysis. Myers (1982) studied flow resistance in wide rectangular channels. Lau (1983) presented the general velocity distribution given by the logarithmic distribution plus the wake function, which describes the velocity throughout the whole depth. Willis (1983) evaluated flow resistance in test channels and gave the formula for friction in channels.

Rijn (1984) presented the classification of bed forms for the prediction of the bed form dimensions and the effective hydraulic roughness of bed forms. Jarrett (1984) worked on hydraulics of high-gradient streams and realised that many studies based on hydraulic theory pertaining to flow resistance have been made and summarised that Limerinos in 1970 (Jarrett, 1984) resistance velocity is most accurate.

Krishnappan (1985) developed a resistance relationship for unsteady flows in alluvial stream. Aziz and Prasad (1985) studied sediment transport in shallow flow and gave a resistance relationship for shear velocity. Vedula (1985) worked out bed shear from velocity profiles approach and obtained the velocity formula for wide channels. Karim and Kennedy (1987) developed a relationship for mean sediment velocity in bed layer. Kirkgoz (1989) studied turbulent velocity profiles for smooth and rough open channel flow and got best-fit expression for velocity-defect distribution on rough bed.

$$\frac{\Delta u}{u_*} = 3.5 \left(\frac{u_* k_s}{\nu} \right)^{0.13} \quad (2.10)$$

in which u_* = shear velocity; k_s = equivalent roughness height; and ν = kinematic viscosity.

Griffiths (1989) studied the form resistance in gravel channels with mobile beds.

Babarutsi et al. (1989) utilised ASCE Task Force approach on friction factor in open channel flow. Phillips (1990) proposed the following equation

$$U = (\rho g RS/f)^{0.5} \quad (2.11)$$

in which U = average velocity; ρ = density of fluid; R = hydraulic radius; S = slope of stream; and f = Darcy-Weisbach friction factor.

Shu-Guang Li et al. (1992) proposed a stochastic theory for irregular stream flow resistance modelling, which gives finally an effective resistance coefficient. Yen et al., (1992) studied aggradation-degradation process in alluvial channels and described

average speed of wave propagation. Lyn (1993) measured and proposed Reynold's shear stress profiles and fitted to an expression in their study on turbulence measurements in open-channel flows over artificial bed forms.

Wang and White (1993) proposed a friction relationship for transition regime in alluvial channel. Griffiths (1993) presented sediment translation wave velocity in braided gravel bed. Yang et al. (1996) studied sediment transport in the Yellow river in China and presented the dimensionless critical velocity at incipient motion. Sturm and Sadiq (1996) studied water surface profiles in compound channel with multiple critical depths and used Keulegan's (Sturm, 1996) expression for Darcy-Weisbach friction factor f in fully rough, turbulent open channel flow, which has given below:

$$\frac{1}{f^{1/2}} = 2.2 + 2.0 \log \left(\frac{R}{k_s} \right) \quad (2.12a)$$

Manning's n that can also be differentiated to obtain dn/dy (Sturm 1992)

$$\frac{n}{k_s^{1/6}} = \frac{\frac{C_n}{\sqrt{8g}} \left(\frac{R}{k_s} \right)^{1/6}}{2.2 + 2.0 \log \frac{R}{k_s}} \quad (2.12b)$$

in which $C_n = 1.0$ for SI unit and 1.49 for FPS unit; and g = acceleration due to gravity.

Song and Graf (1996) described velocity and turbulence distribution in unsteady open-channel flows and used a particular form of the wake law which was given by Nezu and Rodi (Song 1996). Sumer et al. (1996) suggested that for practical purposes, the flow-resistance could be represented by the following empirical expressions

$$\frac{k_s}{d} = 2 + 0.6\theta^{2.5} \quad \text{when } \frac{\omega}{U_f} > 0.8-1 \quad (2.13a)$$

and

$$\frac{k_s}{d} = 4.5 + \frac{1}{8} \exp \left[0.6 \left(\frac{\omega}{U_f} \right)^4 \theta^2 \right] \theta^{2.5} \quad \text{when } \frac{\omega}{U_f} < 0.8 - 1 \quad (2.13b)$$

in which, d = particle diameter; θ = Shield parameter = $U_f / g(s-1)d$; ω = fall velocity of sediment grains; U_f = bed friction velocity; s = relative density of sediment grains; and k_s = equivalent roughness height.

Ervine et al. (2000) proposed in their two-dimensional solution for meandering river, (i) the lateral distribution of boundary shear stress and (ii) the lateral distribution of depth-averaged velocity.

2.5 EXTREMAL HYPOTHESES AND MAXIMUM ENTROPY THEORY

2.5.1 Extremal Hypotheses

Many researchers have worked on extremal hypotheses for study of river behaviour. Yang et al. (1981) identified a parameter, MEDR, termed as 'minimum energy dissipation rate' and stated that a system is in an equilibrium condition when its rate of energy dissipation is at a minimum value. Yang and Song (1979) defined 'minimum unit stream power', which also equals the product of the flow velocity and slope of the channel. The authors stated that channel will adjust its velocity, slope, roughness and geometry in such a manner that a minimum amount of stream power is used to transport a given sediment and water discharge. Chang (1980b) described minimum stream power (MSP) equal to γQS in which γ is unit weight of water, Q is the discharge of water and S is slope of the channel. He stated that the equilibrium occurs

when the stream power per unit length of channel is a minimum subject to given constraints. Davies and Sutherland (1980) stated that maximum friction factor (MFF) 'If the flow of a fluid past an originally plane boundary is stable to deform the boundary to non-planar shape, it will do so in such a way that the friction factor increases to a maximum'. White et al. (1982) state that for a particular water discharge and slope, the width of the channel adjusts to maximise the sediment transport rate. It is used to predict hydraulic and geometrical characteristics of both sand and gravel bed alluvial channels.

2.5.2 Maximum Entropy Theory

Amorocho and Espildora (1973) used the concept of entropy, as introduced in information theory, to characterise the uncertainty of hydrologic occurrence. Entropy is a measure of the degree of uncertainty of a particular outcome in a process; therefore, in dealing with the prediction of a hydrologic and hydraulic variable such as stream flow and channel pattern, one can compute the entropy of this variable from historical data and thus characterise the unexpectedness or variability inherent in the process.

Deng and Singh (1999) have described mechanisms and conditions for change in channel pattern. They also presented channel pattern coefficient and stability criteria of different river channels. Using the entropy theory, they have related the process variables to define a stability parameter related to single and multiple thread streams.

2.6 SCALE MODEL STUDY

Scale models are specifically useful for the design of river improvement works and hydraulic structures, which need detailed information about the associated three-

dimensional, time-dependent phenomena involved. The introduction of morphological processes into scale models considerably enhances the complexity of scaling. Both water movement and sediment movement have to be reproduced at the same time. Smeaton in 1795 described first recognized hydraulic model studies (Jansen et al., 1979). Since Louis Jerome Fargue built the river model in 1875, great advances have been made due to better understanding of the phenomena involved. Fargue's model covered a reach of the Garonne River at Bordeaux (Jansen et al., 1979). The historical development of mobile bed models especially for rivers and estuaries is described by Allen in 1947 and Ippen in 1970 (Modi and Seth, 1982; Jansen et al., 1979)

Many problems in river engineering are sufficiently complicated so that the equations of fluid mechanics cannot be readily applied or do not supply answers. Then the use of a model, which is a miniature prototype, might lead to a much-desired answers. Further useful information on the theory, construction and operation of models was given by Freeman in 1929, Stevens et al. in 1942 and Rzhanitsyn in 1960 (Graf, 1971). Complete dynamic similarity between model and prototype exists if identical types of forces are parallel and have the same model prototype ratio at all points of the corresponding flow fields.

To assess some of the objectives, it is necessary to do scale model study of a braided river. For this study purpose, a particular stretch of the Brahmaputra river in Bangladesh has under taken, which will be reproduced in the laboratory flume.

2.7 CONCLUDING REMARKS

In this chapter, various studies related to formation of braid bars as well as mechanisms responsible for their occurrences have been reviewed. It is obvious that

braiding depends on a multitude of factors including flow, geometry, sediment and fluid related variables. The opinion defers regarding the relative importance of these variables on braiding process. In addition, the flow resistance also considered an important parameter behind the occurrence of braiding. Although the mechanism of braiding is important topic of research, in this phase of the research endeavour, these have not been considered further. Rather, the observations regarding the utility of braiding indicators are considered in this study along with the development of resistance relationships as well as assessment of extremal hypothesis and entropy in studies related to braided streams. With these objectives in view, the chapter has presented a review of work on different resistance laws, which are in general empirical in nature. The different extremal hypotheses are also reviewed and applicability of some of these, finds attention in later chapters. Considering the importance of entropy in other disciplines of engineering and sciences, some coverage to this was also given in this chapter to highlight the application of entropy in characterising braiding condition.

METHODOLOGY AND EXPERIMENTAL PROGRAMME

3.1 GENERAL

Measurement of stream geometry and other geometric features and different fluvial data in the field is laborious and time consuming. Work in quantitative morphology and geometry would progress more rapidly if measurement could be taken from topographic maps having planform of rivers. But it is not possible to collect all data from the topo-sheet, specially the fluvial data. All fluvial data of the Brahmaputra river like water discharge, sediment discharge, water level elevation etc. have been collected from Bangladesh Water Development Board (BWDB) and Surface Water Modelling Centre (SWMC), Dhaka. For laboratory experimental study, a model flume (Experimental set-up) has been constructed in the river engineering laboratory of WRDTC, IIT, Roorkee. The geometrical and fluvial data of the model river have been measured during each experimental run.

3.2 IDENTIFICATION OF STUDY REACH

In the present research, it is proposed to analyse the field data of the Brahmaputra river in Bangladesh, which originates on the Northern slope of the Himalayas and flows

through the state of Assam in India and Bangladesh with its ultimate outfall into the Bay of Bengal. The location of the study reach has been shown in the Fig.3.1. The study reach has been limited between Bahadurabad Ghat (upstream) and Daulatdia-ArichaBaruria (downstream) where the Brahmaputra and the Padma river have made confluence. The planform of the study reach is shown in the Fig.3.2. The longitudinal profile has been shown in the Fig. 3.3. The cross-sections of the different sections of Fig. 3.2 such as A-A, B-B, and C -C from 1988 to 1997 have been shown in the Figs. 3.4a, 3.4b and 3.4c.

3.3 EXPERIMENTAL SET UP AND PROCEDURE

All the experiments are performed in a masonry-recirculating flume, which was constructed in the River Engineering Laboratory of WRDTC. The masonry open channel flume is of 22.5 meter long, 2.60 meter wide and 1.40 meter high. Re-circulating flow of water is supplied to the channel with the help of a centrifugal pump having 10 H.P. electric motor with 4 inch diameter delivery and suction pipe from a masonry underground water storage tank of size 12.5 m x 2m x 2m. The plan of the experimental set-up has been shown in the Fig. 3.5 and Plate 3.1.

Detailed drawing and elevation of experimental set-up and different accessories are shown in the Fig. 3.6. The flume has two walls along its length. Two rails are fitted on the walls. A steel bridge or trolley spans the width of the flume and is mounted on rails on the walls. The bridge or trolley is moved by rope or can be pulled manually and it is equipped with a pointer gauge for measuring elevations of the sand surface and water surface. Scales are installed along the length of the flume and on the bridge and these are used to establish a co-ordinate system and channel morphology is measured in relation to

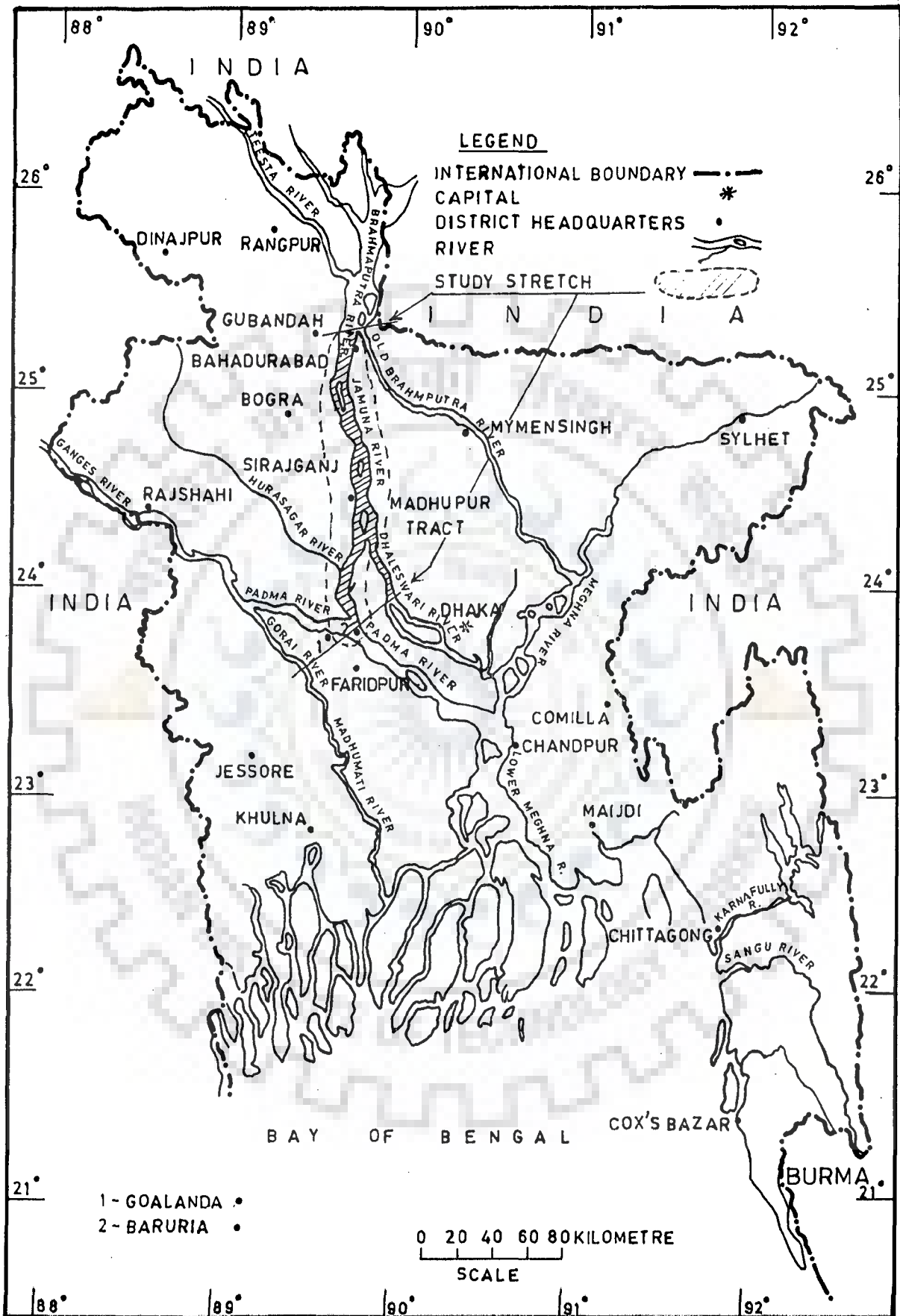


FIG.3.1: LOCATION MAP OF THE MAJOR RIVERS OF BANGLADESH

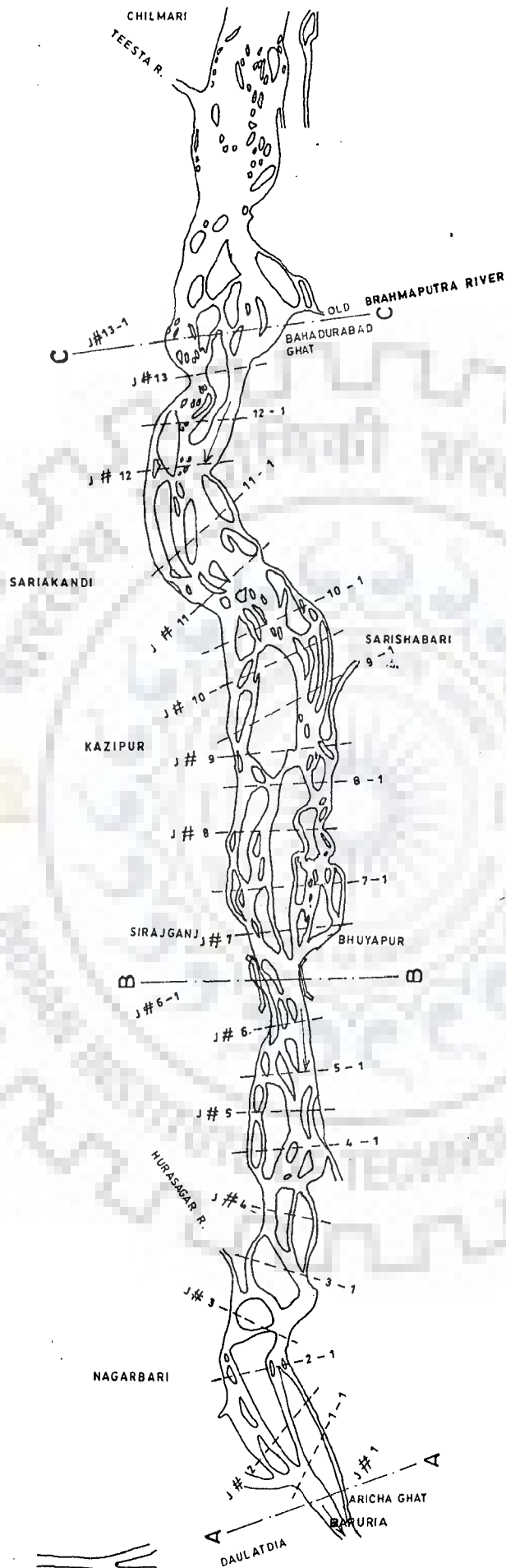


FIG.32: BRAHMAPUTRA RIVER STRETCH UNDER STUDY

SCALE :- NOT TO SCALE

LEGEND

- 1. RIVERS
- 2. CROSS SECTIONS



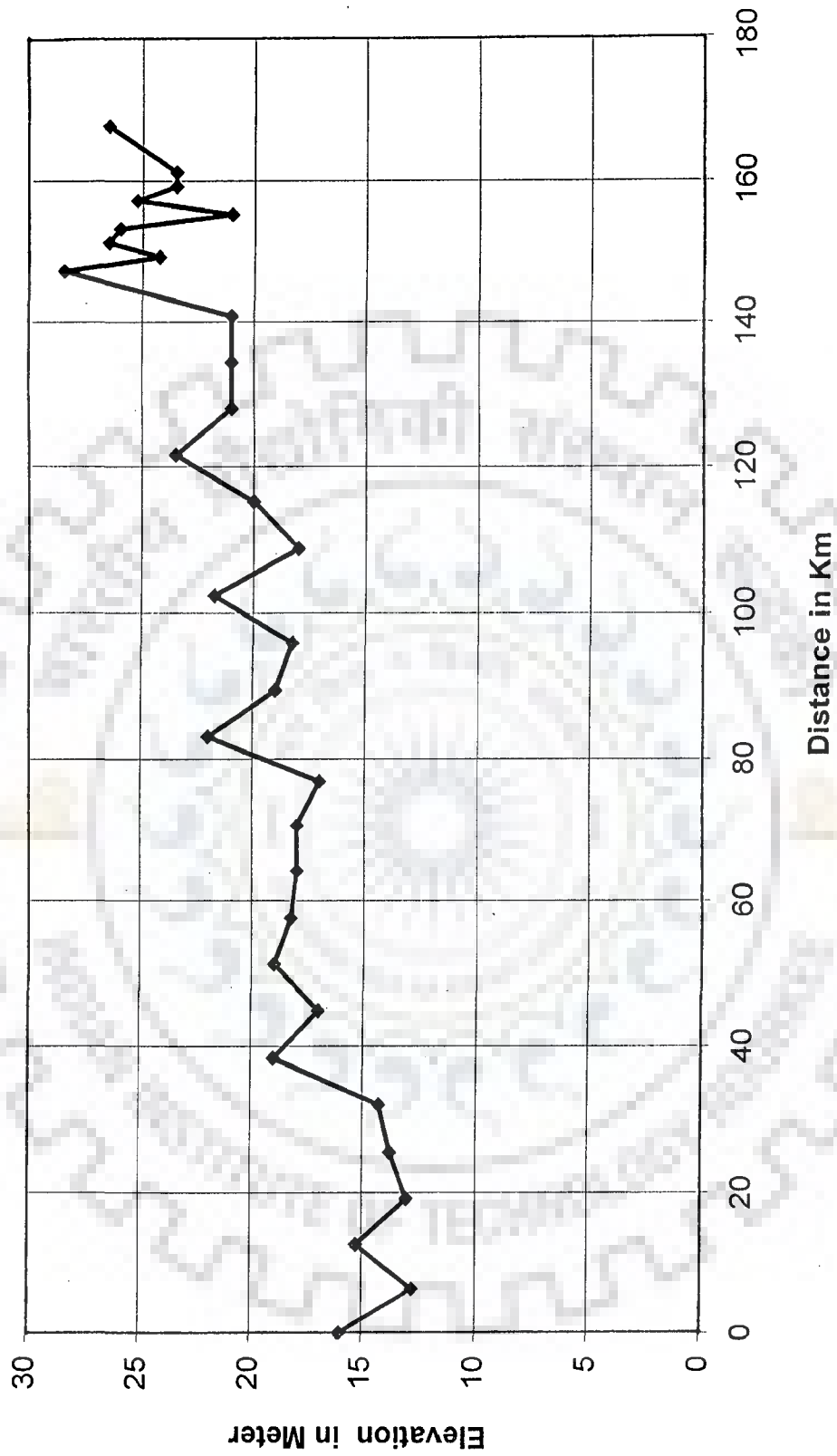


FIG. 3.3: A TYPICAL LONGITUDINAL PROFILE OF STUDY REACH OF THE BRAHMAPUTRA RIVER FOR YEAR 1997-1998

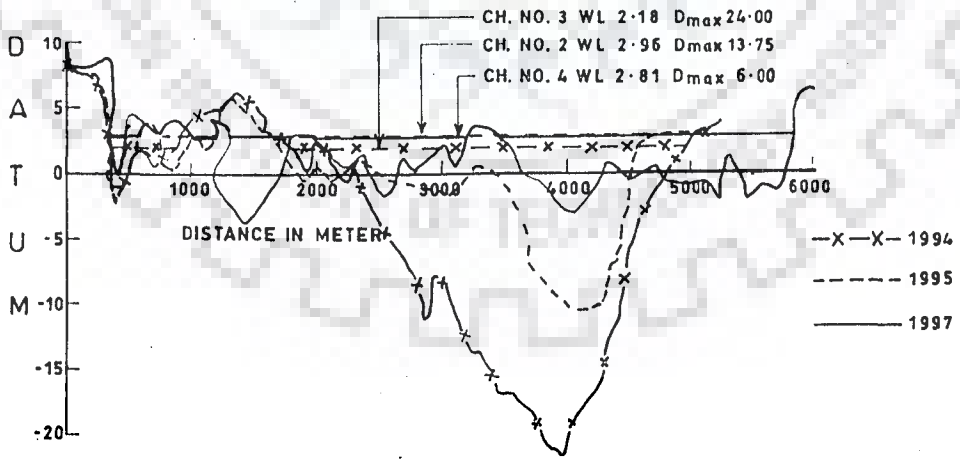
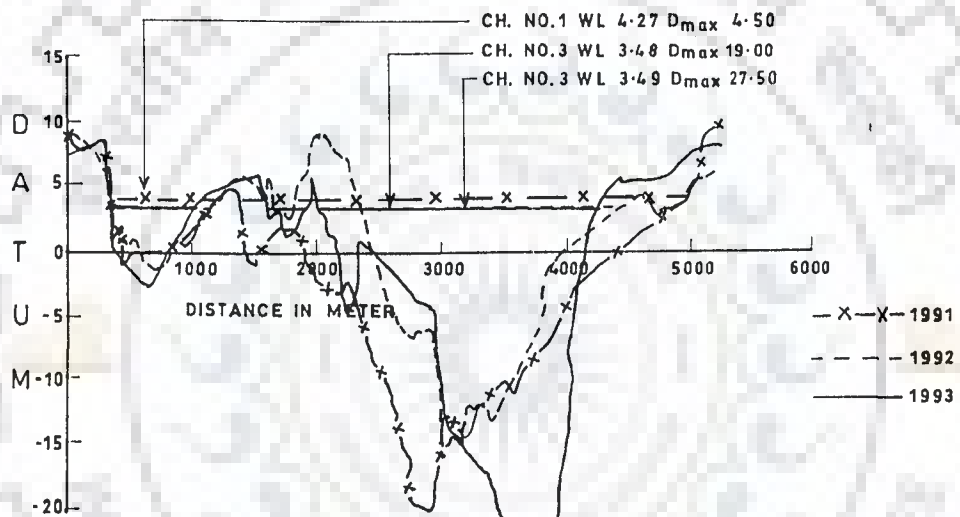
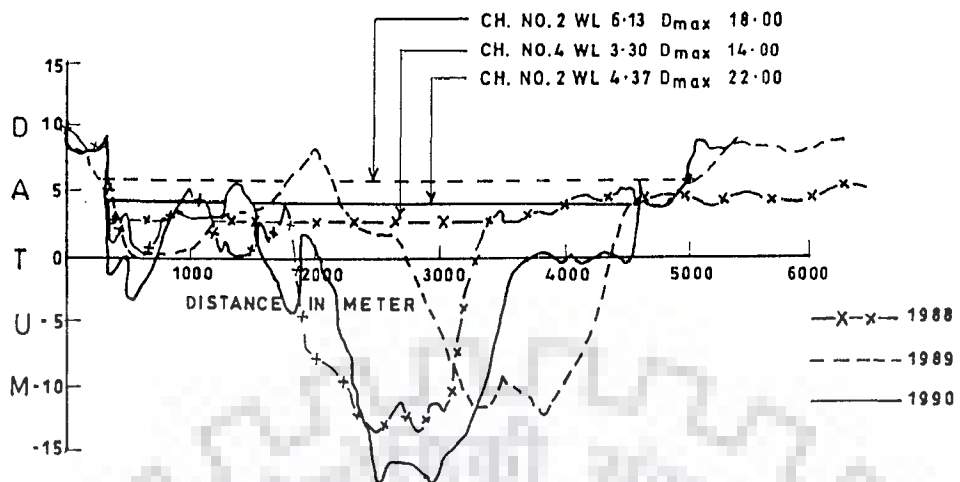


FIG.3.4a: TYPICAL CROSS-SECTION OF BRAHMAPUTRA RIVER AT DOULATDIA-ARICHABARU. (SEE A-A SEC. IN FIG.3.2)

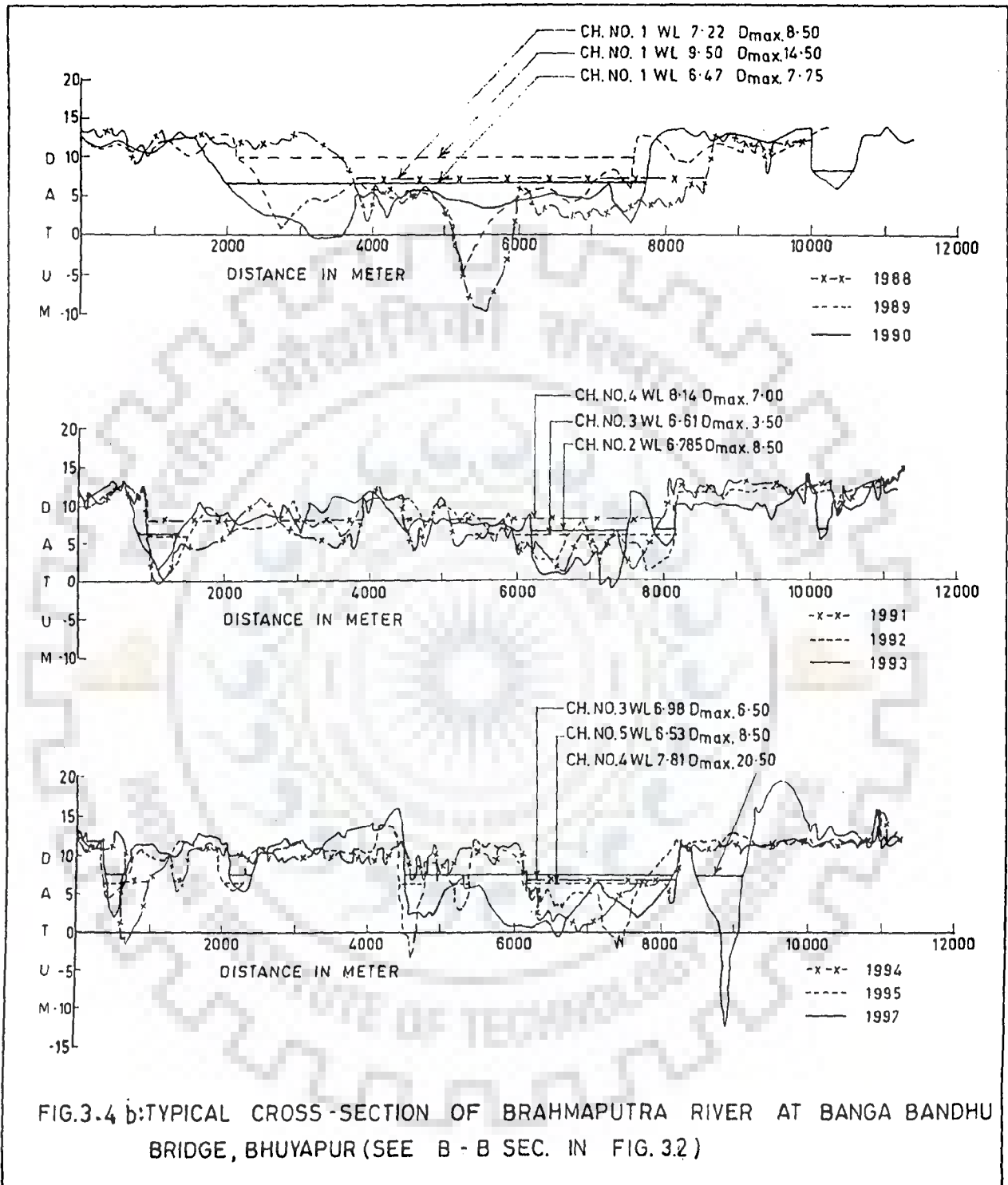
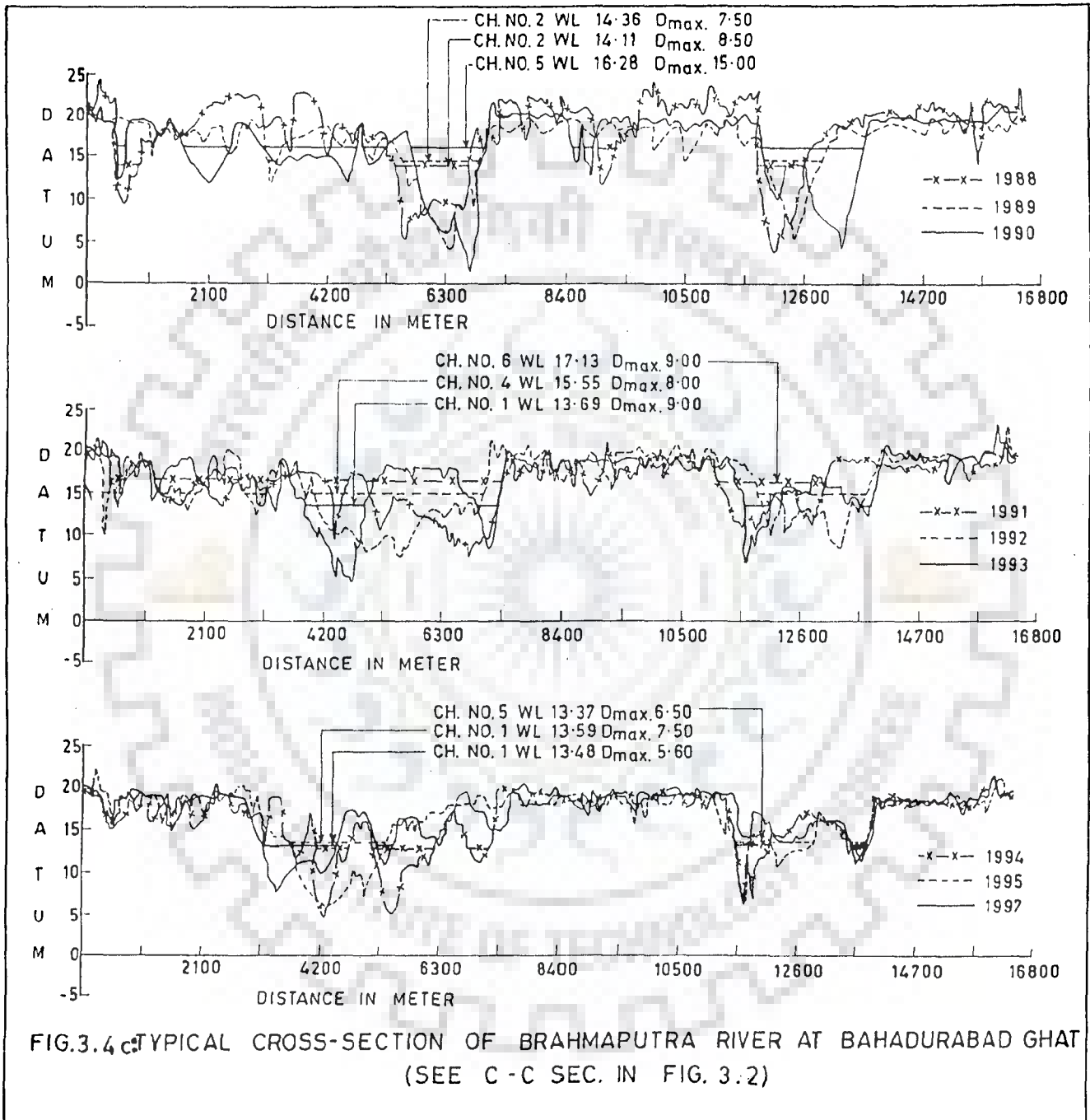


FIG.3-4 b: TYPICAL CROSS-SECTION OF BRAHMAPUTRA RIVER AT BANGA BANDHU BRIDGE, BHUYAPUR (SEE B - B SEC. IN FIG. 3.2)



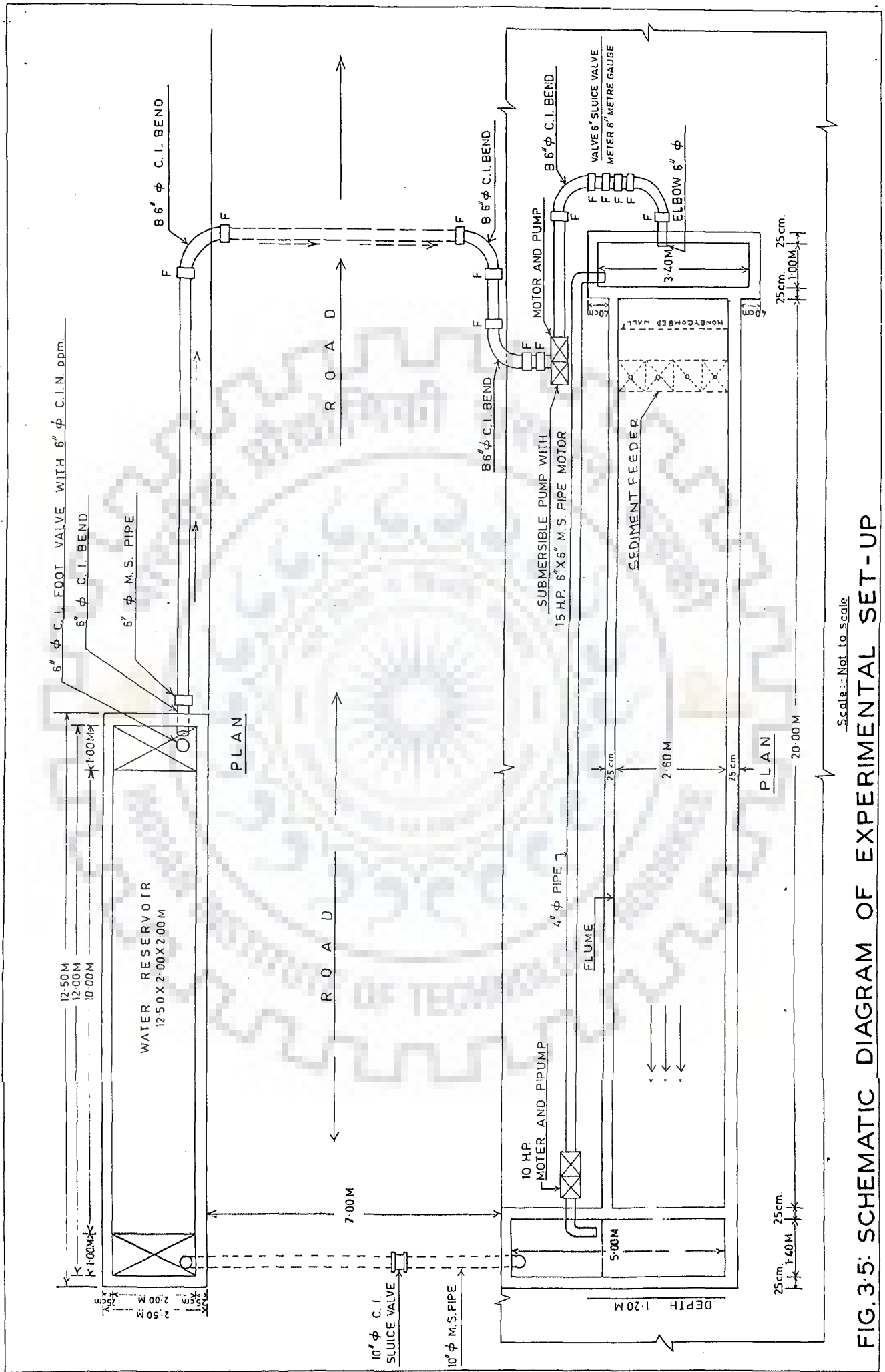


FIG.3.5: SCHEMATIC DIAGRAM OF EXPERIMENTAL SET-UP

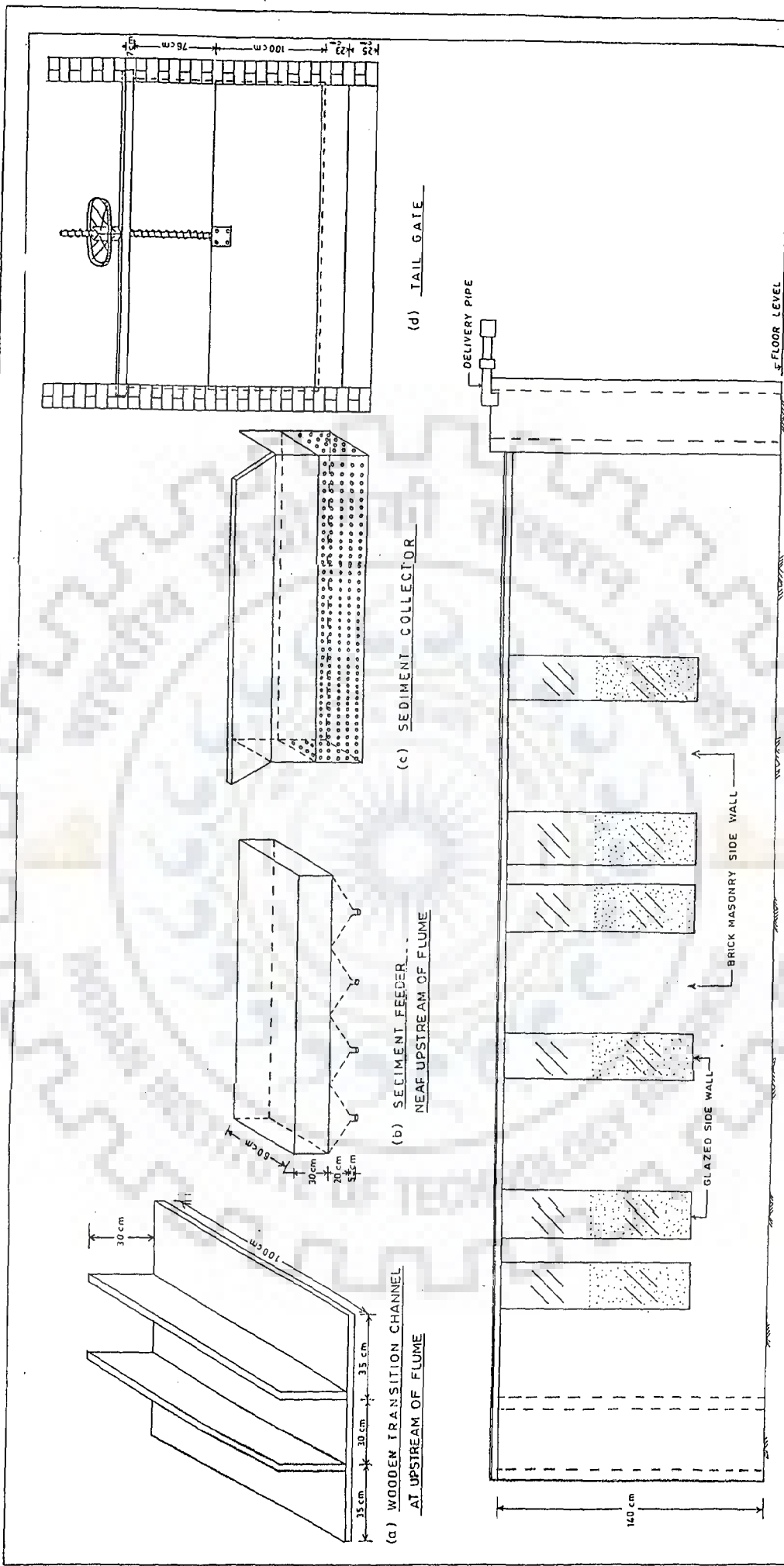


FIG.3.6: LONGITUDINAL ELEVATION OF MASONRY FLUME WITH NECESSARY ACCESSORIES



Plate 3.1: SHOWING LEVELLING PROCEDURE OF RAILS AND TROLLEY AT THE LAST STAGE OF FLUME CONSTRUCTION.



Plate 3.2: WOODEN TRANSITION CHANNEL

it. The flume is filled to a depth of 40 cm with a poorly sorted medium sand having d_{50} around 0.22 mm. Initial channels of required shapes and sizes are moulded by means of template mounted on a moving carriage, the latter carrying a pointer gauge for measuring elevation to an accuracy of 0.001m .

Both water and sediment passed through wooden transition and then through the model sand channel and entered a tail box or sediment collector at the end of the flume. Direction of flow was changed by wooden transition channel as shown in the Fig. 3.6a and Plate 3.2. Another two 6 inch dia. axial flow pumps are used for recirculating the water, when more discharge are required to supply in the flume. The slope of the model channel is maintained with the helps of a dumpy level. Slopes are taken as .005, 0.01, 0.02, 0.03 etc.

Direct discharge meter is connected to the delivery pipe. From the meter or delivery pipe the water flows into a stilling basin and thence through three honeycombed walls for suppressing the turbulence. After flowing through the model-working channel, it enters the tail box and it is re-circulated. Discharges are used in the range 0.00146, 0.002, 0.003, 0.004, 0.005, 0.007, 0.008, 0.010, 0.013 and 0.015 m^3/s . At the downstream end of the sand channel is a rectangular weir, which is made by brick masonry, the elevation of which is kept approximately level with the sand bed of the stream.

Sediment, in the form of dry and wet sand, is fed into the system from the hopper or sediment feeder fixed in the up-stream (Fig.3.6b and Plate 3.3). The sand is introduced at the entrance of the channel to compensate for sediment trapped in the tail-box by sediment collector shown in the Fig.3.6c and Plate 3.4. The rate at which sediment is fed at the hopper is determined by trial and error method. The rate of sediment feed varies



Plate 3.3: SEDIMENT FEEDING SYSTEM WHEN WOODEN TRANSITION AT AN ANGLE 40°



Plate 3.4: SEDIMENT COLLECTOR



Plate 3.5: ACOUSTIC DOPPLER VELOCIMETER (ADV)

from 0 to 1000 gm per minute. A period during which sand and water are delivered to the channel at constant rate is as long as 20-24 hours. The depth of flow is to be controlled when it is required by the tail-gate shown in the Fig. 3.6d.

Velocity of the flowing water in x direction and bed shear stresses are measured by pitot tube and Preston tube respectively as shown in the plate A2.8 of Appendix-II. Acoustic Doppler Velocimeter (ADV) is used for precise measurements of two velocity components of flow in x, and y direction. ADV having side probe has been shown in the plate 3.5 in working condition. During each experiment, elevations of both the bed of the channel and water surfaces are measured by using the pointer gauge. At the end of each experiment, a series of cross-sections and the longitudinal profile are measured.

3.4 EXPERIMENTAL PROGRAMME FOR PHASE-I

3.4.1 Planning of Present Experimental Work Programme Based on Experimental Study and Physical Observation of Past Investigators

Planning of present experimental work programme based on experimental study of past investigators is shown in Table 3.1.

3.4.2 Experimental Condition Phase -I

3.4.2.1 Non-sediment feeding condition for the present study, Phase-I

Table 3.2 represents the non-feeding experimental programme Phase-I.

3.4.2.2 Sediment feeding condition for present experimental study Phase-I

Table 3.3 represents the feeding condition experimental program Phase-I

Table 3.1 BASIS FOR PLANNING OF PRESENT EXPERIMENTAL WORK

Investigator	Length of flume / River	Initial Size, B x D	Slope, S	Discharge, Q	Feeding rate, Q _f , gm/min	Sinuosity, $p_c = L_m/L_s$	Median grain size d_{50}	Sediment concentration, C _s	Velocity, m/s	Bed sand filling	Running time	Remarks
Leopold & Wolman (1957)	18.288 m	38.1cm x 3.81cm	0.01	0.01-0.1 cfs = 2.84 lps	0-200 gm / min	-	0.17 (fine) .62-1mm (medium)	830 ppm	0.173-0.424 m/s	Sand filling in bed 12.7cm	25 hrs	Based on experimental Study
Lane, (1957)	Colorado River, America		1.2 / 5280	2500-190000 cusec			Bed silt 0.10mm					Silt-laden stream Field observation
Peter Ackers (1964)	91.46 m long	B=30.48 m		5 cusec (0.4-5.4)			0.16 mm & 0.34 mm	400 ppm				Experimental study
Peter Ackers & Charlton (1970)				Max. 5 cusec			$d_{50}=0.15$ mm			Sand bed 45cm, underlain 2 ft coarse sand		Meandering geometry arising from varying flow (Flume experiment)
Schumm and Khan (1972)	30.48 m	36.58 cm x 7.62 cm	0.015-0.02	0.15 cfs = 4.25 lps	87-150gm / min	1.07-1.26 existed	0.7 mm	3% sorting index =2.22	0.518-0.732 m/s	Sand Filling 60.96cm	24 hrs	Based on Experimental study
Smith (1974)	6437.45 m	853.45 or 762 m x (0.6096-1.219m)	0.0054-0.0072	2.83 m ³ /s -124 m ³ /s				BRI=3.9				Field observation Kicking Horse River, B.Columbia.

Contd....

Investigator	Length of flume / River	Initial Size ,B x D	Slope, S	Discharge , Q	Feeding rate, Q_s gm/min	Sinuosity, $p_s = L_m/L_s$	Median grain size d_{50}	Sediment concentration	Velocity, m/s	Bed sand filling	Running time	Remarks
Cheetham (1969)	150 m	Increase - 1.0—180	1 in 7 or 1 in 70	2.2 to 2.9	$Q = 3.8$ m ³ /s favour	D increase —46 to 20	0.51 to 0.61 mm	Catchment area 15 km ²	Incr —42 To 10	$\tau_0 = 11-46$ N/m ²		Field observation
Coleman, (1969)	Brahmaputra River 2896.85 km but Study reach 220km	1828.82 m or 510 to 20km x 7.82 to 12.97m	0.00001 136	12200 m ³ /s to 65500 m ³ /s	$Q_s = 168.8$ million tons		$d_{50} = 0.028$ to 0.34mm		2.84 m/s			Field observation of Brahmaputra River Bangladesh
Callander, (1969)		1.207 m to 2.304m x 0.0396 m to 0.0435m	0.00107 9 to 0.00171	0.00793 to 0.039 m ³ /s			0.45 mm			$\tau_0 = 0.00935$ to 0.146 kg/m ²		Physical observation (resistance and sediment transport)
Miall, (1977)	Brahmaputra River =3000km	13000 m x 15m (Brahmaputra) 5000 m x 10m (Ganga)	BR=0.0 0007	100000 cumecs	>11% favours braiding	Sinuosity < 1.3 favours braiding		B/D >40 favours braiding >300 (steep slope)	2.4 m/s (Brahmaputra) & Ganga 3.4 /s			Field observation

Contd....

Best, (1988)	1.7m (confluent channel) to 1.5m (post confluent)	B=0.15m B/d ₅₀ =300 (flume) & 30-4000 (Rivers)					0.49 mm	Sorting co-efficient 0.52-0.59	D/d _m =36-40 (flume) & 30-4000 (Rivers)	R _c =3000-12000(Flume) & >2000-10 ⁶ (Rivers)	Field observation F _r =0.1 to 1.0(Flume) <1.0(Rivers)
Ashmore, (1988)	10m	2m	Slope 0.01—0.015	Q _{m model} =0.0012—0.0045 m ³ /s			d ₅₀ =1.16mm, d ₈₅ =4mm				F _r =0.41—1.08 F _{r model} =0.56—0.93 R _c particle=36-103
Patra and Kar, (2000)	L1=21 m L2=10 m	B=2m B=0.6m	0.00278 -0.0061				Sinuosity =1.043-1.22	B/b=2.13-5.25			Flume exp. On meandering river b=width of main or centre channel

Notes:

A * Khan and Schumm (1972) had given initial bend (IB) at up-stream of channel to create meandering or braiding and achieved sinuosity up to 1.26.

* They had also taken the measurements at the end of each run

B * Leopold and Wolman (1957) had taken the measurements depending on bars / islands formation in the channel. Intervals vary from 3hrs—6hrs - 7 hrs—9 hrs --13 hrs-- 22 hrs.

Table 3.2: DETAILS OF EXPERIMENTS (NON-FEEDING CONDITION) FOR PHASE-I

Run no.	Initial channel Size, BxD	Slope S_0	Water discharge Q in m^3/s	Duration of Experiments in hours	Sinuosity P_c	Remarks
1	30cm x 10cm	0.01	0.005	24	1.00	40° oblique flow or Initial bend
2	30cm x 10cm	0.01	0.0035	20	1.00	20° IB
3	30cm x 10cm	0.01	0.0075	24	1.00	60° IB
4	30cm x 10cm	0.01	0.0056	20	1.05	Straight channel
5	30cm x 10cm	0.01	0.0075	24	1.10	20° IB
6 S	30cm x 10cm	0.02	0.0065	24	1.00	40° OFor IB
7 T	30cm x 10cm	0.02	0.0043	24	1.00	60° IB
8 E	30cm x 10cm	0.02	0.007	24	1.05	Straight channel
9 D	30cm x 10cm	0.02	0.0045	24	1.10	20° IB
10 Y	30cm x 10cm	0.02	0.0075	24	1.00	40° IB
11	30cm x 10cm	0.03	0.006	24	1.00	60° OFor IB
12	30cm x 10cm	0.03	0.0075	24	1.00	40° IB
13	30cm x 10cm	0.03	0.004	20	1.00	60° OFor IB
14	30cm x 10cm	0.03	0.0075	24	1.05	Straight channel
15	30cm x 10cm	0.03	0.0075	24	1.10	20° IB
16 U	30cm x 10cm	0.01	0.0035 / 0.007 / 0.009 / 0.007 / 0.0035	0-4 / 4-8 / 8-12 / 12-16 / 16-20	1.00	20° IB
17 N	30cm x 10cm	0.01	0.0035 / 0.007 / 0.01 / 0.007 / 0.0035	0-4 / 4-8 / 8-12 / 12-16 / 16-20	1.00	40° IB
18 S	30cm x 10cm	0.01	0.0035 / 0.007 / 0.01 / 0.007 / 0.0035	0-4 / 4-8 / 8-12 / 12-16 / 16-20	1.00	60° OFor IB
19 T	30cm x 10cm	0.01	0.0035 / 0.007 / 0.01 / 0.007 / 0.0035	0-4 / 4-8 / 8-12 / 12-16 / 16-20	1.05	Straight channel
20 E	30cm x 10cm	0.01	0.0035 / 0.007 / 0.009 / 0.007 / 0.0035	0-5 / 5-10 / 10-15 / 15-20 / 20-25	1.10	20° IB
21 A	30cm x 10cm	0.02	0.0035 / 0.007 / 0.01 / 0.007 / 0.0035	0-4 / 4-8 / 8-12 / 12-16 / 16-20	1.00	20° IB

Contd....

22	D	30cm x 10cm	0.02	0.0035 / 0.007 / 0.01 / 0.007 / 0.0035	0-4 / 4-8 / 8-12 / 12-16 / 16-20	1.00	40° IB
23	Y	30cm x 10cm	0.02	0.0035 / 0.007 / 0.01 / 0.007 / 0.0035	0-5 / 5-10 / 10-15 / 15-20 / 20-25	1.00	60° OFor IB
24		30cm x 10cm	0.02	0.0035 / 0.007 / 0.01 / 0.007 / 0.0035	0-5 / 5-10 / 10-15 / 15-20 / 20-25	1.05	Straight channel
25		30cm x 10cm	0.02	0.0035 / 0.007 / 0.01 / 0.007 / 0.0035	0-5 / 5-10 / 10-15 / 15-20 / 20-25	1.10	20° IB
26		30cm x 10cm	0.03	0.0035 / 0.007 / 0.01 / 0.007 / 0.0035	0-4 / 4-8 / 8-12 / 12-16 / 16-20	1.00	40° IB
27		30cm x 10cm	0.03	0.0035 / 0.007 / 0.01 / 0.007 / 0.0035	0-4 / 4-8 / 8-12 / 12-16 / 16-20	1.00	60° OFor IB
28		30cm x 10cm	0.03	0.0035 / 0.007 / 0.01 / 0.007 / 0.0035	0-5 / 5-10 / 10-15 / 15-20 / 20-25	1.00	Straight channel
29		30cm x 10cm	0.03	0.0035 / 0.007 / 0.01 / 0.007 / 0.0035	0-5 / 5-10 / 10-15 / 15-20 / 20-25	1.05	channel
30		30cm x 10cm	0.03	0.0035 / 0.007 / 0.01 / 0.007 / 0.0035	0-5 / 5-10 / 10-15 / 15-20 / 20-25	1.10	

Notes : Water level, water surface slope, and bed level profile will be taken 4- 6 hrs interval depending upon development of braid bars in channel.

- Velocity and shear stress measurements are to be taken at bankfull discharge. Sediment size is $d_{50} = 0.22$ mm
- Effective length of the river flume is 15 m and test section is 13 m.
- Sinuosity instead of initial bend of flow at upstream, which is necessary for occurrence of meandering or braiding, suggested by Khan and Schumm (1972), will be provided. Khan and Schumm gave initial bend 40° and got sinuosity up to 1.26.
- From Run-1 to Run-15 having steady flow condition by applying constant discharge and from Run-16 to Run-30 having unsteady flow condition by applying variable discharges.

Table 3.3: DETAILS OF EXPERIMENTS (FEEDING CONDITION) FOR PHASE-I

Run no.	Initial channel Size, W x D	Slope S_b	Water discharge, Q m^3/s	Duration of Experiments in hours.	Sediment Discharge (gm/min)	Sinuosity, $P_c = L_m / L_s$	Remarks
31	30cm x 10cm	0.01		24	455	1.00	40° oblique flow direction
32	30cm x 10cm	0.01	0.004	24	665	1.00	20° IB
33	30cm x 10cm	0.01	0.005	20	560	1.00	60° IB
34	30cm x 10cm	0.01	0.004	24	560	1.05	Straight
35	30cm x 10cm	0.01	0.005	20	630	1.10	Channel
36	S 30cm x 10cm	0.02	0.005	24	280	1.00	20° IB
37	T 30cm x 10cm	0.02	0.006	24	560	1.00	40° OFor IB
38	E 30cm x 10cm	0.02	0.004	20	560	1.00	60° IB
39	D 30cm x 10cm	0.02	0.005	20	490	1.05	Straight
40	Y 30cm x 10cm	0.02	0.0065	20	396.7	1.10	Channel
41	30cm x 10cm	0.03	0.006	20	630	1.00	20° IB
42	30cm x 10cm	0.03	0.0045	20	490	1.00	40° IB
43	30cm x 10cm	0.03	0.004	20	385	1.00	60° OFor IB
44	30cm x 10cm	0.03	0.008	20	700	1.05	Straight
45	30cm x 10cm	0.03	0.0085	24	630	1.10	Channel
46	U 30cm/10cm	0.01	0.004 / 0.007 / 0.01 / 0.007 / 0.004	0-4 / 4-8 / 8-12 / 12-16 / 16-20	280	1.00	20° IB
47	N 30cm x 10cm	0.01	0.0035 / 0.007 / 0.01 / 0.007 / 0.0035	0-4 / 4-8 / 8-12 / 12-16 / 16-20	420	1.00	40° IB
48	S 30cm x 10cm	0.01	0.004 / 0.007 / 0.01 / 0.007 / 0.004	0-4 / 4-8 / 8-12 / 12-16 / 16-20	420	1.00	60° OFor IB
49	T 30cm x 10cm	0.01	0.0035 / 0.007 / 0.01 / 0.007 / 0.0035	0-5 / 5-10 / 10-15 / 15-20 / 20-25	350	1.05	Straight
50	E 30cm x 10cm	0.01	0.0035 / 0.007 / 0.01 / 0.007 / 0.0035	0-4 / 4-8 / 8-12 / 12-16 / 16-20	630	1.10	Channel
51	A 30cm x 10cm	0.02	0.0035 / 0.007 / 0.01 / 0.007 / 0.0035	0-4 / 4-8 / 8-12 / 12-16 / 16-20	546	1.00	20° IB

Contd....

52	D	30cm x 10cm	0.02	0.0035 / 0.007 / 0.01 / 0.007 / 0.0035	0-4 / 4-8 / 8-12 / 12-16 / 16-20	630	1.00	40° IB
53	Y	30cm x 10cm	0.02	0.0035-0.0065-0.01-0.007-0.0035	0-4 / 4-8 / 8-12 / 12-16 / 16-20	392	1.00	60° OFor IB
54		30cm x 10cm	0.02	0.0035 / 0.007 / 0.01 / 0.007 / 0.0035	0-4 / 4-8 / 8-12 / 12-16 / 16-20	560	1.05	Straight
55		30cm x 10cm	0.02	0.0035 / 0.007 / 0.01 / 0.007 / 0.0035	0-5 / 5-10 / 10-15 / 15-20 / 20-25	700	1.10	Channel
56		30cm x 10cm	0.03	0.004 / 0.007 / 0.01 / 0.007 / 0.004	0-5 / 5-10 / 10-15 / 15-20 / 20-25	350	1.00	20° IB
57		30cm x 10cm	0.03	0.0035 / 0.007 / 0.01 / 0.007 / 0.0035	0-4 / 4-8 / 8-12 / 12-16 / 16-20	560	1.00	40° IB
58		30cm x 10cm	0.03	0.0035 / 0.007 / 0.01 / 0.007 / 0.0035	0-4 / 4-8 / 8-12 / 12-16 / 16-20	350	1.00	60° OFor IB
59		30cm x 10cm	0.03	0.0035 / 0.007 / 0.01 / 0.007 / 0.0035	0-4 / 4-8 / 8-12 / 12-16 / 16-20	630	1.05	Straight
60		30cm x 10cm	0.03	0.0035 / 0.007 / 0.01 / 0.007 / 0.0035	0-4 / 4-8 / 8-12 / 12-16 / 16-20	630	1.10	Channel

Notes:

- * measurements were taken every 4-6 hours because in the flume incipient bars are appearing within 4-6 hours only.
- size of feeding sand around $d_{50} = 0.22$ mm
- For feeding sand, newly build-up sediment feeders are fixed at the up stream.
- Feeding time is equal to the running time of the experiment.
- Sediment have been collected from sediment collector which is fitted in the down stream tail box or small water reservoir.
- All measurements are to be taken at 1m interval along the length of the channel in braiding region.
- From Run-31 to Run-45 having steady flow condition by applying constant discharge and from Run-46 to Run-60 having unsteady flow condition by applying variable discharges.

3.5 EXPERIMENTAL PROGRAMME PHASE-II

3.5.1 Physical Model Studies for a Particular Stretch of the Brahmaputra River in Bangladesh

Notwithstanding considerable use of mathematical models in rivers engineering, a large number of problems have to be investigated and solved by means of scale models. The Brahmaputra river stretch is bounded from Bahadurabad to BangaBandhu-Jamuna bridge site has taken for this model study (Fig. 3.2). The length of the stretch is around 83 km and width varies from around 12 to 16 km within the stretch. This stretch is to be reproduced in the laboratory flume of River Engineering Lab. by providing vertical scale 1: 200 and horizontal scale 1: 6000. The use of a model facilitates experimental investigation into veracity of empirical relationships developed between fluvial parameters.

3.5.2 General Characteristics of the Brahmaputra river

The Brahmaputra river in Bangladesh is well suited for such a study because it possesses a highly dynamic fluvial environment. The river exhibits a widely varying discharge, easily eroded banks and highly mobile bed material consisting of medium to fine sand. As a result, the channel morphology responds quickly to fluvial processes and flow-morphology interactions can be observed over short periods. Details of the Brahmaputra river has been presented in the Appendix-I.

3.5.3 Scale Model Experiments

Table 3.4 represents condition for scale model experimental programme Phase-II

Table 3.4: DETAILS OF THE PHYSICAL MODEL EXPERIMENTS (EXPERIMENTAL PROGRAMME PHASE-II)

Model Run number	Over all model channel width	channel width of Prototype	Slope S_0 model	Water discharge Q Litre/ s (Model)	Sedime nt discharge, Q_s	Prototype discharge Q m^3/s	Running time of model Experiments
1	260 cm	15600 m	0.0025	1.4615 / 2.24 / 3 / 3.86 / 4.714 / 5.893	750 gm / min	24802.48 / 38014.06 / 50911.69 / 65506.37 / 79999.23 / 100007.5	0-1 / 1-2 / 2-3 / 3-4 / 4-5 / 5-5.5 / 5.5-6.5 / 6.5-7.5 / 7.5 -8.5 / 8.5-9.5 / 9.5-10.5
2	260 cm	15600 m	0.0025		455 gm / min		Total running time of Flume = 10.5 hrs
3	260 cm	15600 m	0.0025		550 gm / min		
4	260 cm	15600 m	0.0025		833 gm / min		
5	260 cm	15600 m	0.00255		354 gm / min		
6	260 cm	15600 m	0.002899		750 gm / min		
7	260 cm	15600 m	0.002536		450 gm / min		

Notes

- Widths are to be varied at different cross-sections, which have been taken according to horizontal scale 1:6000;
- Vertical scale is 1: 200 and 180 days time span has been considered from observed hydrograph to operate model experiments.
- For calculation of model size, average width of the stretch is to be considered as 15600 m.
- Prototype stretch is from Bahadurabad to Jammuna bridge site having a distance in between 83.2 km.
- Overall length will be considered for making model channel in the laboratory as 83200/6000 = 13.86 m.
- Discharge scale, $Q_r = 16970562.75$
- Roughness scale $n_r = 0.442$
- Velocity scale $V_r = 14.14$
- Slope scale $S_r = 0.03$
- Time scale $T_r = 424.264$

3.5.4 Physical Modelling Details

For simulation of the alluvial river in a model flume, a stretch of the Brahmaputra river in Bangladesh has been adopted as shown in the index plan in Fig 3.1. This stretch is confined between Bahadurabad ghat to Bangabandhu-Jamuna bridge site (Fig.3.2. X-Sections. B-B and C-C). Bangladesh Water Development Board has been measuring 14 cross-sections e.g. bed level profile every year in the lean period within the aforementioned stretch. Cross-sections are selected in such a way that each section is situated 6.4 km apart from the other. Stretch length of the study reach is $6.4 \text{ km} \times 13 = 83.2 \text{ km}$. Water discharge, water level and cross section data have been collected from BWDB for the year 1997 - 1998. It is seen that width of the river within the stretch varies around from 12 km to 16 km and depth ranges from 5 to 20 m during low flow at the time of hydrographic survey. For making model of this stretch, discharge = $24800 \text{ m}^3/\text{s}$, overall width = 15600 m, maximum depth (at low flow) = 20 m, and slope = 0.00008, have been considered according to the field data. The masonry flume of River Engineering Laboratory in WRDTC was used for the present model studies. The layout of the flume is shown in Fig 3.5.

Different sets of the scales, such as; 1 : 3000 H & 1 : 50 V, 1 : 3000 H & 1 : 150 V, 1 : 5000 H & 1 : 200 V, 1 : 6000 H & 1 : 300 V, 1 : 6000 H & 1 : 200 V were considered at the first instance of model design involving estimation of rugosity coefficient 'n'. It was seen that smaller horizontal scale and higher vertical scale gave bigger 'n' value like more than 0.07, with respect to the prototype 'n' value of .03 , which was selected from data supplied by the BWDB and experience of the organization Uttar

Pradesh Irrigation Research Institute (UPIRI). Finally 1 : 6000 H and 1 : 200 V model scale is adopted which gave the result of rugosity coefficient 'n' equal to 0.066 for the model study. This model is not geometrically similar. It has a vertical exaggeration of (VE =) 30. The materials used in model is sand having $d_{50} = 0.22$ mm, which did not give the required model roughness of $n=0.066$. So grasses were fixed in the slope and on the islands top and sides for simulating the roughness of models (Plates 3.6a and 3.6b). Downstream and upstream cross sections were constructed by masonry corresponding to the actual cross-section of prototype (Brahmaputra River). 14 cross-sections (Figs. 3.7 a, b, c & d) have been reproduced in the model by applying horizontal scale 1 : 6000 and vertical scale 1 : 200 . Each cross-section with sub channels was finished by putting small pegs according to the Reduced Level of the respected point in the cross-section line. In the lean period $U = 1.2$ m/s and the high flood $U= 3$ m/s is assumed in the prototype based on the available data. Discharge was measured by flow meter fixed in the system and these discharges were compared with the results obtained by the V - Notch fixed at downstream in the channel and whose C_d has been calibrated as 0.59. Water supply was given by 10 HP motor with 4 inch diameter centrifugal pump having 4 inch diameter suction and delivery pipes (Fig 3.5). Model readings are taken at eight transverse points across the cross-section. For the purpose of simulation of water levels in the model, the measured discharge and stages at section J#13.1(Section C-C), as mentioned in Fig. 3.2, of Bahadurabad of prototype is adopted as the reference for the study. The model was constructed by adopting cross-section data at different survey points and was proved through matching of observed field stage-discharge data at the upstream section J#13.1 of Bahadurabad as shown in Fig. 3.8,. and corresponding water level and stage-discharge

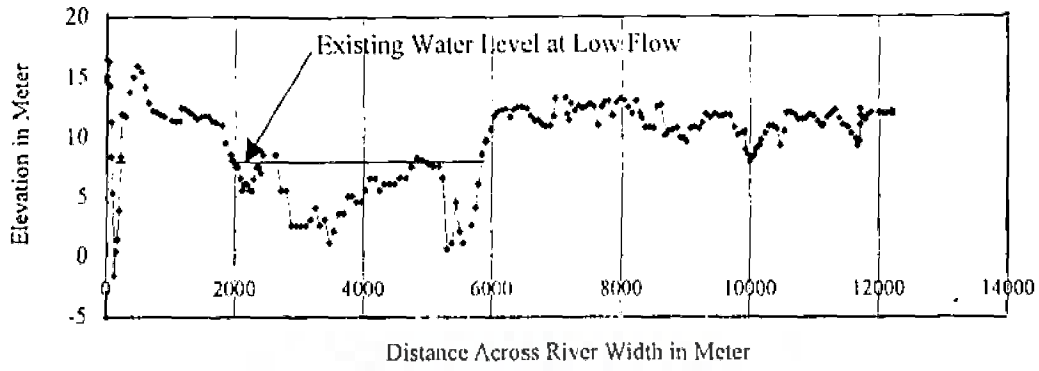


FIG. 3.7a (i): CROSS SECTION OF J# 7 AT JAMUNA BRIDGE SITE

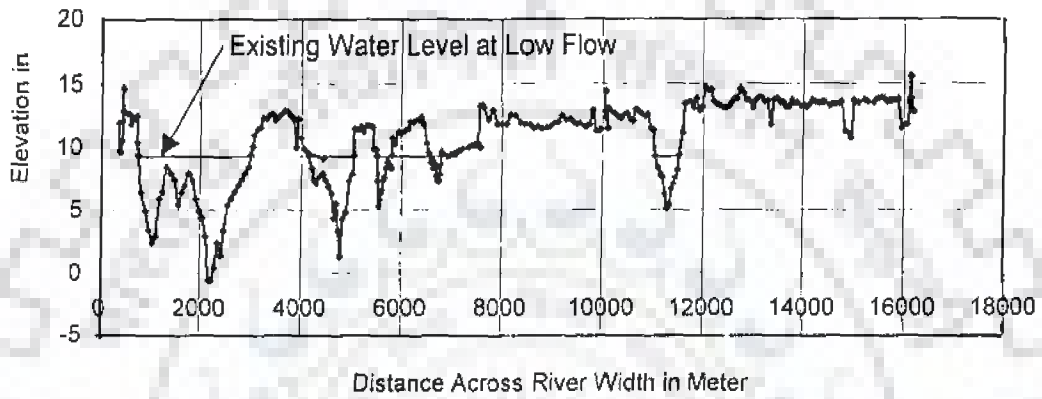


FIG.3.7a (ii): CROSS SECTION OF J# 7-1 OF THE BRAHMAPUTRA RIVER

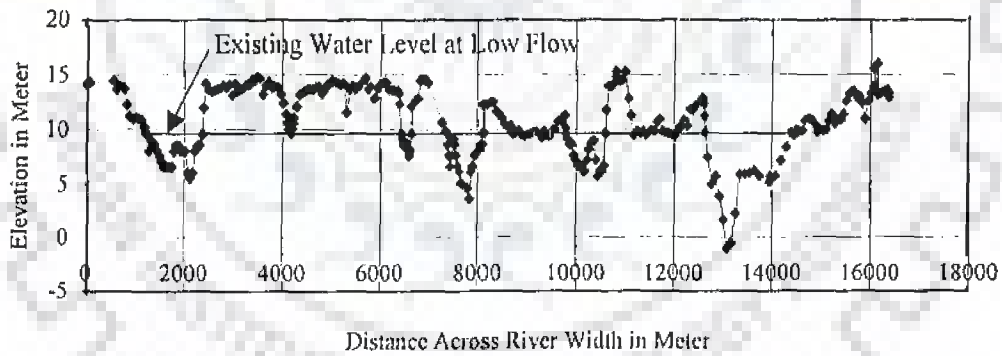


FIG.3.7 a (iii): CROSS SECTION OF J# 8 OF THE BRAHMAPUTRA RIVER

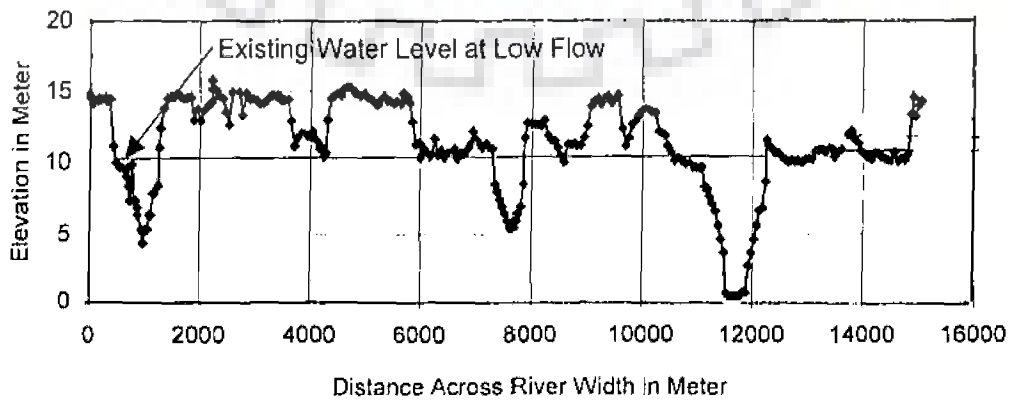


FIG.3.7 a (iv): CROSS SECTION OF J# 8-1 OF THE BRAHMAPUTRA RIVER

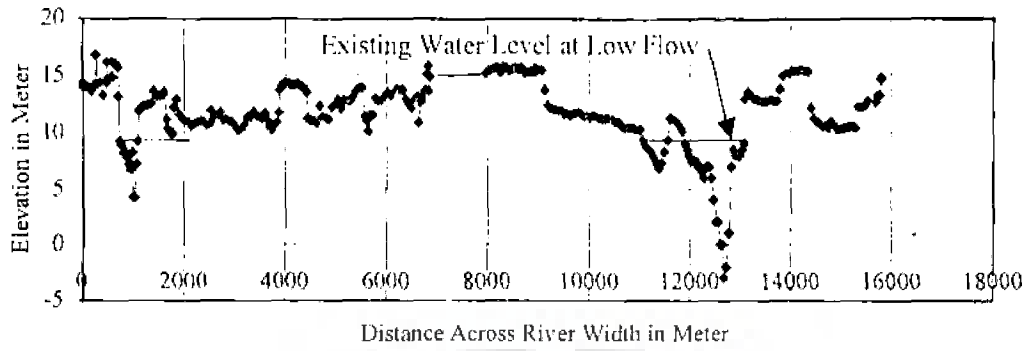


FIG. 3.7 b(i); CROSS SECTION OF J# 9 OF THE BRAHMAPUTRA RIVER

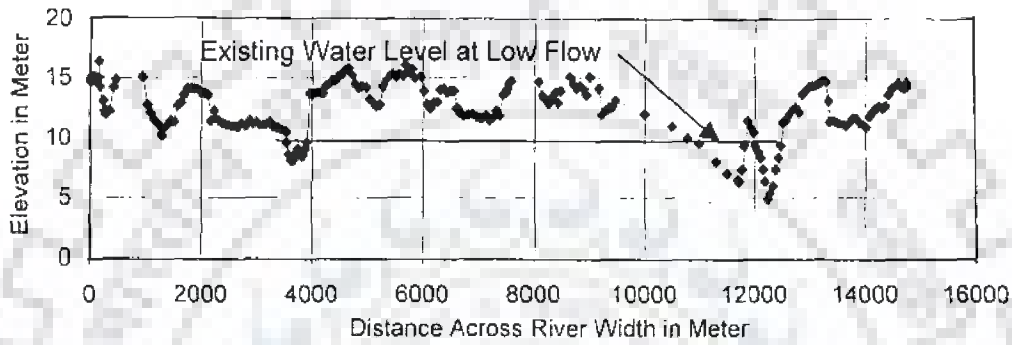


FIG. 3.7b(ii); CROSS SECTION OF at J# 9-1 OF THE BRAHMAPUTRA RIVER

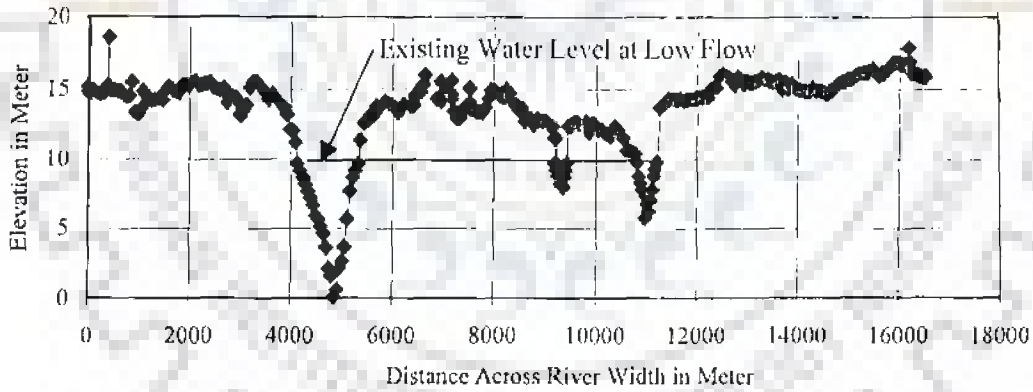


FIG. 3.7 b(iii); CROSS SECTION OF J# 10 OF THE BRAHMAPUTRA RIVER

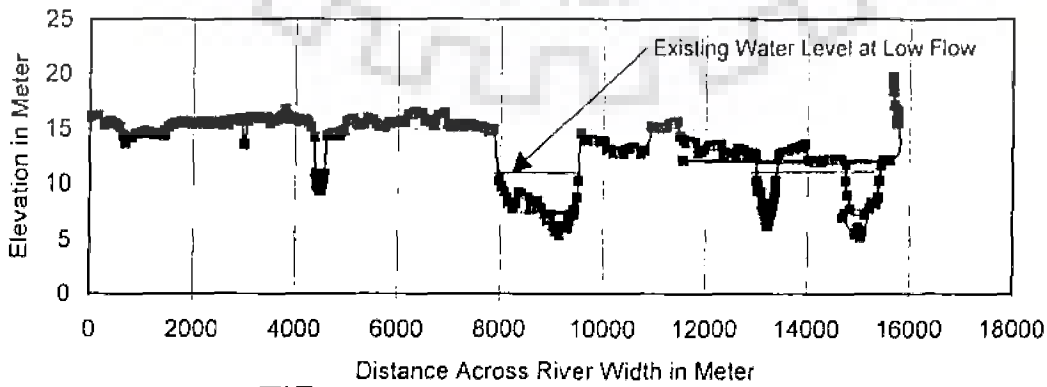
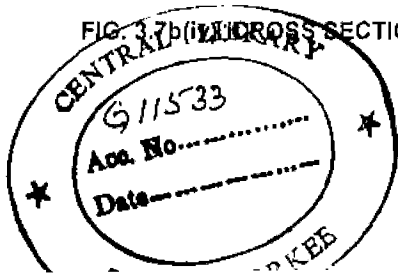


FIG. 3.7 b(iv); CROSS SECTION OF at J# 10-1 OF THE BRAHMAPUTRA RIVER



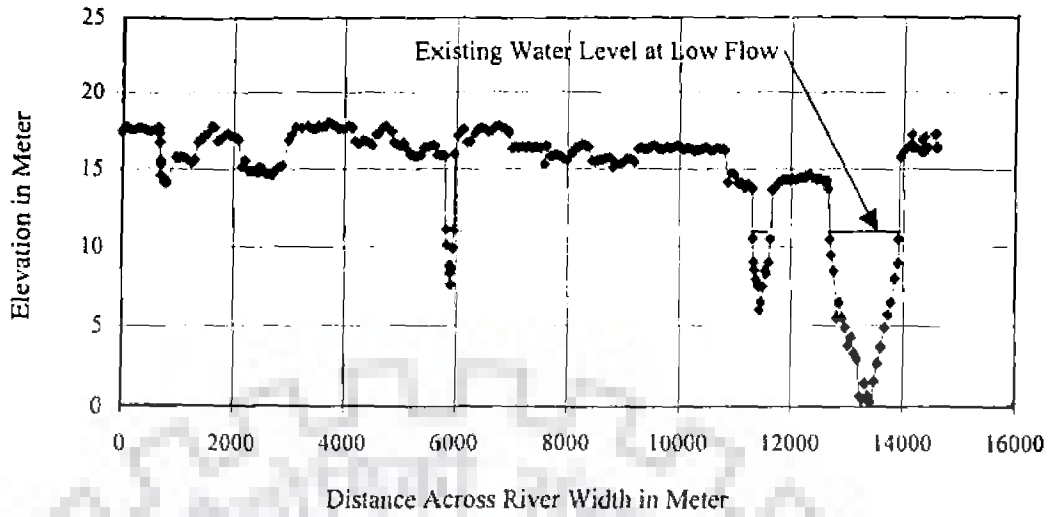


FIG. 3.7 c(i): CROSS SECTION OF J# 11 OF THE BRAHMAPUTRA RIVER

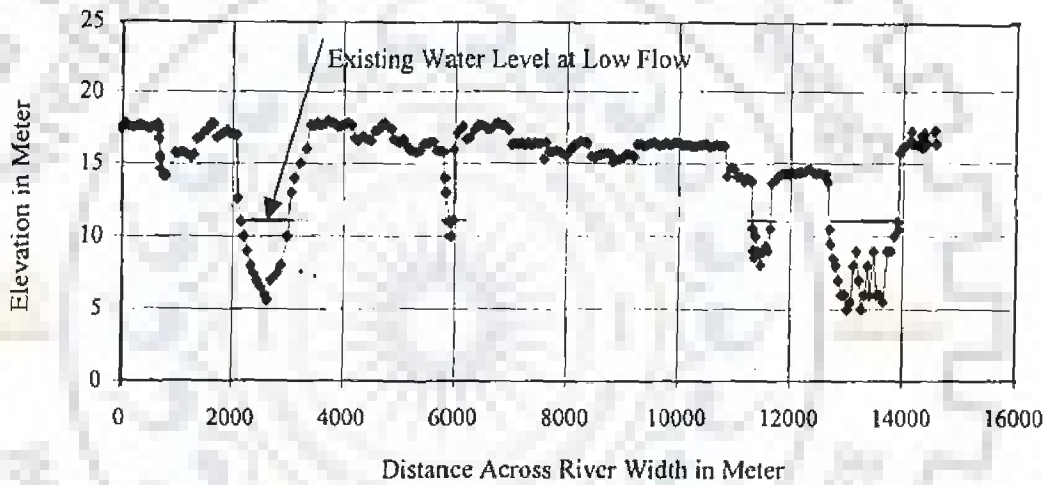


FIG. 3.7 c(ii): CROSS SECTION OF J# 11-1 OF THE BRAHMAPUTRA RIVER

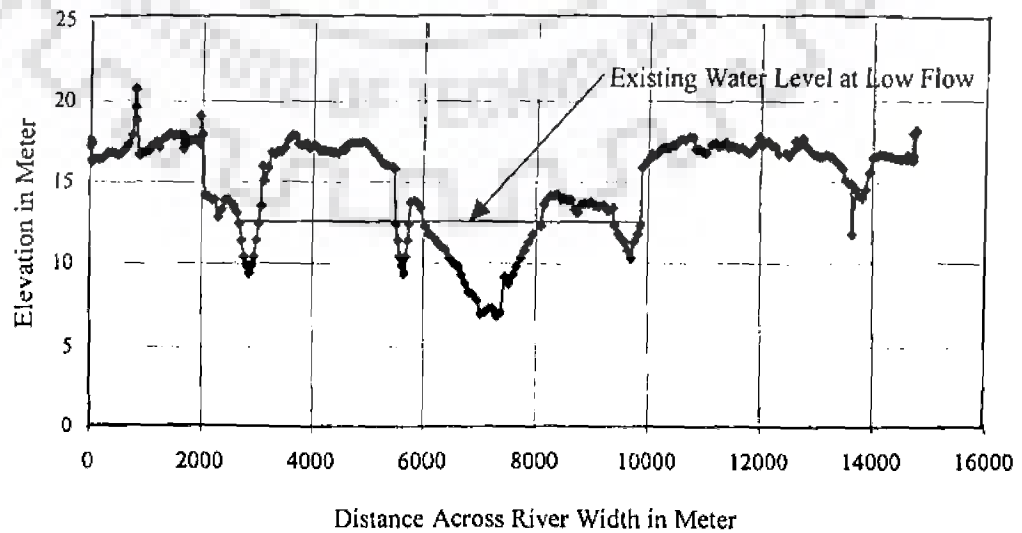


FIG. 3.7c(iii): CROSS SECTION OF J# 12 OF THE BRAHMAPUTRA RIVER

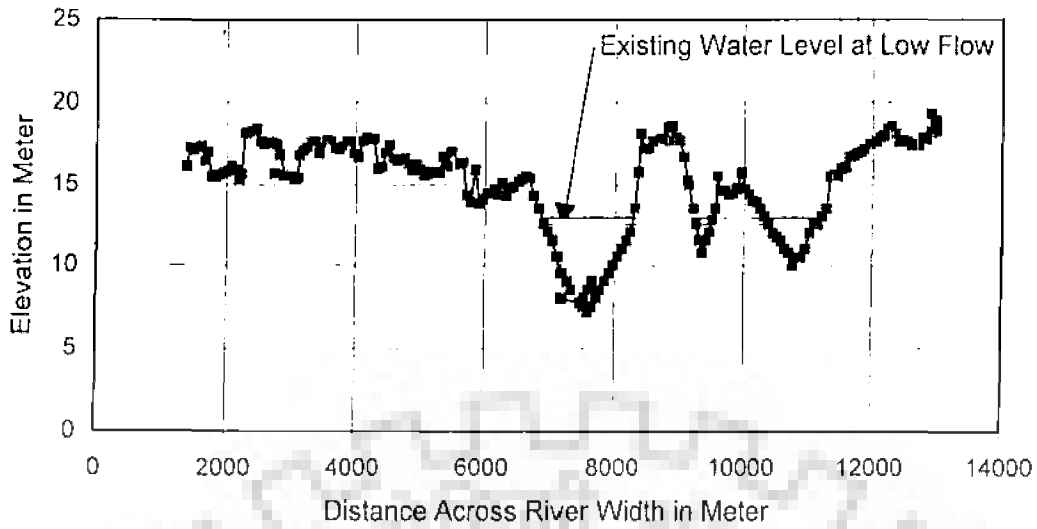
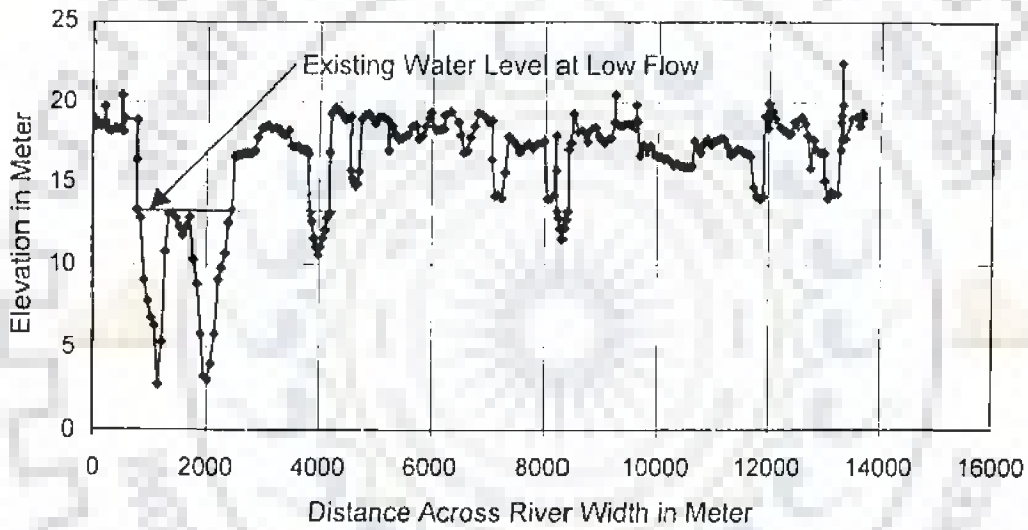


FIG. 3.7 d(i): CROSS SECTION OF J# 12-1 OF THE BRAHMAPUTRA RIVER



3.7 d(ii): CROSS SECTION OF J# 13 OF THE BRAHMAPUTRA RIVER

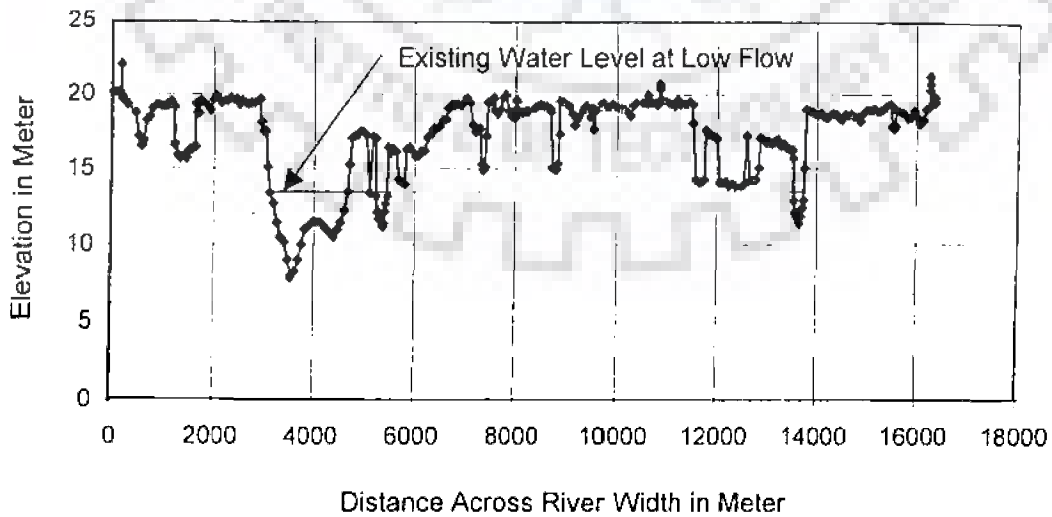


FIG. 3.7 d(iii): CROSS SECTION OF J# 13-1 OF THE BRAHMAPUTRA RIVER



Plate 3.6a: INITIAL PLAN FORM OF EXPERIMENTS OF MODEL BRAHMAPUTRA RIVER*



Plate 3.6b: SIMULATED PLAN FORM OF MODEL STUDIES OF THE BRAHMAPUTRA RIVER IN RUNNING CONDITON

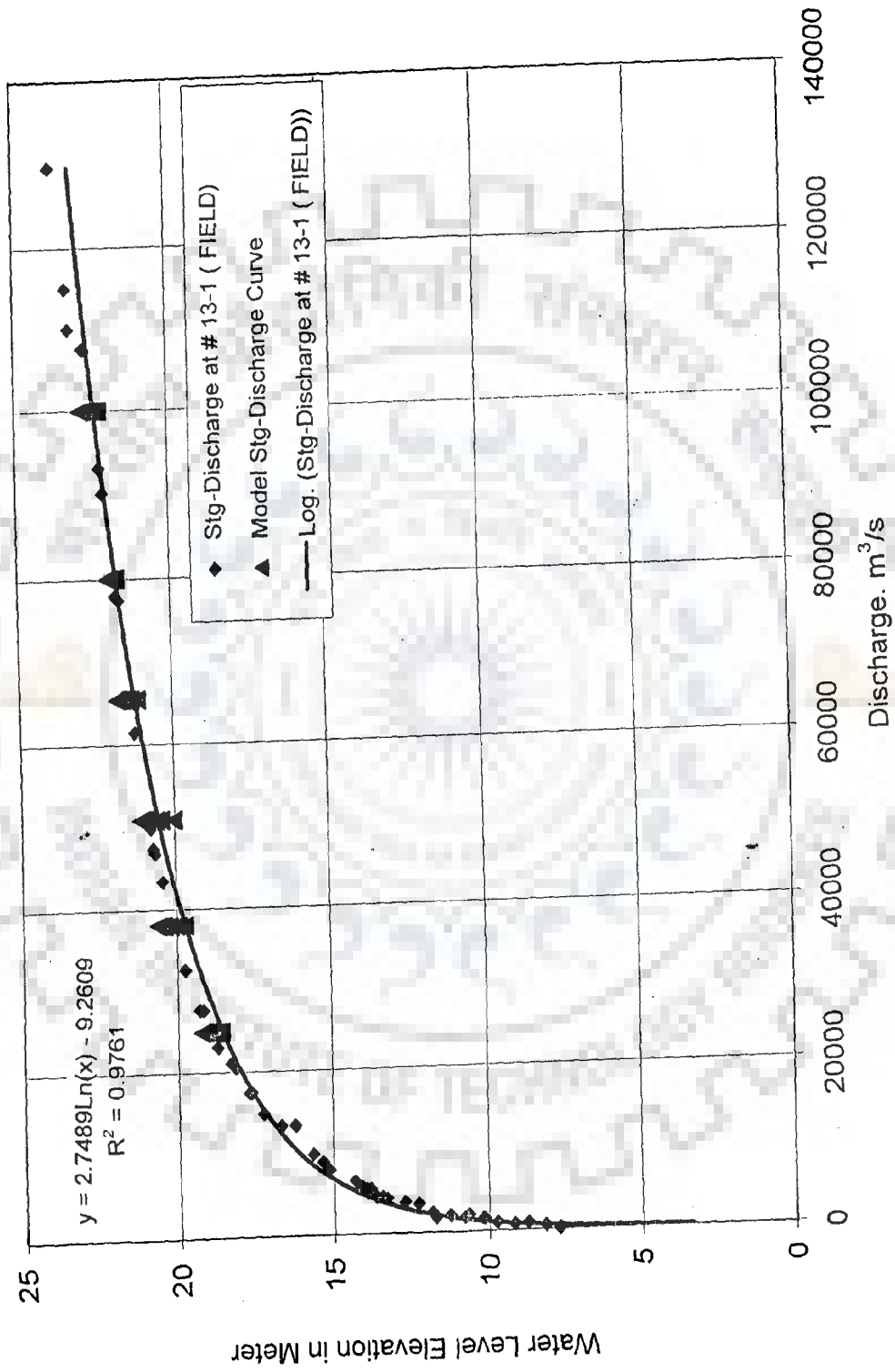


FIG. 3.8: STAGE-DISCHARGE CURVE AT J#13-1 (BAHADURABAD) BASED ON BOTH FIELD AND MODEL STUDY DATA

curve at downstream section J#7 near Jamuna Bridge site and approximate mid point section at J# 10 (Figs. 3.9a and 3.9b).

With the satisfactory accomplishment of the model-proving phase, seven experimental runs were conducted on the model with movable bed and bank, constructed with the model scales worked out earlier. The model experimental runs were operated by using a histogram of applied discharges, which is based on observed hydrograph of the Brahmaputra river at Bahadurabad ghat for 1997-98 (Fig. 3.10a and Fig. 3.10b). The above histogram was formulated by retaining the basic character of the observed hydrographic at Bahadurabad.

To cross-check the correctness of flow simulation in the model, the experimental stage-discharge curve at other three river sections like J#9, J#11 and J#12 were compared with the corresponding available field data. This comparison, as can be seen vide Figs. 3.11 (a, b & c) was found to be satisfactory.

Details of field data of study reach of the Brahmaputra River has been given in the Table A2.1 of Appendix-II. The bed materials grain size analysis of the Brahmaputra River has been shown in Fig. 3.12. Grain size analysis of bed materials of the laboratory flume experiment has been presented in the Fig 3.13a. and grain size analysis of transported materials collected, from the sediment collector, has shown in the Fig 3.13b.

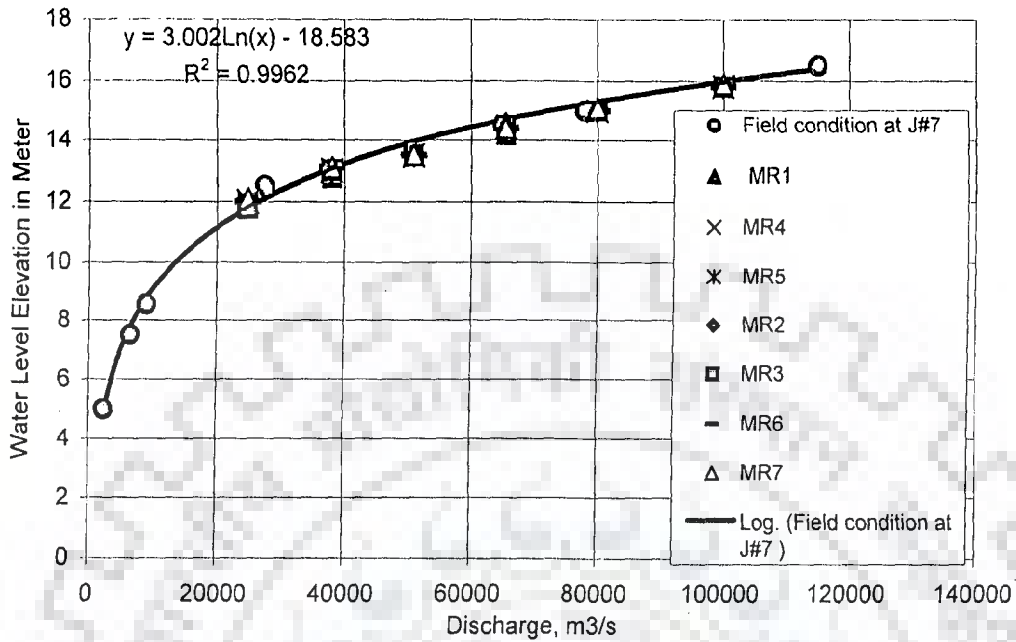


FIG. 3.9 a: STAGE- DISCHARGE CURVE AT SEC. j #7 BASED ON BOTH FIELD AND MODEL STUDY DATA

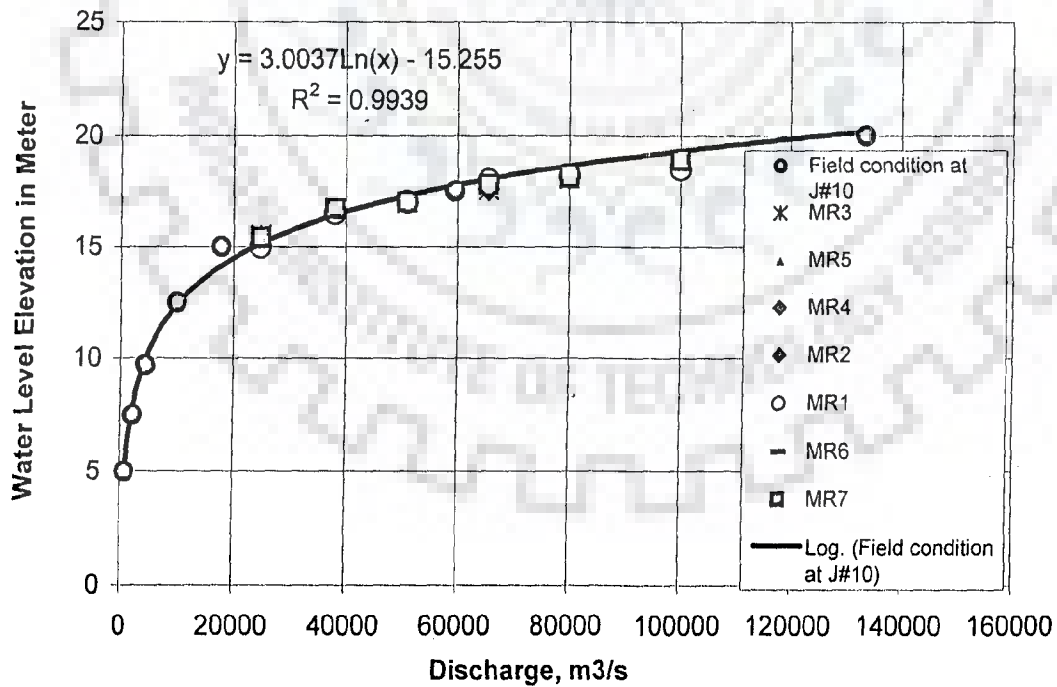


FIG. 3.9b: STAGE- DISCHARGE CURVE AT SEC. j #10 BASED ON BOTH FIELD AND MODEL STUDY DATA

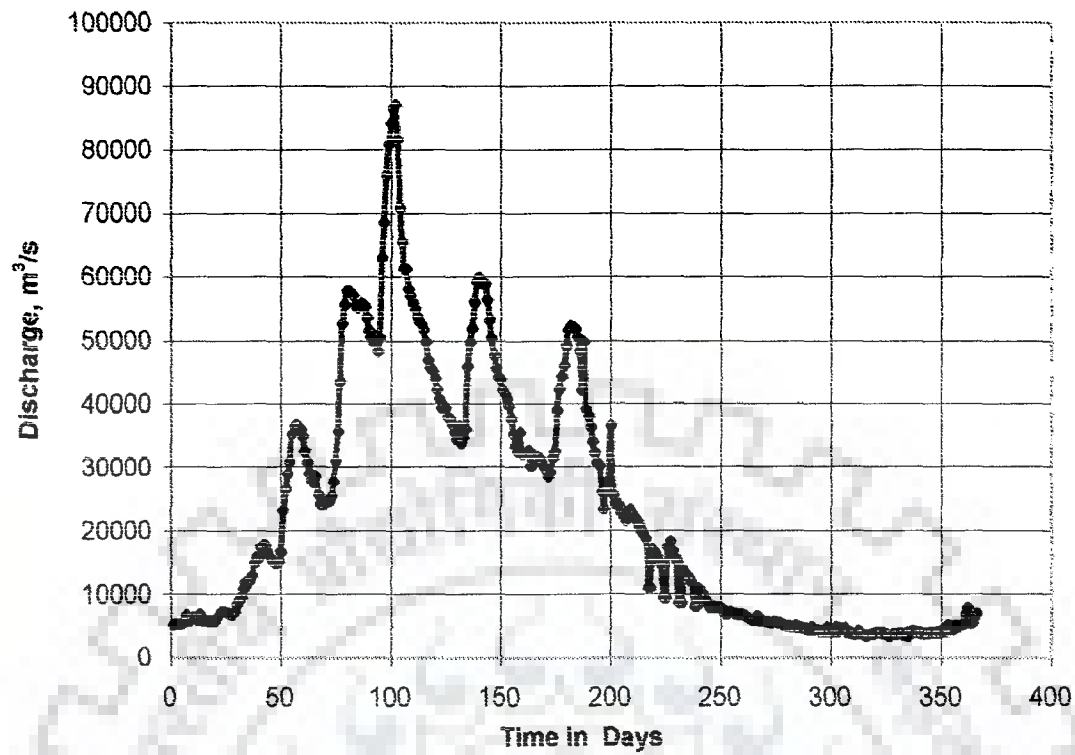


FIG. 3.10a DISCHARGE HYDROGRAPH OF 1997-98 AT BAHADURABAD GHAT TRANSIT

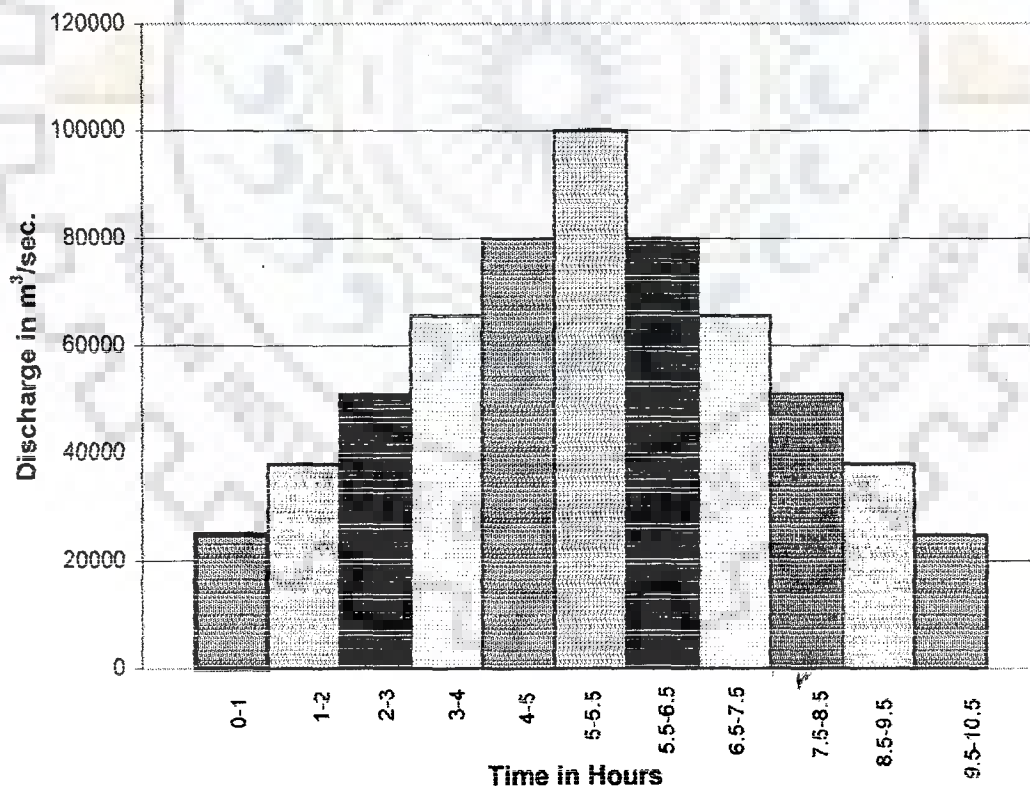


FIG. 3.10b HISTOGRAM OF APPLIED DISCHARGE FOR THE BRAHMAPUTRA MODEL STUDY

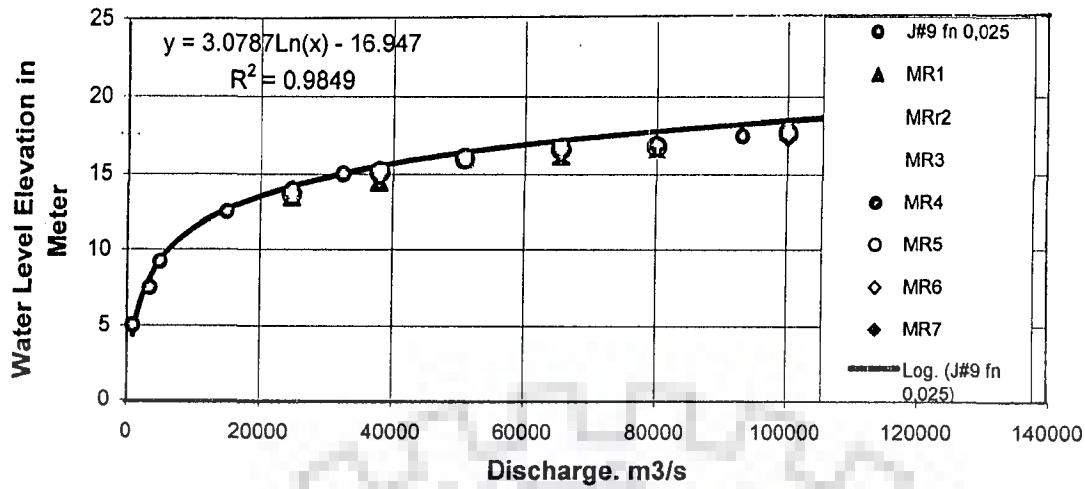


FIG. 3.11 a; STAGE- DISCHARGE CURVE AT SEC. j #9 BASED ON BOTH FIELD AND MODEL STUDY DATA

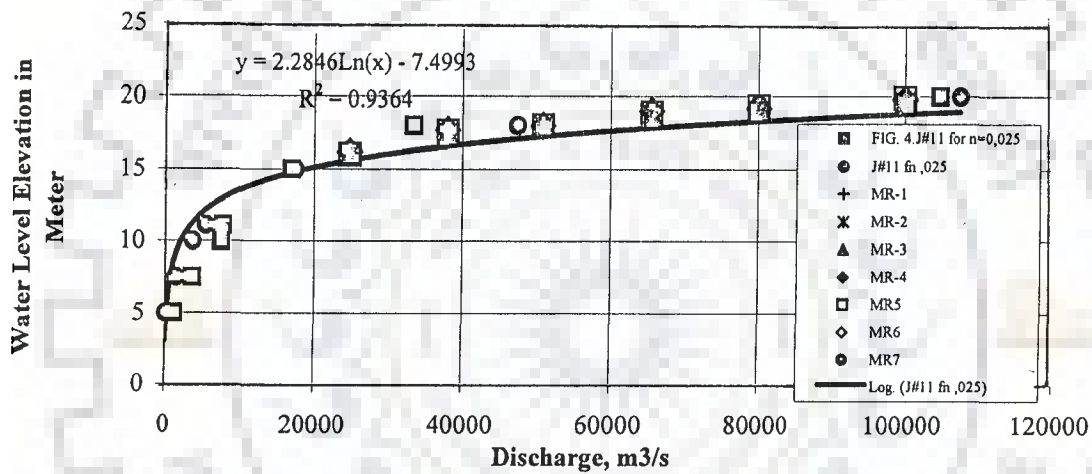


FIG. 3.11 b; STAGE- DISCHARGE CURVE AT SEC. j #11 BASED ON BOTH FIELD AND MODEL STUDY DATA

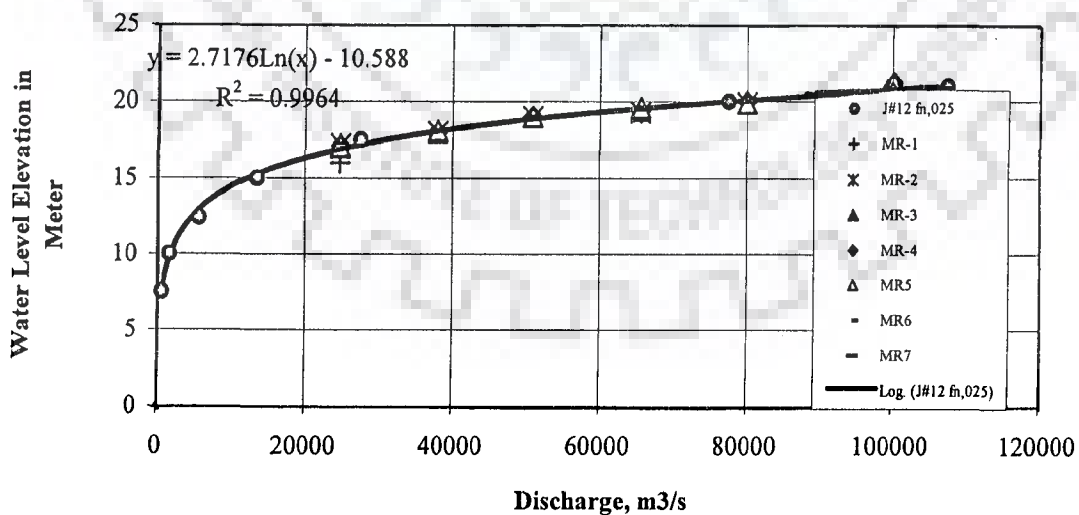


FIG. 3.11c; STAGE- DISCHARGE CURVE AT SEC. j #12 BASED ON BOTH FIELD AND MODEL STUDY DATA

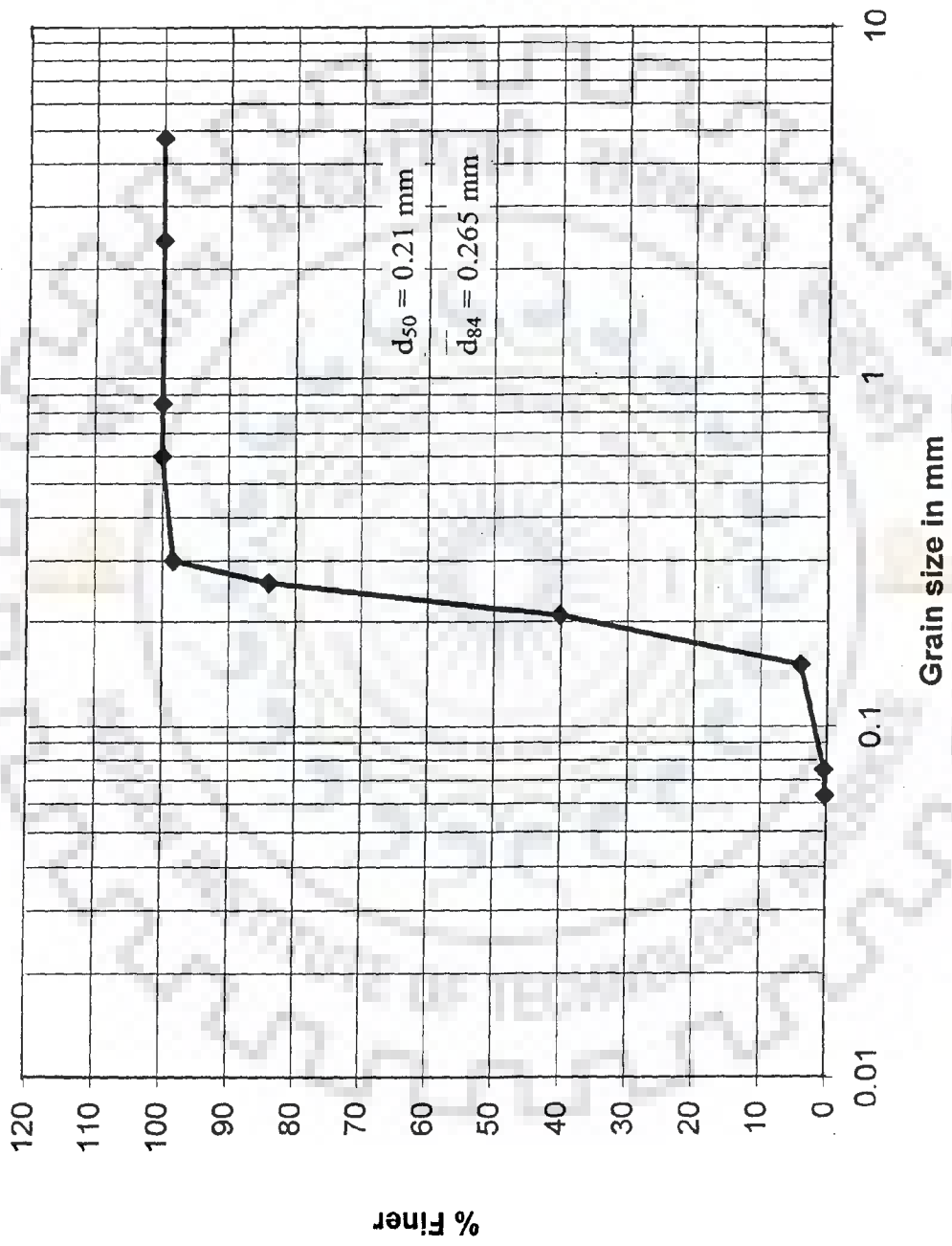


FIG. 3.12: GRAIN SIZE ANALYSIS OF BED MATERIALS OF THE BRAHMAPUTRA RIVER

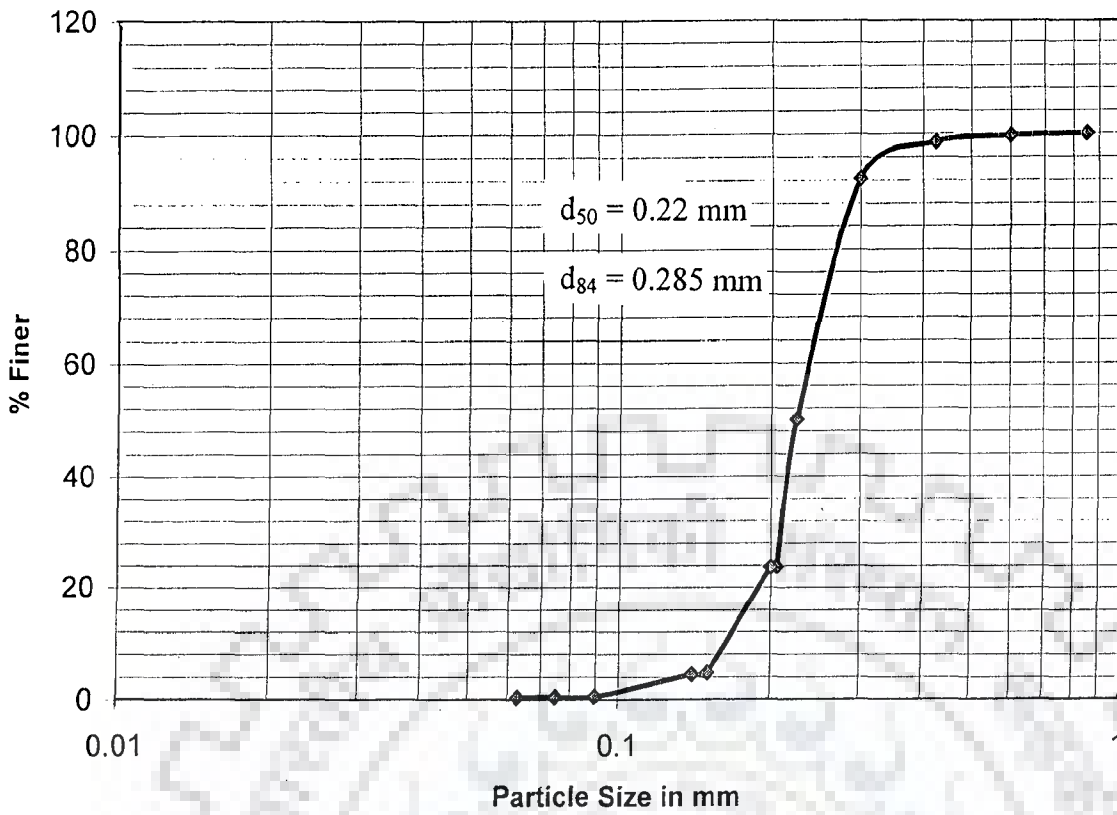


FIG. 3.13a: GRAIN SIZE ANALYSIS OF THE LABORATORY CHANNEL BED MATERIALS

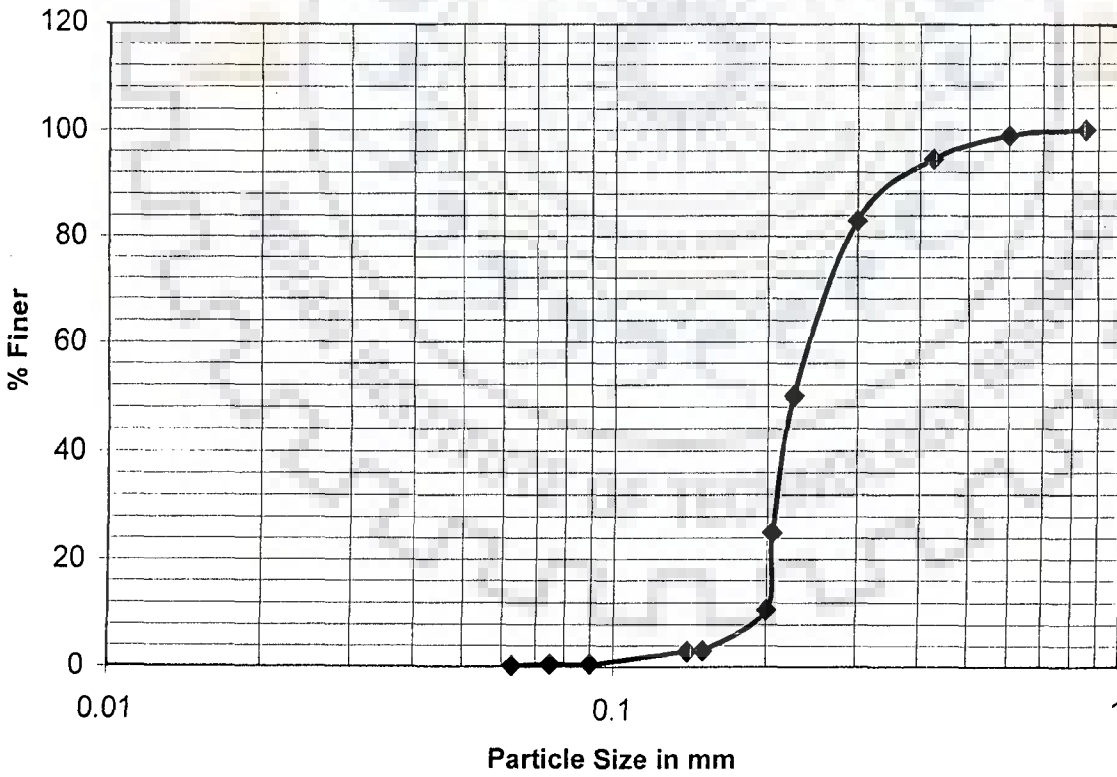


FIG. 3.13b: GRAIN SIZE ANALYSIS OF TRANSPORTED MATERIALS IN THE LABORATORY CHANNEL

3.6 DESIGN AND CONSTRUCTION OF EXPERIMENTAL SET-UP

To conduct the planform changes or similar experiments of a model of large braided river, different sets of data have been collected from the field. It is seen that width of the river varies around from 5 km to 16 km and depth of flow varies from 5m to 50 m at bankfull stage. In the River Engineering Laboratory, WRDTC 25 m x 5 m space was available for construction of a flume for experimental research purpose. Considering the collected field data and available space 22.5 m long including upstream stilling basin and downstream small sump, 2.6 m wide flume river has been constructed, where depth of flume has given 1.4 m high. Now this flume river can easily represents any large alluvial river in the world by providing some horizontal and vertical scale. Fig.3.5 shows the schematic diagram of the experimental set-up (Laboratory Flume). Brief design and construction procedure of the experimental set-up has been given in the Appendix-III and different measuring instruments have been described shortly in the Appendix-IV.

3.7 GENERAL OBSERVATIONS ON THE LABORATORY EXPERIMENTS

In the laboratory experimental study it is seen that when initial channel is straight and direction of flow is along the channel centre line, there were no bar or *char* formation in the down stream zone of the channel, even after 36 hours.

The longitudinal profile of run 43 has been shown in Fig 3.14. It is seen that longitudinal profile were changing with running hours depend upon the sediment movement from upstream to downstream. When initial flow direction at the upstream is kept at an angle between 20° to 60° , it causes secondary circulation that leads to first

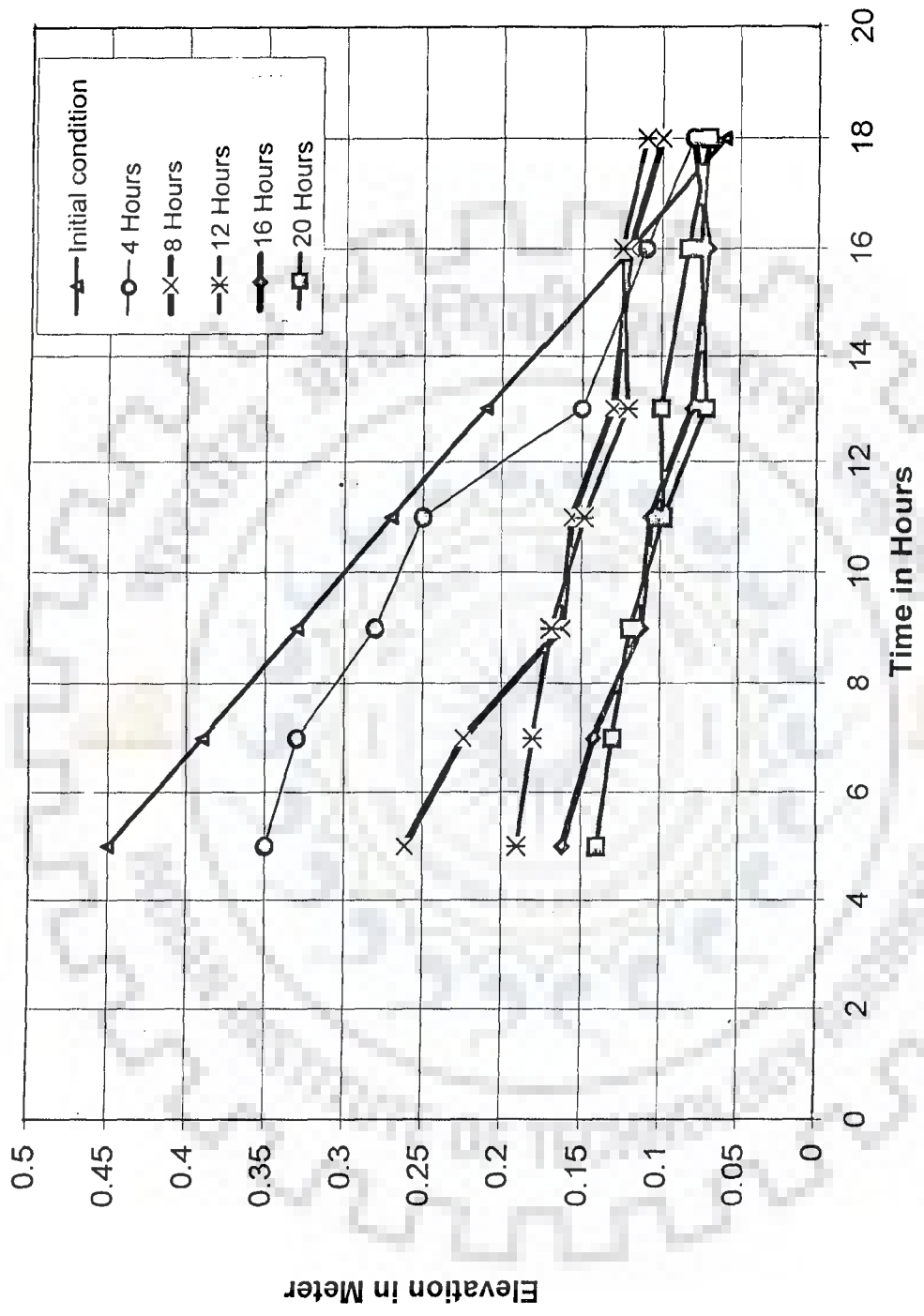


FIG. 3.14 LONGITUDINAL PROFILE OF RUN NO.43 AT DIFFERENT RUNNING TIME

formation of meandering planform, erosion of bank and bed materials and subsequently results in bar formation or braiding condition along the down stream zone. This condition is shown in the Fig. 3.15 a (iii) of experimental run 43. Channel slope weilds a significant influence on braid bar formation in any water course. When slope is more, braiding condition occurred relatively quickly. Without sediment feeding in the channel, braiding was occurring slowly. According to Parker (1976) $Q_s/Q = C_s$, is an important parameter that had influence in the braid bar formation in the channel centre. If sediment concentration is high by feeding sediment at the up stream, formation of multiple channel pattern could be induced along the down stream zone as depicted in Fig. 3.15 b (ii) SEC. 11-16 m zone.

When initial channel planform is given a sinuosity ranging from 1.05 to 1.10 with the initial flow direction being kept straight, then due to initial generation of transverse currents resulting in creation of strong secondary circulation. This exacerbates the meandering phenomenon and by the process the channel ends up in creation of braiding with multiple flow channel configuration and bar formation.

Due to variation and fluctuation of water discharge with constant sediment feeding at the upper end of the flume, bars and islands have formed at the down stream zone as shown in the Appendix-II (Plate A2.12 of Run- 59).

Sometimes local shoaling of thalweg and reverse eddy appeared, which caused deposition and braiding in the channel. The braiding condition occurred mostly when channel widened to the utmost and flow depth became low resulting in emergence of bars above water level along channel centre in the downstream zone as shown in the Figs. 3.15b (IV) and 3.15b (V). It may be noted that Fig 3.15a and 3.15b depict the temporal

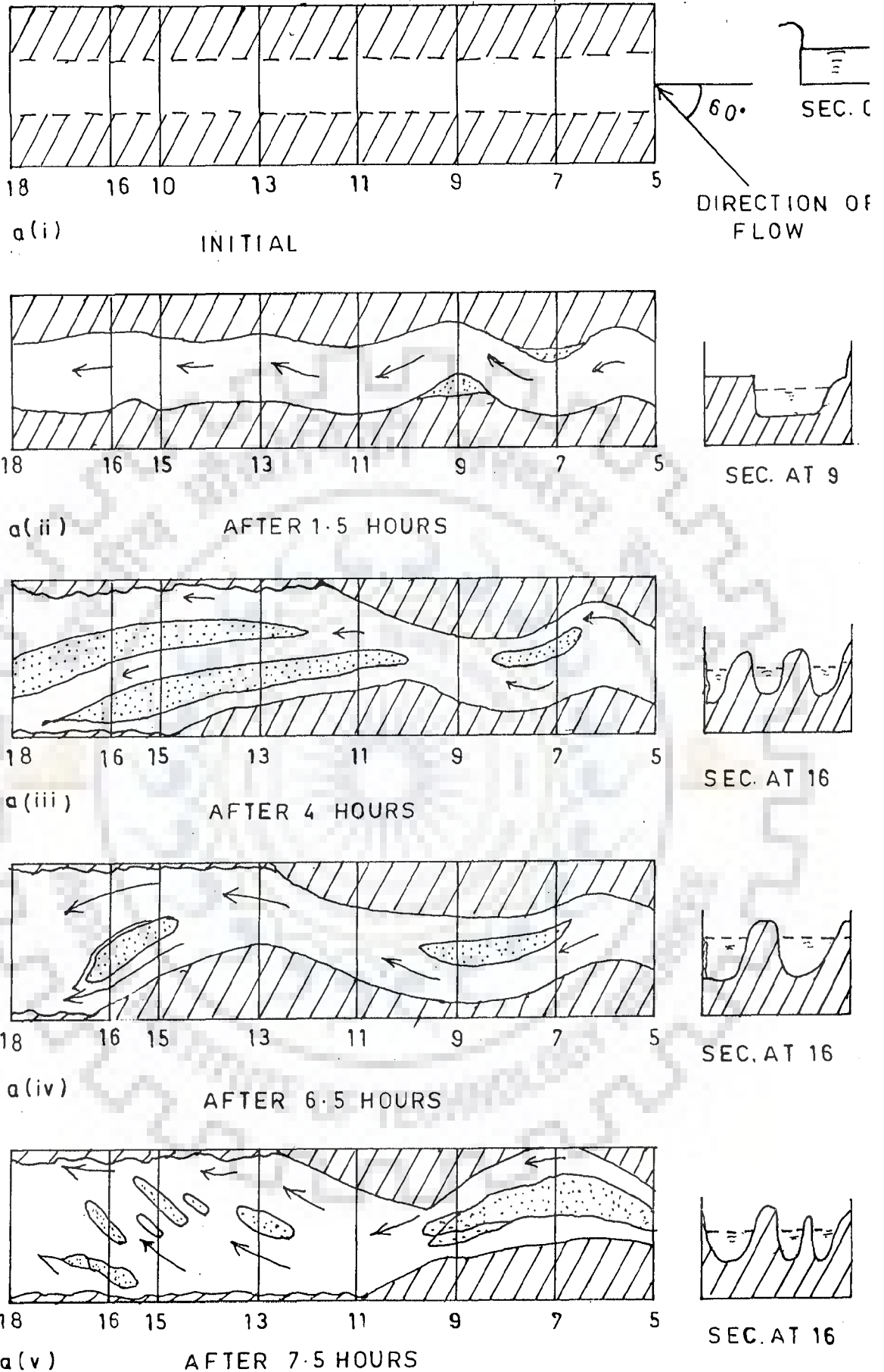


FIG. 3.15 a: SKETCHES AND CROSS SECTION SHOWING PROGRESS IN DEVELOPMENT OF BRAID IN THE LABORATORY EXPERIMENTAL RUN No. 43

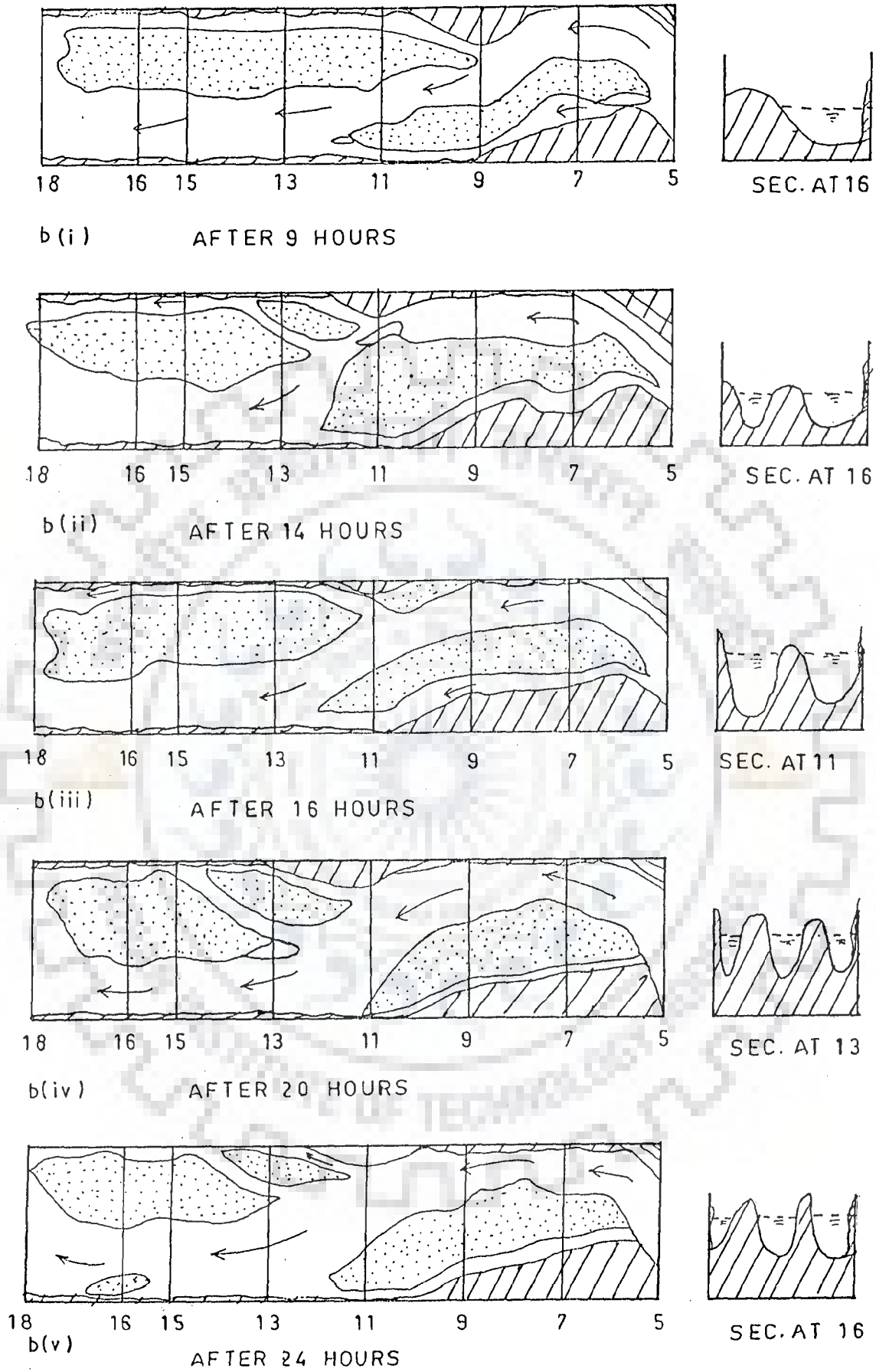


FIG. 3.15 b: SKETCHES AND CROSS SECTION SHOWING PROGRESS IN DEVELOPMENT OF BRAID IN THE LABORATORY EXPERIMENTAL RUN No. 43

and spatial changes of the flume bed during the experimental run number 43 for Phase-I, which are shown herein as example of the general behaviour.

During execution of the laboratory experiments of Phase-I and Phase-II, all data regarding this research work have been measured in a systematic manner and record-keeping. Detail data of run 43 has been given in the Table A2.2 of Appendix II. The sample data of experimental study phase-I have been presented in the Table A2.3 of Appendix II. The data of model experimental study Phase-II have been presented in the Table A2.4 of Appendix-II.

Photographs of different laboratory experimental runs (Phase-I) with different categories have been shown in Plate A2.1 to A2.12 of Appendix-II.

3.8 VARIATION OF SINUOSITY WITH RUNNING TIME AND SLOPE OF CHANNEL

Variation of sinuosity during processing of experimental data was investigated with the help of graphical plots to study this aspect as can be seen in Figs.3.16(a,b) and 3.17(a,b). Fig. 3.18 represents the variation of channel sinuosity with slope and this variation is similar to that suggested by Schumm and Khan (1972).

3.9 SUMMARY

Details of the experiments conducted in the study are given in this chapter. The data are also presented in the Appendix-II. Variation of sinuosity with time during certain experiments is shown in Figs.3.16 and 3.17. Fig. 3.18 represents the variation of channel sinuosity with channel slope, similar to those reported in the literature.

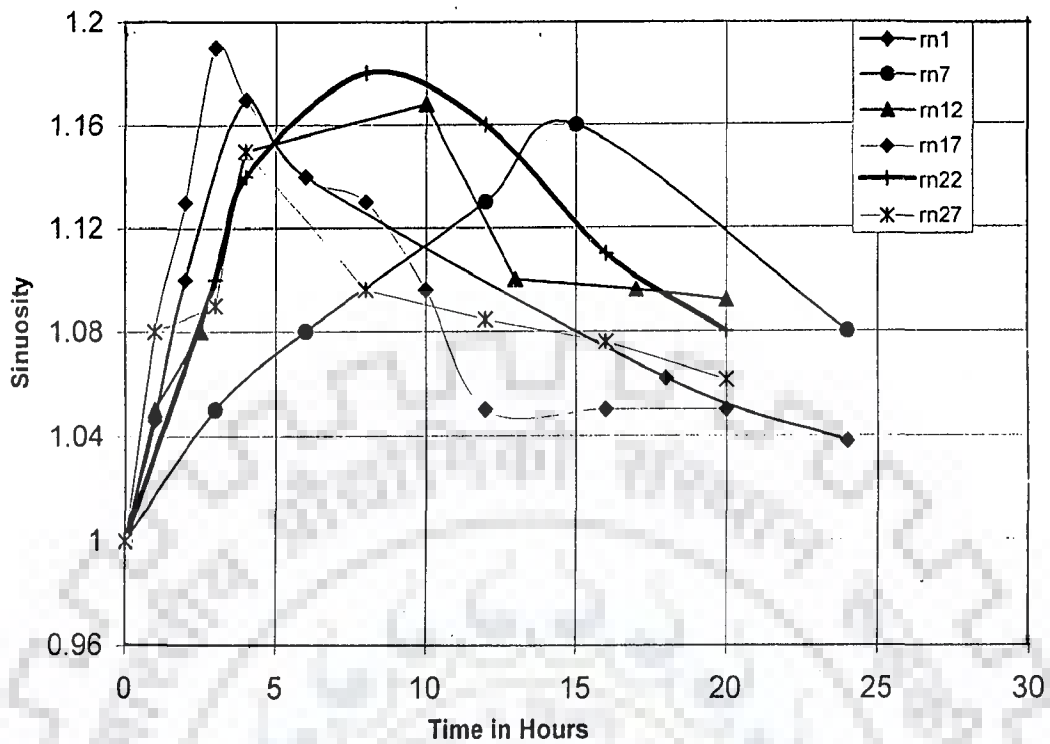


FIG. 3.16 a; SHOWING SINUOSITY VERSUS RUNNING TIME FOR NON-SEDIMENT FEEDING CONDITION WITH OBLIQUE FLOW AT AN ANGLE=40°

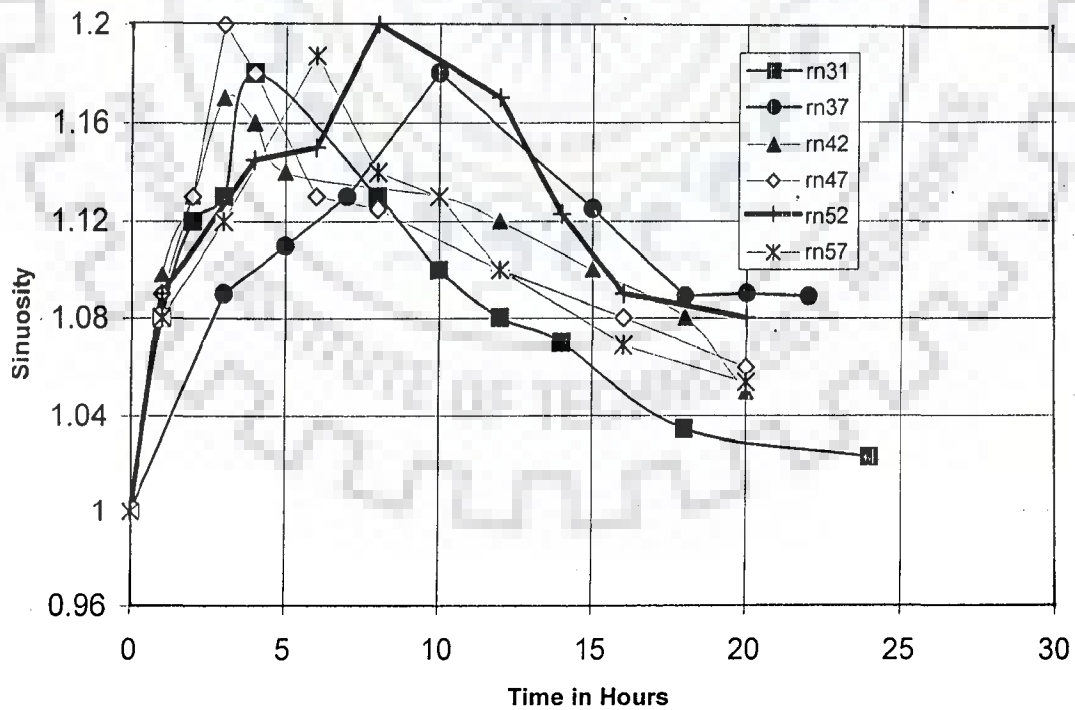


FIG. 3.16 b; SHOWING SINUOSITY VERSUS RUNNING TIME FOR SEDIMENT FEEDING CONDITION WITH OBLIQUE FLOW AT AN ANGLE=40°

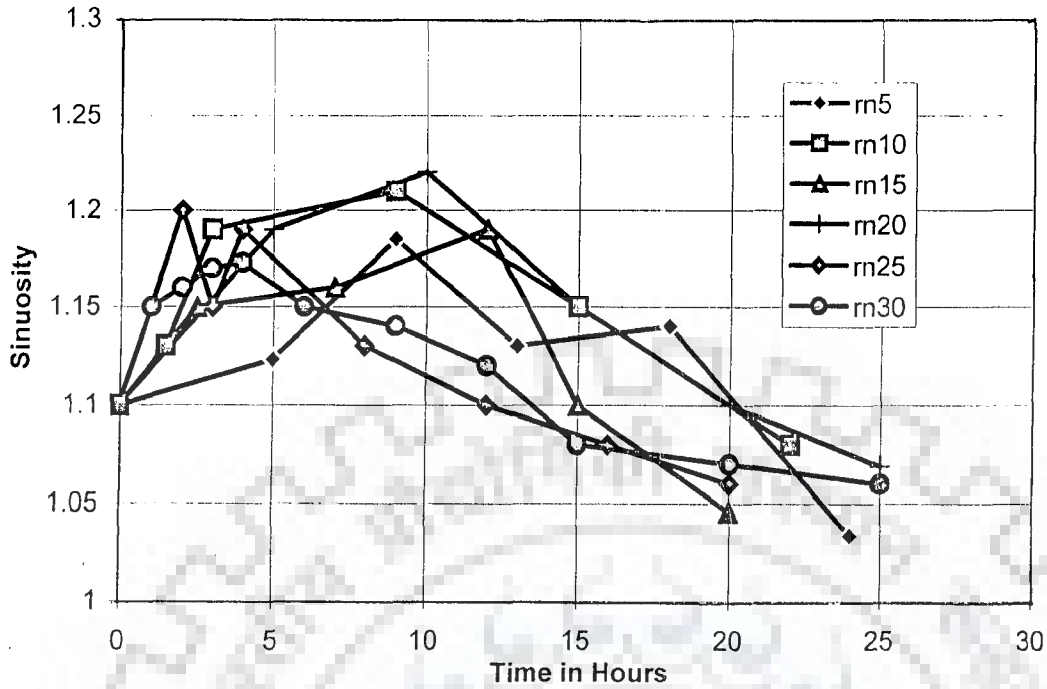


FIG. 3.17a: SHOWING SINUOSITY VERSUS RUNNING TIME FOR OBLIQUE FLOW = 0° WITH NON-SEDIMENT FEEDING CONDITION AND INITIAL SINUOSITY = 1.10

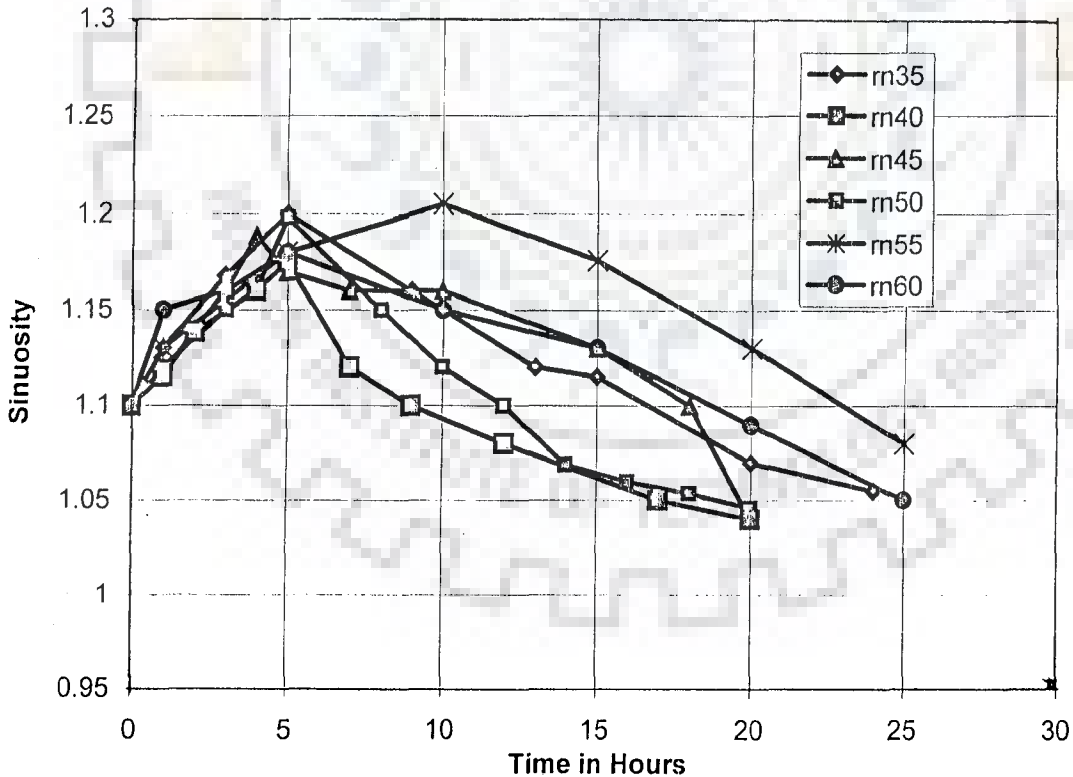


FIG. 3.17b: SHOWING SINUOSITY VERSUS EXPERIMENTAL RUNNING TIME FOR INITIAL SINUOSITY = 1.10 AND OF = 0° WITH SEDIMENT FEEDING CONDITION

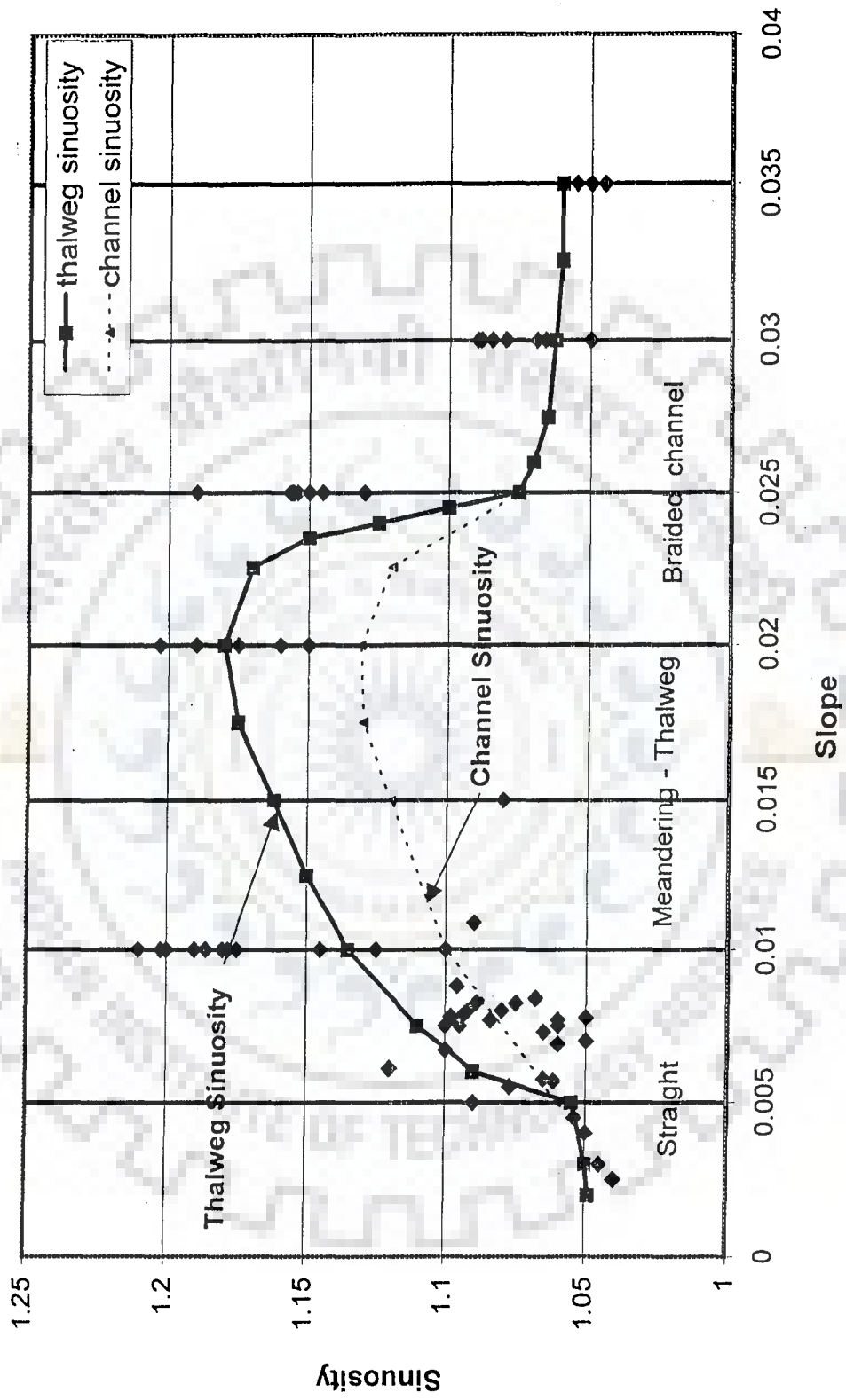


FIG. 3.18: PLOT OF SINUOSITY AGAINST SLOPE OF CHANNEL FOR LABORATORY EXPERIMENTAL DATA OF SEDIMENT FEEDING CONDITION

BRAIDING INDICATORS

4.1 GENERAL

The braiding indicators have been used for quantitative description of braiding phenomenon. Many times these have been used to assess the extent or severity of braiding in a stream. It is well recognised that bed topography and planform geometry is the result of complex interaction of fluid flow with the channel boundaries and sediment transport. The secondary flow component also contributes to the growth of channel deformations (Bathurst et al., 1979). For an unstable channel, the channel deformation dictates whether the channel will meander or braid. To model the channel deformations in an unstable state is not simple and investigators have preferred to use braiding indicators as a means of studying the braiding characteristics of the alluvial streams. In this chapter, different types of braiding indicators are analysed. Later on using the data from the Brahmaputra river in Bangladesh in conjunction with data of laboratory experimental runs conducted in the present study, the braiding indicators i.e. indices are evaluated. A comparison also has been made with the values of these indicators reported by other investigators in case of different alluvial rivers.

4.2 EXISTING BRAIDING INDICATORS

Several studies have presented discrimination between straight, meandering and braided streams on the basis of discharge and channel slope. Lane (1957) suggested the following criterion for the occurrence of braiding

$$S > 0.004 (Q_m)^{-0.25} \quad (4.1)$$

in eq. (4.1) Q_m = mean annual discharge; and S = channel slope.

Using bankfull discharge Q_b , Leopold and Wolman in 1957 (Richards, 1982) proposed a relationship for braiding to occur, which also predicts braids at higher slopes and discharges.

$$S > 0.013 Q_b^{-0.44} \quad (4.2)$$

in eq. (4.2) Q_b = bankfull discharge.

Leopold and Wolman (1957) also indicated that braided and meandering streams can be separated by the relationship

$$S = 0.06 Q^{-0.44} \quad (4.3)$$

in eq. (4.3) S = channel ; and Q = water discharge. Thus, for the streams they studied, higher slopes for given discharges tend to favour braided pattern rather than meandering.

Antropovskiy (1972) developed the following criterion for the occurrence of braiding

$$S > 1.4 Q_b^{-1} \quad (4.4)$$

in eq. (4.4) S = channel slope; and Q_b = bank for full discharge.

However, these indicators have been criticised by Schumm and Khan (1972) as none of these recognizes the importance of sediment transport. These results imply a higher power expenditure rate in braided streams, a conclusion reinforced by Schumm and Khan's (1972) flume experiments. However, none of these investigators recognises the control of channel pattern by sedimentology. Since bed material transport and bar formation is necessary in both meander and braid development processes, the threshold between the patterns should relate to bedload calibre.

Henderson (1961) re-analysed Leopold and Wolman's data to derive an expression including d_{50} , median grain size (mm).

$$S > 0.002 d_{50}^{1.15} Q_b^{-0.46} \quad (4.5)$$

in eq. 4.5 d_{50} = median grain size; and Q_b = bankfull discharge.

According to equation (4.5), a higher threshold slope is necessary for braiding in coarse bed materials. Bank material resistance affects rate of channel migration and should also influence the threshold, although its effect may be difficult to quantify and also be non linear since greater stream power is required to erode clays and cobbles than sands.

Parker's stability analysis (1976) indirectly illustrates the effects of bank material resistance by defining the meander - braid threshold as

$$S/F_r = D/B \quad (4.6)$$

in eq. (4.6), D = mean depth of the flow; B = width of the stream, and F_r = Froude number. However, depth, width and Froude number may be expressed in terms of discharge and bank silty-clay percentage, as suggested by Schumm (Richards, 1982).

Meandering occurs for $S/F_r \leq D/B$ and braiding occurs for $S/F_r \geq D/B$, and transition occurs in between $S/F_r \sim D/B$.

Ferguson (1981) suggested for braiding to occur, which predicts steeper threshold slopes for braiding in channels with resistant silty banks.

$$S > 0.0028 (Q_b)^{-0.34} B_c^{0.90} \quad (4.7)$$

In eq. (4.7) B_c = percentage of silty clay content in the bank material.

Measures of the degree of braiding generally fall into two categories: (i) the mean number of active channels or braid bars per transects across the channel belt; and (ii) the ratio of sum of channel lengths in a reach to a measure of reach length (total sinuosity).

The sinuosity, P_c is thalweg length / valley length.

Smith (1970) illustrated the measurement of cross - section bed relief, measured by the index.

$$BRI = \frac{2[(T_1+T_2+\dots+T_n)-(t_1+t_2+t_3+\dots+t_n)] \pm T_{e1}, T_{e2}}{B_L} \quad (4.8)$$

in eq. (4.8) T_i = height maxima between hollows; t_i = minima between peaks.; B_L = transect length; and T_e = end heights.

Miall (1977) also suggested Table -4.1 for the classification of channel patterns.

Different types of indices have been given in the Table-4.2

Table 4.1: CLASSIFICATION OF RIVER TYPES (MIALL, 1977)

Type	Morphology	Sinuosity	Load type	Bed load percent (of total load)	Width/depth ratio	Erosive behaviour	Depositional behaviour
Meandering	Single channels	> 1.3	Suspension or Mixed load	< 11	< 40	Channel incision, meander widening	Point-bar formation
Braided	Two or more channels with bars and small islands	< 1.3	Bed load	> 11	> 40	Channel widening	Channel aggradation mid-channel bar formation
Straight	Single channel with pools and riffles, meandering thalweg	< 1.5	Suspension, mixed or bedload	< 11	< 40	Minor channel widening and incision	Side channel bar formation
Anastomosing	Two or more channels with large, stable islands	> 2.0	Suspension load	< 3	< 10	Slow meander widening	Slow bank accretion

Table-4.2 DIFFERENT TYPES OF INDICES

Brice (1960, 1964)	Braiding Index = $\frac{2(\text{Sum of lengths of bars or islands in a reach})}{\text{Centre line reach length}}$
Howard, Keetch and Vincent (1970)	Average number anabranches bisected by several transects perpendicular to flow direction
Engelund and Skovgaard (1973), Parker (1976), Fuzita (1989)	Mode = Number of rows of alternate bars (and sinuous flow paths) = 2 times the number of braid bars and number of side (points) bars per transect.
Rust (1978a)	Number of braids per mean curved channel wave length = mode - 1
Hong and Davies (1979)	Total sinuosity = $\frac{\text{Length of channel segments}}{\text{Channel belt length}}$ Number of braids or channels in cross -section
Mosley (1981)	Braiding index = $\frac{\text{Total length of bankful channels}}{\text{Distance along main channel}}$
Richards (1982) Robertson - Rintoul and Richardes (1993)	Total sinuosity = $\frac{\text{Total active channel lenth}}{\text{Valley length}}$
Ashmore (1991a)	Mean number of active channels per transect Mean number of active channel links in braided network
Friend and Sinha (Best and Bristow, 1993)	Braid channel ratio = $\frac{\text{Sum of mid - channel lengths of all channels in reach}}{\text{Length of mid - line of widest channel}}$

Howard et al. (1970) proposed three different topological indices namely alpha (α) index, beta (β) index, and gamma (γ) index

$$\text{Alpha } (\alpha) \text{ Index} = \frac{t-(n+e)+1}{2(n+e)-5} \quad (4.9)$$

$$\text{Beta } (\beta) \text{ Index} = \frac{t}{n+e} \quad (4.10)$$

$$\text{Gamma } (\gamma) \text{ index} = \frac{t}{3(n+e-2)} \quad (4.11)$$

in eqs. (4.9), (4.10) and (4.11), t = total number of segments; e = number of bisected segments; and n = number of nodes.

Sharma (1995) proposed flow geometry index (FGI), plan form index (PFI) and cross-slope ratio for identifying the degree of braiding of highly braided river. The FGI, PFI and cross- slope formulae have been given as below:

$$\text{i) Plan Form Index} = \frac{\frac{W}{B} \times 100}{N} \quad (4.12)$$

$$\text{ii) Flow Geometry Index} = \left[\frac{\sum d_i x_i}{WxD} \right] \times N \quad (4.13)$$

$$\text{iii) Cross-slope} = \frac{\frac{B_L}{2}}{(\text{Bank level} - \text{Av. bed level})} \quad (4.14)$$

in eqs. (4.12) to (4.14), W = flow top width; B = overall width of the channel; B_L = Transect length across river width; N = numbers of braided channel; d_i and x_i are depth and top lateral distance of submerged sub-channel; and D = hydraulic mean depth.

4.3 DISCUSSION OF RESULTS

4.3.1 Existing Braiding Indicators

Eqs. (4.1) to (4.8) except eq.(4.6) have not been considered for the present analysis because of lack of data in the required format. Due to unavailability of data from the field, eqs. (4.9) to (4.11) have not been used for field study but these equations are considered in the model studies of a typical reach of the Brahmaputra river in Bangladesh.

According to Parker's (1976) stability analysis, Fig 4.1 was plotted with the Brahmaputra river data for demarcating the braided river zone with meandering or straight river. The necessary field data have been collected from Bangladesh Water Development Board. Fig. 4.2 is indicative of the braiding, meandering and straight river zones according to Parker's (1976) criterion for the present laboratory experimental data. Similar plot has been made according to Parker (1976) for demarcating braiding and meandering- straight river zone for the data of different investigators as shown in the Fig.4.3. In the Fig. 4.4 (a, b), specific energy and velocity head have been plotted against width to depth ratio, D/B for field data according to Richardson and Thorne, (2001). Figs. 4.5 (a, b) show the plot between specific energy, velocity head and D/B ratio for the laboratory experimental data. Similarly, plot has been made according to Richardson and Thorne (2001) for demarcating braiding and meandering - straight river zone for the data of different investigators as shown in the Fig. 4.6. The above plots demarcate the braiding and meandering- straight region. A good relationship has come out between FGI and PFI of Sharma (1995) using field data. It is seen that FGI and PFI have depicted good relationship with cross-slope for field data of the Brahmaputra river (Table 4.3). Cross-slope is basically a form ratio indicator and its higher value may indicate higher braiding intensity. For laboratory data,

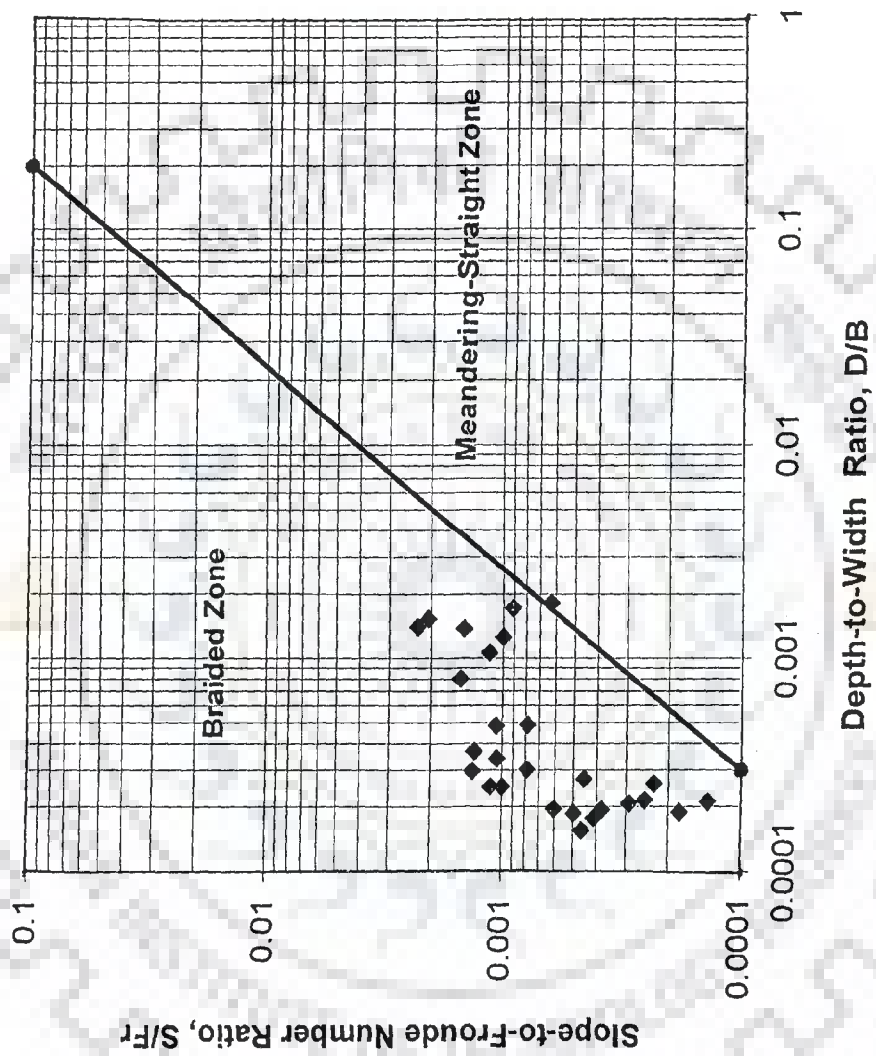


FIG. 4.1: DEMARCATION OF BRAIDING ZONE USING S/Fr , VS D/B DIAGRAM FOR OBSERVED DATA OF THE BRAHMAPUTRA RIVER

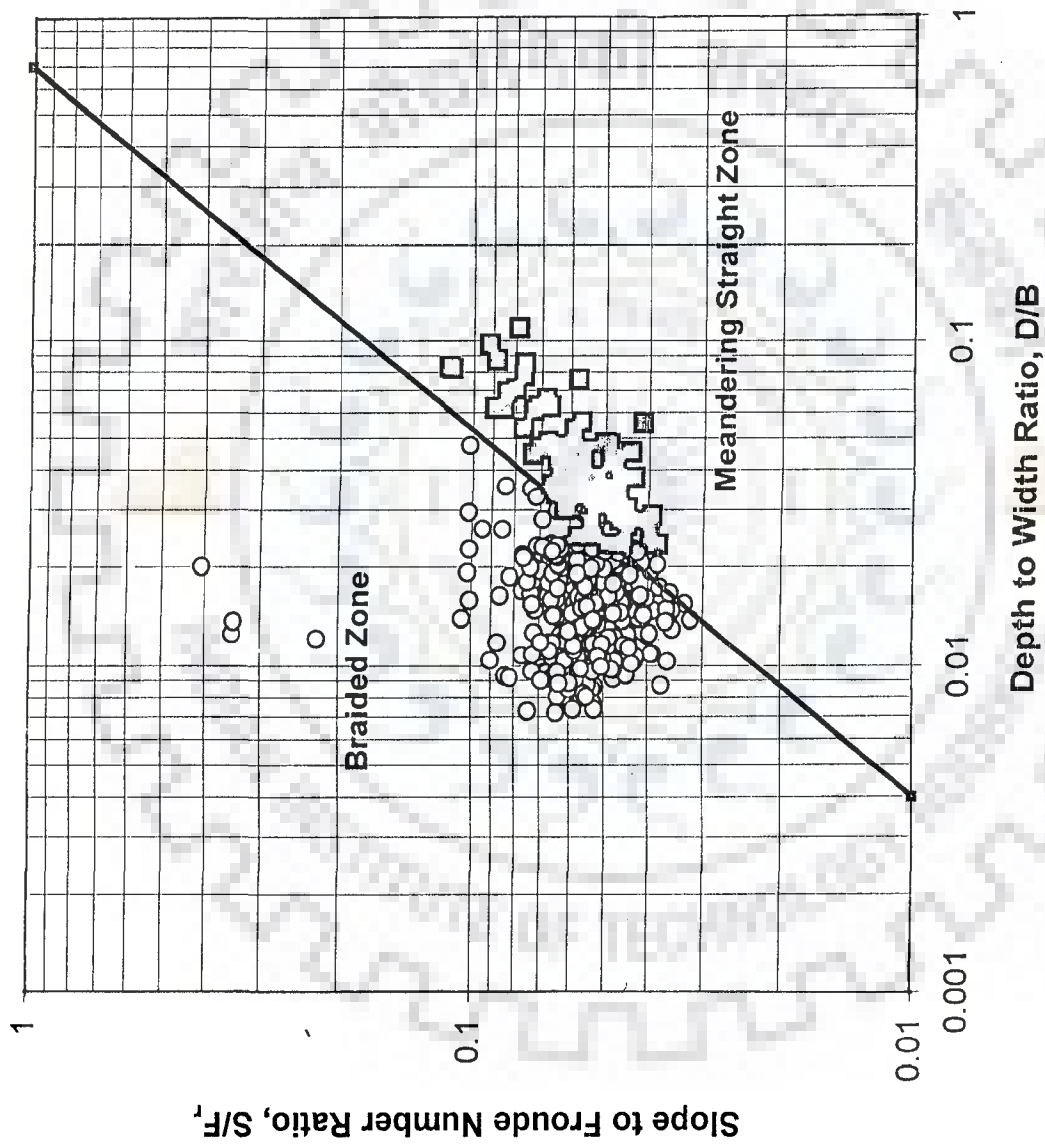


FIG. 4.2 : DEMARICATION OF BRAIDING ZONE USING S/F_r VS D/B FOR LABORATORY EXPERIMENTAL DATA

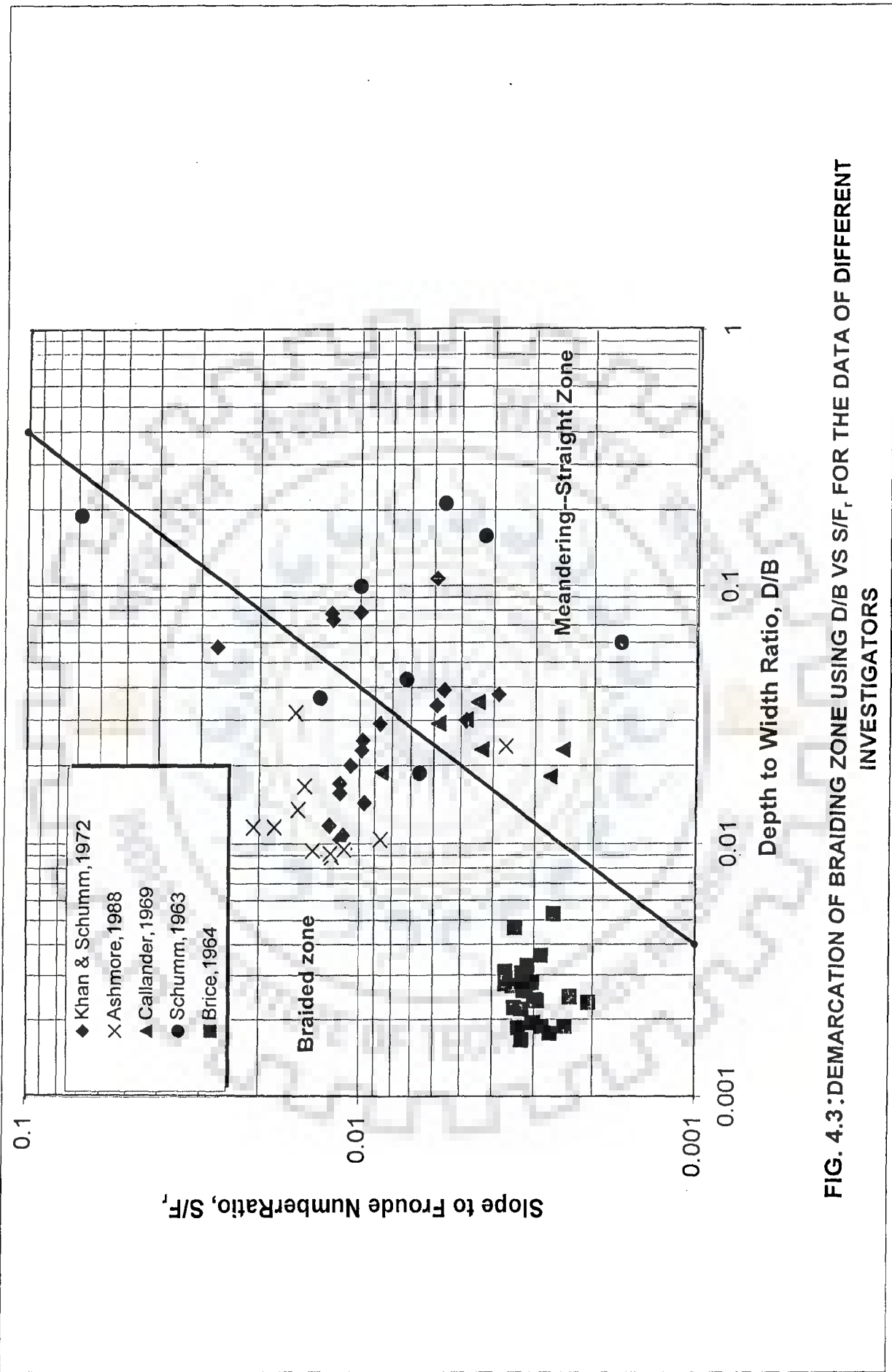


FIG. 4.3: DEMARCATION OF BRAIDING ZONE USING D/B VS S/F_r , FOR THE DATA OF DIFFERENT INVESTIGATORS

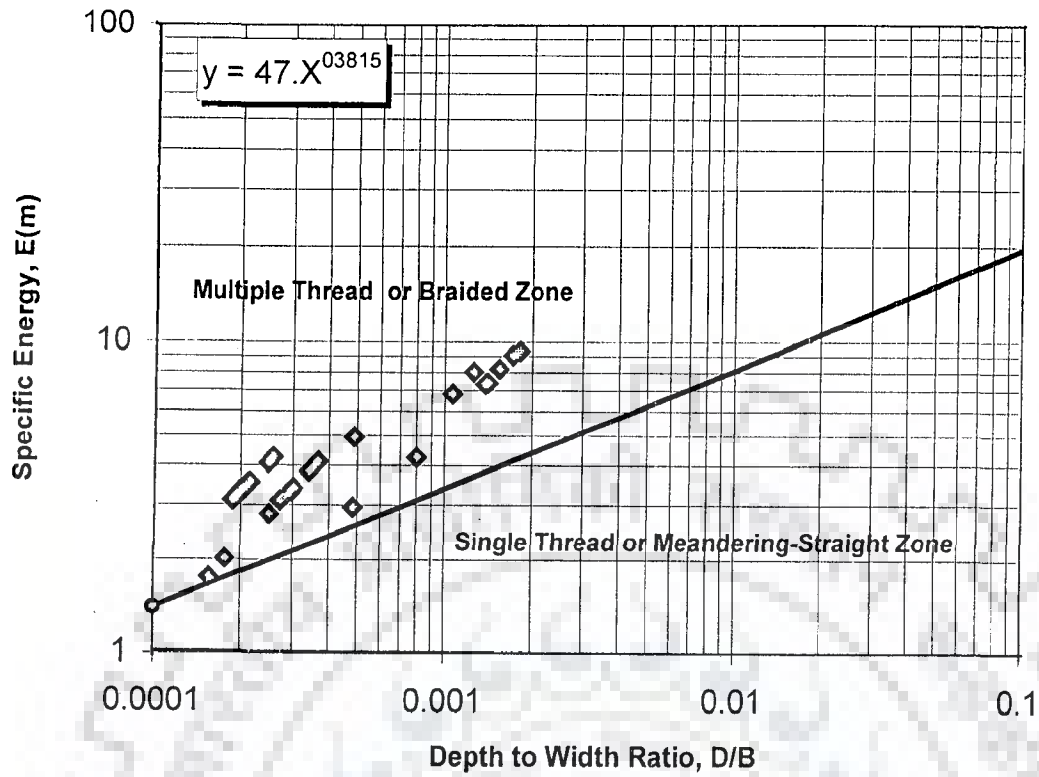


FIG. 4.4 a PLOT OF SPECIFIC ENERGY (E) AGAINST DEPTH-TO- WIDTH RATIO (D/B) FOR 27CROSS-SECTIONS OF THE BRAHMAPUTRA RIVER.

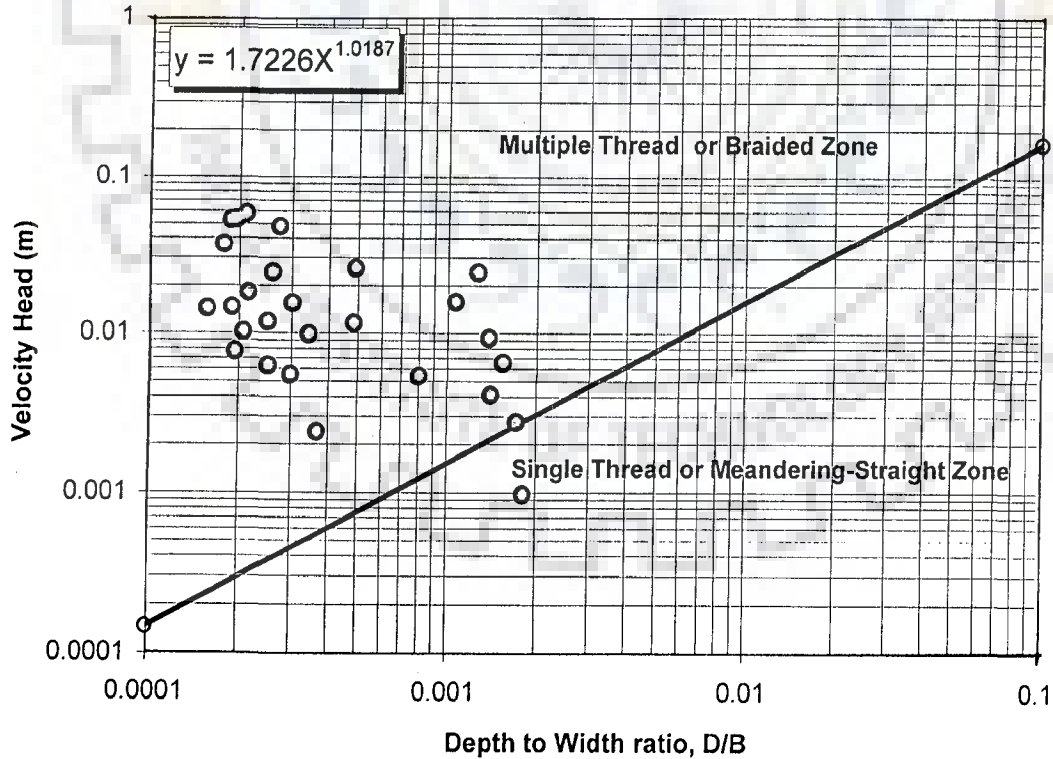


FIG. 4.4'b PLOT OF VELOCITY HEAD AGAINST DEPTH-TO WIDTH RATIO (D/B) FOR 27 CROSS-SECTIONS OF THE BRAHMAPUTRA RIVER.

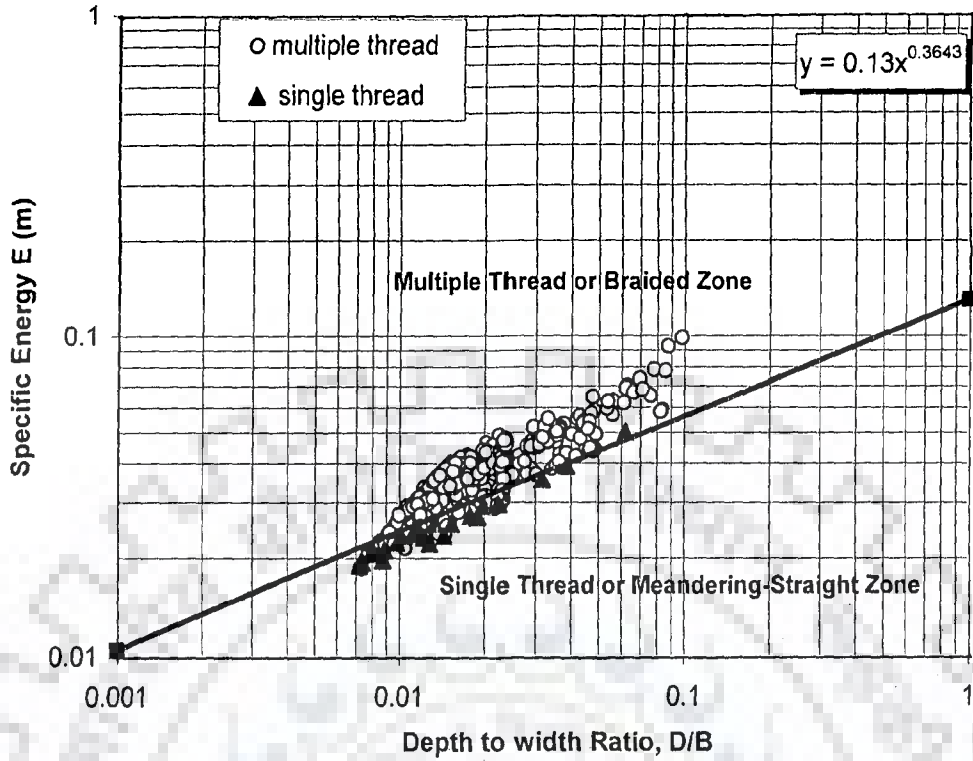


FIG. 4.5a; PLOT OF SPECIFIC ENERGY (E) AGAINST DEPTH-TO-WIDTH RATIO (D/B) FOR LABORATORY EXPERIMENTAL DATA

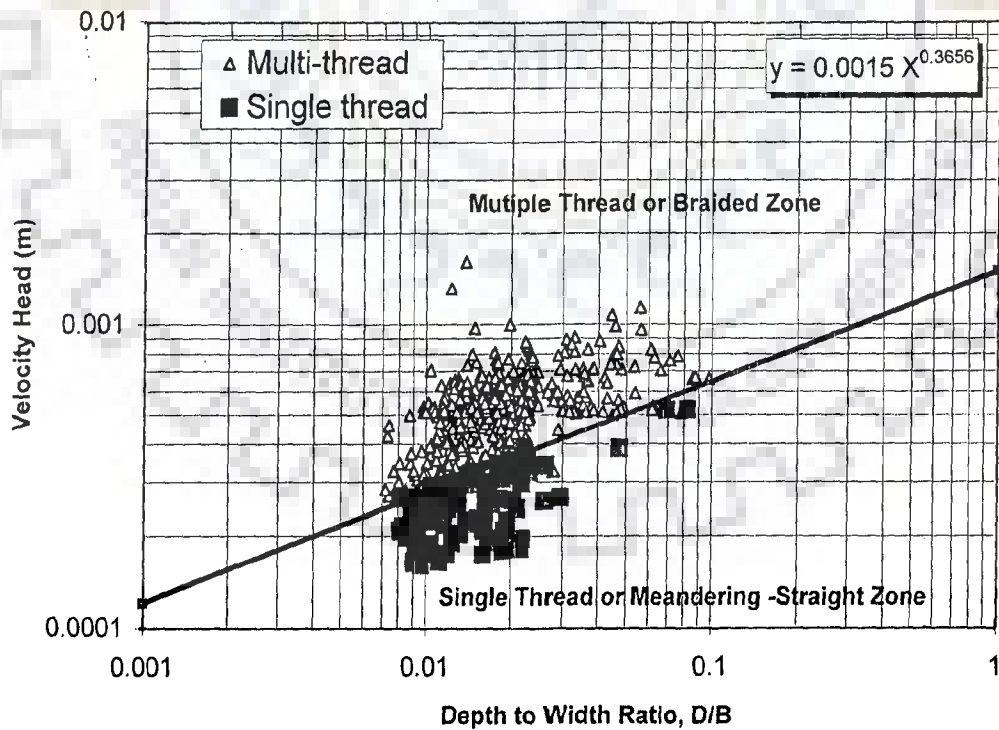


FIG. 4.5b; PLOT OF VELOCITY HEAD AGAINST DEPTH-TO-WIDTH RATIO (D/B) FOR LABORATORY EXPERIMENTAL DATA

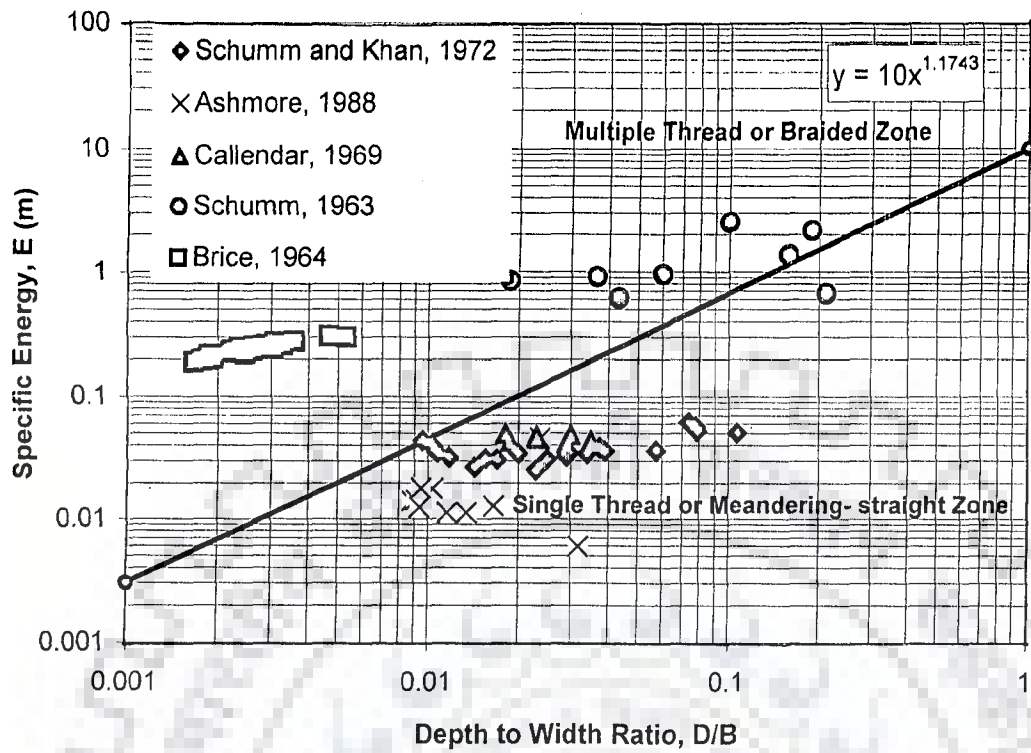


FIG. 4.6a: PLOT OF SPECIFIC ENERGY (E) AGAINST DEPTH-TO-WIDTH (D/B) FOR THE DATA OF DIFFERENT INVESTIGATORS

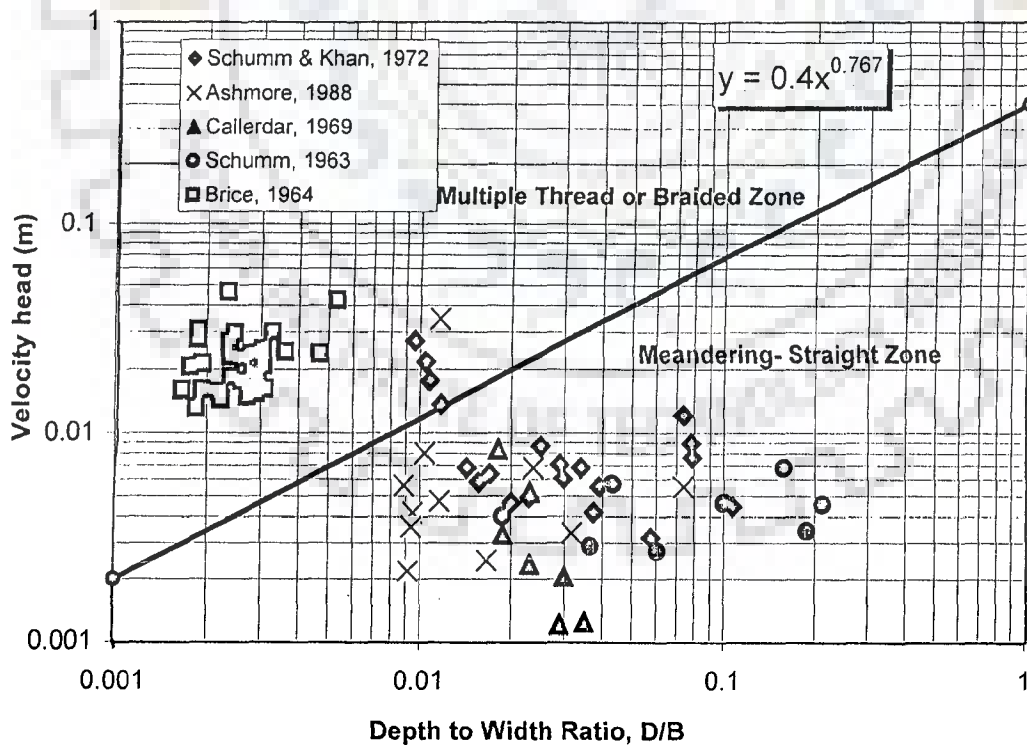


FIG. 4.6b: PLOT OF VELOCITY HEAD AGAINST DEPTH-TO-WIDTH (D/B) FOR THE DATA OF DIFFERENT INVESTIGATORS

Table 4.3: RELATIONSHIP BETWEEN DIFFERENT PARAMETERS FOR DEMARCATING THE CHANNEL PATTERNS

Investigators	Y-axis	X-axis	Relationship	Remark	R ² value
Richardson and Thorne (2001)	E	D/B	$Y=47 X^{0.3815}$	Field data	
Richardson and Thorne(2001)	E	D/B	$Y=0.13 X^{0.3643}$	Lab. data	
Sharma (1995)	FGI	PFI	$Y=9.7533 e^{-0.0196 X}$	Field data	0.40
Sharma (1995)	FGI	Cross slope	$Y=323.2 e^{0.05 X}$	Field data	0.1283
Sharma (1995)	PFI	Cross slope	$Y=38.7 e^{-0.0022 X}$	Field data	0.4611
Sharma (1995)	FGI	B/D	$Y=.0032 X + 4.4$	Field data	0.23
Sharma (1995)	PFI	B/D	$Y= -3.6 \ln (X) + 34.6652$	Field data	0.117
Brice (1964) and Mosley (1981)	B.I.	T.S (Richards, 1982)	$Y= -0.6148X^2 + 3.8146 X - 3.3112$ $Y = 0.1047 X^2 + 0.561 X + 3207$	Lab. data	0.4885 0.9632
Friend and Sinha (1993)	B.C.R.	T.S.	$Y = 0.6663 e^{0.5081x}$	Lab. data	0.8092
Richardson and Thorne (2001)	Velocity Head, $V^2/2g$	D/B	$Y = 1.722 X^{1.0187}$	Field data	
Richardson and Thorne (2001)	Velocity Head, $V^2/2g$	D/B	$Y = 0.0015 X^{0.3656}$	Lab. data	
New approach	Composite Index I ₁	B/D	$Y = 9*10^7 X^{-0.7734}$	Field data	0.4328
New approach	Composite Index I ₂	B/D	$Y = 0.0882 X^{0.2811}$	Field data	0.269

no relationships exist between B/D ratio and FGI or PFI according to Sharma (1995), as shown in the Table 4.3. Several graphical plots were made between braiding indices proposed by different investigators with respect to B/D, and R^2 values based on the best fit curves in case of different indices such as Brice (1964), Mosley (1981) and Friend and Sinha (1993) have been shown in the Table 4.3. These indices in fact, do not vary with B/D ratio for laboratory data. Further study is required to validate the above relationships whether these would have a great role with braiding condition or to elicit information pertaining to the degree of braiding.

Agreement between braiding index (Brice, 1964, Mosley, 1981) and total sinuosity has been depicted in the Fig. 4.7a. Also Fig. 4.7b indicates the good agreement between braid channel ratio (Friend and Sinha, 1993) and total sinuosity (Richards, 1982).

4.3.2 Proposed Braiding Index

The existing braid indicators like bed relief index, braid intensity, sinuosity may not be adequate to properly describe the braiding phenomenon in terms of key variables like water level, hydraulic radius and these also do not account for underwater braid bars, which play a significant role in the energy loss process. In this context, the following new modified indices in line with those formulations by Sharma (1995) are proposed in this work:

$$i) \quad \text{Composite index} \quad I_1 = \left(\frac{\frac{W}{B} \times 100}{N} \right) / S^{pi} \quad (4.15)$$

$$ii) \quad \text{Composite index} \quad I_2 = \left(\left[\frac{\sum d_i x_i}{W \times D} \right] \times N \right) \times C_s^{pi} \quad (4.16)$$

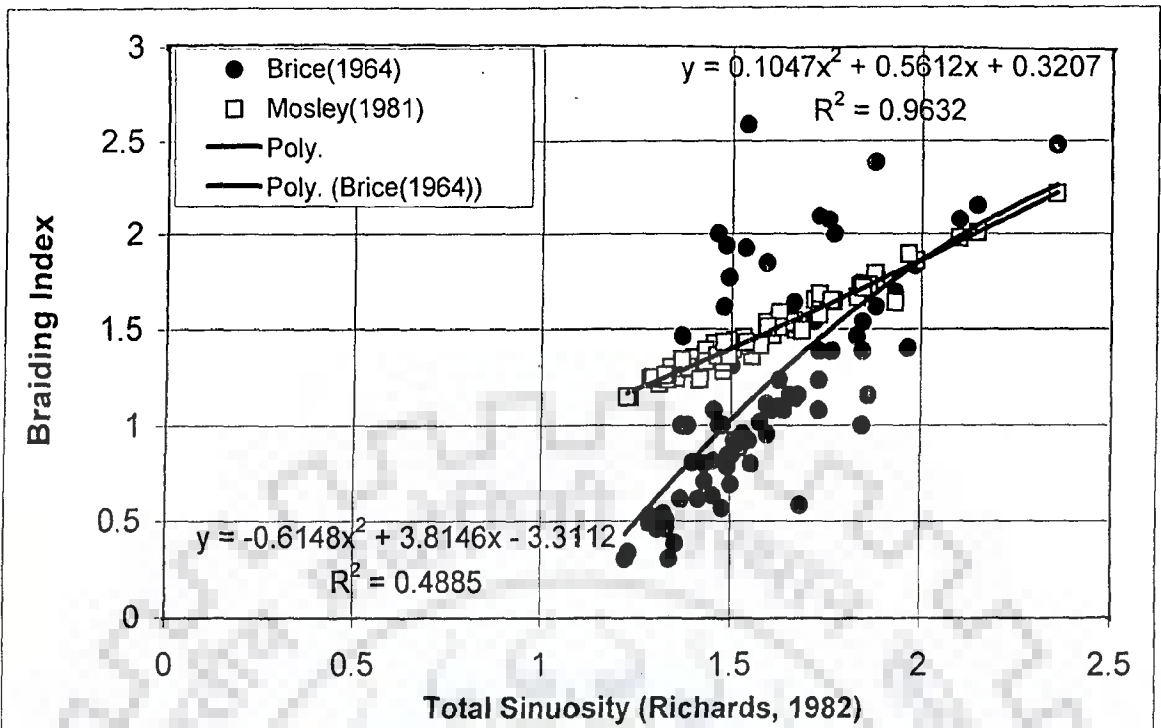


FIG. 4.7a: Variation of Braiding Index with Total Sinuosity (Richards, 1982)

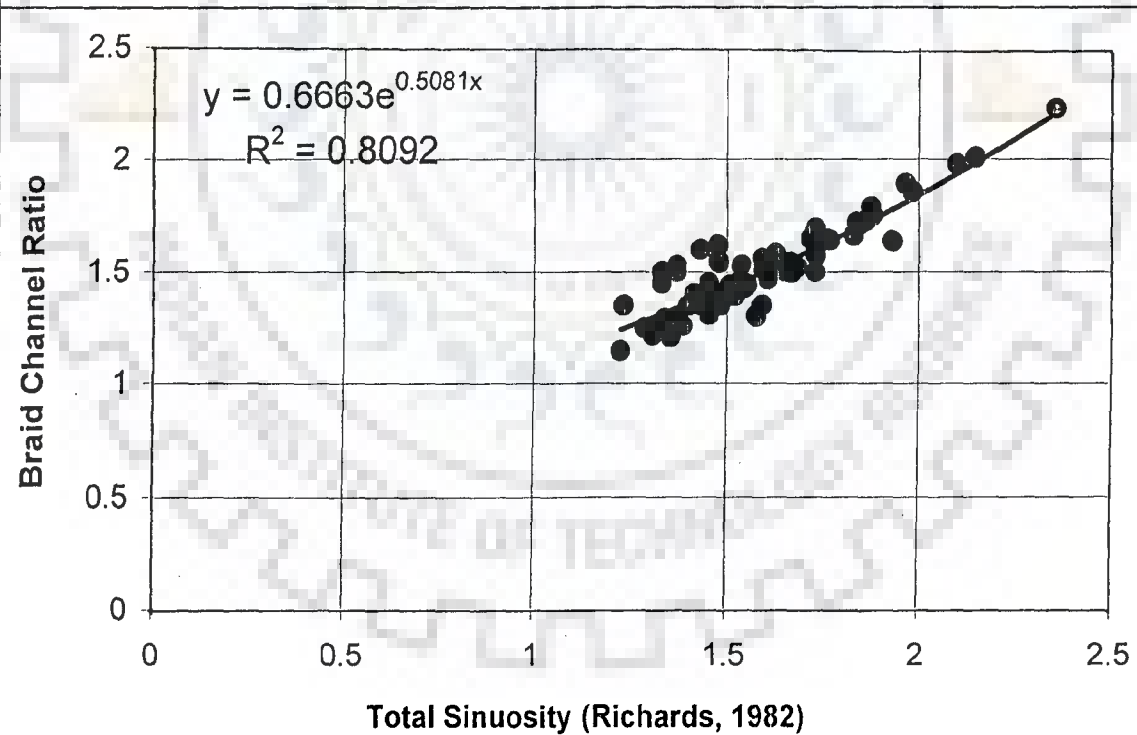


FIG. 4.7b: Variation of Braid Channel Ratio (Friend and Sinha, 1993) with Total Sinuosity for Laboratory data

in eqs. (4.15) and (4.16), W = flow top width; B = overall river width; N = Nos. of braided channel; S = slope of stream; d_i and x_i = depth and top lateral distance of submerged sub-channel; D = hydraulic mean depth and C_s = dimensionless sediment concentration = Q_s/Q . P_i = exponent of S and C_s . The influence of varying the exponents of S and C_s is shown in Table 4.4a and 4.4b. The idea behind developing the composite index is to see if these lead to serve as a better indicator. From a perusal of Table 4.3 and Table 4.4, there is certainly some improvement in using the composite indicators.

Fig. 4.8a shows the variation of composite index I_1 with B/D ratio for field data and variation of composite index I_2 with B/D ratio for field data has been shown in the Fig.4.8b. In these figures, certain trend appears to prevail between composite index I_1 and composite index I_2 with B/D values.

Figs. 4.9 (a, b & c) represent the hypothetical streams to be used for the appraisal of approach suggested by Howard et al. (1970). Here, the hypothetical streams have been created in such a way that one can identify the streams in terms of the severity of the braiding. For example, one can see that the braiding intensifies from top to bottom (Fig. 4.9a). For different figures including Fig.4.9a to Fig.4.9c, the values of alpha (α), beta (β), gamma (γ) index have been given in the Table 4.5. It can be seen that with the intensification of braiding, all the indices show an increasing trend. When the pattern of braiding changes (Figs. 4.9a and 4.9 b), certain influence of this can be also seen on the values of indices in Table 4.5.

Table 4.4a ANALYSIS OF DIFFERENT PARAMETERS OF COMPOSITE INDEX I₁ AND COMPOSITE I₂ FOR FIELD DATA

Composite Index I ₁ = Y-axis	B/D= X-axis	Best fit equation	R ² value	Remarks
$Y = (W/B \times 100)/(N \times S^{1/2})$	B/D	$633140 X^{-0.7696}$	0.5261	Field Data
$Y = (W/B \times 100)/(N \times S^{+2})$	B/D	$2X10^2 X^{-0.7812}$	0.2162	Do
$Y = (W/B \times 100)/(N \times S^{(-1/2)})$	B/D	$31.012 X^{-0.7618}$	0.3762	Do
$Y = (W/B \times 100)/(N \times S^{-1})$	B/D	$0.217 X^{-0.7579}$	0.2598	Do
$Y = (W/B \times 100)/(N \times S^{-2})$	B/D	$1 X 10^{-5} X^{-0.7502}$	0.1256	Do
Composite Index I₂				
$Y = (\sum xidi/WD) \times N \times C^{0.5}$	B/D	$0.0005 X + 1.2178$ $0.266 X^{0.2811}$.3767 0.2691	Field Data
$Y = (\sum xidi/WD) \times N \times C^{-0.5}$	B/D	$0.0041 X + 11.071$	0.3767	Do
$Y = (\sum xidi/WD) \times N \times C^{-0.5}$	B/D	$24154 X^{0.2811}$	0.2691	Do
$Y = (\sum xidi/WD) \times N \times C^{-1}$	B/D	$7.2917 X^{0.2811}$	0.2691	Do
$Y = (\sum xidi/WD) \times N \times C^{+2}$	B/D	$0.1125 X + 303.45$	0.3767	Do
$Y = (\sum xidi/WD) \times N \times C^{-2}$	B/D	$66.288X^{0.2811}$	0.2691	Do

Table 4.4b ANALYSIS OF DIFFERENT PARAMETERS OF COMPOSITE INDEX I₁ AND COMPOSITE I₂ FOR LABORATORY EXPERIMENTAL DATA

Composite Index I ₁ =Y-axis	B/D = X-axis	Best fit equation	R ²	Remarks
$Y = (W/B \times 100)/(N \times S^{+1})$	B/D	$4113.3 X^{0.0321}$	0.0049	Lab. Data
$Y = (W/B \times 100)/(N \times S^{-0.5})$	B/D	$0.0420 X^{0.148}$	0.001	Lab. Data
$Y = (W/B \times 100)/(N \times S^{+0.5})$	B/D	$0.402 X^{0.0297}$	0.423	Lab. Data
$Y = (W/B \times 100)/(N \times S^{-1})$	B/D	$0.3757 X^{0.0073}$	0.0002	Lab. Data
Composite Index I₂		B/D ratio		
$Y = (\sum xidi/WD) \times N \times C^{+1}$	B/D	$0.0005 X + 0.2424$	0.003	Lab. Data
$Y = (\sum xidi/WD) \times N \times C^{+0.5}$	B/D	$0.0002 X + 7802$	0.236	Lab. Data
$Y = (\sum xidi/WD) \times N \times C^{-0.5}$	B/D	$-0.0225 X + 8.75$	0.0084	Lab. Data
$Y = (\sum xidi/WD) \times N \times C^{-1}$	B/D	$-0.119 X + 30.639$	0.0135	Lab data

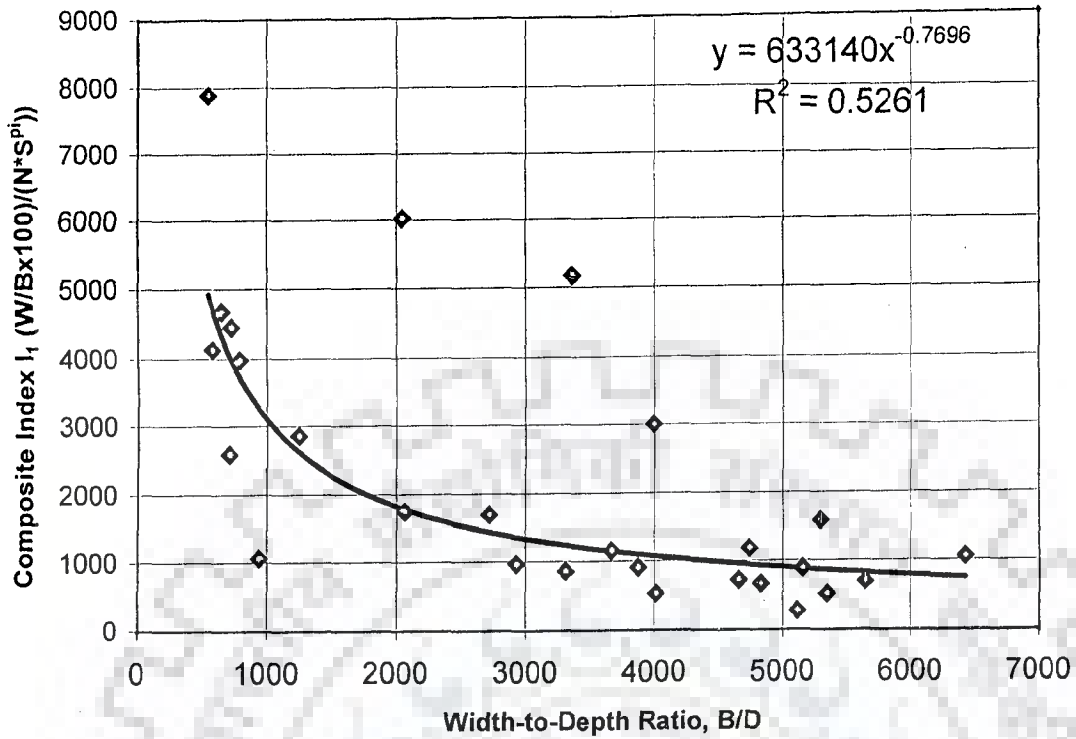


FIG. 4.8a: VARIATION OF COMPOSITE INDEX I_1 WITH B/D RATIO FOR FIELD DATA OF THE BRAHMAPUTRA RIVER (EXPONENT OF $S=0.5$)

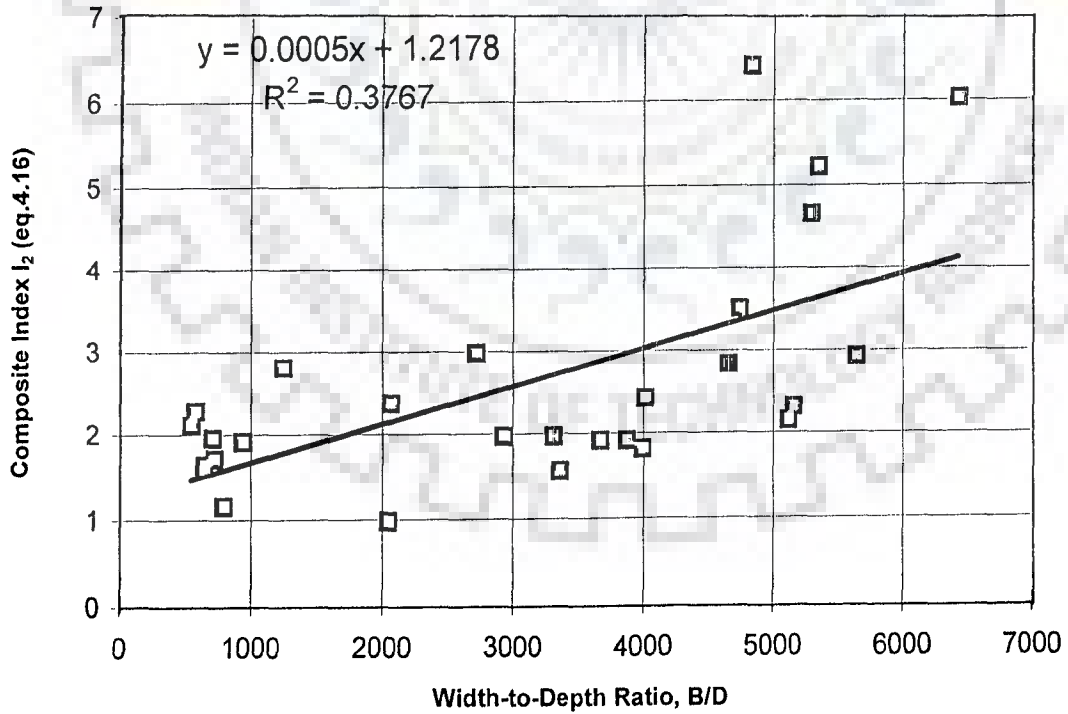


FIG. 4.8b: VARIATION OF COMPOSITE INDEX I_2 WITH B/D RATIO FOR FIELD DATA OF THE BRAHMAPUTRA RIVER (WHEN EXPONENT OF $C_f=0.5$)

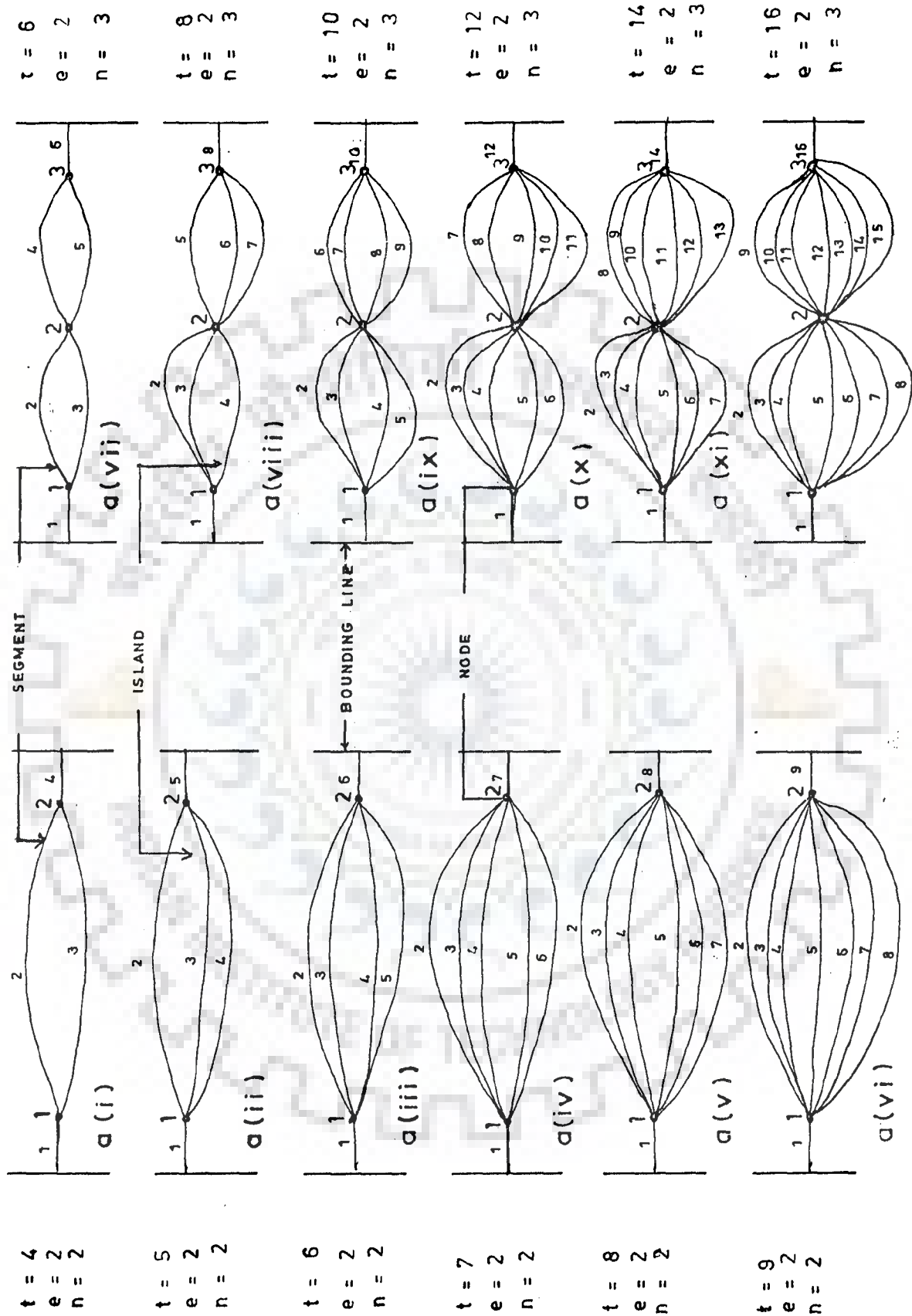


FIG. 4.9: HYPOTHETICAL TOPOLOGY REPRESENTING EXTENT OF BRAIDING

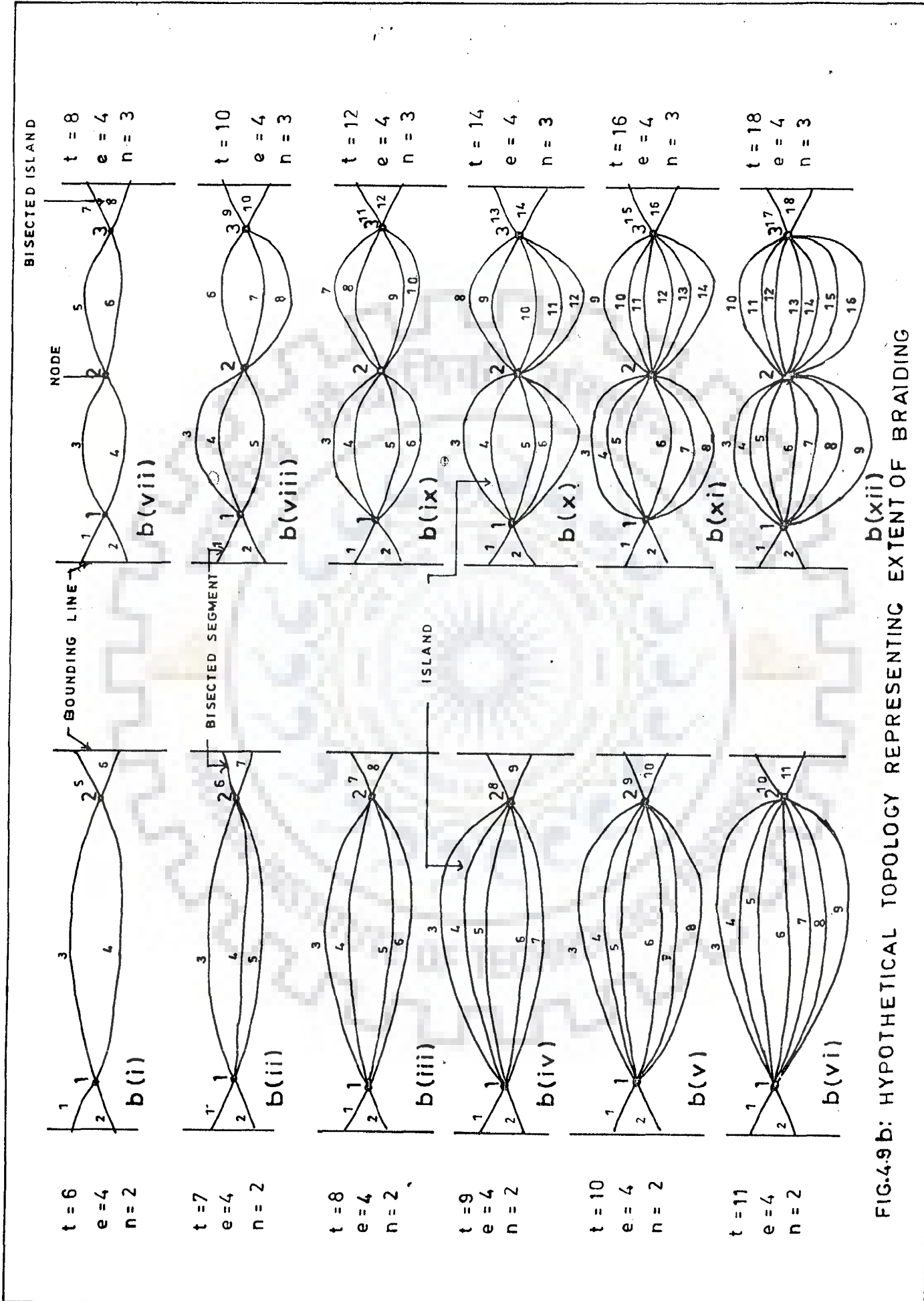
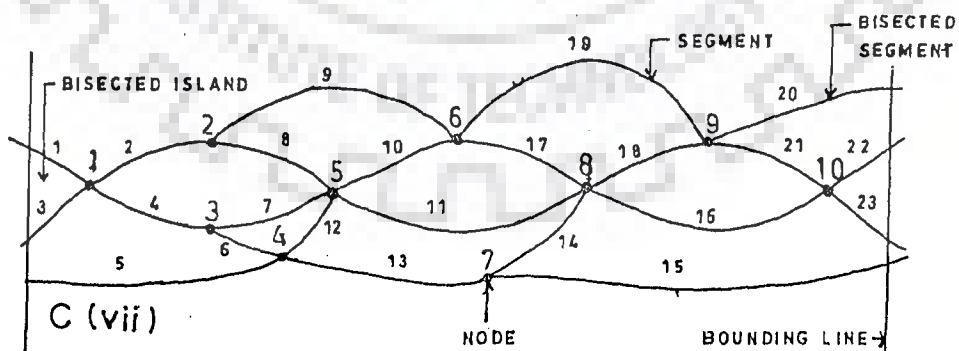
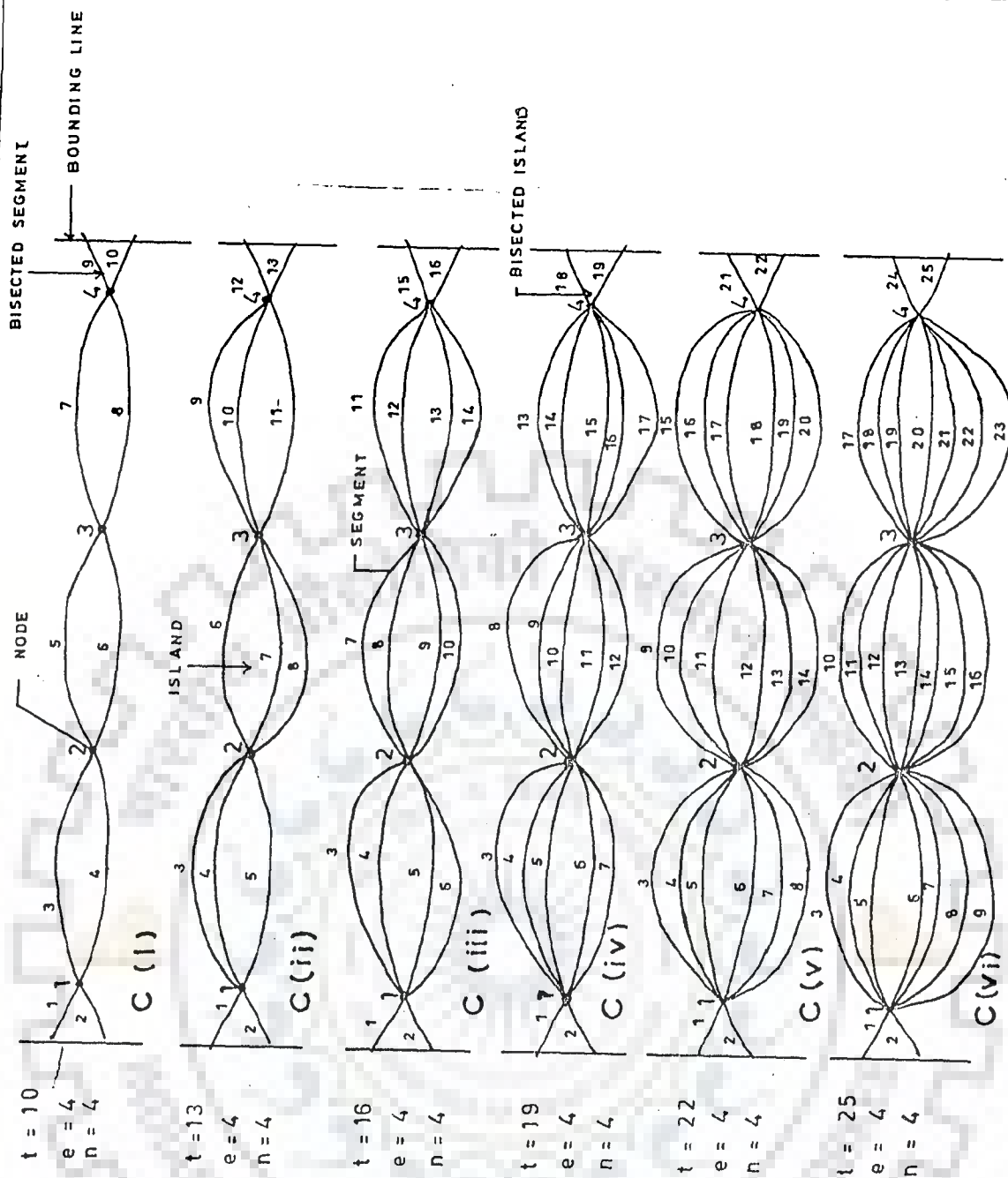


FIG.4-9b: HYPOTHETICAL TOPOLOGY REPRESENTING EXTENT OF BRAIDING



$c = 16$
 $p = 5$
 $i = 7$

α - Index = .24
 β - Index = 1.35
 γ - Index = .51

FIG.4.9 C: HYPOTHETICAL TOPOLOGY REPRESENTING EXTENT OF BRAIDING

Table 4.5: DIFFERENT HYPOTHETICAL TOPOLOGICAL INDICES VIZ α -INDEX, β -INDEX AND γ -INDEX (HOWARD ET AL. 1970) FOR UNDERSTANDING BRAIDING PHENOMENON

Figure No.	Variables	α -Index	β -Index	γ -Index
4.9a (i)	t = 4 e = 2 n = 2	0.33	1.0	0.67
4.9a (ii)	t = 5 e = 2 n = 2	0.67	1.25	.83
4.9a (iii)	t = 6 e = 2 n = 2	1.0	1.5	1.0
4.9a (iv)	t = 7 e = 2 n = 2	1.33	1.75	1.16
4.9a (v)	t = 8 e = 2 n = 2	1.67	2.0	1.33
4.9a (vi)	t = 9 e = 2 n = 2	2.0	2.25	1.50
4.9a (vii)	t = 6 e = 2 n = 3	0.4	1.20	0.67
4.9a (viii)	t = 8 e = 2 n = 3	0.80	1.60	0.88
4.9a (ix)	t = 10 e = 2 n = 3	1.20	2.0	1.10
4.9a (x)	t = 12 e = 2 n = 3	1.6	2.4	1.33
4.9a (xi)	t = 14 e = 2 n = 3	2.0	2.8	1.56
4.9a (xii)	t = 16 e = 2 n = 3	2.4	3.2	1.78
4.9b (i)	t = 6 e = 4 n = 2	0.143	1.00	0.50
4.9b (ii)	t = 7 e = 4 n = 2	0.285	1.167	0.58
4.9b (iii)	t = 8 e = 4 n = 2	0.428	1.33	0.67

Contd....

4.9b (iv)	t = 9 e = 4 n = 2	0.571	1.5	0.75
4.9b (v)	t = 10 e = 4 n = 2	0.714	1.67	0.83
4.9b (vi)	t = 11 e = 4 n = 2	0.857	1.83	0.916
4.9b (vii)	t = 8 e = 4 n = 3	0.222	1.142	0.53
4.9b (viii)	t = 10 e = 4 n = 3	0.444	1.428	0.667
4.9b (ix)	t = 12 e = 4 n = 3	0.666	1.714	0.8
4.9b (x)	t = 14 e = 4 n = 3	0.88	2	0.933
4.9b (xi)	t = 16 e = 4 n = 3	1.11	2.285	1.066
4.9b (xii)	t = 18 e = 4 n = 3	1.33	2.57	1.20
4.9c (i)	t = 10 e = 4 n = 4	0.27	1.25	0.555
4.9c (ii)	t = 13 e = 4 n = 4	0.54	1.625	0.722
4.9c (iii)	t = 16 e = 4 n = 4	0.818	2.0	0.88
4.9c (iv)	t = 19 e = 4 n = 4	1.09	2.378	1.055
4.9c (v)	t = 22 e = 4 n = 4	1.36	2.75	1.222
4.9c (vi)	t = 25 e = 4 n = 4	1.636	3.125	1.388
4.9c (vii)	t = 23 e = 7 n = 10	0.24	1.35	0.51

4.3.3 Results Pertaining to Model Experiments

In order to test some of the results, additional data are generated by constructing a laboratory model of a reach of the Brahmaputra river in Bangladesh, as described in Chapter 3. A set of seven experiments conducted on this model is used to develop following figures. Fig 4.10 indicates braiding and meandering zone according to Parker (1976) for model study data. Interestingly, all the lab data, which pertain to a braided stream stretch, are correctly represented in the braiding zone, as demarcated by Parker's criteria. Fig 4.11a and Fig.4.11b show the plot of data points of specific energy and velocity with D/B ratio for model study. However, from the Fig.11a indicated the braiding and meandering zone where all data points fall in the braiding zone, seem to a trend line. Here velocity head is very small due to low discharges in the model. Fig 4.12a indicates variation between composite index I_1 and B/D ratio for model study. Fig 4.12b shows the relation between composite index I_2 and B/D for the model study. Figs. 4.13 (a, b, c & d) show topological channel pattern analysis for the seven model experiments for a particular stretch of the river Brahmaputra. The values of alpha (α) beta (β) gamma (γ) index have been shown in the Table 4.6. For stream having, complex braiding patterns, the indices proposed by Howard et al. (1970) also show lesser values and some times these do not reflect any consistent variation. Ranges of values of different braiding indices have been given in the Table 4.7.

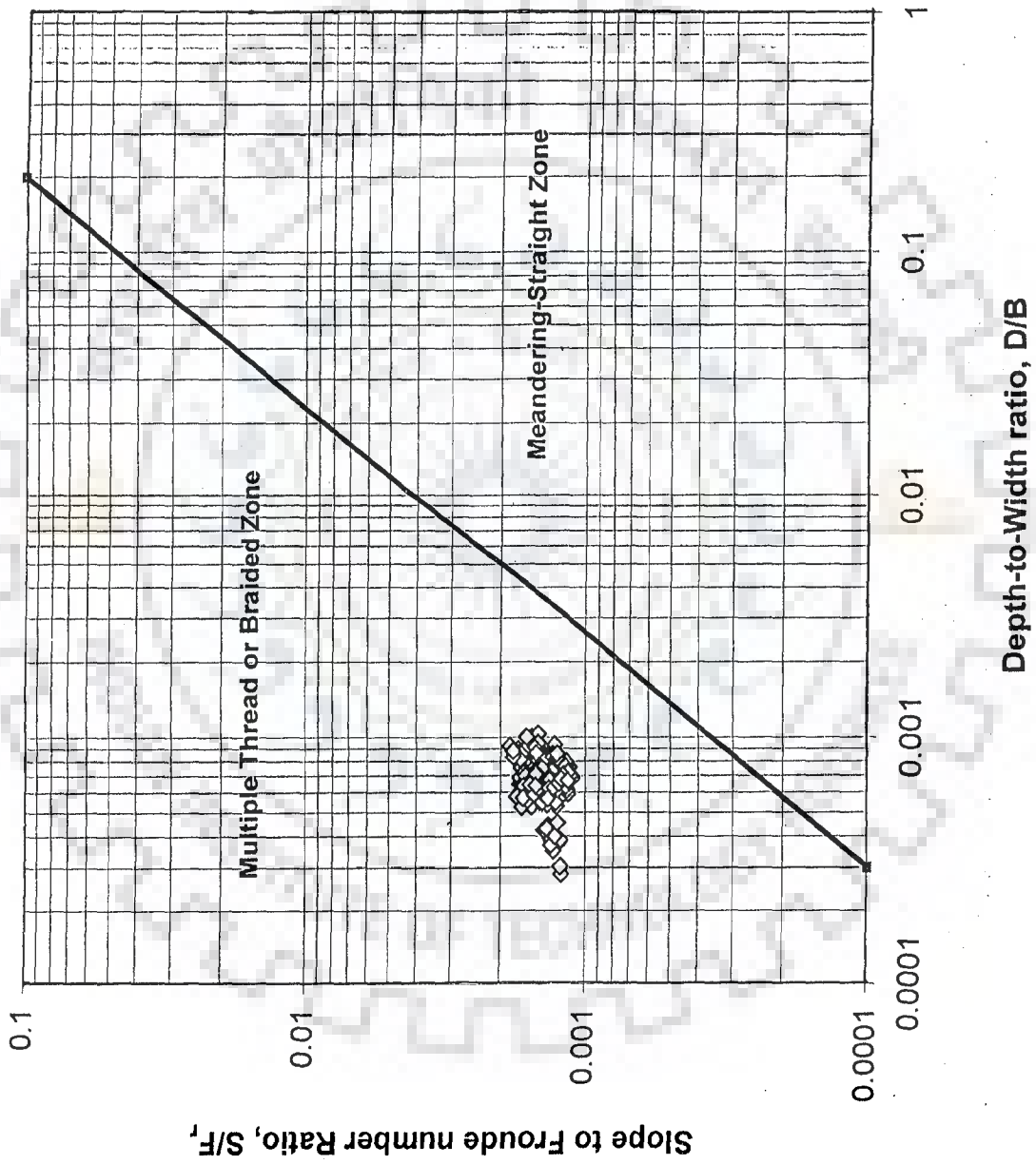


FIG. 4.10: DEMARCATION OF BRAIDING INDICATORS USING D/B VS S/F_r FOR MODEL STUDY

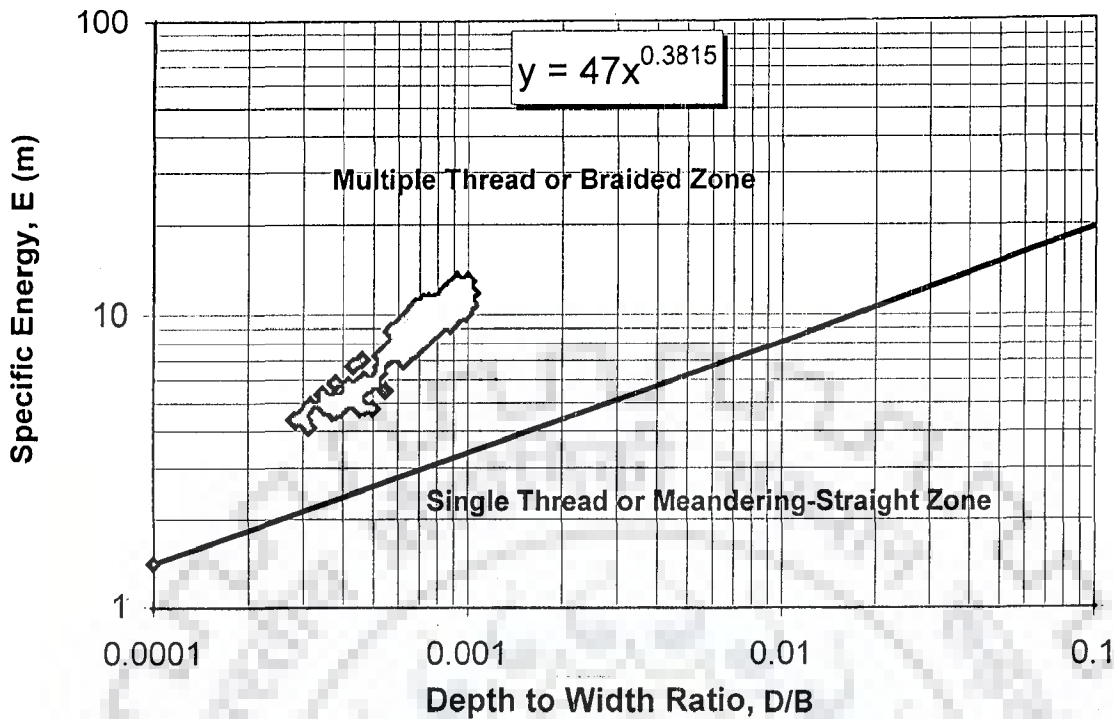


FIG. 4.11a: PLOT OF SPECIFIC ENERGY, E AGAINST DEPTH TO WIDTH RATIO, D/B FOR MODEL STUDY

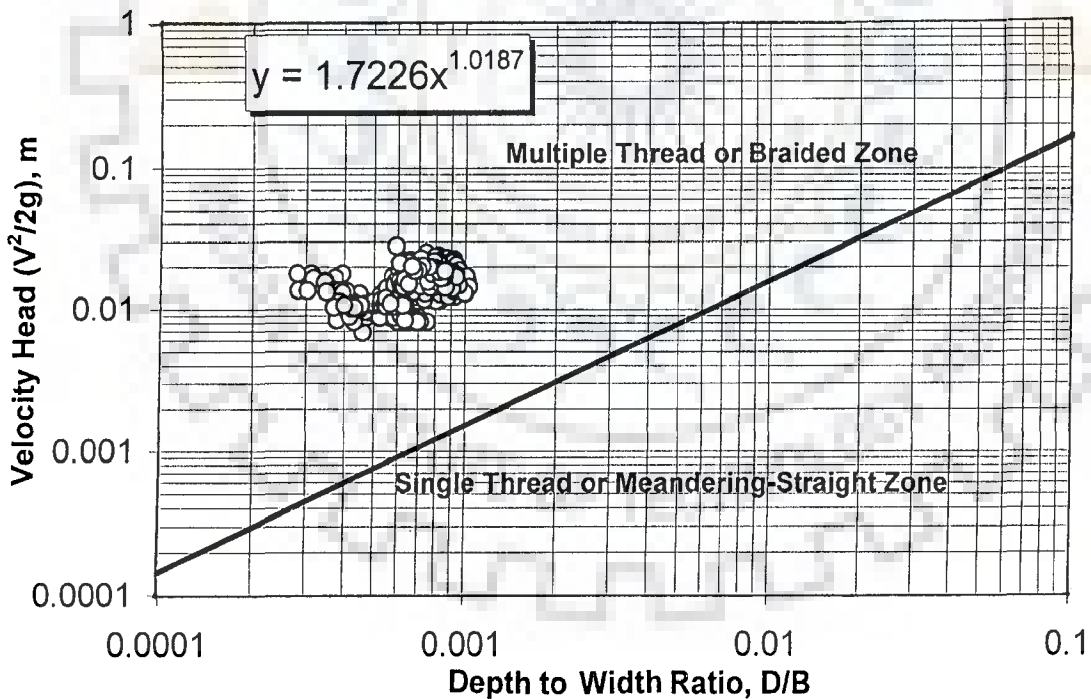


FIG. 4.11 b: VARIATION OF VELOCITY HEAD WITH D/B ACCORDING TO RICHARDSON & THORNE (2001) FOR MODEL STUDY

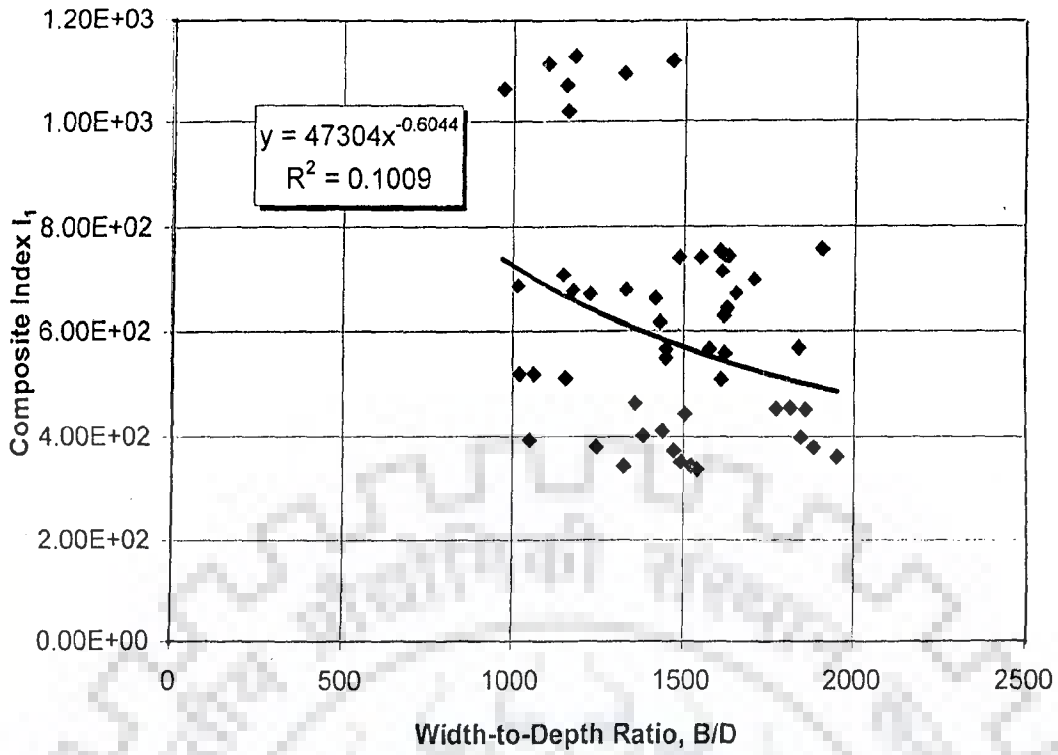


FIG. 4.12 a: VARIATION OF COMPOSITE INDEX I_1 WITH B/D RATIO FOR MODEL STUDY

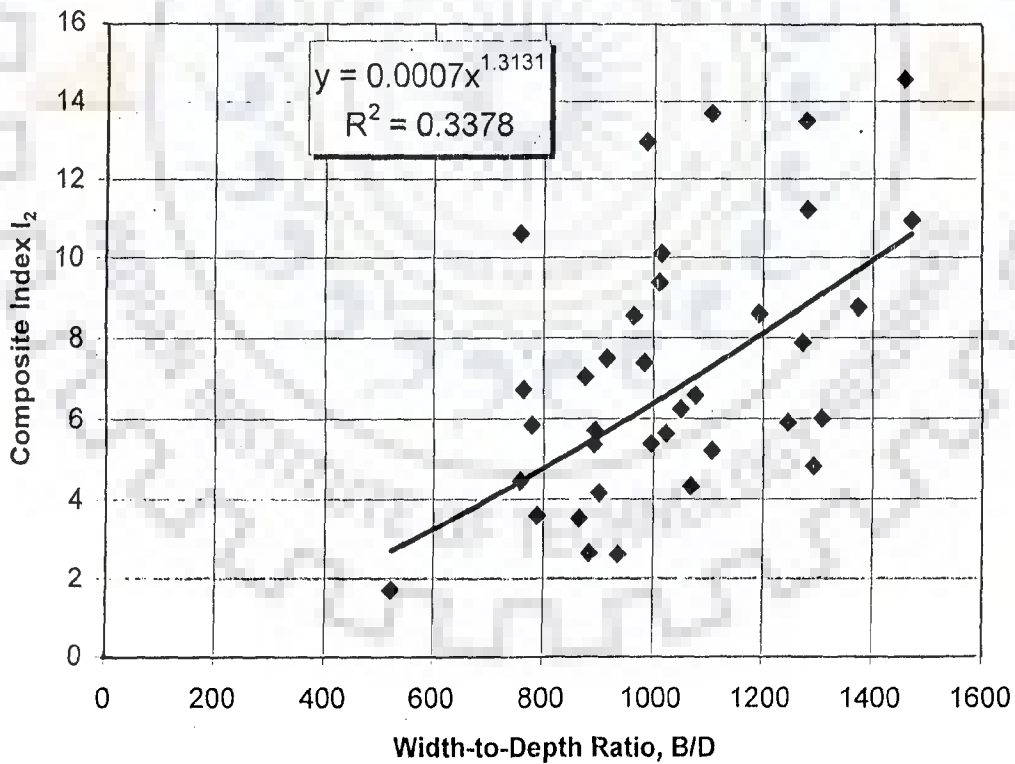


FIG. 4.12 b: VARIATION OF COMPOSITE INDEX I_2 WITH B/D RATIO FOR MODEL STUDY

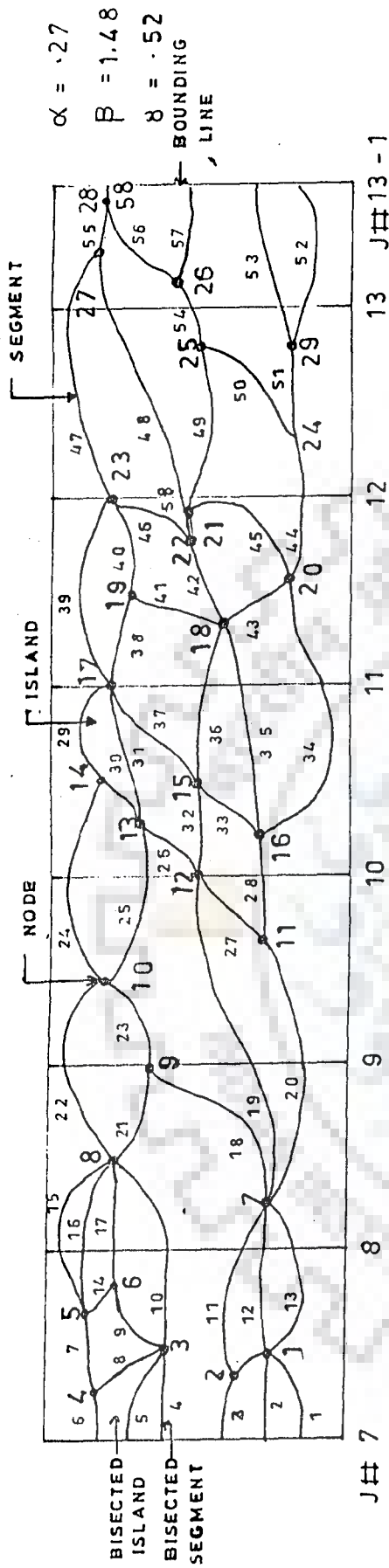


FIG. 6 (i) INITIAL TOPOLOGIC CONDITION OF MODEL RUN (1 to 7)

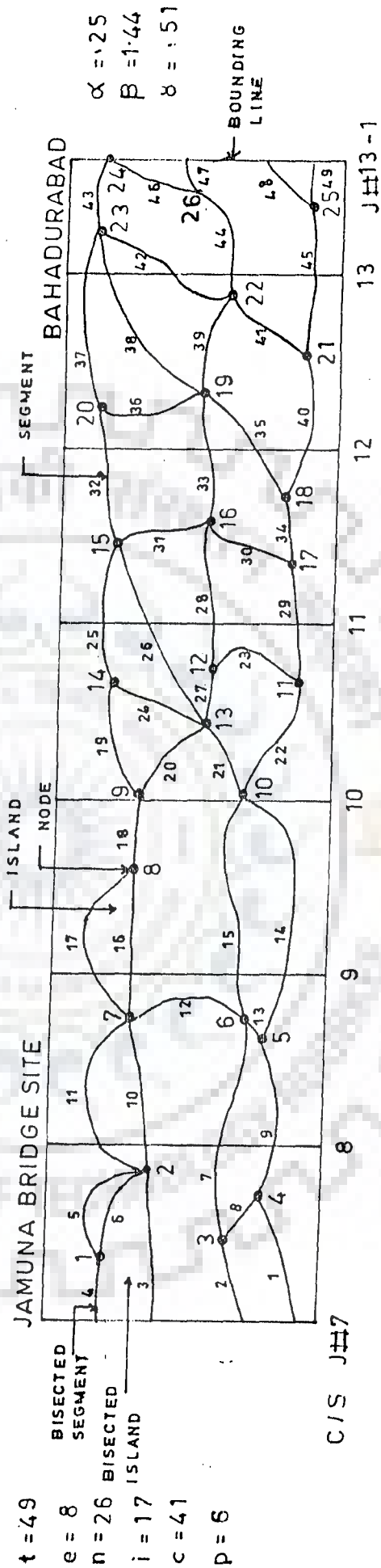
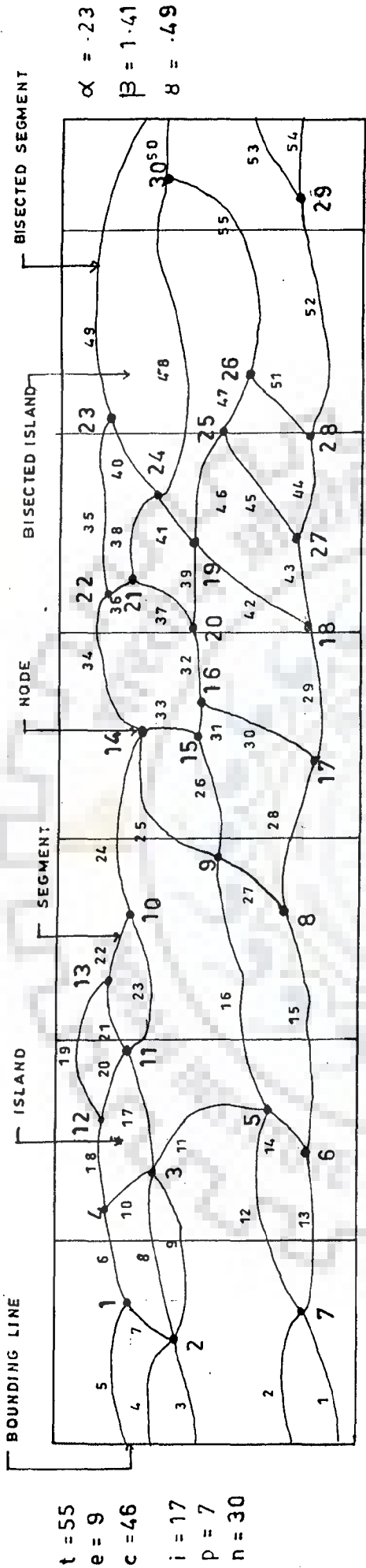


FIG. 4.13G (ii): TOPOLOGIC CONDITION OF MODEL RUN 1

FIG. 4.13a: TOPOLOGIC DEFINITION ON BRAIDED STREAMS FOR MODEL STUDY OF BRAHMAPUTRA RIVER

$t = 58$
 $e = 10$
 $n = 29$
 $p = 8$
 $i = 22$
 $c = 48$

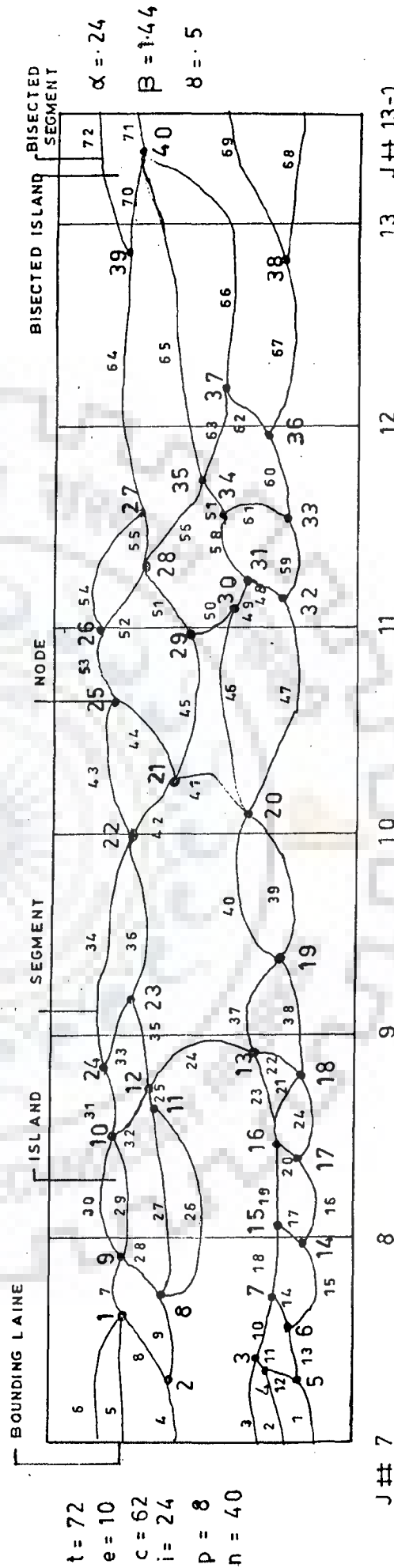
$t = 49$
 $e = 8$
 $n = 26$
 $i = 17$
 $c = 41$
 $p = 6$



J#7

8 9 10 11 12 13 J#13-1

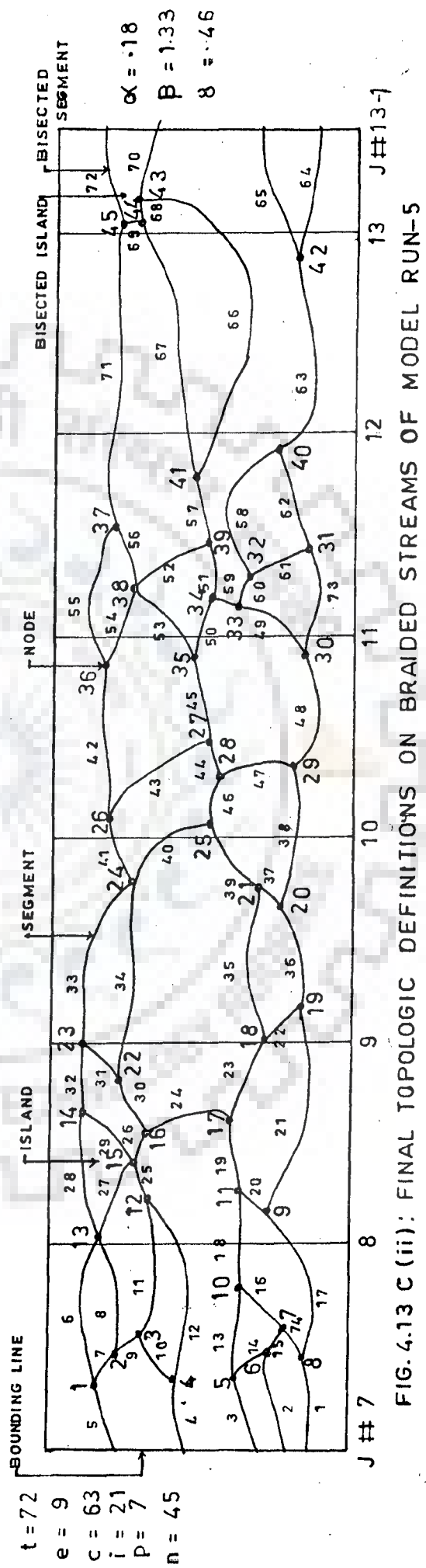
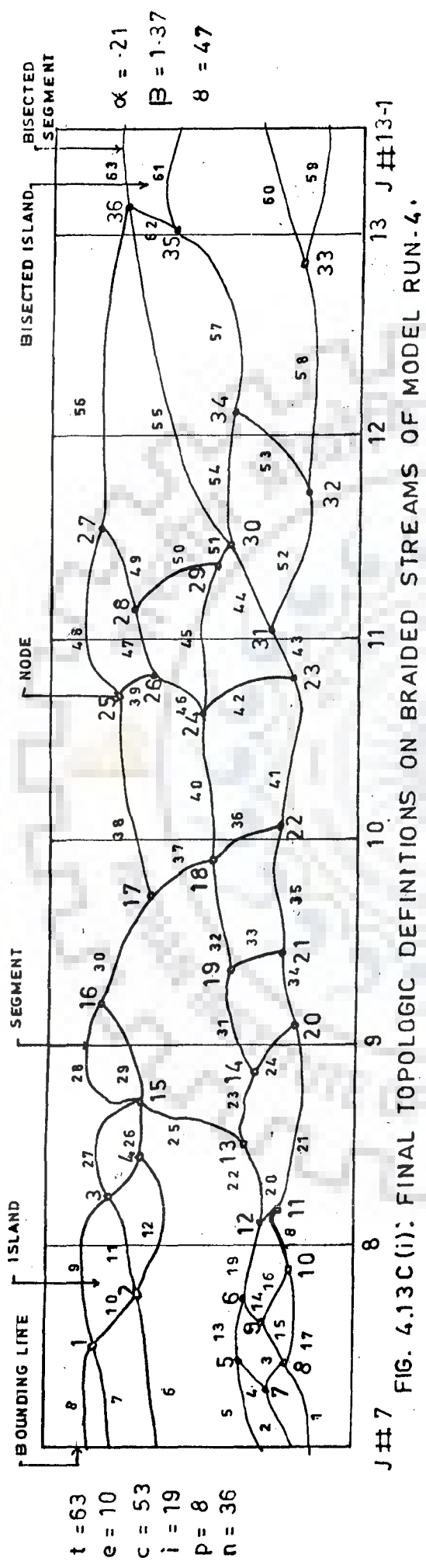
FIG. 4.13b(i): FINAL TOPOLOGIC DEFINITIONS ON BRAIDED STREAMS OF MODEL RUN-2



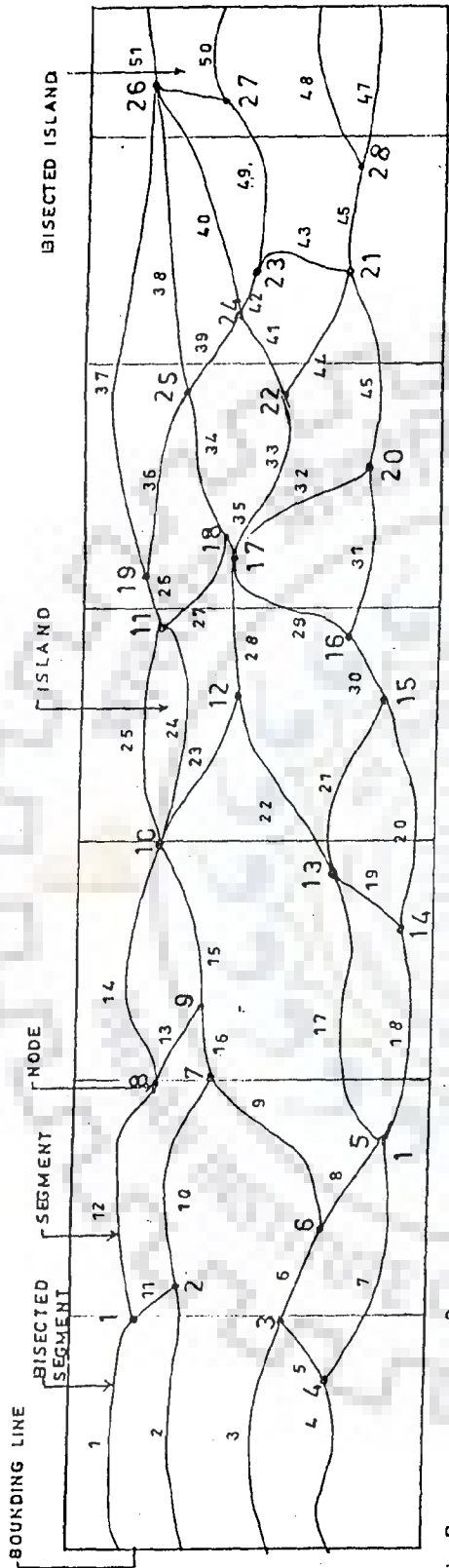
J#7

8 9 10 11 12 13 J#13-1

FIG. 4.13b(ii): FINAL TOPOLOGIC DEFINITIONS ON BRAIDED STREAMS OF MODEL RUN-3



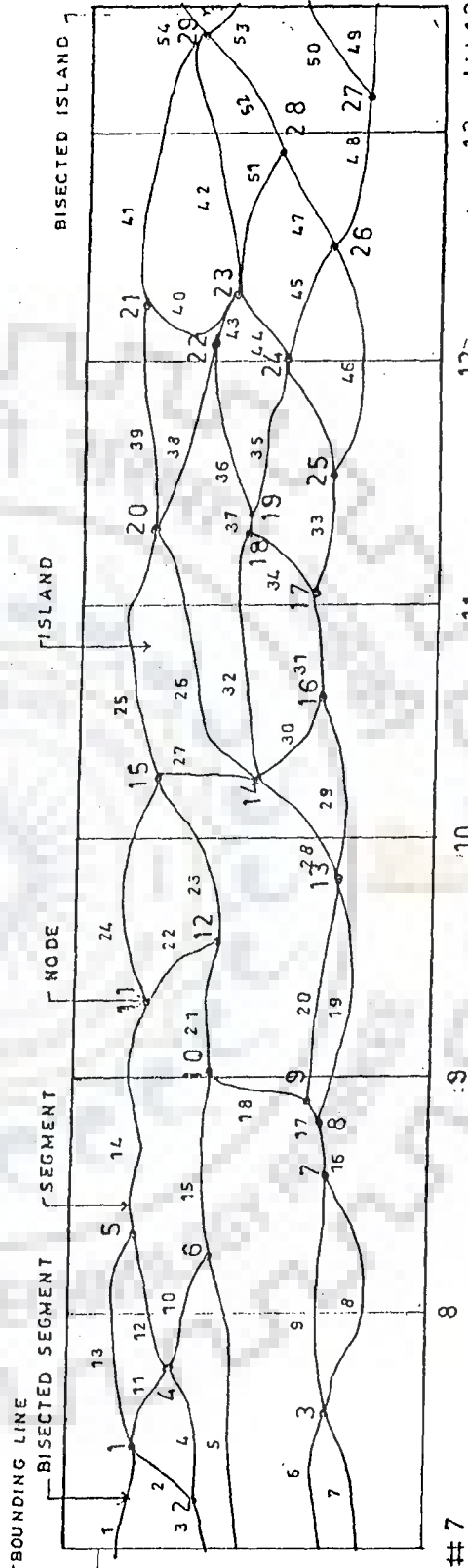
t = 51
 e = 8
 n = 28
 C = 43
 i = 17
 p = 6



$\alpha = .27$
 $\beta = 1.14$
 $\delta = .5$

J# 7 8 9 10 11 12 13 J# 13-1
 FIG. 4.13d(i): FINAL TOPOLOGIC DEFINITIONS ON BRAIDED STREAM OF MODEL RUN-6

t = 54
 e = 9
 n = 29
 C = 45
 i = 18
 p = 7



$\alpha = 24$
 $\beta = 1.42$
 $\delta = .5$

J# 7 8 9 10 11 12 13 J# 13-1
 FIG. 4.13d(ii): FINAL TOPOLOGIC DEFINITIONS ON BRAIDED STREAM OF MODEL RUN-7

Table 4.6: VALUES OF ALPHA (α), BETA (β) AND GAMMA (γ) INDEX FOR MODEL STUDY (HOWARD ET AL. 1970)

Run no.	Values of parameters	Alpha Index		Beta Index		Gamma Index		Remarks
		Initial	Final	Initial	Final	Initial	Final	
MR1	t =49 e =8 n =26	0.27	0.25	1.48	1.44	0.52	0.51	Model study Brahmapur ra river
MR2	t =55 e =9 n =30	0.27	0.23	1.48	1.41	0.52	0.49	
MR3	t =72 e =10 n =40	0.27	0.24	1.48	1.44	0.52	0.5	
MR4	t =63 e =10 & n =36	0.27	0.21	1.48	1.37	0.52	0.47	
MR5	t =72 e = 9 & n =45	0.27	0.18	1.48	1.33	0.52	0.46	
MR6	t =51 e =8 & n =28	0.27	0.27	1.48	1.14	0.52	0.5	
MR7	t =54 e =9 n =7	0.27	0.24	1.48	1.42	0.52	0.5	

Table-4.7 RANGES OF VALUES OF PFI, FGI, CROSS-SLOPE, BRAIDING INDEX, TOTAL SINUOSITY AND COMPOSITE INDEX I₁ AND COMPOSITE INDEX I₂

Different Parameters	Range for moderately braided (Sharma, 1995)	Laboratory Experimental Data	Field Data of Bramaputra R.	Model Experiments	MDBJR*-EGIS and Delft Hydraulics (1997)
Cross-slope (Sharma, 1995)	170-800		157-1062.2		
Plan Form Index (Sharma, 1995)	19-4	23.86-96.3	2.79-53.93		
Flow Geometry Index (Sharma, 1995)	7-35	0.23-19.94	2.953-19.31		
Braiding Index (Brice 1964)		0.307-2.58	-		
Braiding Index (Mosley 1981)		1.14-2.22	-		
Braid Channel Ratio (Friend & Sinha, 1993)		1.144-2.226	-		
Total Sinuosity (Richards, 1982)		1.23-2.35	-		
Braiding Index :					
(a) Braiding intensity					2.67 - 7.33 (EGIS) 1.60 - 4.30 (Klassen & Vermeer in 1988 (MDBJR*-EGIS, 1997))
(b) Total Sinuosity					2.38 - 7.70 (EGIS) 3.06 - 7.72 (FAPI)
Composite Index I ₁ (Proposed)		228.43-922.35	266.47-7889.7	336.63-1125.42	<
Composite Index I ₂ (Proposed)		0.067-5.13	0.979-6.41	1.6999-14.529	

* Morphological Dynamics of the Brahmaputra - Jamuna River

4.4 CONCLUDING REMARKS

In this Chapter, different indicators have been studied for their performance evaluation as an braiding index. Many a time, these do not show any consistent or discernible trend with the B/D ratio. This raises a doubt over their use as a braiding indicator. In this respect, use of two composite indicators through suitable modification of the indices formulated by Sharma (1995) has been also explored in this work and partially better results have been obtained. Parker's approach works well for the demarcation of braided regime. Richardson and Thorne (2001) approach also works well for the demarcation of multi-thread and single thread rivers. Indices proposed by Howard et al. (1970) work well for well-defined topological patterns. However, it is difficult to interpret these indices for complicated topological patterns.

MODELLING OF FLOW RESISTANCE IN A BRAIDED STREAM

5.1 INTRODUCTION

In Indian sub-continent, the river Brahmaputra is recognised as one of the most important rivers. On a global level too, the river ranks, fifth in terms of discharge, third in terms of sediment discharge, and eleventh in terms of drainage area (Thorne et al., 1993). The river is particularly known for its braiding characteristics. To-date the resistance relationship in case of such a braided river is hardly investigated, although existing design of hydraulic structures on the river Brahmaputra imply Manning's relationship as the representative of appropriate resistance relationship. The consequences of using a constant value of Manning's rugosity co-efficient have not been investigated in case of a braided stream like the Brahmaputra. The present study considers a typical stretch of river Brahmaputra in Bangladesh. The length of this river stretch under study is approximately 160 km. and width of the river varies around from 5 to 16 km within this stretch. Based on the data spanning nearly a decade, the study considers use of constant Manning's rugosity co-efficient. Based on such an evaluation, it is found that Manning's 'n' is not a constant and it depends on the flow and channel characteristics. Subsequently, several alternate expressions for Manning's rugosity coefficient have been either derived or used as reported in the literature. Poor performance of these expressions has led to the

development of a semi-empirical relationship for the Manning's n . Using this relationship, it was observed that the calibrated Manning's rugosity co-efficient, when used to calculate water discharges in the river reflects better agreement with the observed discharges.

Modelling of flow resistance in alluvial rivers is a very old practice. The widely used flow resistance relationship is the one proposed by an Irish Engineer, Robert Manning. This relationship, referred to as Manning's relationship in this study, is also known as Gauckler-Manning-Strickler relationship (Hager, 2001) and has been used to describe flow resistance in several studies. Other resistance laws have been also proposed from time to time. A comparison between many resistance relationships with the Manning's relationship indicates that Manning's rugosity coefficient, ' n ', can not be always assumed constant and it may be necessary to include certain functional relationship for Manning's n . This will mean an identification of appropriate relationship for Manning's n . Hager (2001) correctly points out that the Gauckler-Manning-Strickler formula is currently the most popular power formula for estimating the relationship between cross-sectional average velocity, hydraulic gradient, and hydraulic radius for both closed-conduit and uniform open-channel flows. Beltaos (2001) has shown the application of Manning's relationship in representing the roughness of ice jams. This study also presents certain relationships involving friction factor and Manning's rugosity coefficient.

The Brahmaputra river is known for its braiding characteristics (Goswami, 1985; Richardson and Thorne, 2001). In case of the Brahmaputra river, no serious attempts were made in the past to collect the data. This is also apparent from the studies of

Goswami (1985), where hardly any information about the resistance relationship in case of such a highly braided stream, is provided. With a view to investigate the flow resistance characteristics of this large braided river, it has been possible to have access to nearly a decade's data from the authorities in Bangladesh, who have been collecting the data in a typical stretch of this river.

In fact, the availability of the data has prompted to perform the analysis of flow resistance in this stretch of the river. Fig. 3.1 provides a general layout of the river in Bangladesh. Fig. 3.2 depicts the river stretch. The study reach is confined from Bahadurabad to Daulatdia-ArichaBaruria that has braidplains width up to 20 km. and carries 500 million tones sediments annually. In the study reach, the river is braided with numerous small bars and fewer large islands, locally called *chars*, which divide the flow into sub-channels called anabranches. Prior to the analysis of flow resistance in the study reach, certain relationships for the Manning's rugosity coefficient are reviewed and tested for their performance. In addition, certain new relationships for this coefficient are also derived. During the modelling of the flow resistance, limitations of these relationships in representing the flow resistance was observed. With this in view, several attempts were made to search for alternate relationships. The present study outlines such alternate relationships for Manning's n in describing the flow resistance of this highly braided stream of Indian subcontinent.

5.2 MANNING'S RESISTANCE RELATIONSHIP

Many resistance relationships have been used to describe the flow resistance in alluvial streams; however, Manning's resistance relationship enjoys the popularity because of its simplicity. The relationship is expressed as

$$U = \frac{1}{n} R^{2/3} S^{1/2} \quad (5.1)$$

in which U = average velocity in m/s; R = hydraulic radius in meter; and S = slope of channel.

In equation (5.1), n is known as Manning's rugosity coefficient.

Hager [1989] considers the applicability of equation (5.1) to hydraulically rough surface, when the following conditions are satisfied, i.e.

$$\epsilon \geq 30 \nu [Q(gS)]^{-0.2} \quad (5.2a)$$

$$0.004 \leq \frac{\epsilon}{R} \leq 0.04 \quad (5.2b)$$

in which ϵ = average roughness height of the channel surface; ν = kinematic viscosity of the water; and Q = channel or stream discharge.

Despite the condition imposed by (5.2), Manning's equation has found that application is describing flow resistance of alluvial streams. This has resulted in several expressions for n , some of which are described for their relevance to the present study.

In terms of d_{50} size of the bed material, Strickler (Garde and Ranga Raju, 2000) proposed the following equation for n , i.e.

$$n = \frac{d_{50}^{1/6}}{25.6} \quad \text{in SI unit} \quad (5.3)$$

in which d_{50} = median grain size in mm

Limerinos (Beltaos, 2001) proposed the following expression

$$n = \frac{0.113 R^{1/6}}{1.16 + 2.0 \log \frac{R}{d_{84}}} \quad (5.4)$$

in which d_{84} = the intermediate particle size diameter; n = Manning's roughness coefficient; and R = hydraulic radius. It is noted that eq. (5.4) is in MKS units. Jarrett (1984) observed the very good performance of eq. (5.4) with many data.

In addition, several resistance relationships can be used to derive expression for n . For example, Leopold et al. (1964) as referred by Burkham and Dawdy (1976) proposed the following relationship

$$\frac{U}{U_*} = 2.83 + 5.75 \log \frac{D}{d_{84}} \quad (5.5)$$

in eq. (5.5), D = mean depth of flow in cross section; d_{84} = particle size at which 84% of bed material by weight is finer; and U_* = shear velocity.

Shear velocity is given by

$$U_* = \sqrt{g R S} \quad (5.6)$$

Thus, using eq. (5.5) and eq. (5.6) and a comparison with eq. (5.1), leads to the following expression for 'n':

$$n = \frac{R^{1/6}}{\sqrt{g} \left(2.85 + 5.75 \log \frac{D}{d_{84}} \right)} \quad (5.7)$$

5.3 MANNING'S RESISTANCE RELATIONSHIP BASED ON A GENERALISED FRICTION FACTOR MODEL

The relationships available for coefficient of friction can be utilized to obtain an expression for n . For example, similar to a pipe flow, one can use Darcy-Weisbach expression for a channel

$$h_f = \frac{f L U^2}{8 g R} \quad (5.8)$$

For a uniform flow, $S = h_f / L$.

Thus,

$$U = 2^{3/2} \sqrt{g} R^{1/2} S^{1/2} f^{-0.5} \quad (5.9)$$

Comparing eq. (5.9) with eq. (5.1) may lead to the following relationship between n and f .

$$n = \frac{R^{1/6}}{\sqrt{g}} \cdot \frac{1}{2^{3/2}} \cdot \sqrt{f} \quad (5.10)$$

For open channel flow, Friction [1963] has given the following expression

$$f = 1.325 \left[\ln \left(\frac{\epsilon}{12R} + \frac{0.625\nu}{UR\sqrt{f}} \right) \right]^{-2} ; 10^3 \leq \frac{UR}{\nu} \leq 10^8 ; 10^{-6} \leq \frac{\epsilon}{R} \leq 10^{-2} \quad (5.11)$$

From eq. (5.9), one gets

$$U\sqrt{f} = 2^{3/2} \sqrt{g} R^{1/2} S^{1/2} \quad (5.12)$$

Substituting for $U f^{0.5}$ from eq. (5.12) into eq. (5.11), one obtains

$$f = 1.325 \left[\ln \left(\frac{\epsilon}{12R} + \frac{0.625\nu}{2^{3/2} R \sqrt{g} R S} \right) \right]^{-2} \quad (5.13)$$

From eq. (5.13), one can obtain

$$\sqrt{f} = \sqrt{1.325} \cdot \frac{1}{\ln\left(\frac{\epsilon}{12R} + \frac{0.625 \nu}{2^{3/2} R \sqrt{gRS}}\right)} \quad (5.14)$$

$$\text{or, } \sqrt{f} = -\sqrt{1.325} \cdot \frac{1}{\ln\left(\frac{\epsilon}{12R} + \frac{0.625 \nu}{2^{3/2} R \sqrt{gRS}}\right)} \quad (5.14a)$$

Using eq. (5.10) and eq. (5.14 b), the following expression for n is written

$$n = \frac{-R^{1/6} \sqrt{1.325}}{\sqrt{g}} \cdot \frac{1}{2^{3/2} \ln\left(\frac{\epsilon}{12R} + \frac{0.221 \nu}{2^{3/2} R \sqrt{gRS}}\right)} \quad (5.15)$$

Or,

$$n = \frac{R^{1/6}}{\sqrt{g}} \cdot (-2.457) \cdot \frac{1}{\ln\left(\frac{\epsilon}{12R} + \frac{0.221 \nu}{R \sqrt{gRS}}\right)} \quad (5.16)$$

5.4 DETAILS OF DATA

Discharge and water level data (1988-1997) of the Brahmaputra river at Bahadurabad and ArichaBaruria transit have been collected from the Hydrology Department of Bangladesh Water Development Board (BWDB). The required water surface slopes for different discharges have been worked out by considering the water levels at Bahadurabad and ArichaBaruria Transit along the river Brahmaputra. The areas of cross-section data for the period of 1988-1997 at the three different sections have been collected from the river morphology department of BWDB. Figs.3.4 (a, b & c) show the cross-sections at sections A-A, B-B and C-C of Fig. 3.2 for different years of period 1988-1997. The relative data for this study are indicated in the Table A2.1 of Appendix-

II. Hydraulic mean depth, D is obtained by dividing the total flow cross-sectional area by effective water width, as suggested by Brice (1964). The water surface slope has been considered channel in the present analysis. The values of d_{50} and d_{84} are 0.21 mm and 0.265 mm, respectively. Table 5.1 represents different n values calculated by different approach.

5.5 ANALYSIS OF DATA

To describe the resistance relationship, we considered three strategies: A, B and C. The strategy A considers the use of a constant value of n . The reason for choosing this strategy is that this has been used in the past as a basis of describing flow resistance of this river and designing of some hydraulic structures (Report, 1999). The strategy B considers the evaluation of Limerinos relationship. This relationship is very similar in functional form to a class of relationships referred by Burkham and Dawdy (1976). The strategy C is based on eq. (5.16). In contrast to strategy B, strategy C is based on a generalised friction factor expression and to the best of existing knowledge, this strategy has so far not been attempted in describing the flow resistance of alluvial streams. To rank the relative performance of different strategies, the following error metric is used:

$$E = \frac{100}{N} \sum_{i=1}^N \left| \frac{Q_{observed} - Q_{computed}}{Q_{observed}} \right| \quad (5.17)$$

In eq.(5.17), N represents the number of data points and i is the index. Table 5.2 summarizes the performance of error metric for different strategies. Almost in all the strategies, E is large indicating the need for further reduction of it through development of an improved relationship for Manning's rugosity coefficient.

Table- 5.1: VALUE OF 'n' AS PER DIFFERENT APPROACHES FOR FIELD DATA

Existing 'n'	Constant 'n'	Limerinos 'n'	'n' based on eq. (5.16)	'n' based on eq.(5.18)	'n' based on eq. (5.19)
0.057	0.010	0.015	0.056	0.086	0.070
0.051	0.010	0.016	0.055	0.104	0.083
0.075	0.010	0.016	0.055	0.093	0.075
0.102	0.010	0.016	0.055	0.107	0.086
0.116	0.010	0.016	0.055	0.094	0.076
0.088	0.010	0.016	0.054	0.088	0.074
0.096	0.010	0.016	0.054	0.070	0.061
0.070	0.010	0.015	0.061	0.050	0.040
0.042	0.010	0.015	0.066	0.035	0.028
0.059	0.010	0.015	0.064	0.038	0.030
0.036	0.010	0.015	0.059	0.060	0.048
0.049	0.010	0.015	0.067	0.031	0.025
0.019	0.010	0.015	0.066	0.035	0.028
0.017	0.010	0.014	0.075	0.021	0.017
0.048	0.010	0.015	0.062	0.045	0.036
0.035	0.010	0.015	0.064	0.039	0.031
0.021	0.010	0.014	0.078	0.017	0.013
0.080	0.010	0.015	0.061	0.042	0.035
0.046	0.010	0.015	0.061	0.048	0.038
0.019	0.010	0.015	0.061	0.037	0.03
0.011	0.010	0.015	0.064	0.029	0.024
0.020	0.010	0.015	0.065	0.037	0.029
0.017	0.010	0.016	0.065	0.022	0.019
0.020	0.010	0.015	0.063	0.030	0.025
0.024	0.010	0.015	0.064	0.027	0.023
0.029	0.010	0.015	0.065	0.027	0.022
0.022	0.010	0.015	0.065	0.040	0.032

Table 5.2: AVERAGE PERCENTAGE ERROR WITH DIFFERENT APPROACHES FOR FIELD AND LABORATORY DATA

Approach	FIELD (Total Cross-Section)	EXP.LAB. STUDY	FIELD (Sub-division Cross-Section)	MODEL STUDY
	Error Metric, E	Error Metric, E	Error Metric, E	Error Metric, E
Constant n based on bed particle size $d_{50} = 0.21$ mm for field and $d_{50} = 0.22$ mm for lab. (eq.5.3)	393.20	131.5004	454.58	140.23
Limerinos (eq. 5.4)	212.00	83.36	247.71	93.26
Leopold et al. (eq. 5.7)	212.00	232	222	214
Total friction factor (eq. 5.16)				
$\epsilon = d_{84}$	48.30	54.5	62.62	67
$\epsilon = 2 d_{84}$	50.10	55.66	65	80.2
$\epsilon = 3.16 d_{84}$	51.20	59.88	67	87.5
Proposed approach (eq. 5.18) for field data	31.90		37.85	33.90
Proposed approach (eq. 5.19) for field data	31.75		38.2	
Equation (5.20a) for lab. experiments Phase-I		11.3		
Equation (5.20b) for lab. experiments Phase-I		12.5		

5.6 TESTING OF NEW RELATIONSHIP

Thus, in view of Table 5.2, an attempt is made herein to relate Manning's n with other flow parameters. From eq. (5.16), it can be seen that Manning's n is related to two dimensionless groups, i.e. d_{50}/R , and $v/(gR^3S)^{0.5}$. Using these groups, various relationships for n were attempted including power relations as well as linear combinations. The one, which corresponded to a minimum E , had the following functional form

$$n = 3.0 \times 10^{-7} * \left[\frac{0.15 d_{50}}{12 R} + \frac{0.221 * 0.85 * v}{R \sqrt{g R S}} \right]^{-0.8933} \quad (5.18)$$

Average error associated with the use of equation eq. (5.18) is estimated as 31.9% at existing water level and this is much better when compared with the average errors reported in Table 5.2. Fig. 5.1 presents the agreement diagram between observed and computed discharges using eq. (5.18). It can be seen that 80% of the data fall within a 30% error bandwidth. Another relationship, which is dimensionless in nature, is also obtained as

$$\frac{n \sqrt{g}}{R^{\frac{1}{6}}} = 3.9 \times 10^{-6} * \left[\frac{0.15 d_{50}}{12 R} + \frac{0.221 * 0.85 * v}{R \sqrt{g R S}} \right]^{-0.7723} \quad (5.19)$$

The error with eq. (5.19) is found nearly same as eq.(5.18). The agreement diagram using eq.(5.19) is also shown in Fig. 5.2.

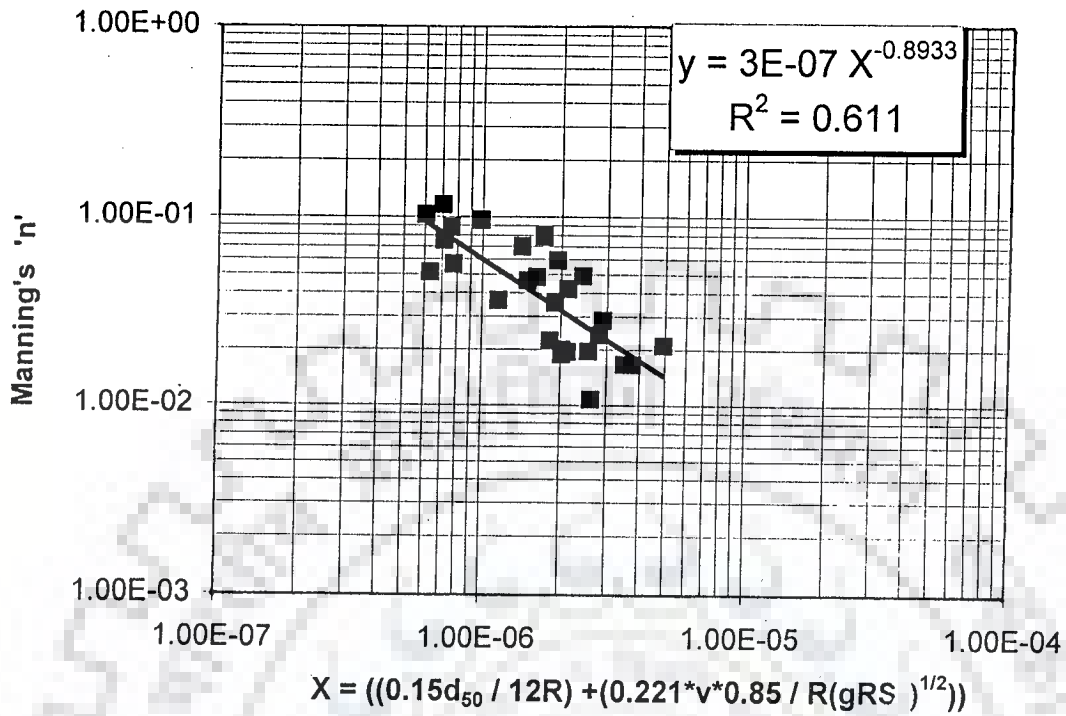


FIG. 5.1a: VARIATION OF MANNING'S 'n' WITH PROPOSED DIMENSIONLESS TERM, X FOR FIELD DATA

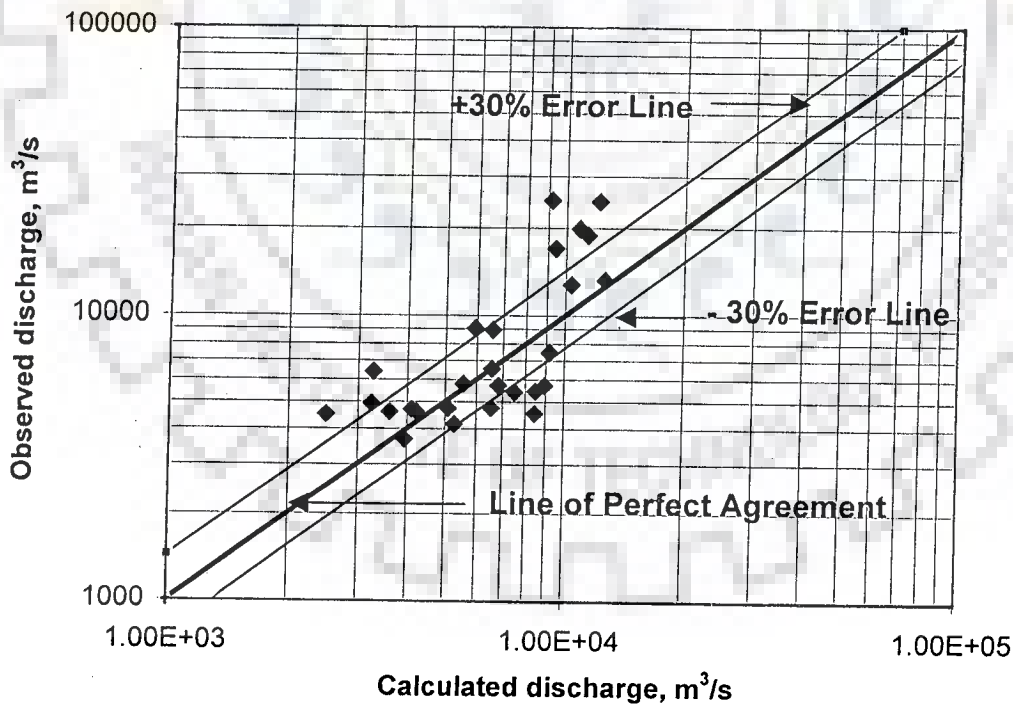


FIG. 5.1b: AGREEMENT BETWEEN CALCULATED (CONSIDERING TOTAL CROSS-SECTION) AND OBSERVED DISCHARGES

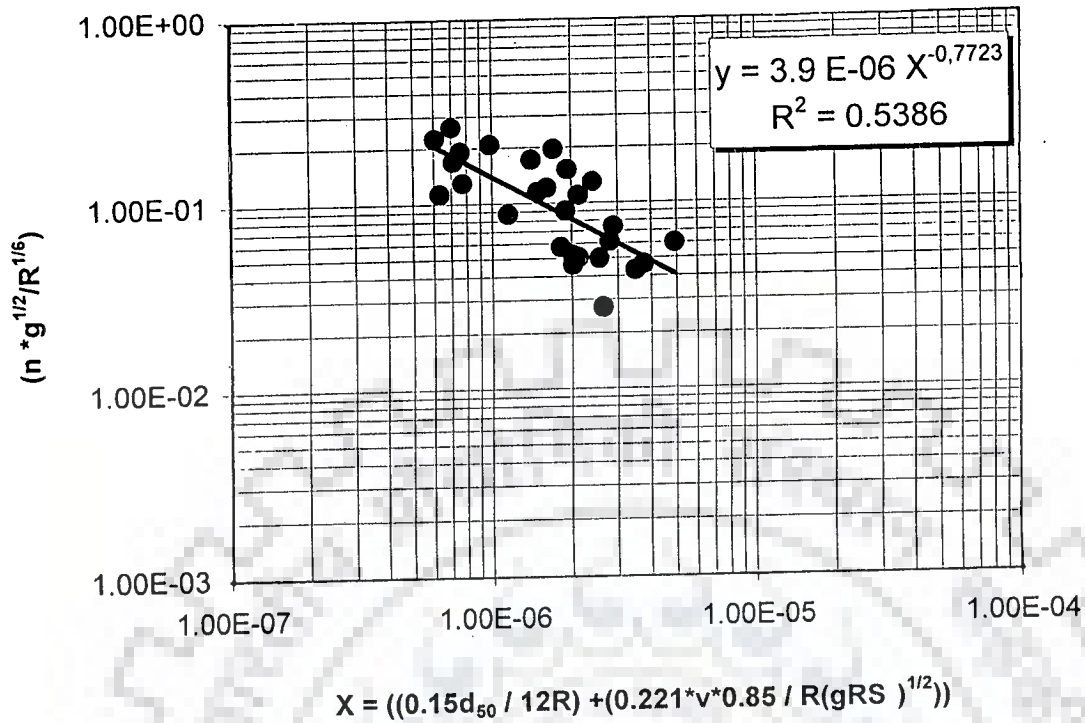


FIG. 5.2a: VARIATION OF $(n * g^{1/2} / R^{1/6})$ WITH PROPOSED DIMENSIONLESS TERM, X FOR FIELD DATA

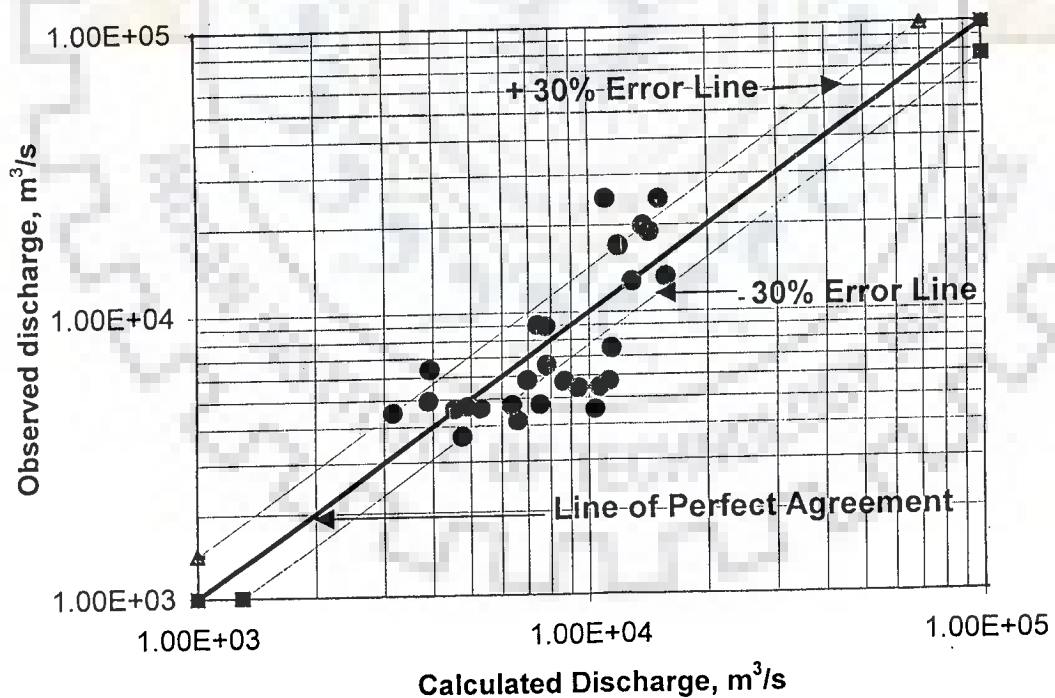


FIG. 5. 2b: AGREEMENT BETWEEN CALCULATED (CONSIDERING TOTAL CROSS-SECTION) AND OBSERVED DISCHARGES

5.7 DISCUSSION OF RESULTS

The data analysis of the present study has clearly shown that use of a constant value of rugosity coefficient 'n' in Manning's equation for the case of a braided stream is fraught with substantial degree of error of the order of about 400%, which is expected to adversely reflect on the resultant hydraulic computations. Thus, one should avoid using a Manning's n based on a given bed particle size. The error metric may very well be reduced by using an optimized value of constant n. In the present work, this possibility was investigated and it was observed that at a constant n value of 0.059155, E drops to as low as 47.30 %.

Moreover, the utility of functional forms of Limerinos (Beltaos, 2001) and eq. (5.16) was also considered in this work. However, in none of the situations, E could be reduced below that obtained using eq. (5.18) or eq. (5.19). However, in preference to the Limerinos or Leopold relationship, eq. (5.16) showed a better performance in obtaining lesser E (Table 5.2). From Table 5.2 it can be seen that the error metric is sensitive to the choice of ϵ . Results for three different values of ϵ are shown in the Table-5.2. In a recent study, Beltaos (2001) has also used $\epsilon = 3.16 d_{84}$. The merit of eq.(5.16 or 5.14) lies in the fact that it helped us to identify the important dimensionless groups leading to the functional form of eq. (5.18). In this context, it is noted that the performance of eq.(5.16), despite the variability of ϵ with d_{84} , is better than the existing relationships. At this stage, it is equally important to realise that the performance of eq. (5.16) has been compared with existing relationships under same set of conditions. It is also possible to divide the cross-sections into many parts and refine the analysis. An attempt in this regard was also made. However, even with smaller cross-sections, similar performance of resistance

relationships was observed and eq. (5.16) still maintained its superiority. Results for sub-cross sections are reported in the Table 5.2. We also believe that as eq. (5.16) represents a generalisation of Manning's n relationship based on a generalised friction factor formula, it will have a better potential of representing flow resistance.

To further evaluate the utility of the functional representation given by eqs. (5.18) and (5.19), the model runs of phase-I are also analysed. The following relationship for Manning's rugosity coefficient has been calibrated

$$n = 0.0044 \times \left(\frac{0.15d_{50}}{12R} + \frac{0.85 \times 0.221v}{R\sqrt{gRS}} \right)^{-0.1732} \quad (5.20a)$$

and another relationship, which is dimensionless in nature, is also calibrated as

$$\frac{n\sqrt{g}}{R^{1/6}} = 0.0616 \times \left(\frac{.15d_{50}}{12R} + \frac{0.85 \times 0.221v}{R\sqrt{gRS}} \right)^{-0.0744} \quad (5.20b)$$

The agreement diagram using eq. (5.20a) is shown in Fig. 5.3a. It can be seen that 70 % of the computed discharge data fall within 11% error band width. The agreement diagram using eq. (5.20b) is shown in Fig. 5.3b. Using the scaled discharges of the phase-II experiments, an attempt has been also made to test the validity of eq. (5.18). The agreement diagram has shown in the Fig. 5.4. for model study phase-II using eq.(5.18) for n . The error metric has got 33.90% for this model study, which is almost similar to the error metric (E) of the field study. The values of d_{50} and d_{84} are 0.22 mm and 0.285mm, respectively for laboratory channel bed materials.

Resistance parameters have been used as an index to characterise the braiding phenomenon as shown in Figs. 5.5a, 5.5b, 5.6a and 5.6b.

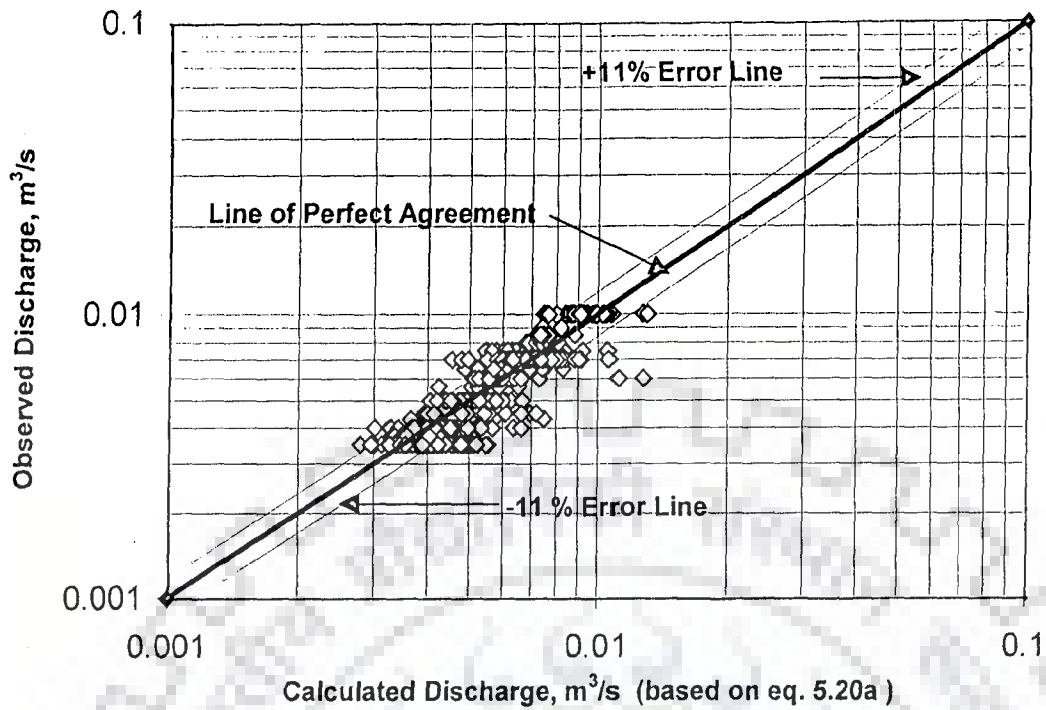


FIG. 5.3 a: AGREEMENT BETWEEN OBSERVED AND CALCULATED DISCHARGES FOR LABORATORY EXPERIMENTAL DATA

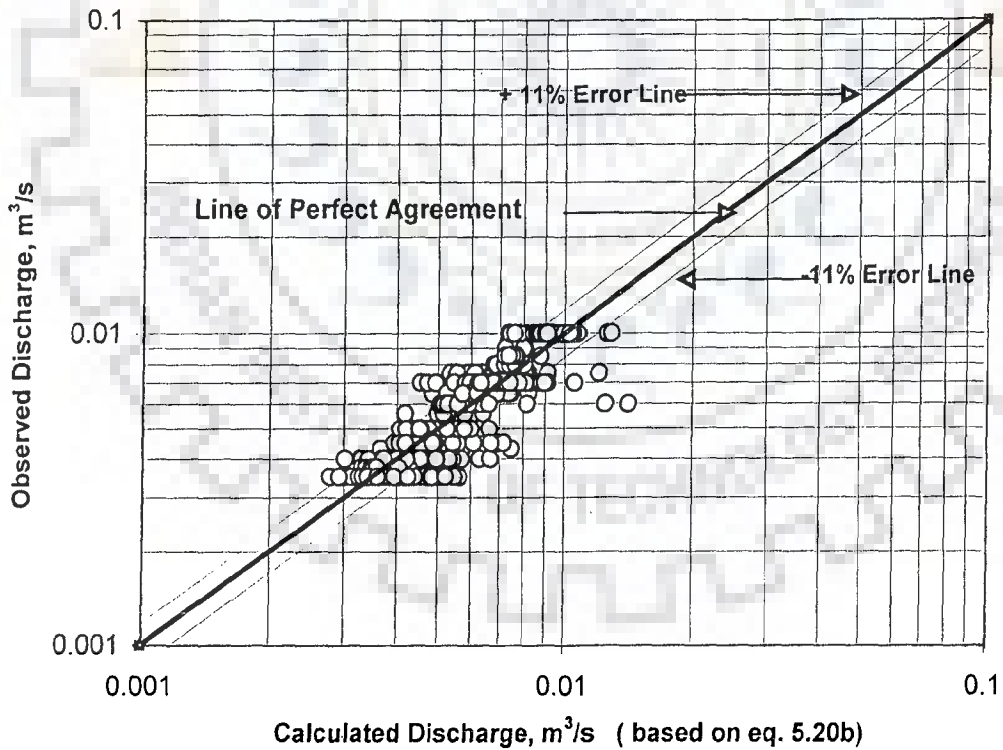


FIG. 5.3b : AGREEMENT BETWEEN OBSERVED AND CALCULATED DISCHARGES FOR LABORATORY EXPERIMENTAL DATA

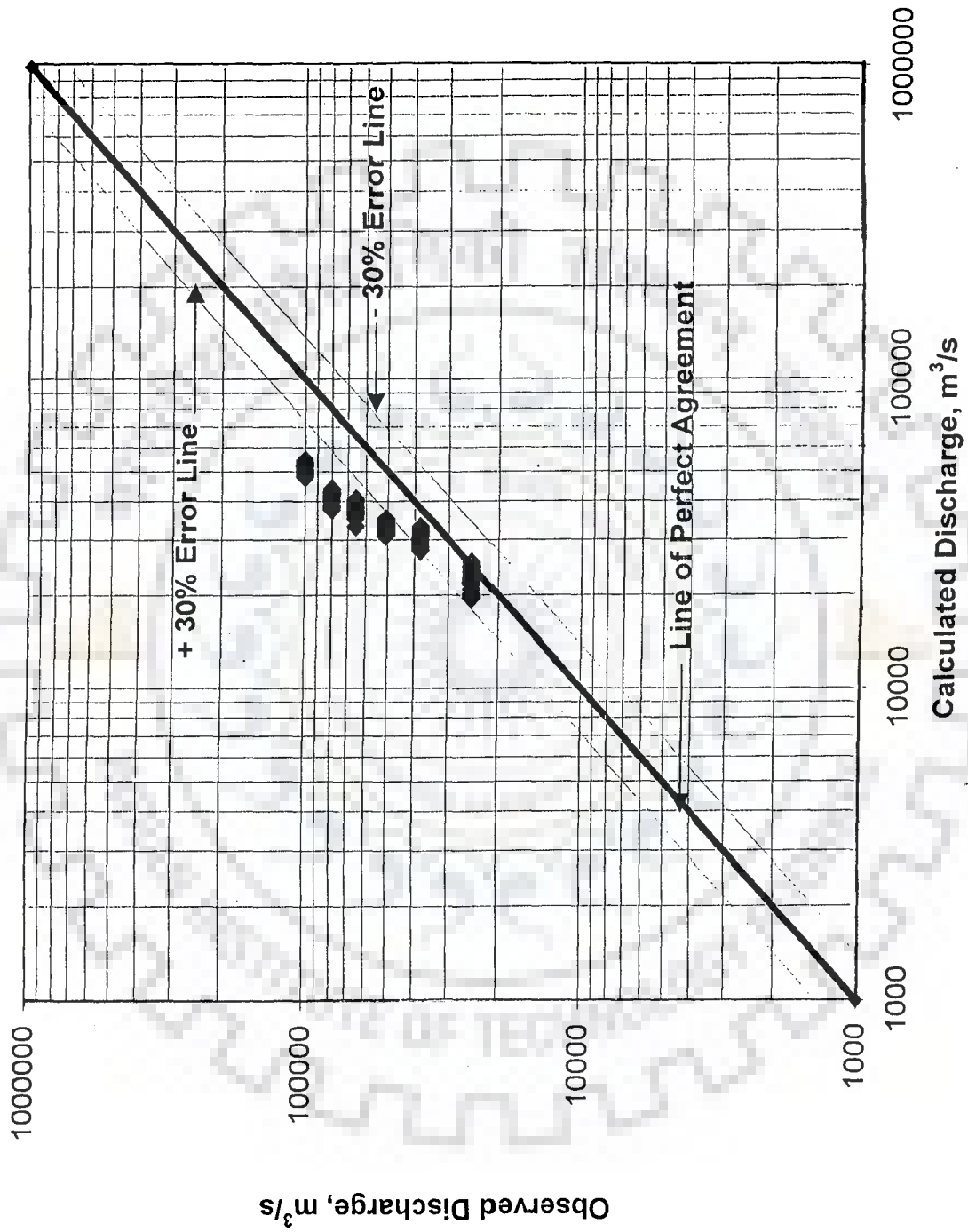


FIG. 5.4; AGREEMENT BETWEEN OBSERVED AND CALCULATED DISCHARGES FOR MODEL STUDY BASED ON EQ.(5.18)

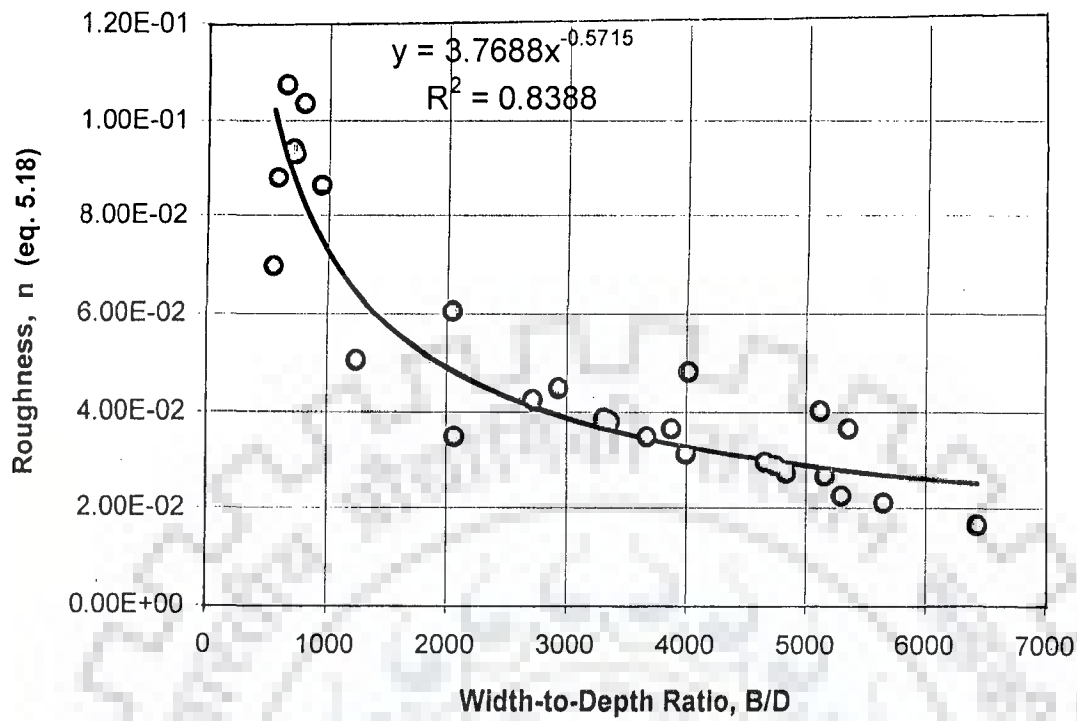


FIG. 5.5a: VARIATION OF ROUGHNESS 'n' (EQ. 5.18) WITH B/D RATIO FOR FIELD DATA

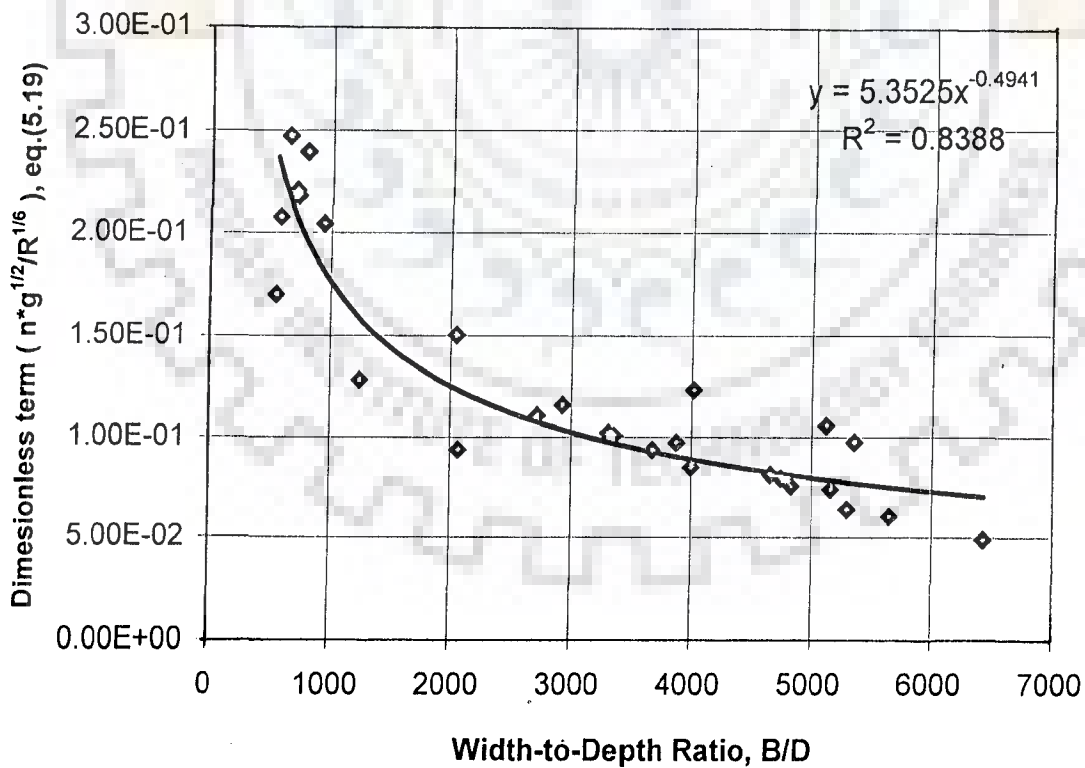


FIG. 5.5 b: VARIATION OF DIMENSIONLESS TERM ($n \cdot g^{1/2} / R^{1/6}$) WITH B/D RATIO FOR FIELD DATA

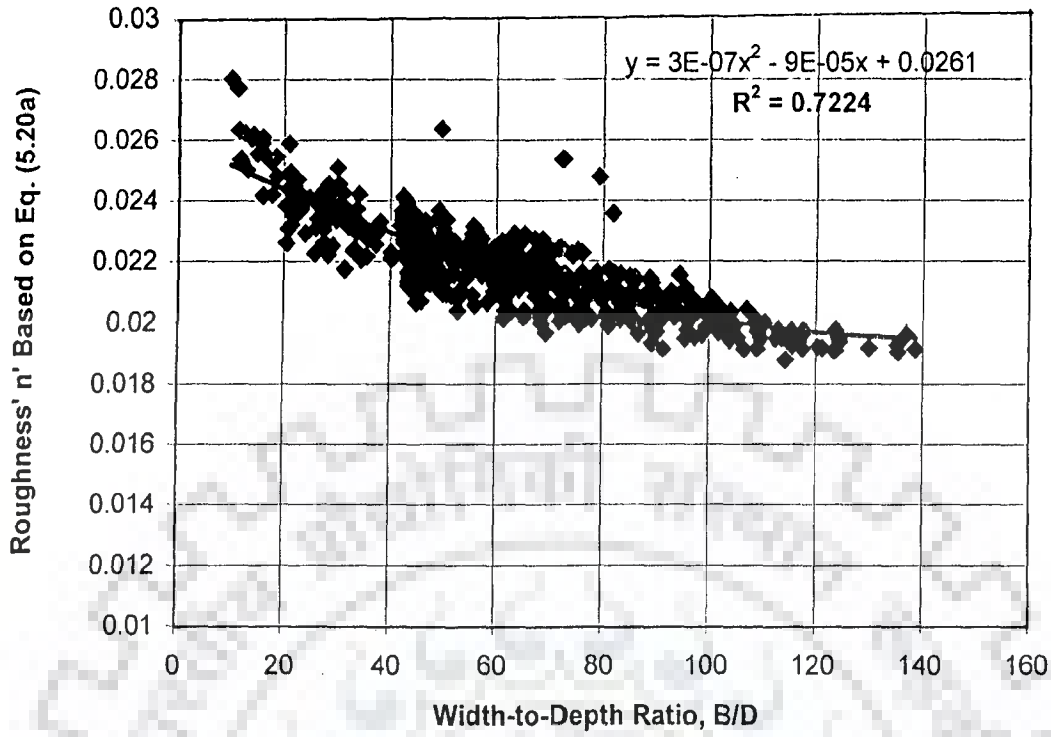


FIG. 5.6a VARIATION OF ROUGHNESS 'n' BASED ON PROPOSED TERM X (EQ. 5.20a) WITH B/D RATIO FOR LABORATORY EXPERIMENTAL DATA

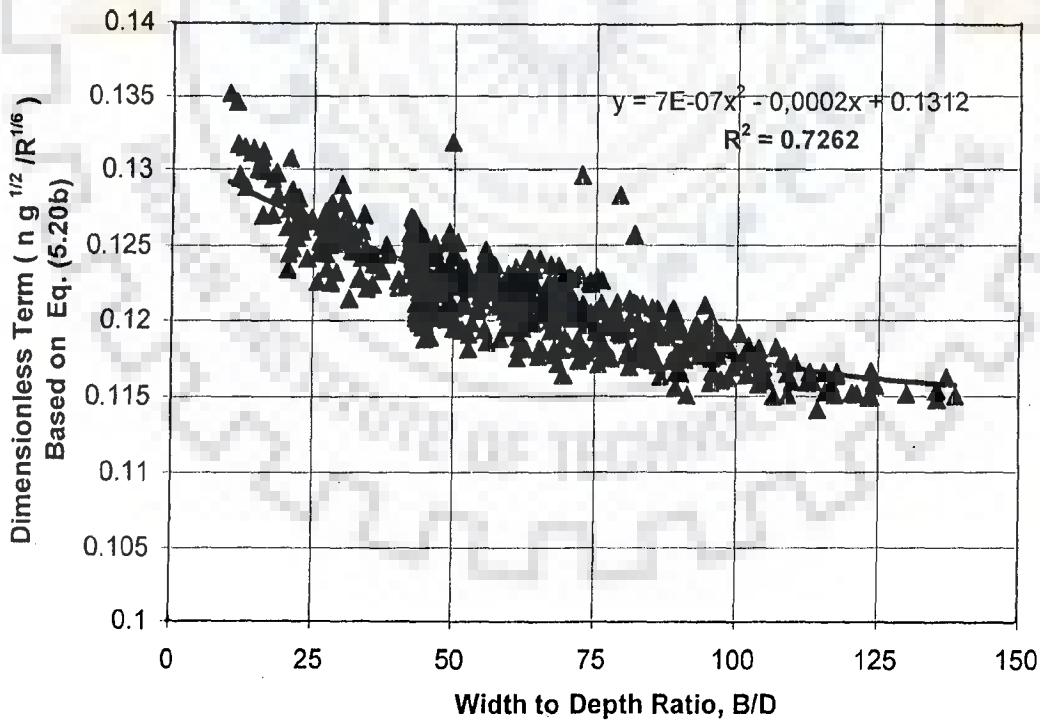


FIG. 5.6b VARIATION OF DIMENSIONLESS TERM ($n g^{1/2} / R^{1/6}$) BASED ON Eq. (5.20b) WITH B/D RATIO FOR LABORATORY EXPERIMENTAL DATA

5.8 CONCLUDING REMARKS

Based on this study, the following conclusions can be made:

- Use of constant value of Manning's n based on a given bed particle size may not always be a better indicator of flow resistance.
- Performance of certain well-established relationship including Limerinos (Beltaos, 2001) and Leopold et al. (Burkham and Dawdy, 1976) is not very satisfactory in describing the flow resistance of braided stream like the Brahmaputra.
- A formula for Manning's n based on a generalised friction factor has been developed and is likely to have merit over using the formulae, which are particular cases of it.
- Using the dimensionless groups of the proposed Manning's relationship using a generalised friction formula, empirical relationships, which describe the flow resistance in a typical stretch of the river Brahmaputra are developed in this work. These relationships are found to have an edge over some of the popular resistance relationships tested in this study.
- Resistance parameter can also be used as an index to characterise the braiding phenomenon.

EXTREMAL HYPOTHESES AND ENTROPY THEORY

6.1 INTRODUCTION

In recent years, researchers are devoted in understanding how the geometry of self-formed alluvial streams achieves equilibrium. In this work, it has been attempted to apply extremal hypotheses for prediction of probable channel behaviour. The thrust is on examining the potential of the extremal hypotheses in application to morphological study of braided streams involving laboratory as well as field data. Entropy of various systems is also found helpful in explaining many of their characteristics. With this in view, entropy related aspects applied to braided streams are presented and analysed.

6.2 EXTREMAL HYPOTHESES

Many researchers have worked on Extremal Hypotheses for study of river behaviour. Yang et al. (1981) identified a parameter, MEDR, termed as 'minimum energy dissipation rate' and stated that 'a system is in an equilibrium condition when its rate of energy dissipation is at a minimum value. This minimum value depends on the constraints applied to the system. When a system is not in an equilibrium condition, its rate of energy dissipation is not at its minimum value. However, the system will adjust in

such a manner that the rate of energy dissipation can be reduced until it reaches the minimum and regains equilibrium'. The rate of energy dissipation Φ_t in a stream system of reach L carrying sediment is given by Yang et al. (1981) as

$$\Phi_t = (Q\gamma + Q_s\gamma_s)LS \quad (6.1)$$

in which Q = water discharge; Q_s = sediment discharge; γ = specific weight of water; γ_s = specific weight of sediment; and S = channel slope.

When the total sediment concentration $C = Q_s / Q$ is less than 1000 ppm by weight, the error in neglecting the $Q_s \gamma_s$ term is less than 0.1 % , eq. (6.1) can be also written as

$$\Phi_t \cong \gamma QLS \quad (6.2)$$

Chang (1980b) described minimum stream power (MSP) equal to γQS and stated that 'for an alluvial channel, the necessary and sufficient condition of equilibrium occurs when the steam power per unit length of channel γQS is a minimum subject to given constraints. Hence, an alluvial channel with water discharge Q and sediment load Q_s as independent variables, tends to establish its width, depth and slope such that γQS is a minimum'. Since Q is a given parameters, minimum γQS also means minimum channel slope S.

$$\text{MSP} = \gamma QS \quad (6.3)$$

Yang and Song (1979) defined 'minimum unit stream power', which also equals the product of the flow velocity and slope of the channel, and stated that 'for subcritical flow in an alluvial channel, the channel will adjust its velocity, slope, roughness and

geometry in such a manner that a minimum amount of unit stream power is used to transport a given sediment and water discharge. The value of minimum unit stream power depends on the constraints applied to the channel. If the flow deviates from its equilibrium condition, it will adjust its velocity, slope, roughness and channel geometry in such a manner that the unit stream power is minimized until the equilibrium condition can be regained. Unit stream power Φ_u is defined as stream power per unit weight of water, which is given by

$$\Phi_u = \frac{\Phi_s}{\rho g B D L} = \frac{Q \gamma L S}{\rho g B D L} = U S \quad (6.4)$$

in which U = average velocity ; B = width of river; ρ = density of water ; g = acceleration due to gravity; and S = channel slope .

Davies and Sutherland (1980) proposed the hypothesis of maximum friction factor (MFF) and stated that 'if the flow of a fluid past an originally plane boundary is able to deform the boundary to a non-planar shape, it will do so in such a way that the friction factor increases. The deformation will cease when the shape of the boundary is that which gives rise to a local maximum of friction factor. Thus, the equilibrium shape of a non-planar self-formed flow boundary or channel corresponds to a local maximum of friction factor'. The friction, or coefficient of resistance to flow, is defined as

$$f = \frac{8gDS}{U^2} = \frac{8gB^2D^3S}{Q^2} \quad (6.5)$$

White et al. (1982) stated maximum sediment transport rate (MSTR) that ' for a particular water discharge and slope, the width of the channel adjusts to maximise the

sediment transport rate'. This hypothesis has been used to predict hydraulic and geometrical characteristics of both sand and gravel bed alluvial channels.

To explain the equilibrium flow conditions of alluvial streams in laboratory and field conditions, extremal hypotheses will be used to identify the inter-relationships between B/D ratio and the different indicators, such as minimum energy dissipation rate, minimum stream power and maximum friction factor.

6.3 MAXIMUM ENTROPY THEORY

6.3.1 General

The term entropy is used to describe the disorder of a system. Entropy is a measure of the degree of uncertainty of a particular outcome in a process. For a closed system, the entropy always tends to increase. In thermodynamics, entropy is usually defined in terms of the irreversible component of heat. In hydraulics, for a fluid to maintain its flow, it has to perform work to overcome frictional forces resisting flow. This involves conversion of flow energy into heat energy through friction, and this conversion of energy is irreversible. Thus, the increase in entropy in a hydraulic system usually occurs due to this irreversible conversion of flow energy (mechanical) into heat through friction. This conversion represents the loss of energy and is non-recoverable. The heat energy is conducted through the fluid and its bounding walls, if any, into the atmosphere and eventually is dissipated through space. The amount of energy so deployed is a function of the system geometry and the types of forces or energy affecting the system. The quantitative formulation of this function can be called the process equation, which is what leads to the resistance equation in hydraulics.

Thus, it can be concluded that every flow process is a conservation process, according to the energy conservation principle (the first law of thermodynamics) and a decay process according to the entropy-increase principle (the second law of thermodynamics) (Singh, 1996). Based on the principle of maximum entropy, Jaynes (1957) has proved that any system in equilibrium under steady constraints tends to maximize its entropy.

Using the principle of maximum entropy, Deng and Singh (1999) studied the stability of different alluvial rivers. They derived three sets of parameters and studied the variation of these parameters for different streams. Using the laboratory and field data collected in this study, it is envisaged to study the variation of these parameters and to establish whether the entropy based conclusions of Deng and Singh (1999) are validated.

6.3.2 Mechanism of Channel Pattern Changes

To introduce various parameters defining the stability of alluvial rivers, it is considered relevant to present certain details related to entropy principle and its application. Deng and Zhang (1994) derived a set of river morphologic equations using the principle of maximum entropy, which were in good agreement with 260 sets of field data from more than one hundred rivers. Principle of maximum entropy is applied to study the change in channel pattern and hydraulic geometry or morphology of alluvial river.

Assuming that the flow thalweg in alluvial rivers is a random walk path (Fig. 6.1), the maximum entropy principle results in the following mathematical statement (Deng and Zhang, 1994)

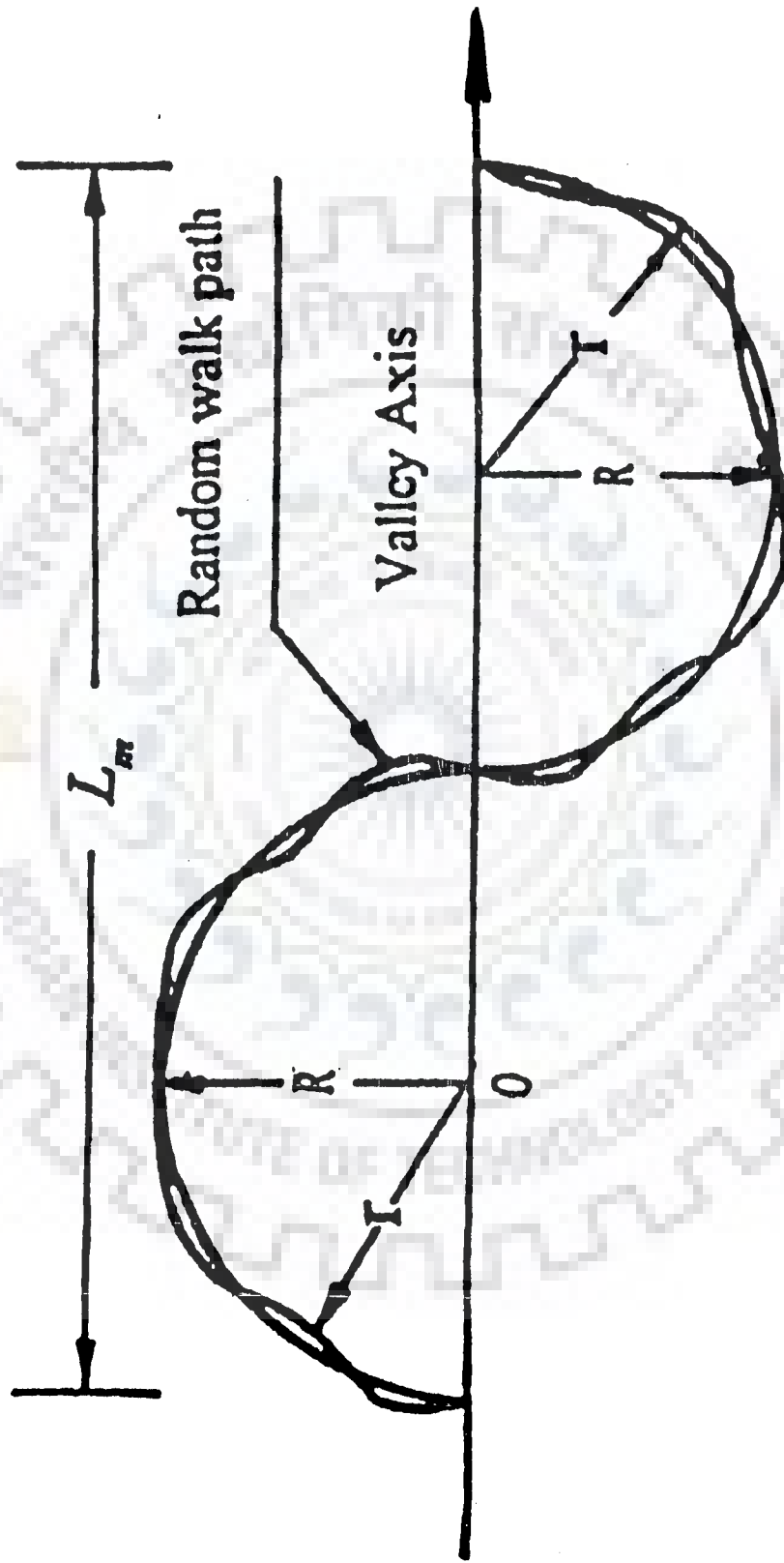


FIG. 6.1: RANDOM WALK PATH OF FLOW THALWEG IN ALLUVIAL RIVERS

$$\text{Maximize } E(r) = - \int_0^R p(r) \ln p(r) dr \quad (6.6)$$

$$\text{Subject to } \int_0^R p(r) dr = 1 \quad (6.7)$$

in which $p(r)$ = the probability density function of the state variable r ; $p(r) dr$ = the probability of the state variable being between r and $r+dr$; and $E(r)$ = entropy of the river system. Under the only constraint expressed by Eq. (6.6), Eq. (6.7) is valid if $p(r)$ satisfies the following condition

$$p(r) = \frac{1}{R} \quad (6.8)$$

and channel sinuosity P_c

$$P_c = \frac{L_s}{L_m} = \frac{\text{Thalweg length}}{\text{Valley length}} = \frac{2 \pi R}{4 R} = \frac{\pi}{2} = 1.57 \quad (6.9)$$

in which R = maximum distance perpendicular from thalweg to valley axis; r = radius of channel curvature; $L_m = 4 R$; and L_s = curved thalweg length around the river.

Equation (6.9) indicates that an alluvial river, with $P_c = 1.57$, conforms to the principle of maximum entropy and represents the natural tendency of fluvial process or river self-adjustment and thus maintains a dynamic equilibrium state.

6.3.3 Condition for Channel Pattern Changes

An alluvial river, conveying a constant discharge 'Q', can be considered to possess three degrees of freedom because it may independently adjust its bankfull channel width 'B', average flow depth 'D', and roughness coefficient 'n', to fit the changes of stream energy with time and longitudinal distance. The only source of natural

stream energy is its potential energy 'Y_E'. The derivative of 'Y_E' with respect to time 'T' is just the unit stream power US (Yang 1973), i.e.

$$\frac{dY_E}{dT} = \frac{dx}{dT} \frac{dY_E}{dx} = US \quad (6.10)$$

where $U = \frac{Q}{B \cdot D}$ (6.11)

Using Manning's equation

$$Q = A \cdot U = B \cdot D \cdot \frac{1}{n} D^{2/3} S^{1/2} \quad (6.12)$$

and equations (6.11) and (6.12), one can get the following expression of unit stream power

$$U \cdot S = \frac{Q^3 n^2}{B^3 D^{13/3}} \quad (6.13)$$

in which S = channel slope; [here notation J used for channel slope by Deng & Singh has been taken as S] and n = Manning's rugosity coefficient.

The derivative of US with respect to longitudinal distance 'x' along the river can be expressed as:

$$\frac{D(US)}{dx} = \frac{\partial(US)}{\partial B} \frac{dB}{dx} + \frac{\partial(US)}{\partial D} \frac{dD}{dx} + \frac{\partial(US)}{\partial n} \frac{dn}{dx} \quad (6.14)$$

$$= -\frac{3Q^3 n^2}{B^4 D^{13/3}} \frac{dB}{dx} - \frac{13Q^3 n^2}{3B^3 D^{16/3}} \frac{dD}{dx} + \frac{2Q^3 n}{B^3 D^{13/3}} \frac{dn}{dx} \quad (6.15)$$

Eq. 6.15 shows that the increment of the unit stream power, US, consists of three parts, that is an alluvial river dissipates its unit stream power US in three ways; (i) adjustment of river width. (ii) adjustment of flow depth, (iii) overcoming the friction of channel boundary.

Let

$$P_B = -\frac{3Q^3 n^2}{B^4 D^{13/3}} \cdot \frac{dB}{dx} \left/ \left[\frac{d(US)}{dx} \right] \right. \quad (6.16a)$$

$$P_D = -\frac{13Q^3 n^2}{3B^3 D^{16/3}} \cdot \frac{dD}{dx} \left/ \left[\frac{d(US)}{dx} \right] \right. \quad (6.16b)$$

$$P_n = \frac{2Q^3 n}{B^3 D^{13/3}} \cdot \frac{dn}{dx} \left/ \left[\frac{d(US)}{dx} \right] \right. \quad (6.16c)$$

$$\text{then, } 1 = P_B + P_D + P_n \quad (6.16d)$$

or

$$1 = \frac{1}{d(US)/dx} \left[-\frac{3Q^2 n^2}{B^4 D^{13/3}} \cdot \frac{dB}{dx} - \frac{13Q^3 n^2}{3B^3 D^{16/3}} \cdot \frac{dD}{dx} + \frac{2Q^3 n}{B^3 D^{13/3}} \cdot \frac{dn}{dx} \right] \quad (6.16e)$$

It is apparent that P_B , P_D , P_n represent the probability of adjustment of river width 'B' and flow depth D as well as flow friction n, respectively.

Based on the principle of maximum entropy, Jaynes (1997) has proved that any system in equilibrium under steady constraints tends to maximize its entropy. It means that the entropy of a river system, having reached its dynamic equilibrium state, achieves its maximum value if and the following equation is valid.

$$P_B = P_D = P_n \quad (6.17)$$

Using eq.(6.17), following relationships have been obtained by Deng and Singh (1999).

$$\xi_0 = \frac{B^{9/13}}{D} \quad (6.18)$$

in which

$$B = \xi_B Q^{13/28} / S^{13/56} \quad (6.19)$$

and

$$D = \xi_D Q^{9/28} / S^{9/56} \quad (6.20)$$

The morphologic coefficients can be expressed as follows:

$$\xi_o = (0.5m)^{84/65} / n^{3/5} \quad (6.21)$$

$$\xi_B = 0.5m \quad (6.22)$$

$$\xi_D = [n/(0.5m)]^{3/5} \quad (6.23)$$

$$\xi_p = Bn^{2/3} \quad (6.24)$$

In eqs. 6.18 to 6.24, ξ stands for different types of indicators.

Using these indicators, Deng and Singh (1999), proposed the stability index, S_{cr} , defined as

$$\text{Stability index 'S}_{cr}\text{'} = \left[\frac{0.319n^{11/30}}{S^{13/56} \sqrt{\xi_o}} \right] \quad (6.25)$$

Substitution of eq. (6.19) into eq.(6.24) and use of dimensional analysis yield

$$\xi_p = S_{cr} Q^{13/28} m^{107/65} \quad (6.26)$$

in which m = channel side slope in m horizontal units to 1 vertical unit.

S_{cr} comprehensively reflects the stability of an alluvial river, and the greater the value of the stability index, ' S_{cr} ', the more stable the river is.

It was also suggested that different river patterns can be identified by the thresholds of river stability criterion ' S_{cr} ' and channel sinuosity ' p_c ', i.e.

- (a) $S_{cr} \leq 0.07$ for wandering pattern
- (b) $0.07 < S_{cr} \leq 0.1$ for anabranching pattern
- (c) $S_{cr} > 0.1$ for single channel pattern including meandering and straight pattern

The channel sinuosity $p_c > 1.57$ and $p_c < 1.57$ correspond to meandering and straight rivers, respectively.

6.4 ANALYSIS OF DATA

6.4.1 Extremal Hypotheses

Based on analyzed data from field as well as laboratory experimentation, several plots have been made to get an insight into the behaviour of the morphological parameters involved.

6.4.1.1 Variation of MEDR

Figs. 6.2 to 6.11 vividly depict the general trend of variation of MEDR with B/D ratio for the laboratory based experiments, conducted in phase-I. Similarly, Fig. 6.12 and 6.13 show the variation of MEDR with B/D ratio for the model experiments and field data, respectively. From a perusal of the graphical plots, mentioned for laboratory data, it could be easily discerned that the dominant trend of variation of MEDR with B/D is in conformity on expected line. The values of MEDR flows a descending path with increase in the ratio of B/D. In other words as the river section approaches some sorts of equilibrium conditions by progressive minimization of energy dissipation rate, there is clear exacerbation of braiding intensity by way of higher B/D ratio.

6.4.1.2 Variation of MSP

Figs. 6.14. to Fig.6.23 vividly depict the general trend of variation of MSP with B/D ratio for the laboratory based experiments, conducted in phase-I. Similarly, Fig. 6.24

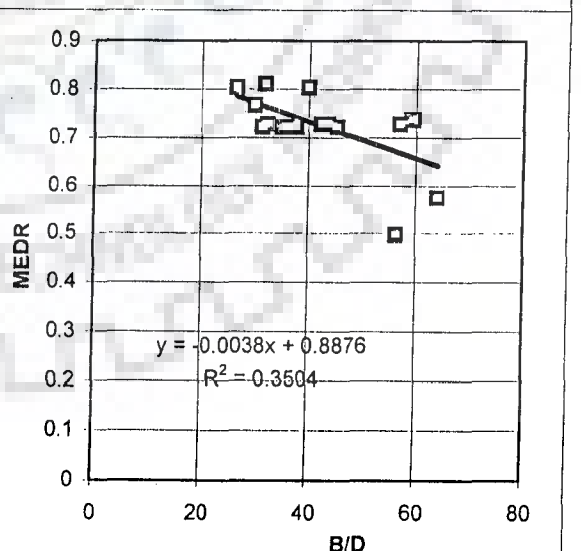
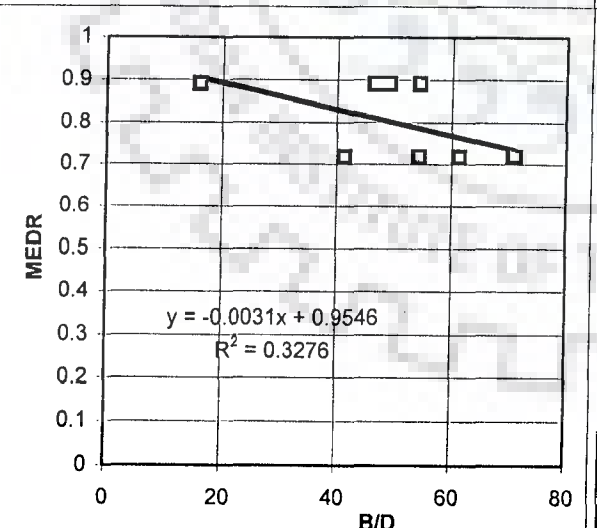
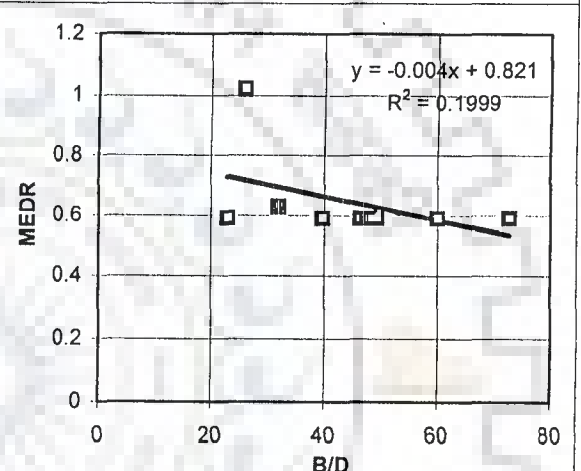
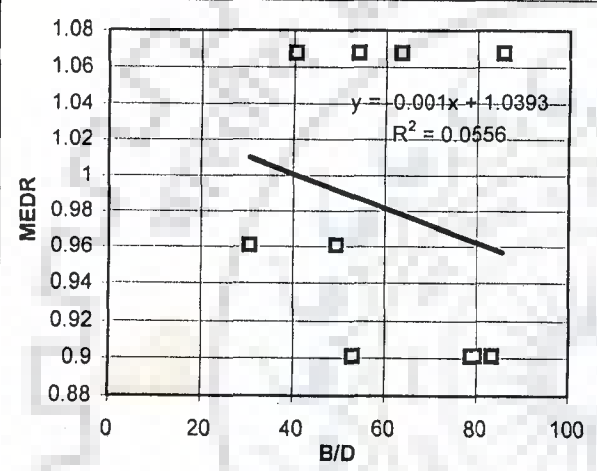
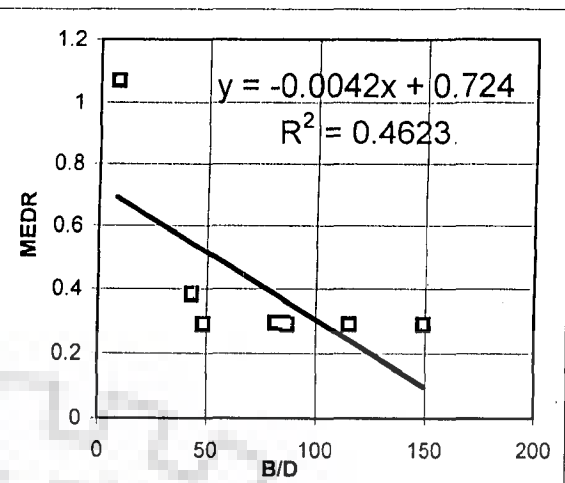
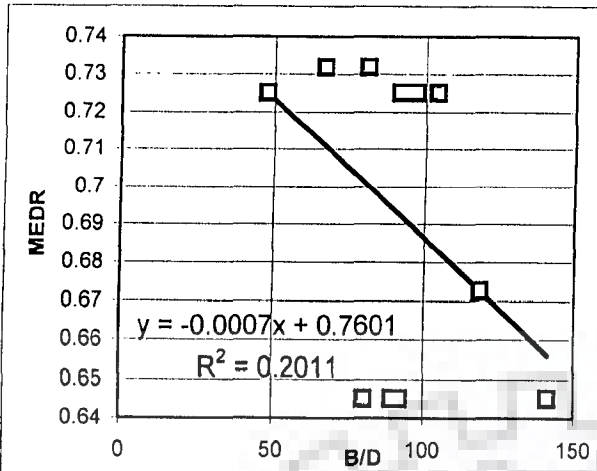


FIG. 6.2 a,b,c,d,e,f; VARIATION OF 'MEDR' WITH B/D RATIO FOR LAB. DATA

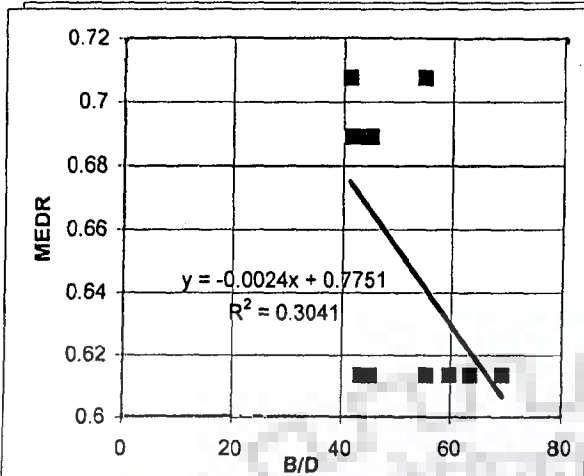


FIG. 6.3a Variation of MEDR with B/D ratio for Run-7

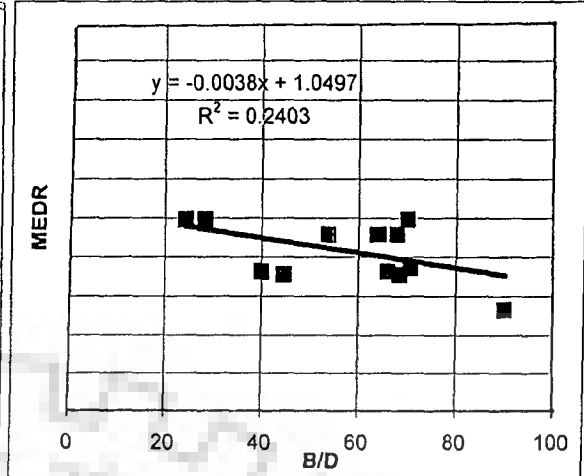


FIG. 6.3b Variation of MEDR with B/D ratio for Run-8

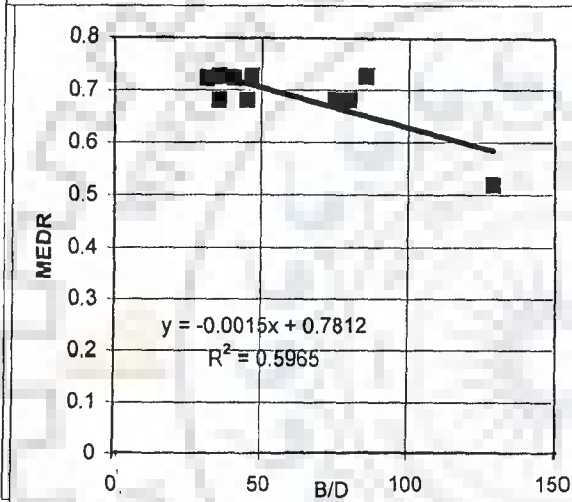


FIG. 6.3c Variation of MEDR with B/D ratio for Run-9

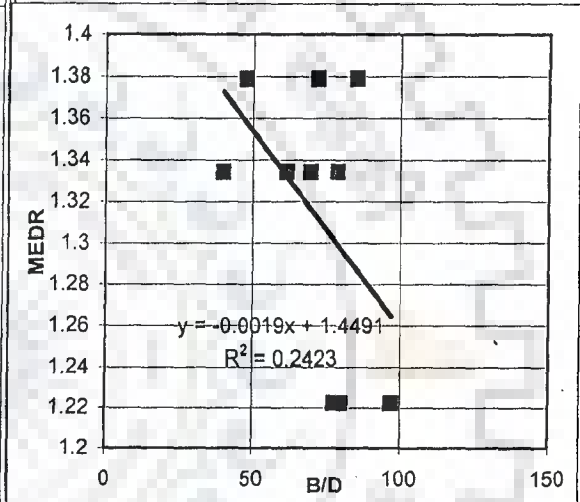


FIG. 6.3d Variation of MEDR with B/D ratio for Run-10

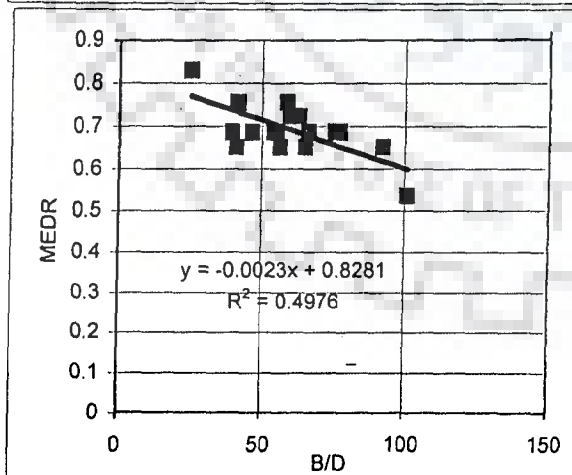


FIG. 6.3e Variation of MEDR with B/D ratio for Run-11

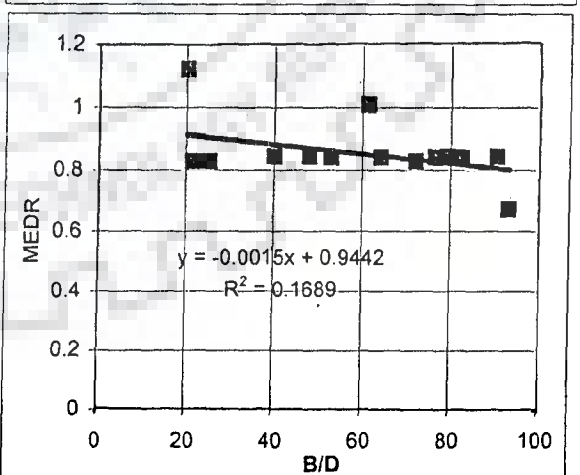


FIG. 6.3f Variation of MEDR with B/D ratio for Run-12

FIG. 6.3 a,b,c,d,e,f: VARIATION OF 'MEDR' WITH B/D RATIO FOR LAB. DATA

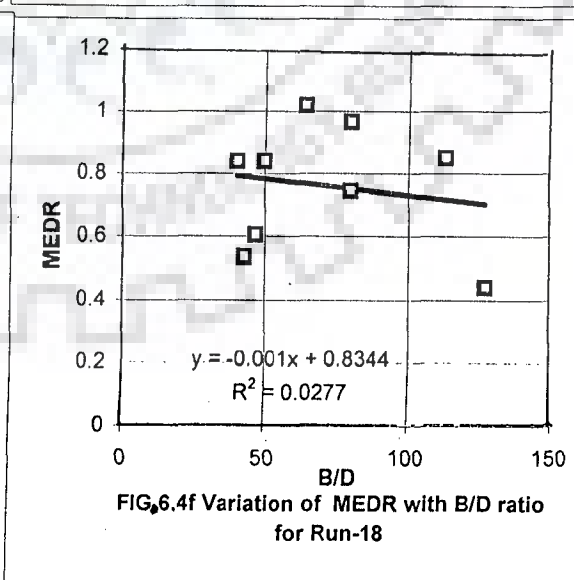
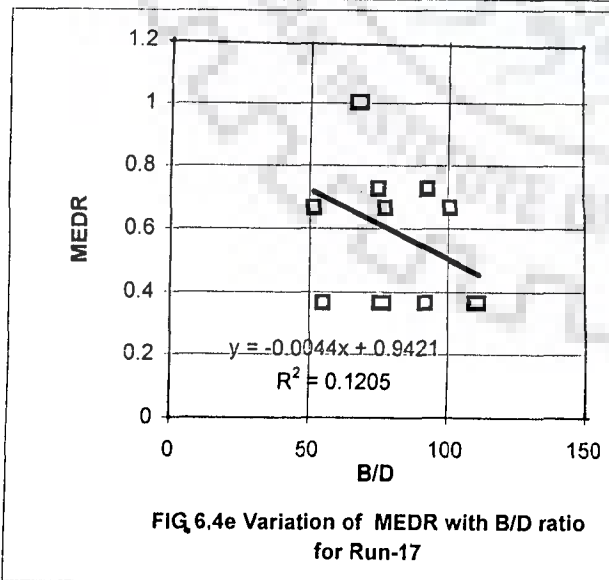
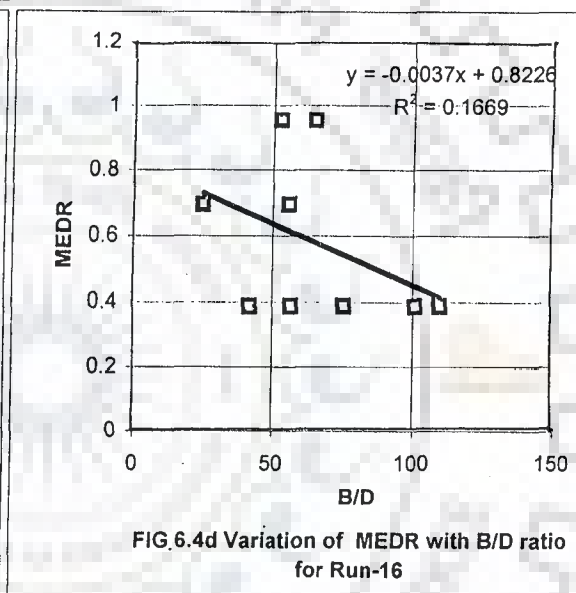
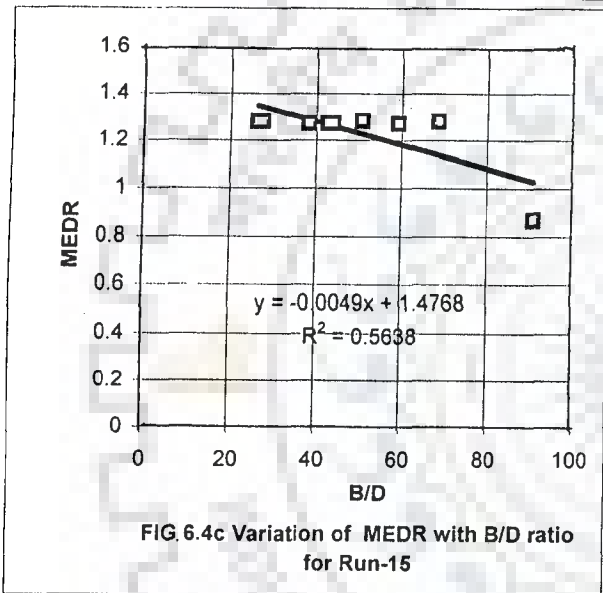
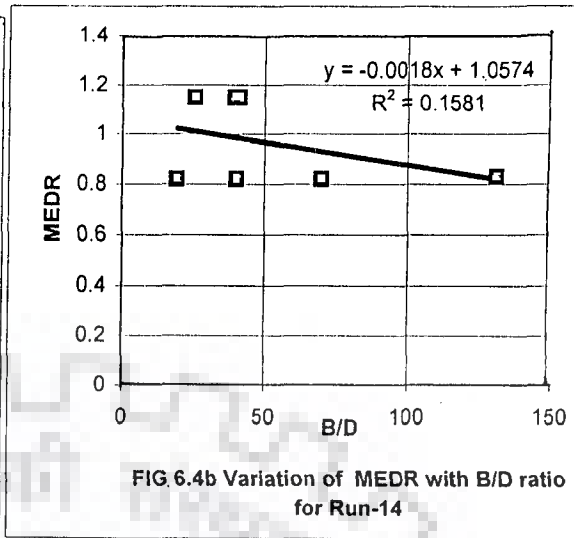
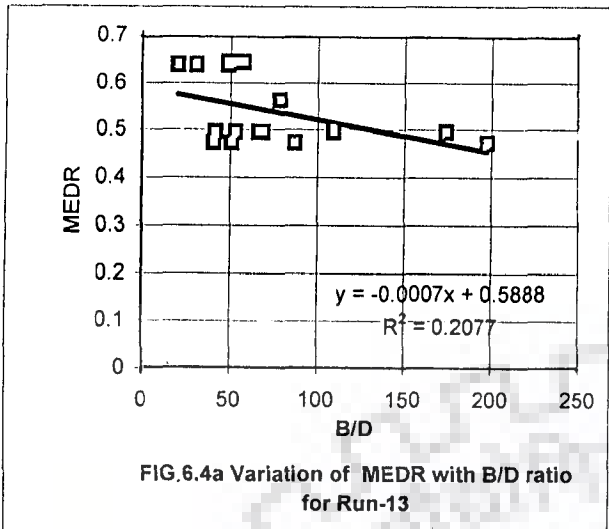


FIG. 6.4 a,b,c,d,e,f: VARIATION OF 'MEDR' WITH B/D RATIO FOR LAB. DATA

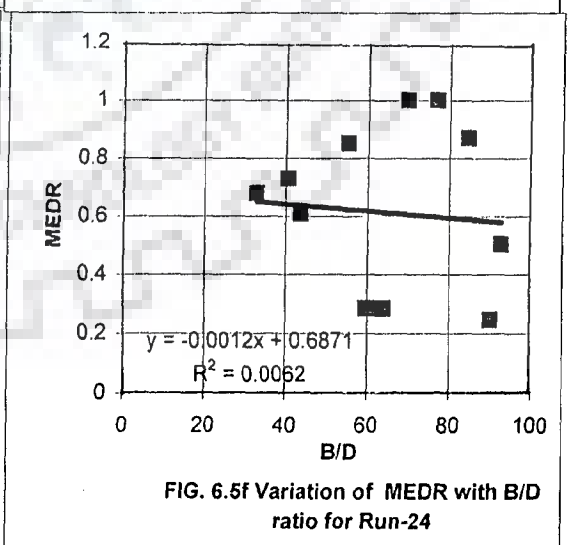
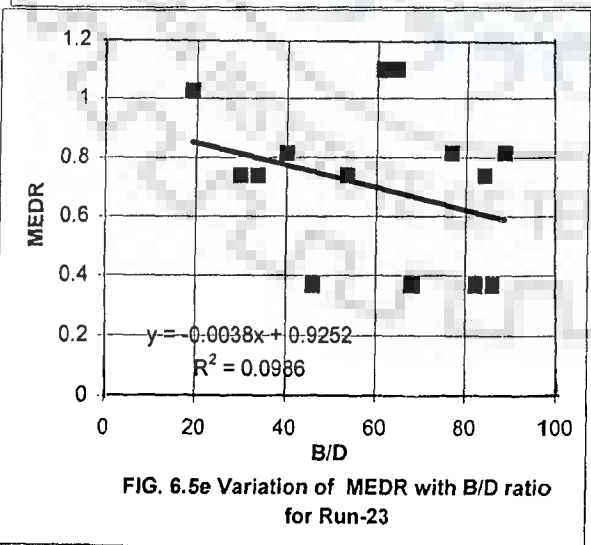
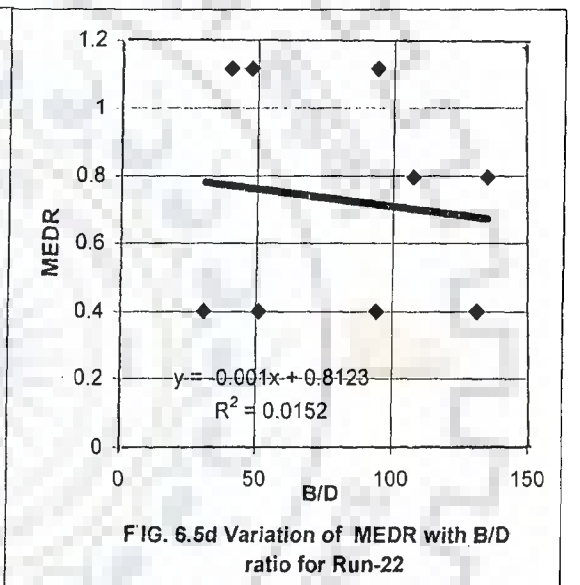
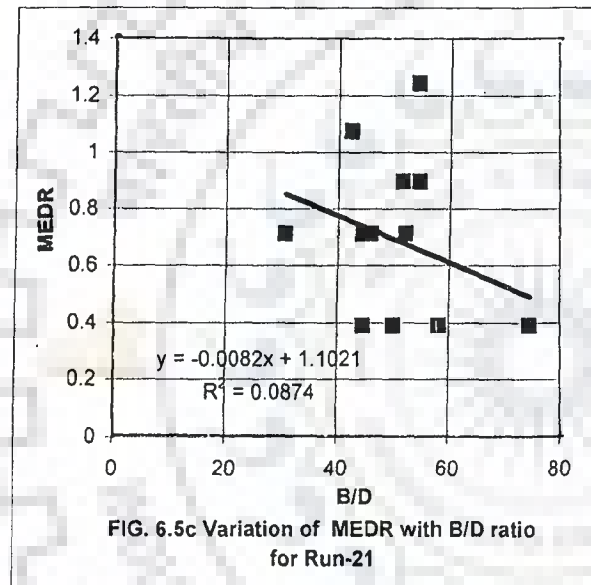
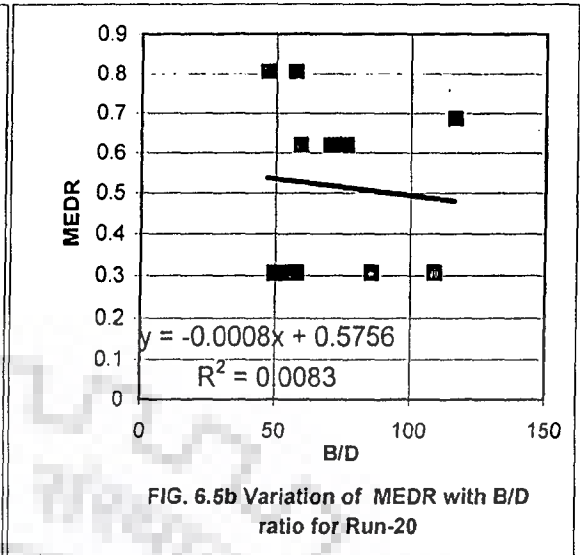
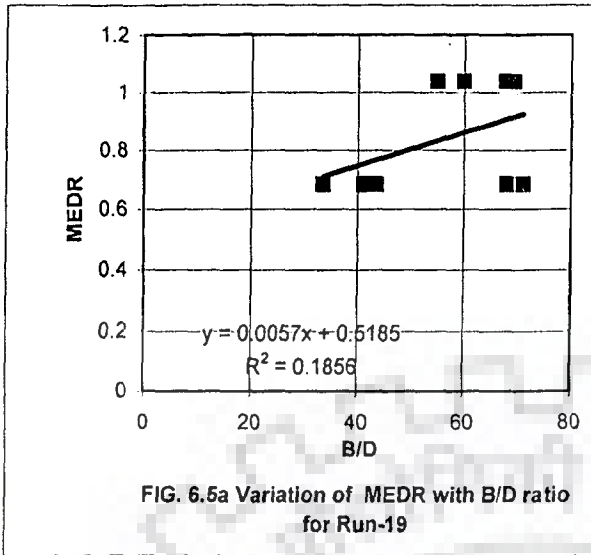


FIG. 6.5 a,b,c,d,e,f; VARIATION OF 'MEDR' WITH B/D RATIO FOR LAB. DATA

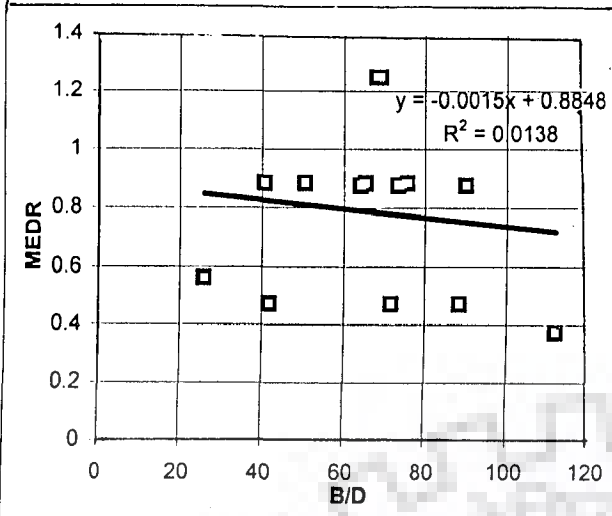


FIG. 6.6a Variation of MEDR with B/D ratio for Run-25

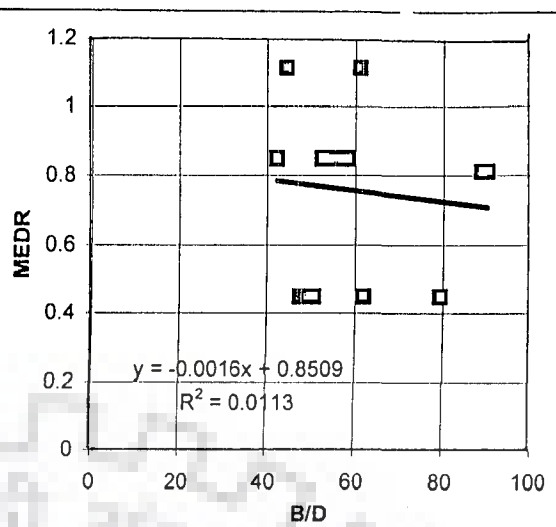


FIG. 6.6b Variation of MEDR with B/D ratio for Run-26

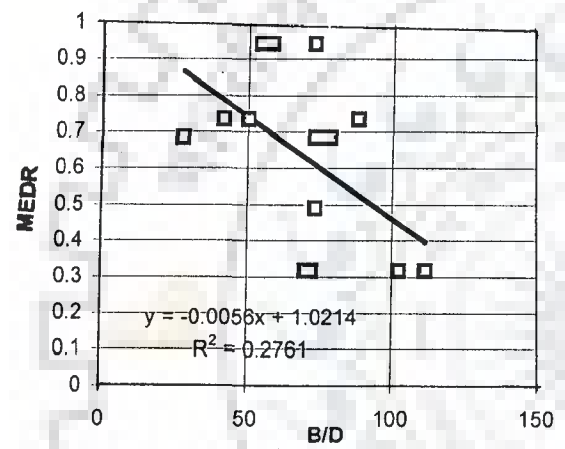


FIG. 6.6c Variation of MEDR with B/D ratio for Run-27

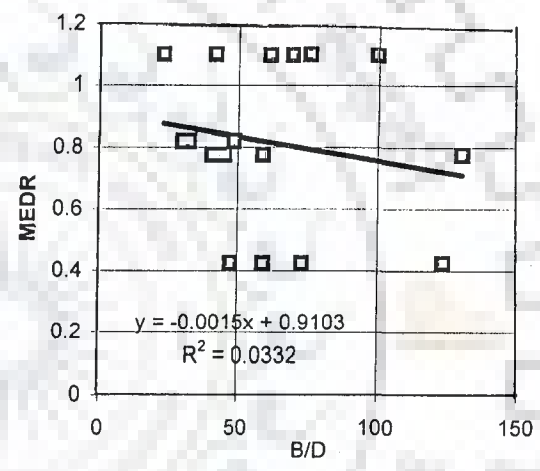


FIG. 6.6d Variation of MEDR with B/D ratio for Run-28

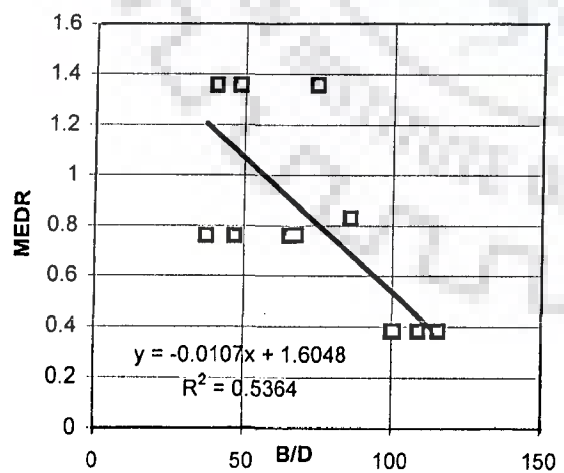


FIG. 6.6e Variation of MEDR with B/D ratio for Run-29

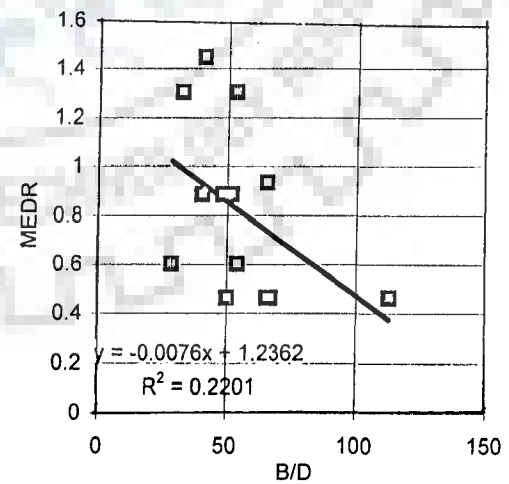


FIG. 6.6f Variation of MEDR with B/D ratio for Run-30

FIG. 6.6 a,b,c,d,e,f: VARIATION OF 'MEDR' WITH B/D RATIO FOR LAB. DATA

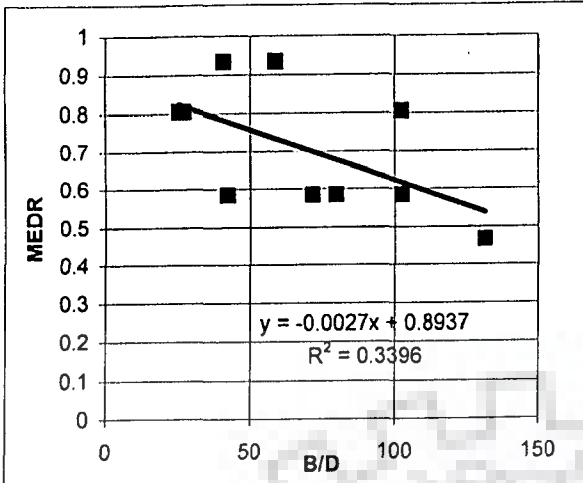


FIG. 6.7a Variation of MEDR with B/D ratio for Run-31

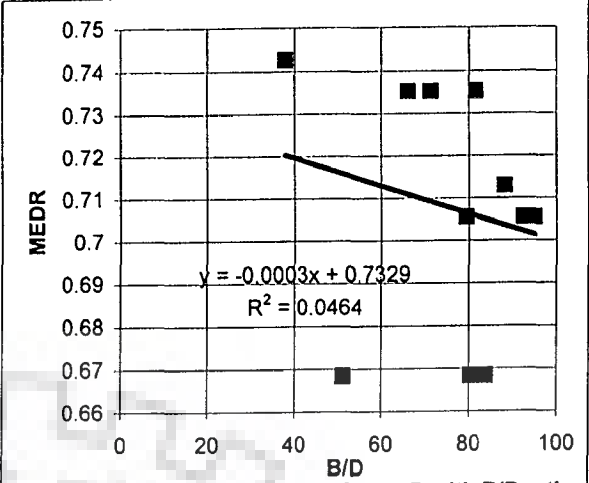


FIG. 6.7b Variation of MEDR with B/D ratio for Run-32

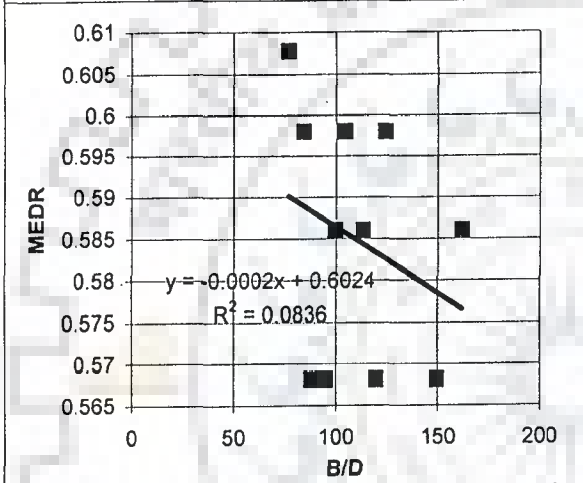


FIG. 6.7c Variation of MEDR with B/D ratio for Run-33

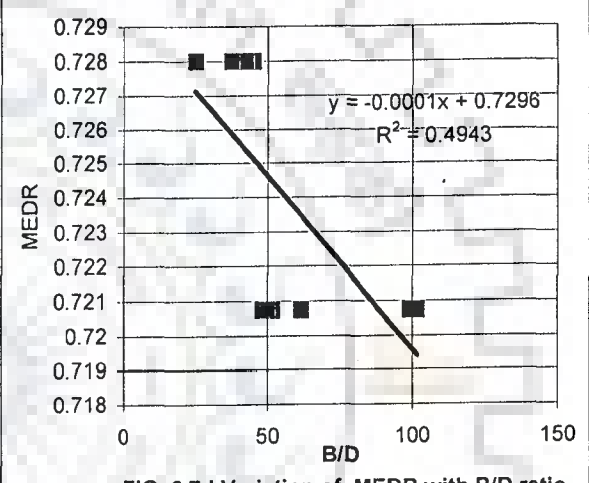


FIG. 6.7d Variation of MEDR with B/D ratio for Run-34

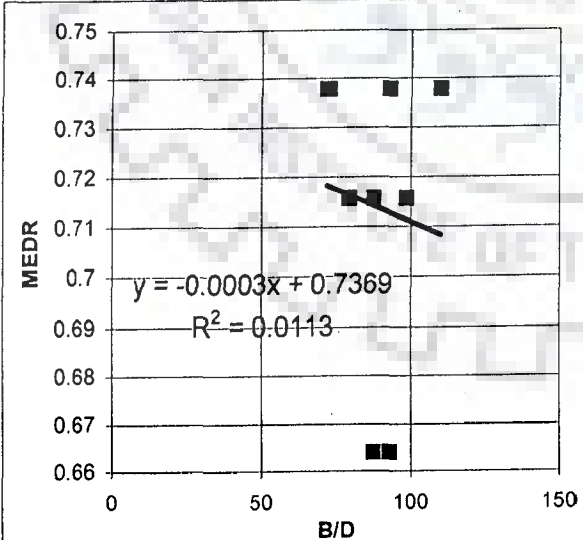


FIG. 6.7e Variation of MEDR with B/D ratio for Run-35

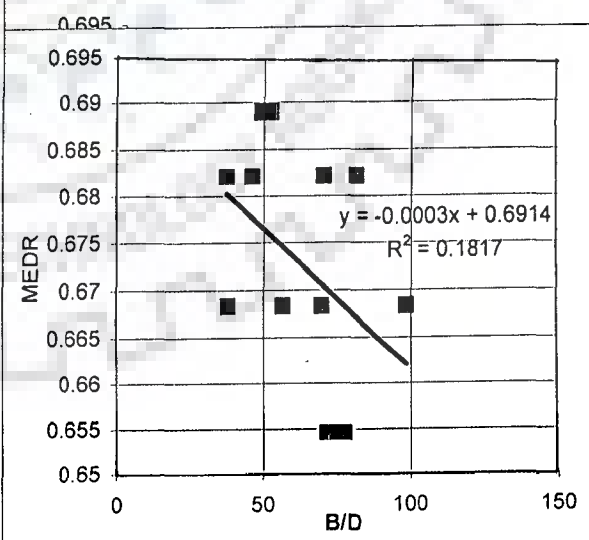


FIG. 6.7f Variation of MEDR with B/D ratio for Run-36

FIG. 6.7 a,b,c,d,e,f: VARIATION OF 'MEDR' WITH B/D RATIO FOR LAB. DATA

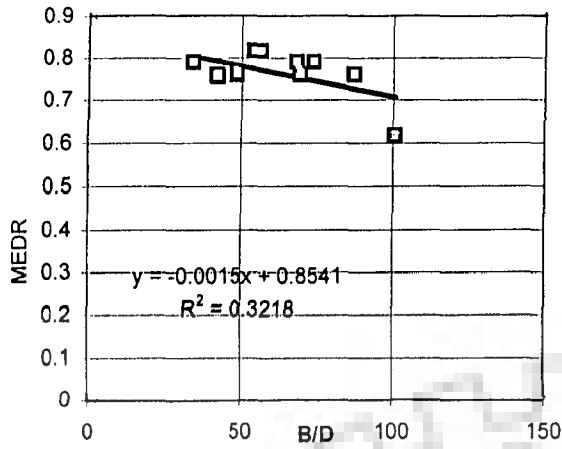


FIG. 6.8a Variation of MEDR with B/D ratio for Run-37

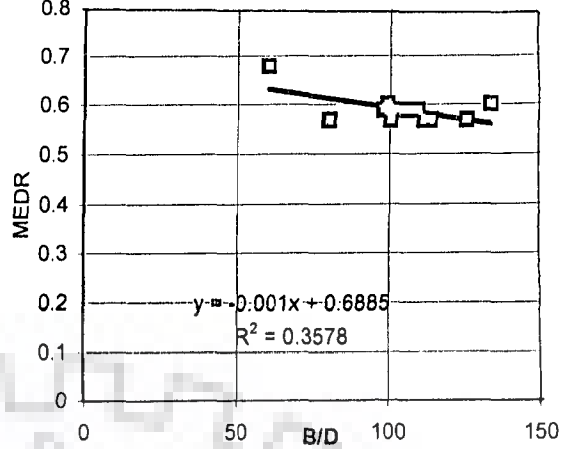


FIG. 6.8b Variation of MEDR with B/D ratio for Run-38

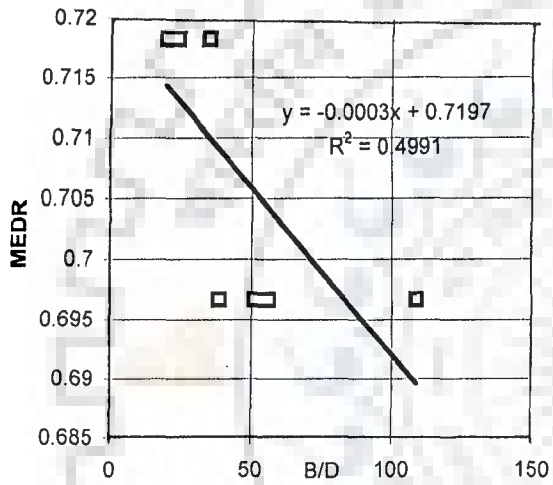


FIG. 6.8c Variation of MEDR with B/D ratio for Run-39

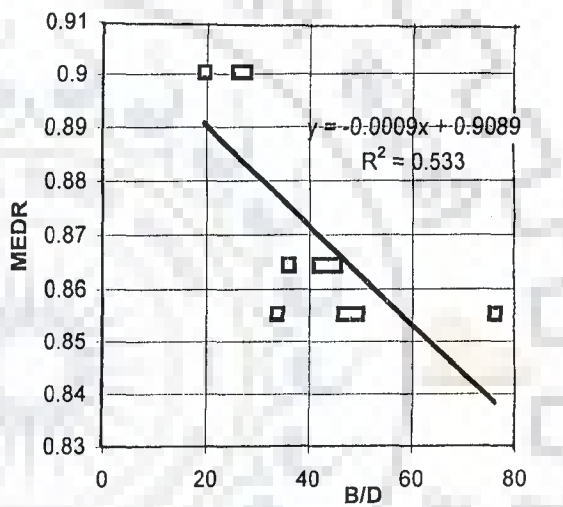


FIG. 6.8d Variation of MEDR with B/D ratio for Run-40

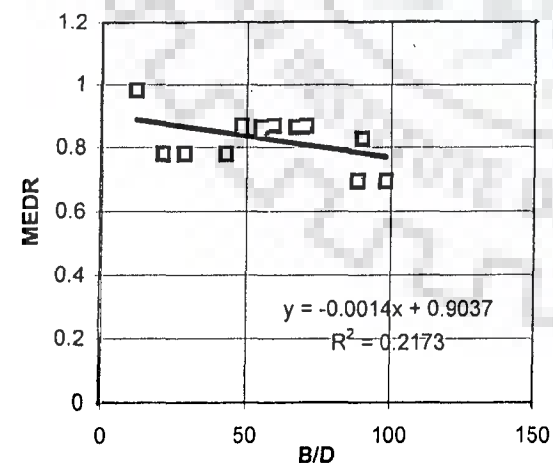


FIG. 6.8e Variation of MEDR with B/D ratio for Run-41

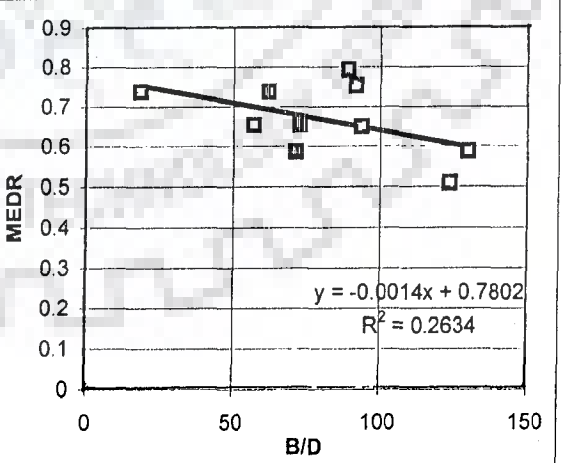


FIG. 6.8f Variation of MEDR with B/D ratio for Run-42

FIG. 6.8 a,b,c,d,e,f: VARIATION OF 'MEDR' WITH B/D RATIO FOR LAB. DATA

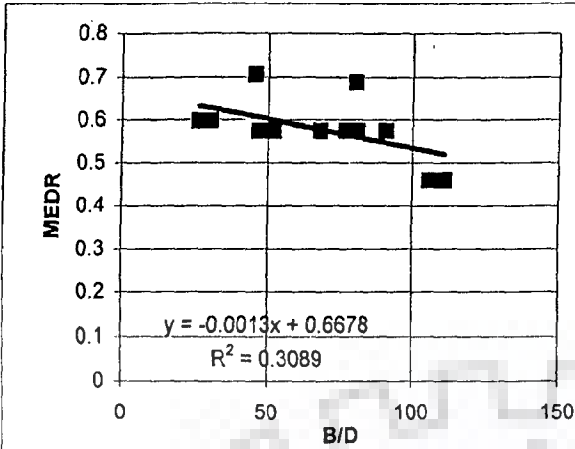


FIG. 6.9a Variation of MEDR with B/D ratio for Run-43

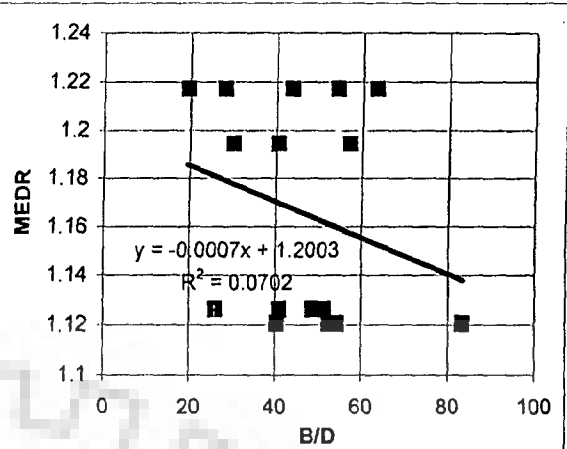


FIG. 6.9b Variation of MEDR with B/D ratio for Run-44

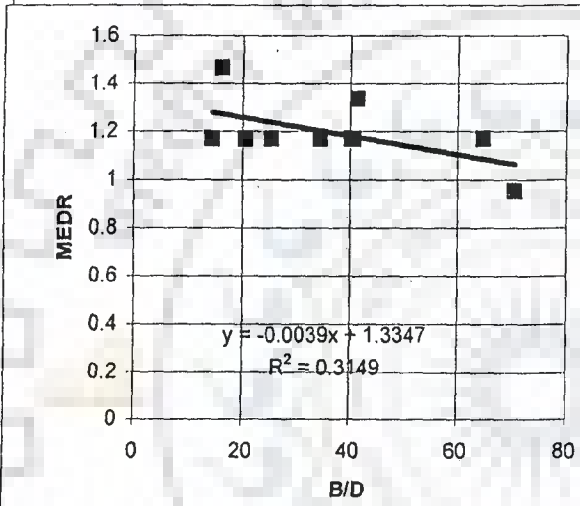


FIG. 6.9c Variation of MEDR with B/D ratio for Run-45

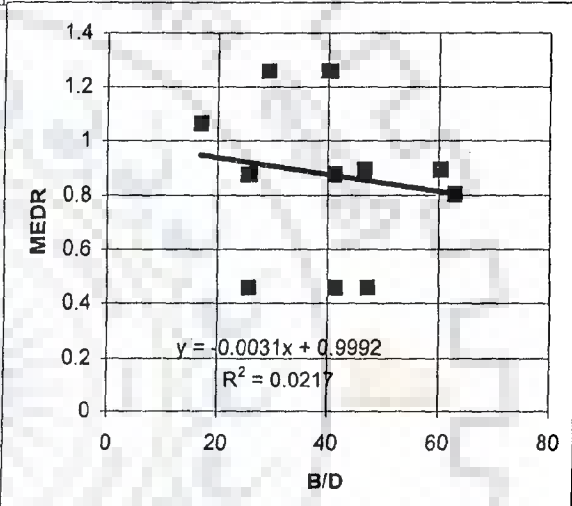


FIG. 6.9d Variation of MEDR with B/D ratio for Run-46

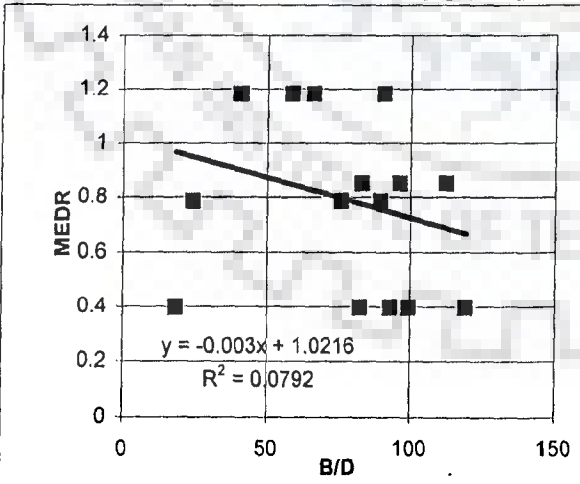


FIG. 6.9e Variation of MEDR with B/D ratio for Run-47

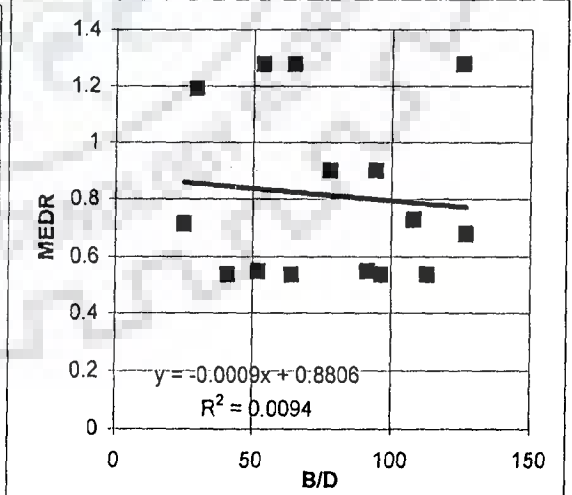


FIG. 6.9f Variation of MEDR with B/D ratio for Run-48

FIG. 6.9 a,b,c,d,e,f; VARIATION OF 'MEDR' WITH B/D RATIO FOR LAB. DATA

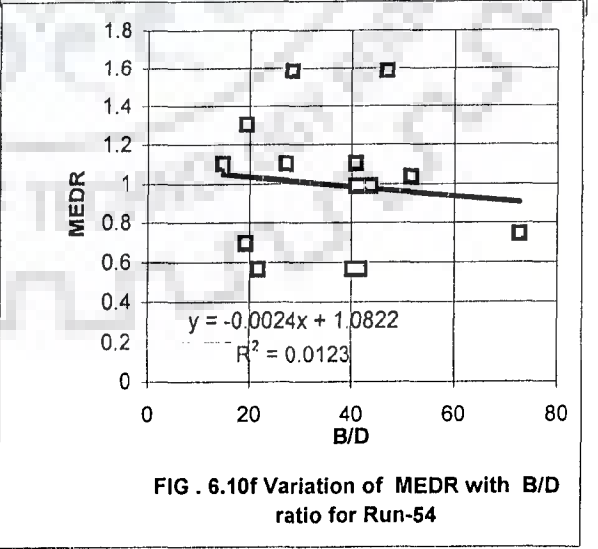
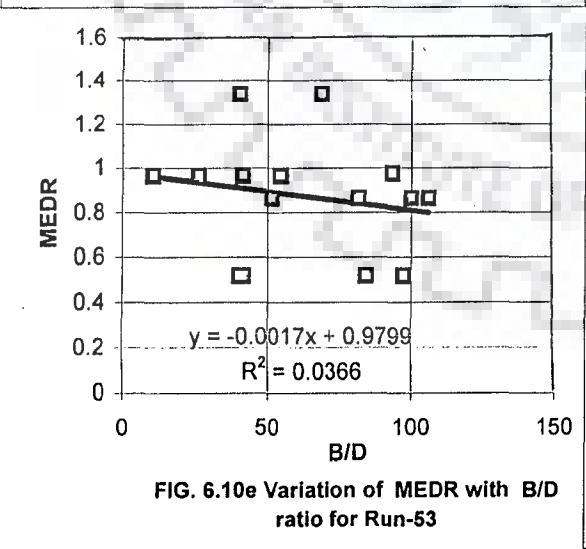
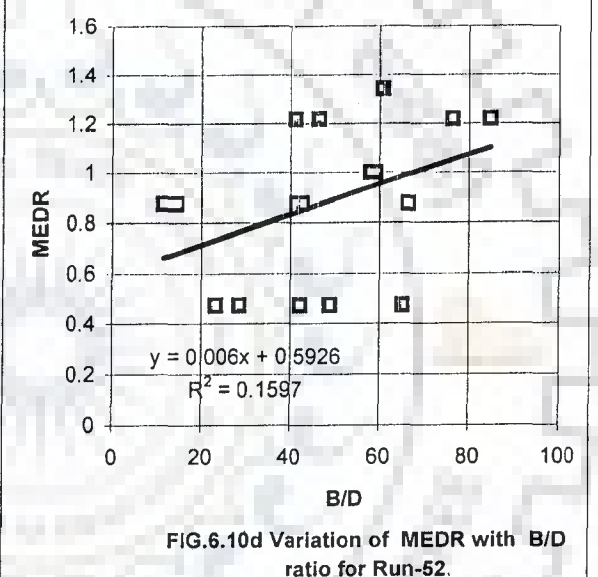
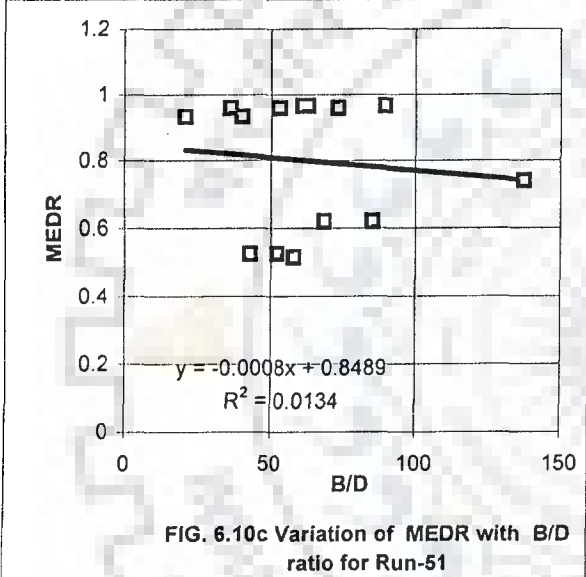
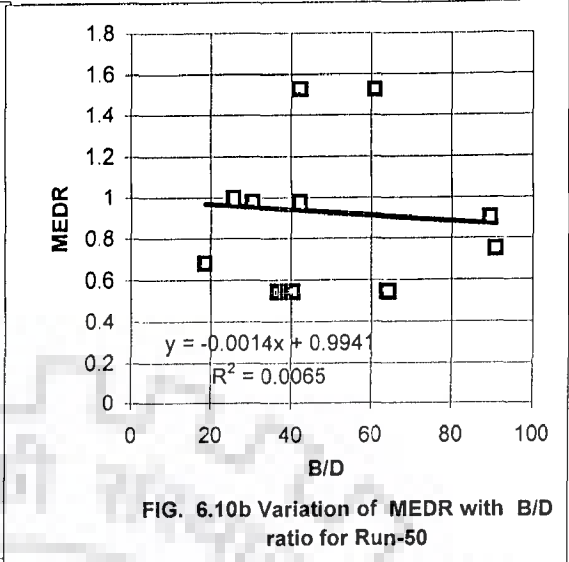
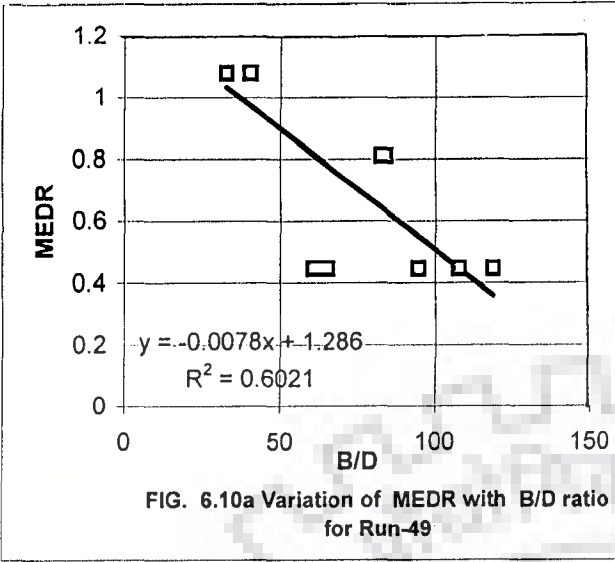


FIG. 6.10 a,b,c,d,e,f; VARIATION OF 'MEDR' WITH B/D RATIO FOR LAB. DATA

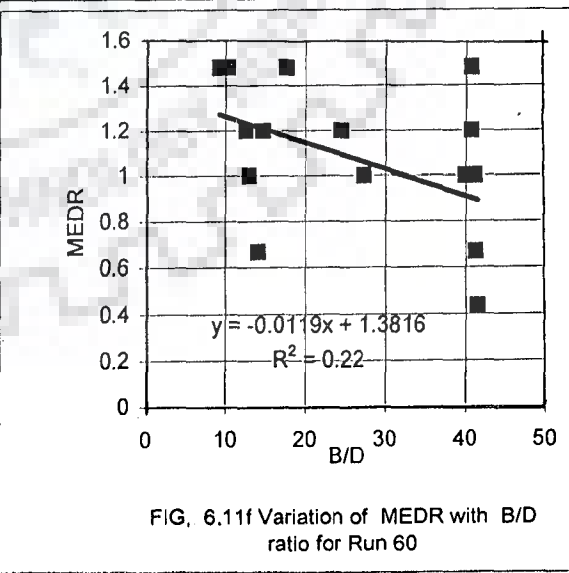
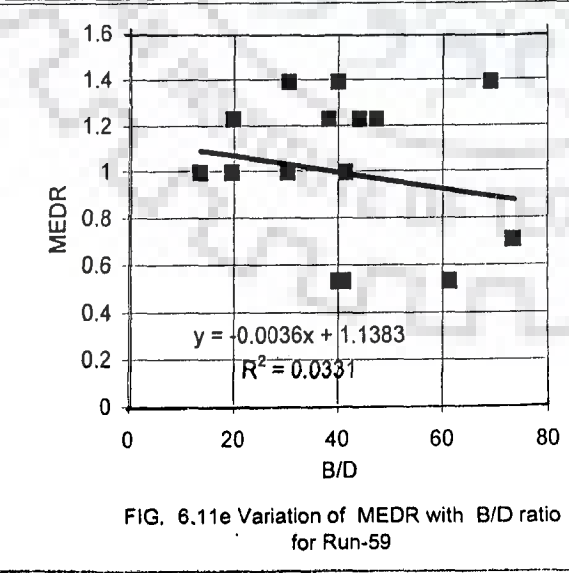
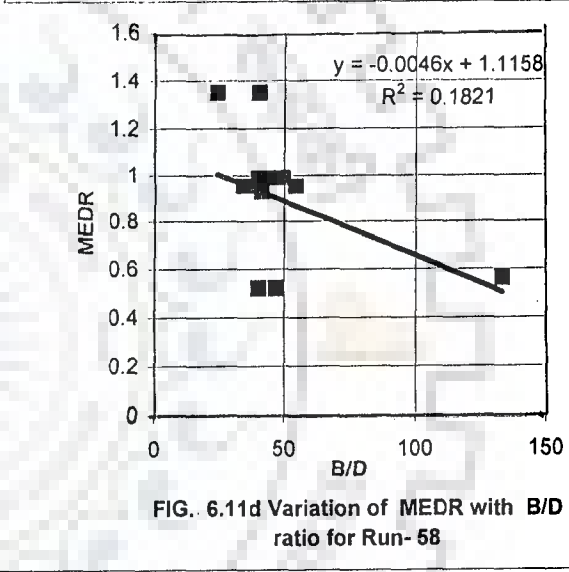
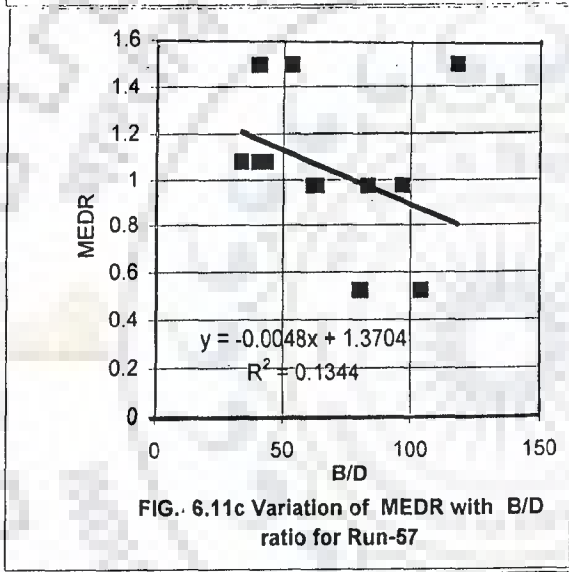
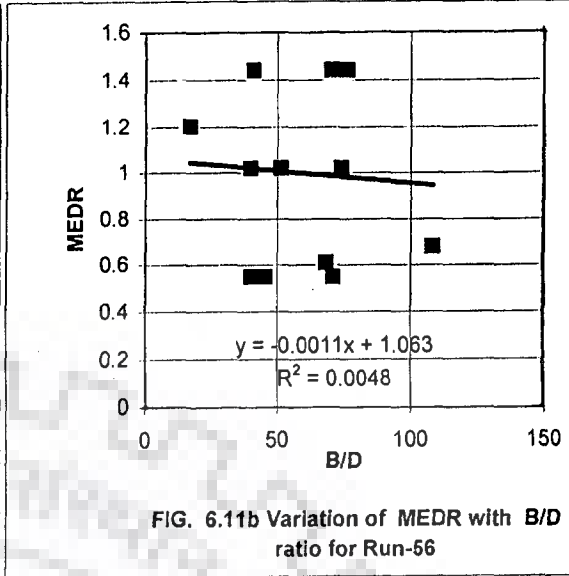
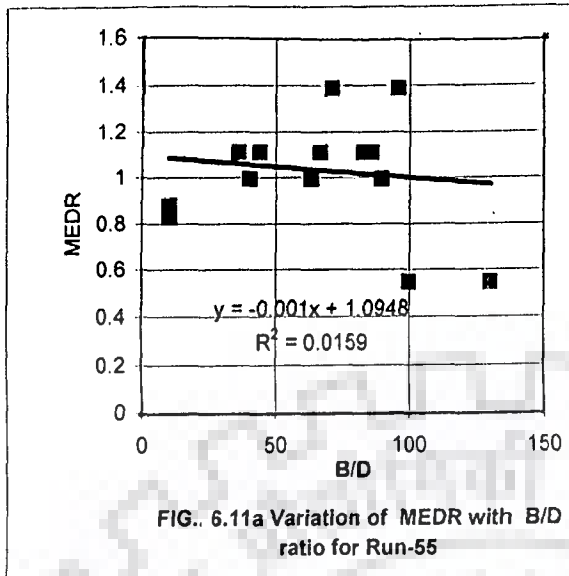


FIG. 6.11 a,b,c,d,e,f: VARIATION OF 'MEDR' WITH B/D RATIO FOR LAB. DATA

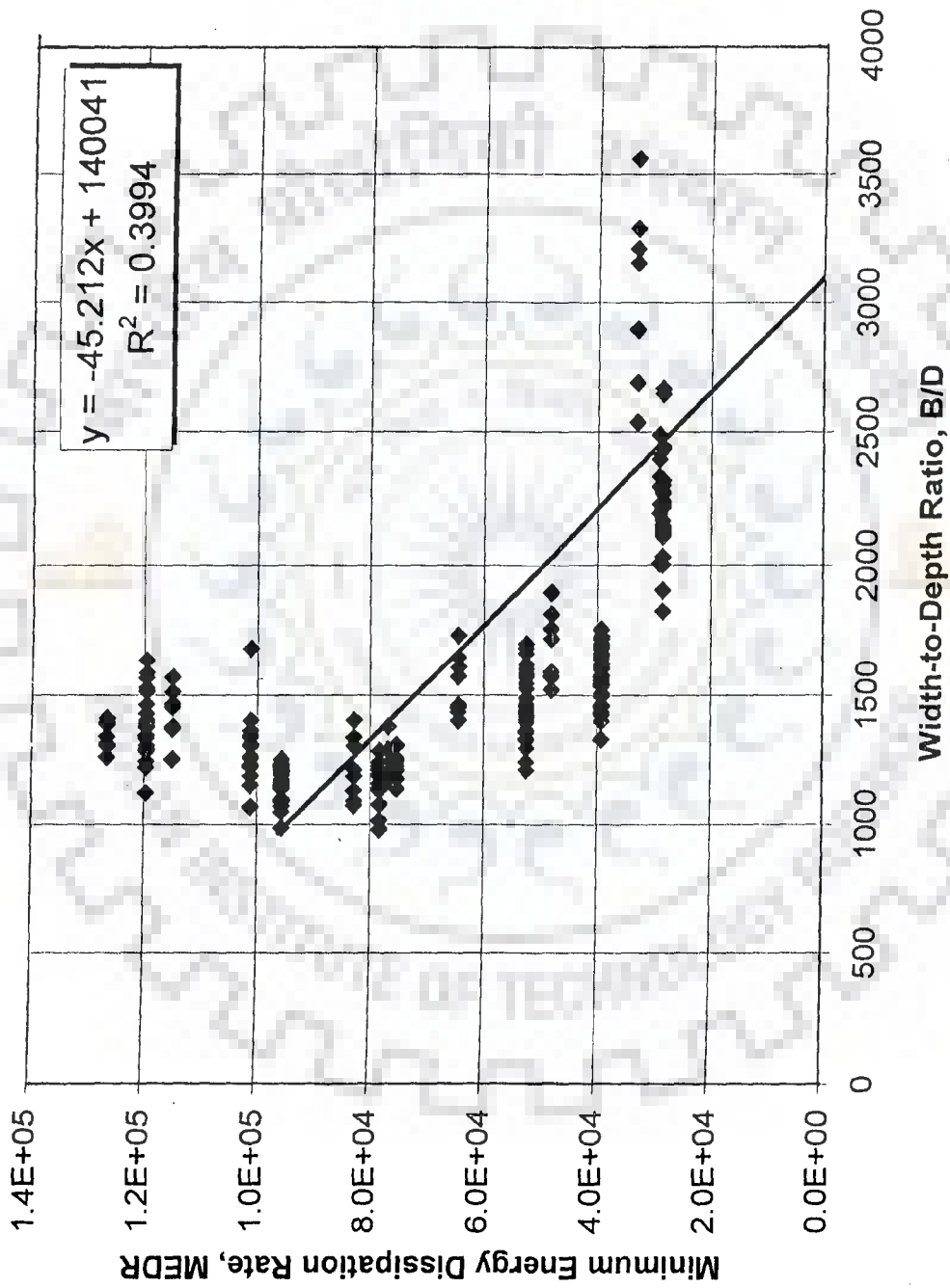


FIG. 6.12: VARIATION OF 'MEDR' WITH B/D RATIO FOR MODEL STUDY OF A PARTICULAR STRETCH OF THE BRAHMAPUTRA RIVER

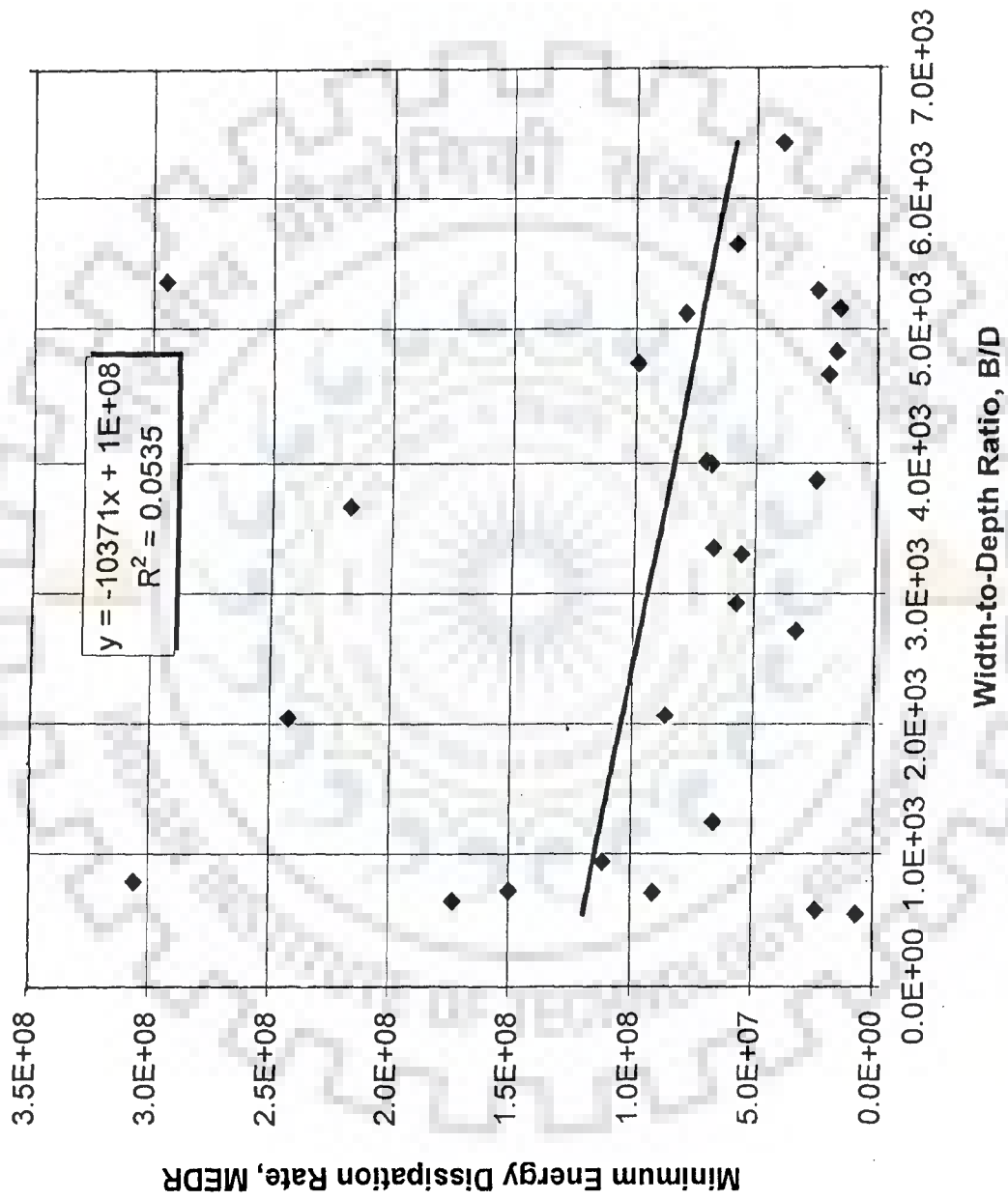


FIG. 6.13: VARIATION OF MEDR WITH B/D RATIO FOR FIELD DATA

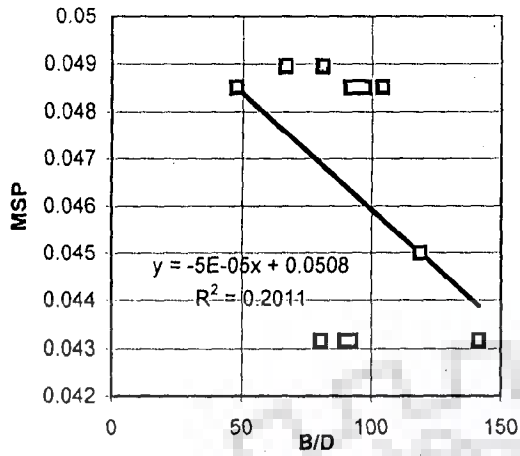


FIG. 6.14a Variation of MSP with B/D ratio for Run-1

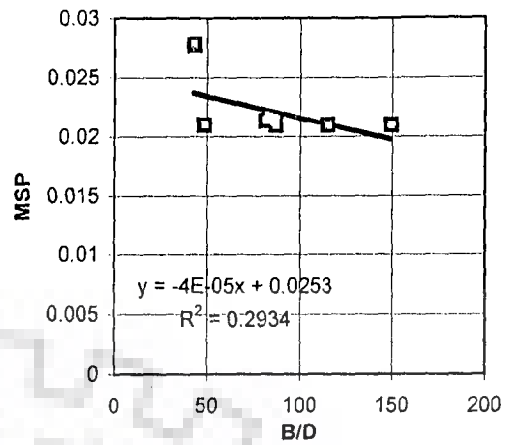


FIG. 6.14b Variation of MSP with B/D ratio for Run-2

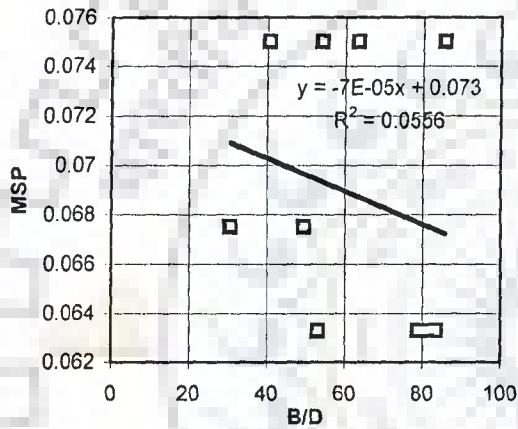


FIG. 6.14c Variation of MSP with B/D ratio for Run-3

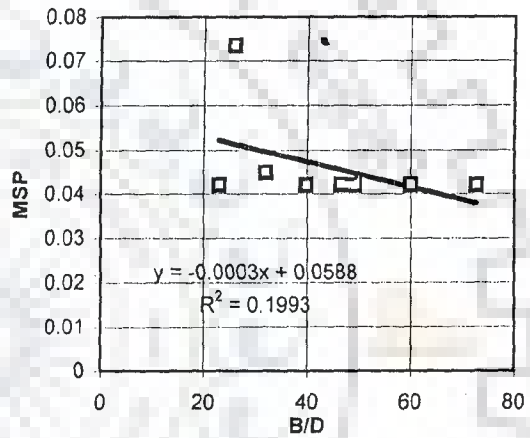


FIG. 6.14d Variation of MSP with B/D ratio for Run-4

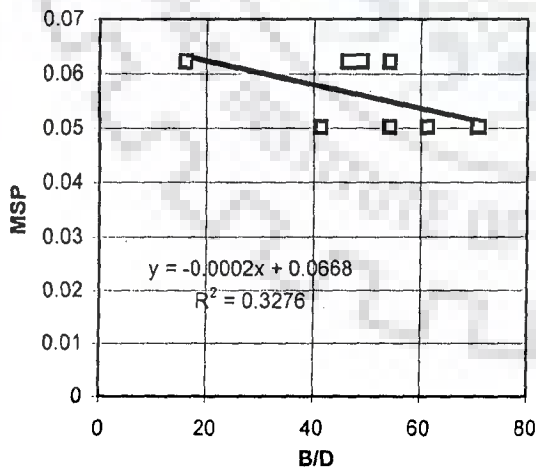


FIG. 6.14e Variation of MSP with B/D ratio for Run-5

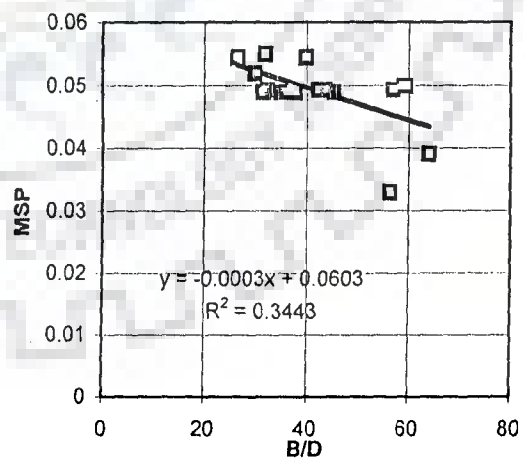


FIG. 6.14f Variation of MSP with B/D ratio for Run-6

FIG. 6.14 a,b,c,d,e,f: VARIATION OF MSP WITH B/D RATIO FOR LAB. DATA

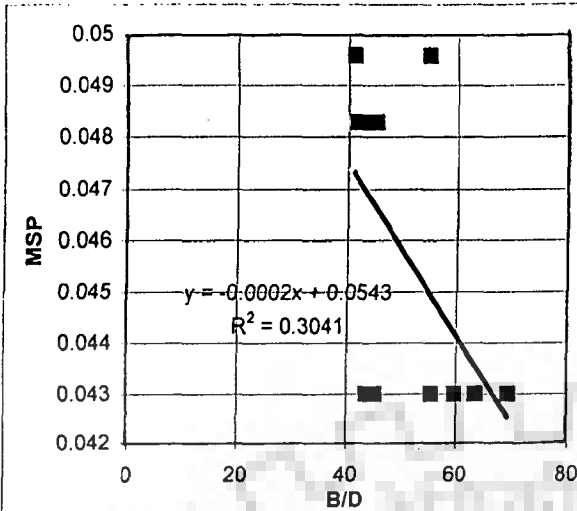


FIG. 6.15a Variation of MSP with B/D ratio for Run-7

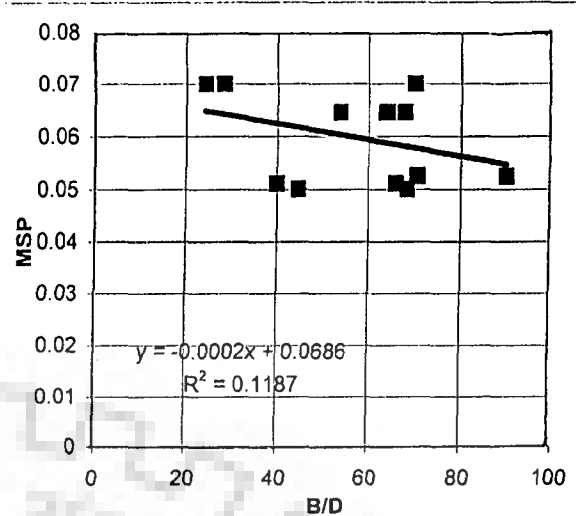


FIG. 6.15b Variation of MSP with B/D ratio for Run-8

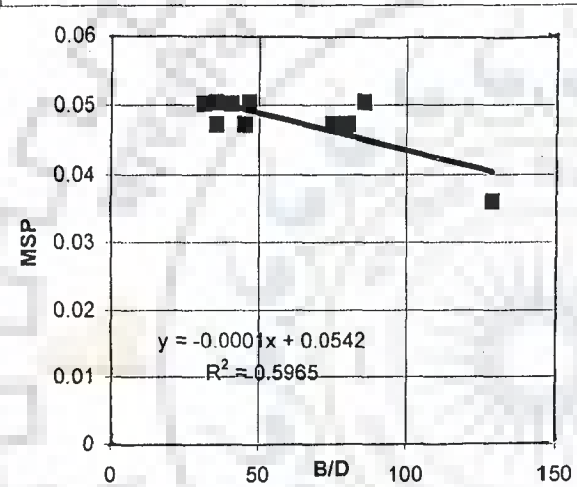


FIG. 6.15c Variation of MSP with B/D ratio for Run-9

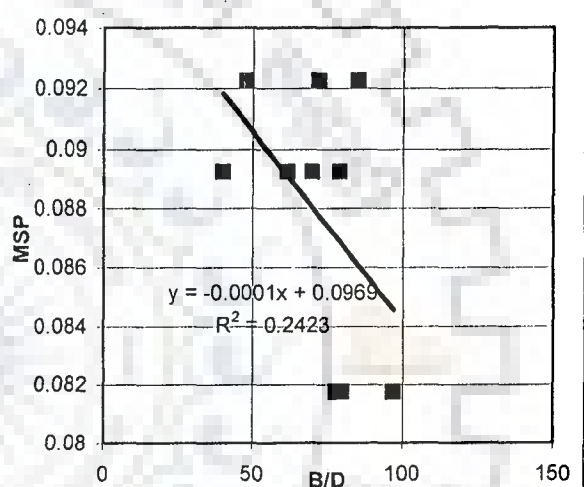


FIG. 6.15d Variation of MSP with B/D ratio for Run-10

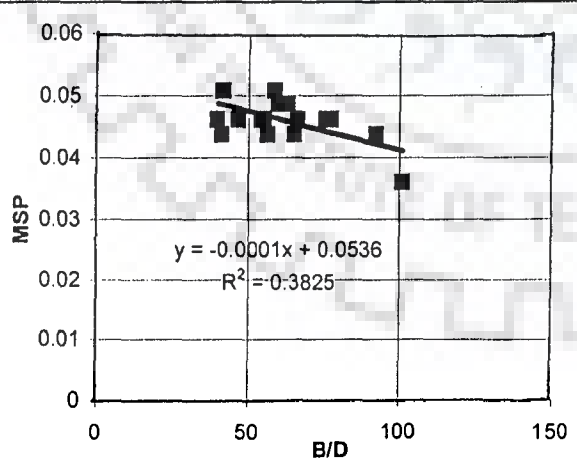


FIG. 6.15e Variation of MSP with B/D ratio for Run-11

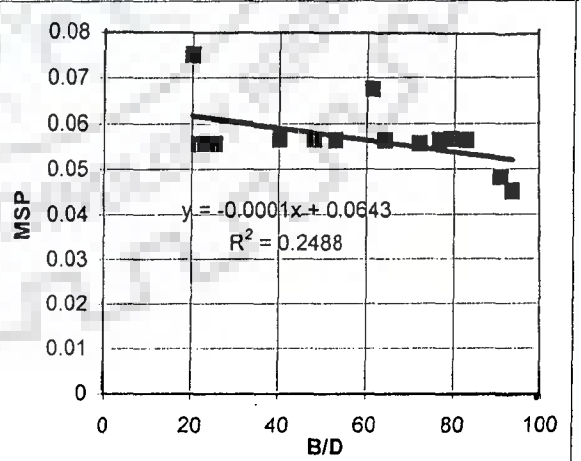


FIG. 6.15f Variation of MSP with B/D ratio for Run-12

FIG. 6.15 a,b,c,d,e,f; VARIATION OF 'MSP' WITH B/D RATIO FOR LAB. DATA

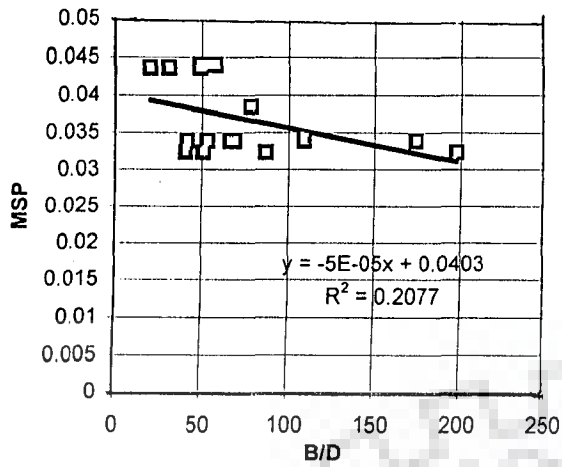


FIG. 6.16a Variation of MSP with B/D ratio for Run-13

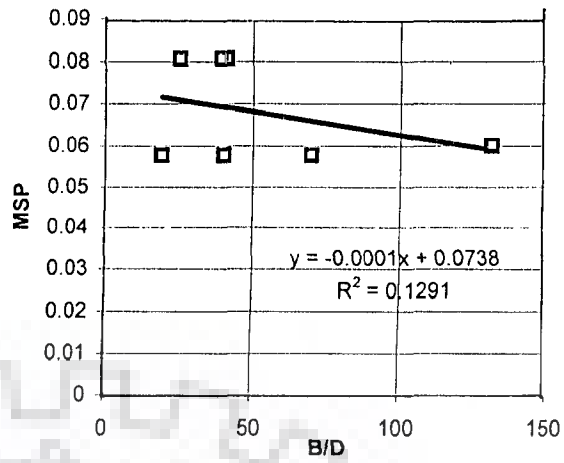


FIG. 6.16b Variation of MSP with B/D ratio for Run-14

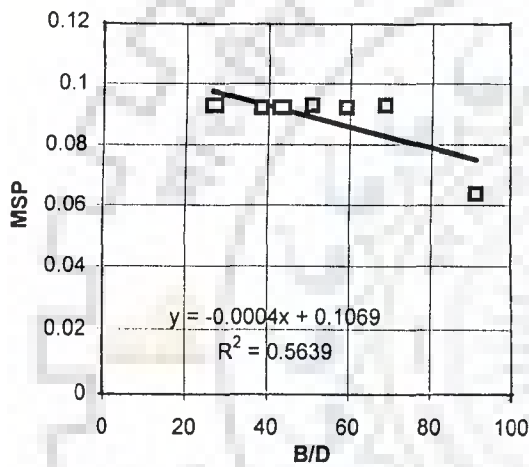


FIG. 6.16c Variation of MSP with B/D ratio for Run-15

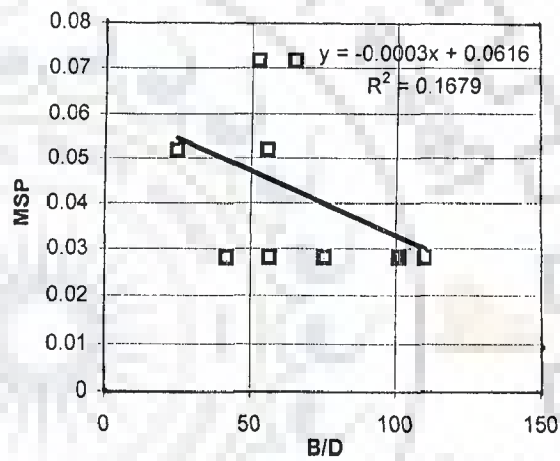


FIG. 6.16d Variation of MSP with B/D ratio for Run-16

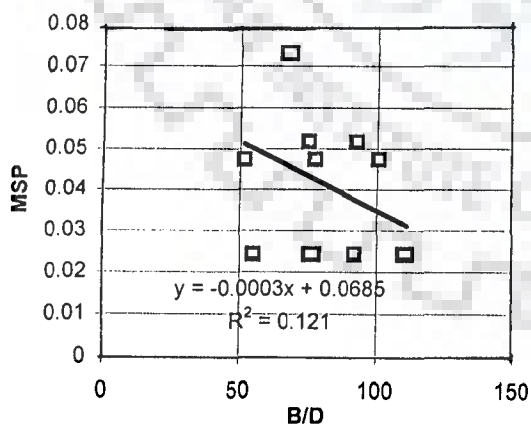


FIG. 6.16e Variation of MSP with B/D ratio for Run-17

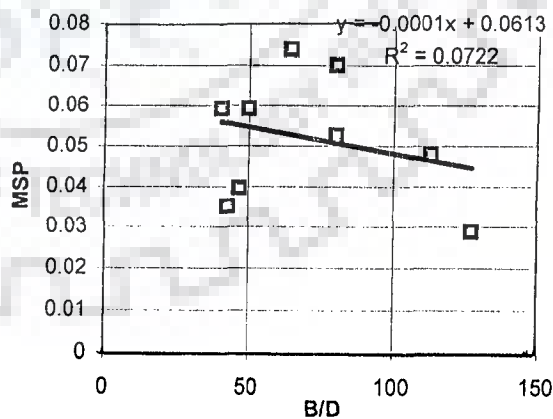


FIG. 6.16f Variation of MSP with B/D ratio for Run-18

FIG. 6.16 a,b,c,d,e,f: VARIATION OF 'MSP' WITH B/D RATIO FOR LAB. DATA

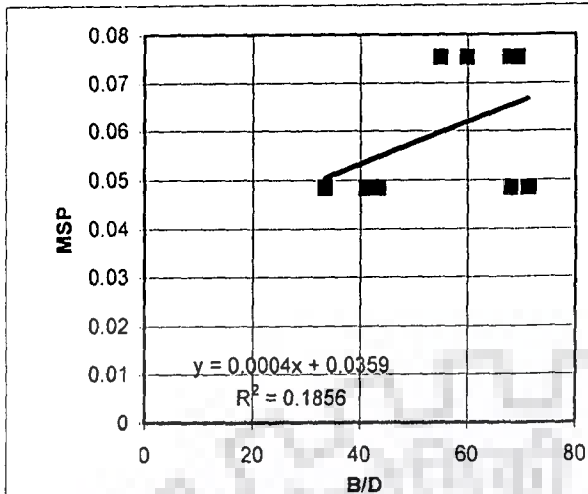


FIG. 6.17a Variation of MSP with B/D ratio for Run-19

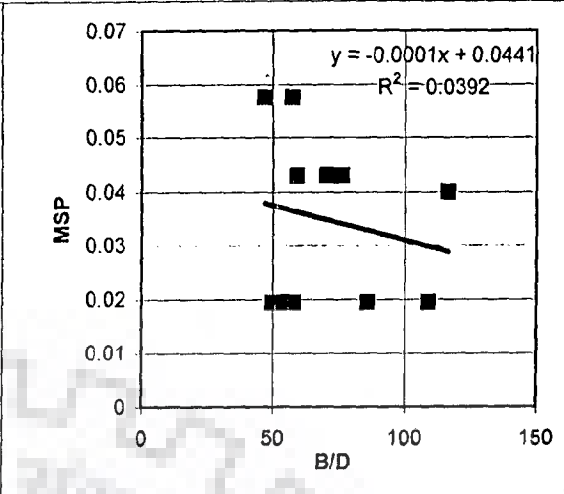


FIG. 6.17b Variation of MSP with B/D ratio for Run-20

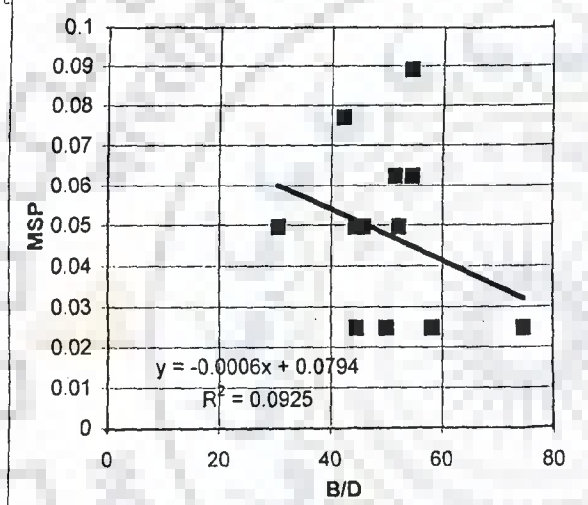


FIG. 6.17c Variation of MSP with B/D ratio for Run-21

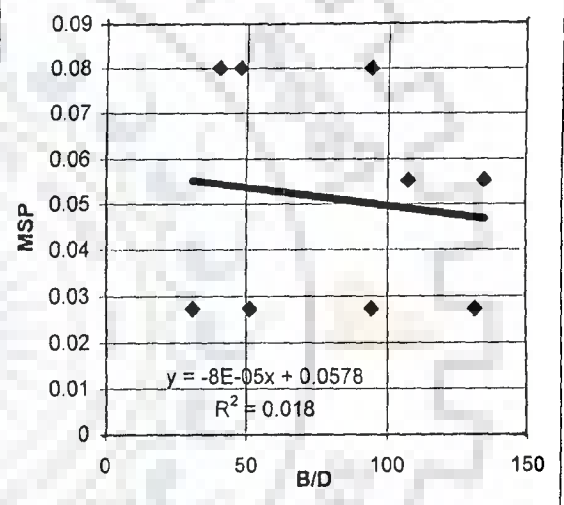


FIG. 6.17d Variation of MSP with B/D ratio for Run-22

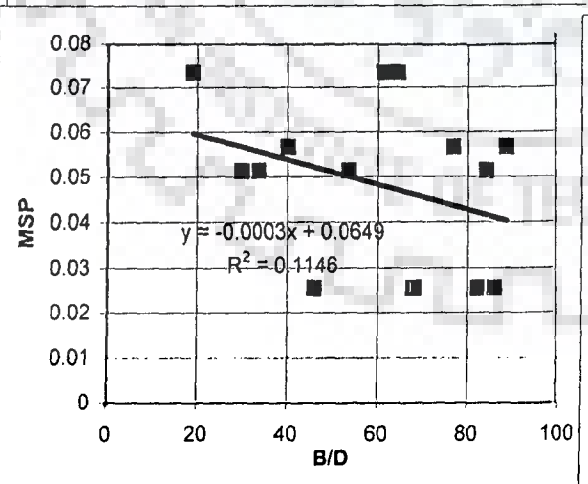


FIG. 6.17e Variation of MSP with B/D ratio for Run-23

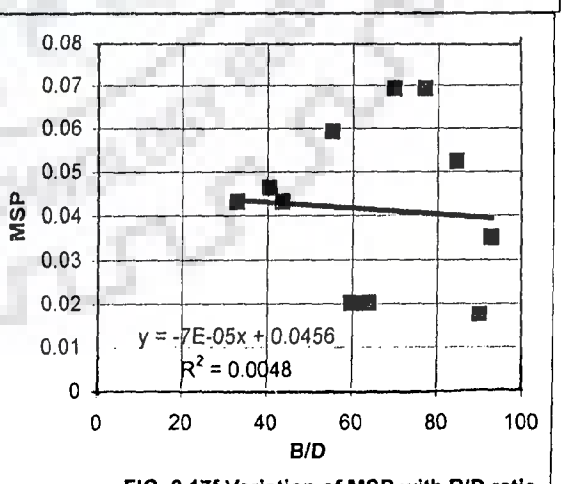


FIG. 6.17f Variation of MSP with B/D ratio for Run-24

FIG. 6.17 a,b,c,d,e,f: VARIATION OF 'MSP' WITH B/D RATIO FOR LAB. DATA

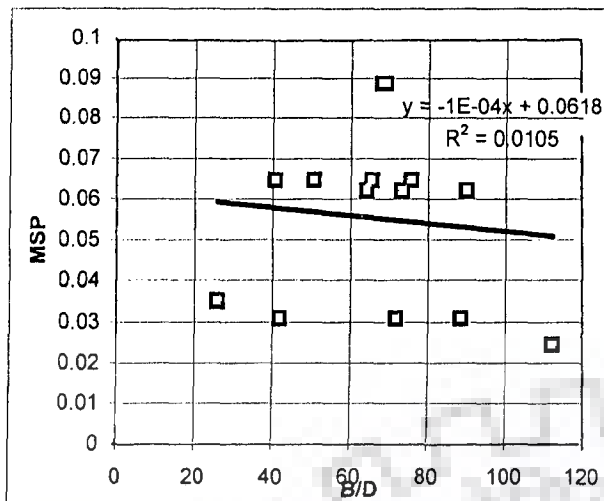


FIG. 6.18a Variation of MSP with B/D ratio for Run-25

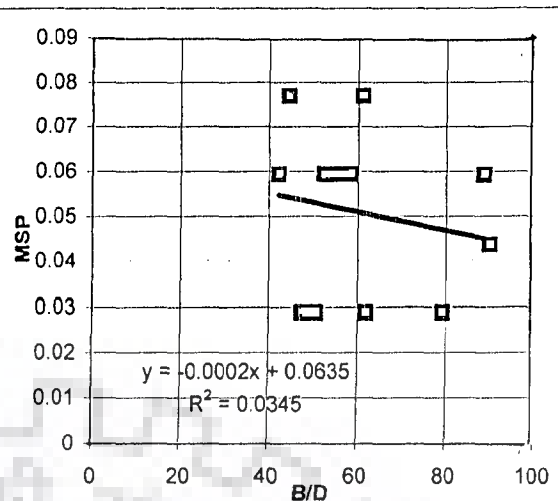


FIG. 6.18b Variation of MSP with B/D ratio for Run-26

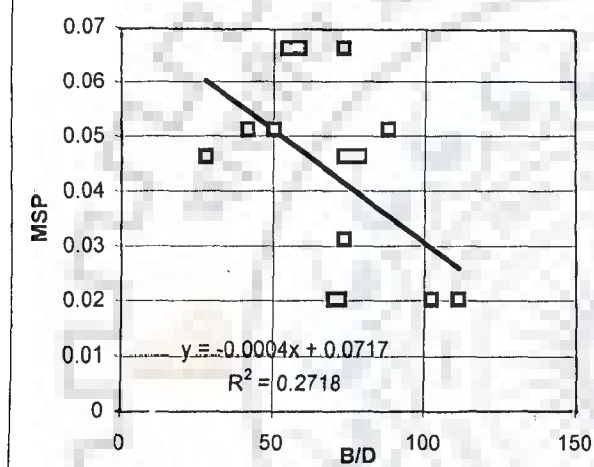


FIG. 6.18c Variation of MSP with B/D ratio for Run-27

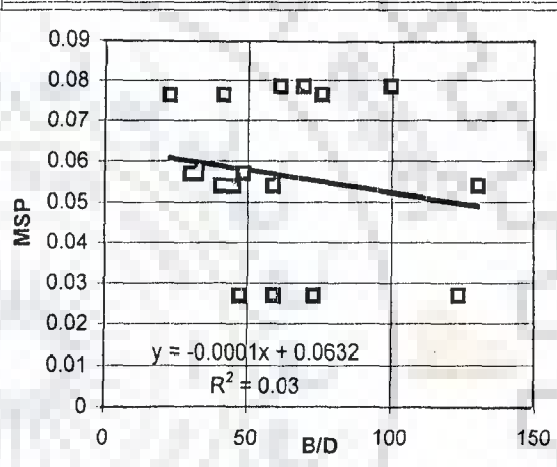


FIG. 6.18d Variation of MSP with B/D ratio for Run-28

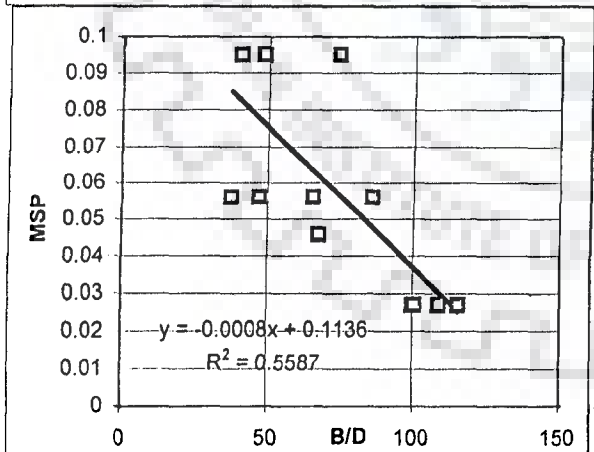


FIG. 6.18e Variation of MSP with B/D ratio for Run-29

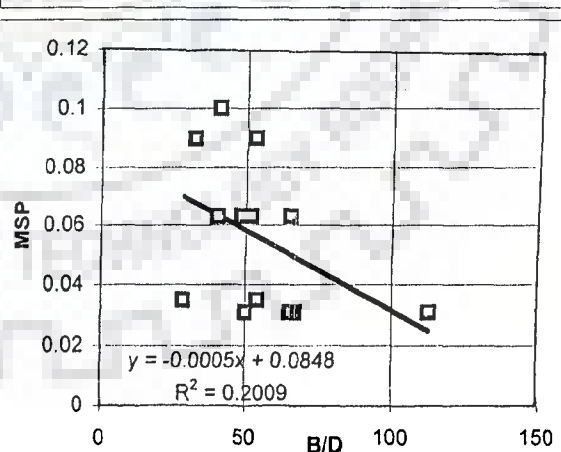


FIG. 6.18f Variation of MSP with B/D ratio for Run-30

FIG. 6.18 a,b,c,d,e,f; VARIATION OF 'MSP' WITH B/D RATIO FOR LAB. DATA

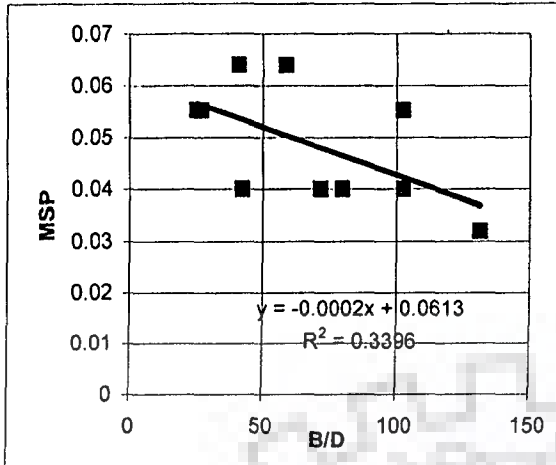


FIG. 6.19a Variation of MSP with B/D for Run-31

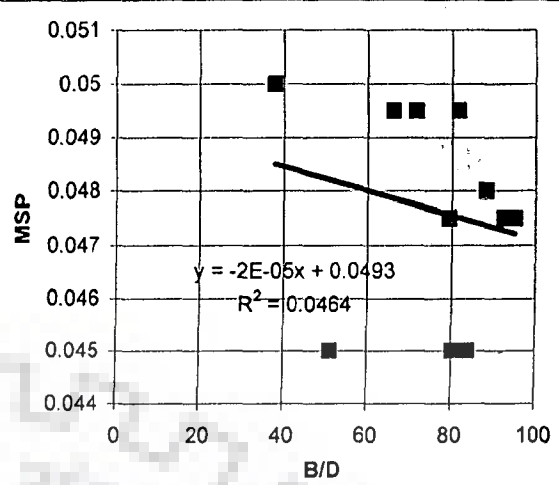


FIG. 6.19b Variation of MSP with B/D for Run-32

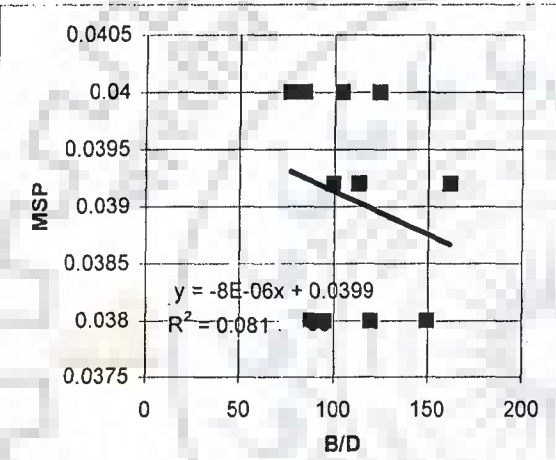


FIG. 6.19c Variation of MSP with B/D for Run-33

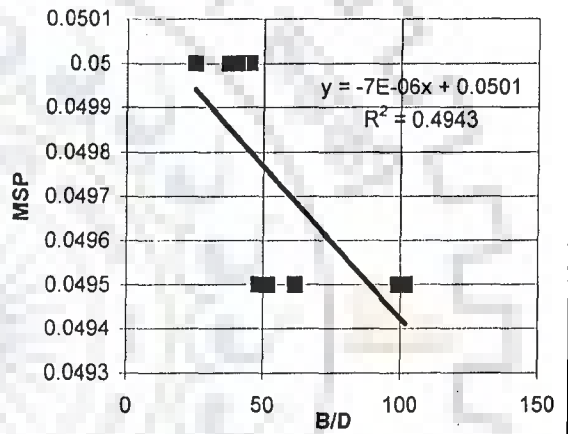


FIG. 6.19d Variation of MSP with B/D for Run-34

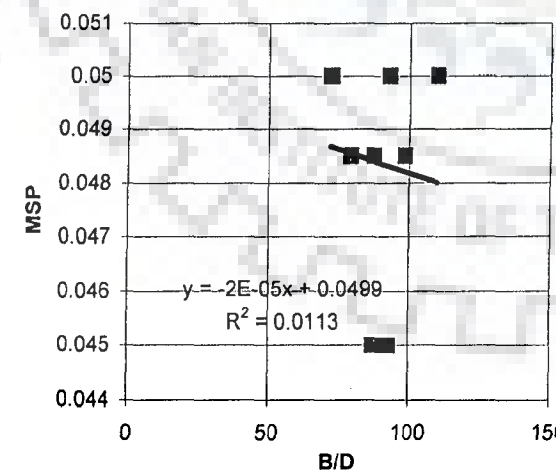


FIG. 6.19e Variation of MSP with B/D ratio for Run-35

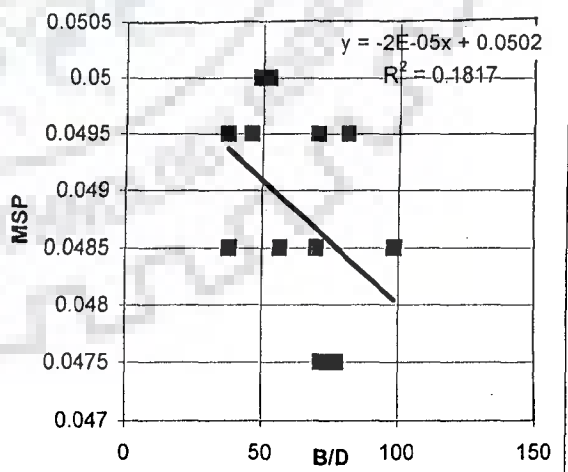


FIG. 6.19f Variation of MSP with B/D ratio for Run-36

FIG. 6.19 a,b,c,d,e,f; VARIATION OF 'MSP' WITH B/D RATIO FOR LAB. DATA

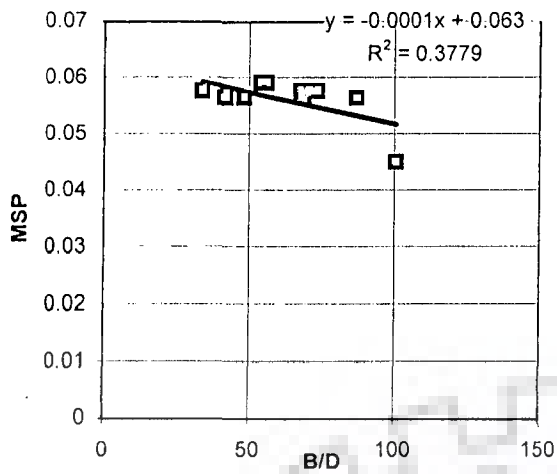


FIG. 6.20a Variation of MSP with B/D ratio for Run-37

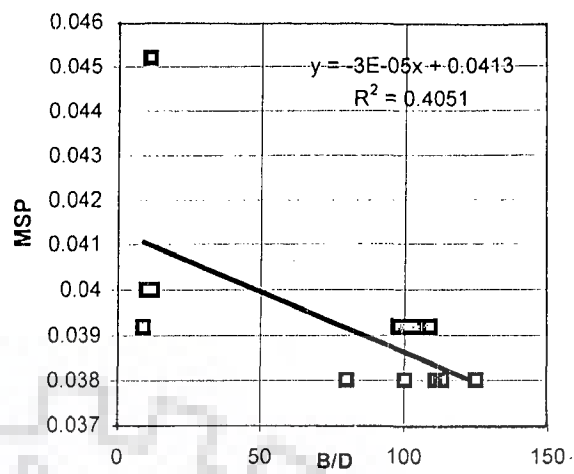


FIG. 6.20b Variation of MSP with B/D ratio for Run-38

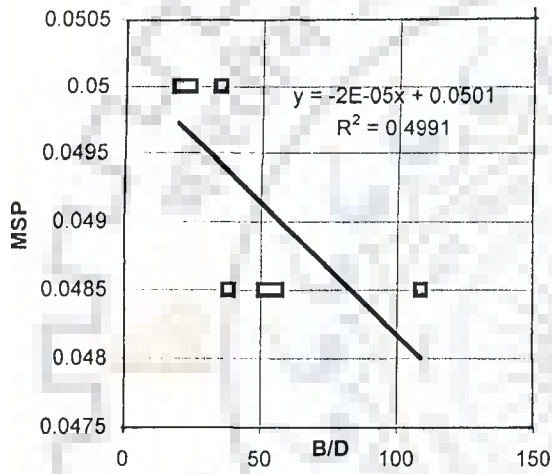


FIG. 6.20c Variation of MSP with B/D ratio for Run-39

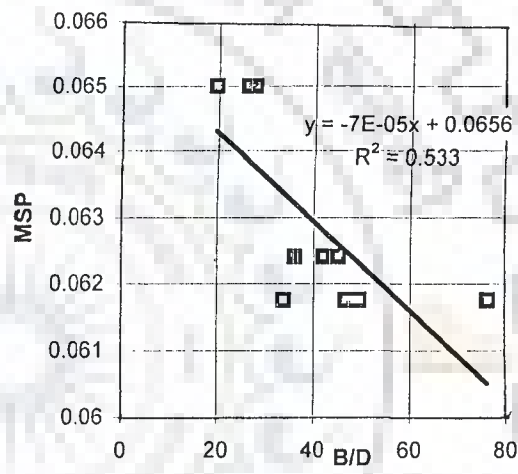


FIG. 6.20d Variation of MSP with B/D ratio for Run-40

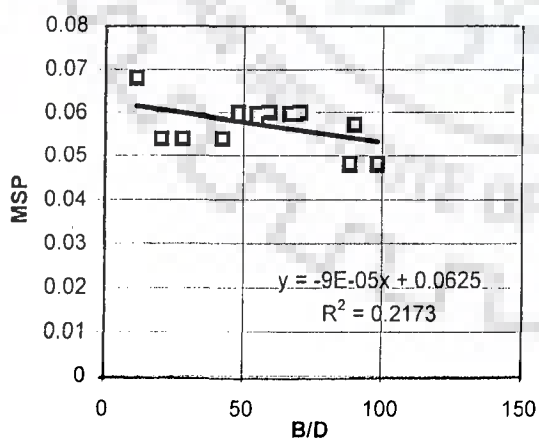


FIG. 6.20e Variation of MSP with B/D ratio for Run-41

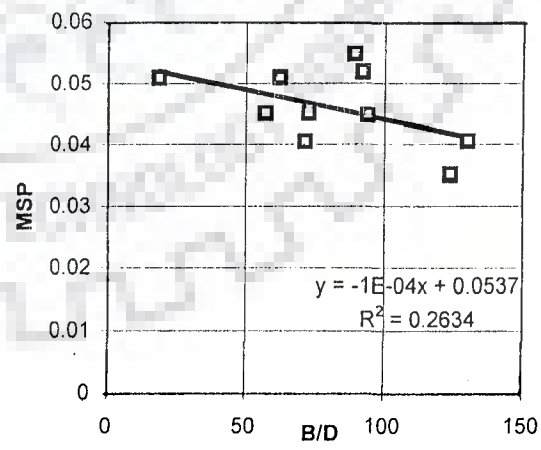


FIG. 6.20f Variation of MSP with B/D ratio for Run-42

FIG. 6.20 a,b,c,d,e,f: VARIATION OF 'MSP' WITH B/D RATIO FOR LAB. DATA

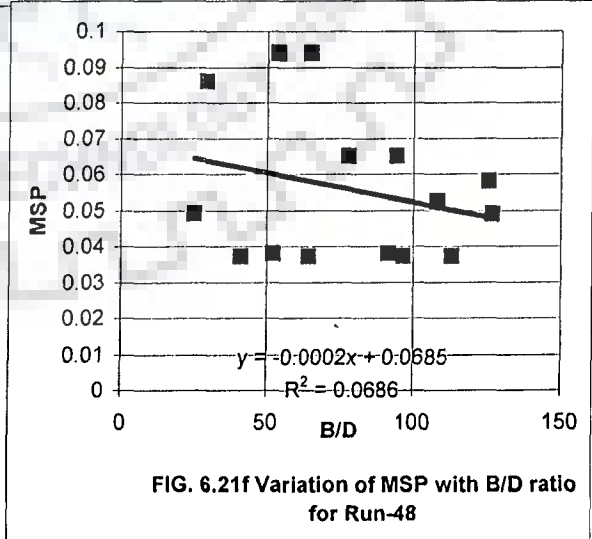
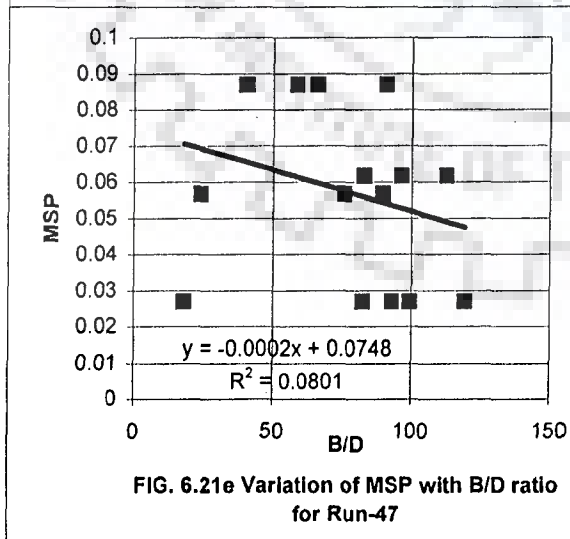
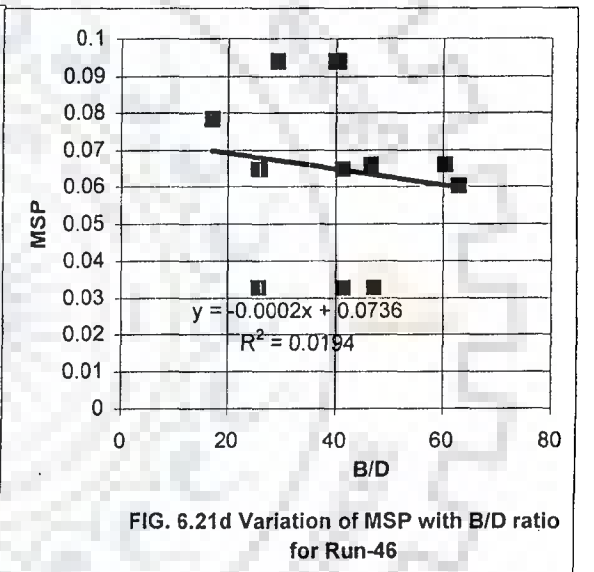
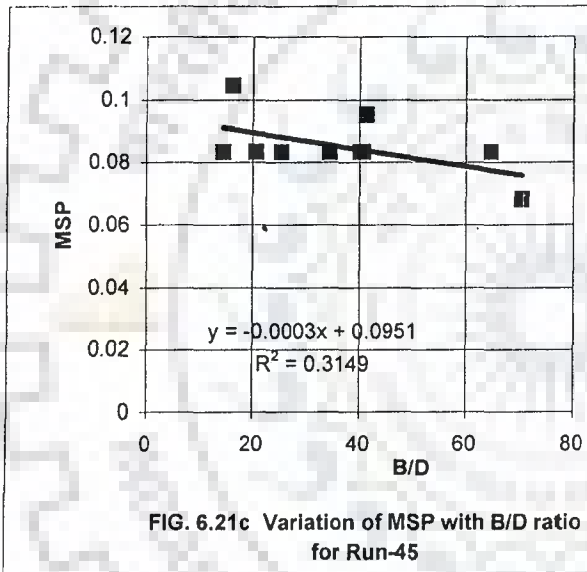
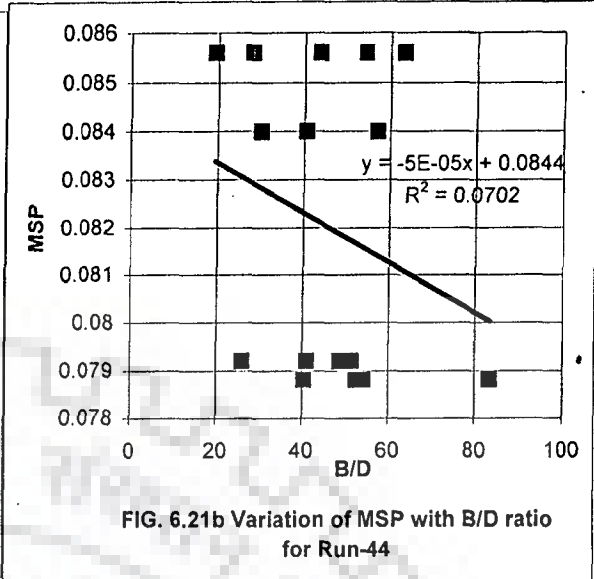
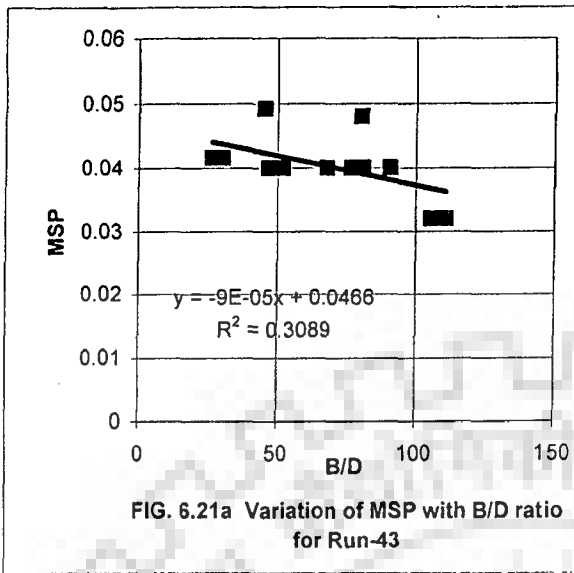


FIG. 6.21 a,b,c,d,e,f-VARIATION OF 'MSP' WITH B/D RATIO FOR LAB. DATA

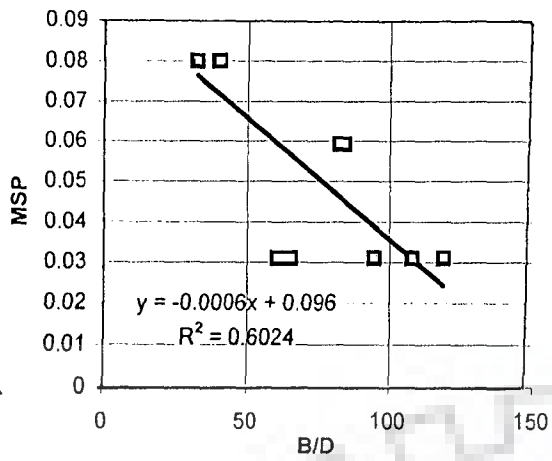


FIG. 6.22a Variation of MSP with B/D ratio for Run-49

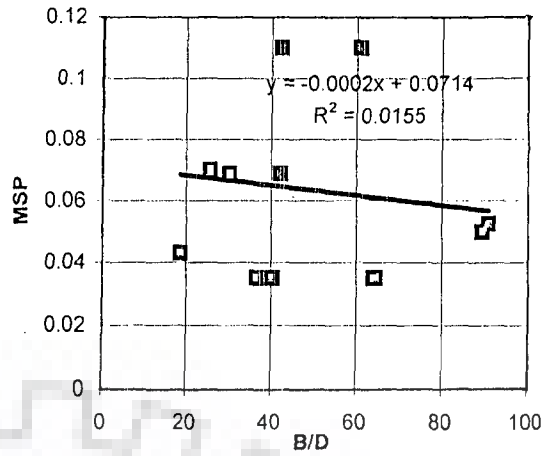


FIG. 6.22b Variation of MSP with B/D ratio for Run-50

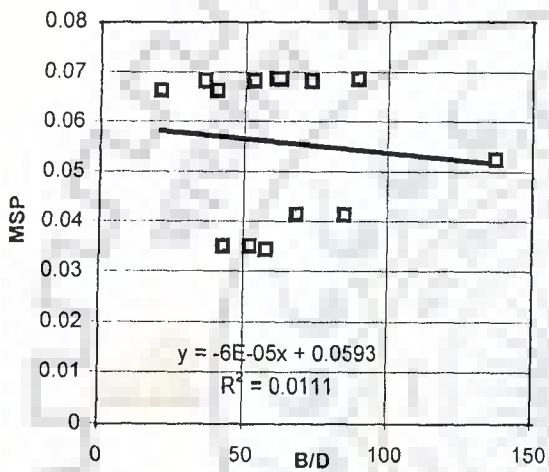


FIG. 6.22c Variation of MSP with B/D ratio for Run-51

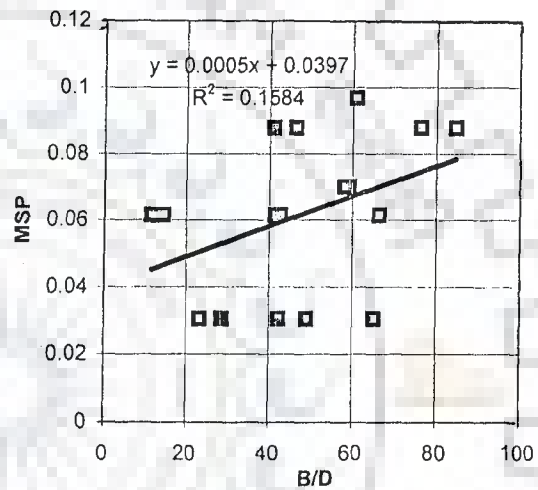


FIG. 6.22d Variation of MSP with B/D ratio for Run-52

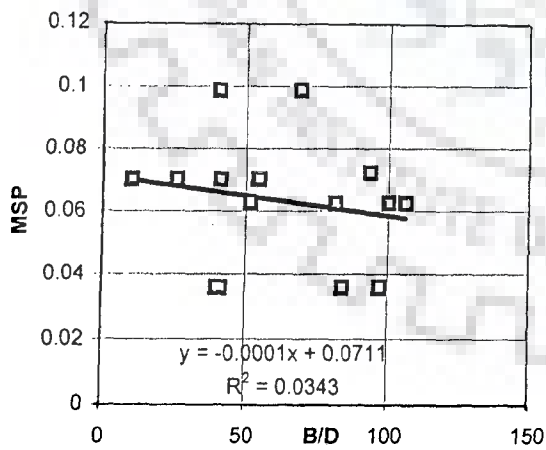


FIG. 6.22e Variation of MSP with B/D ratio for Run-53

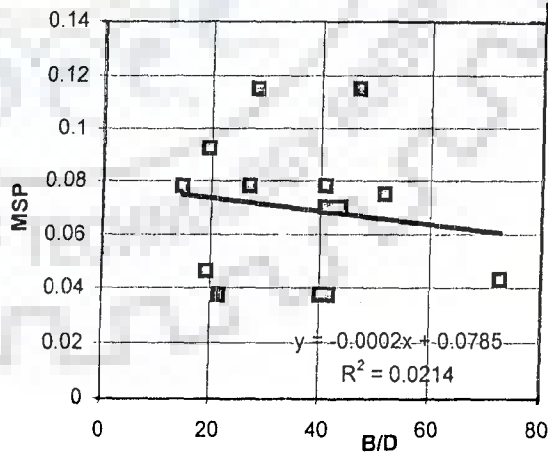


FIG. 6.22f Variation of MSP with B/D ratio for Run-54

FIG. 6.22 a,b,c,d,e,f; VARIATION OF 'MSP' WITH B/D RATIO FOR LAB. DATA

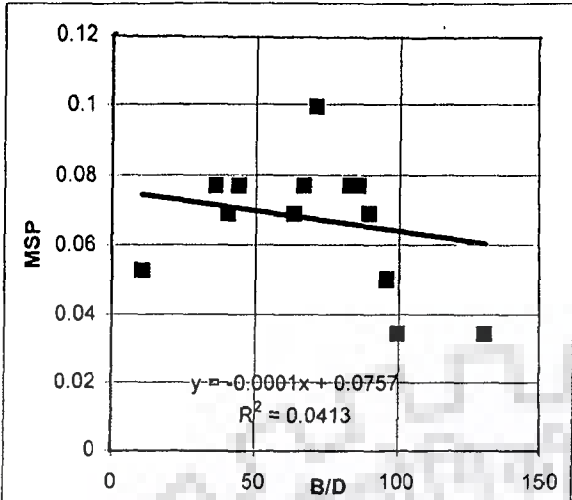


FIG. 6.23a Variation of MSP with B/D ratio for Run-55

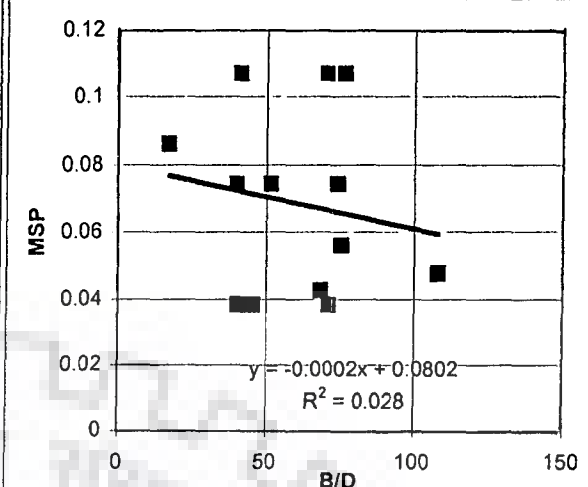


FIG. 6.23b Variation of MSP with B/D ratio for Run-56

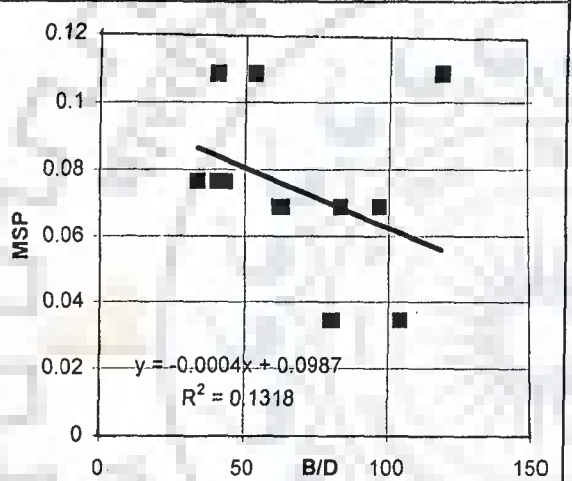


FIG. 6.23c Variation of MSP with B/D ratio for Run-57

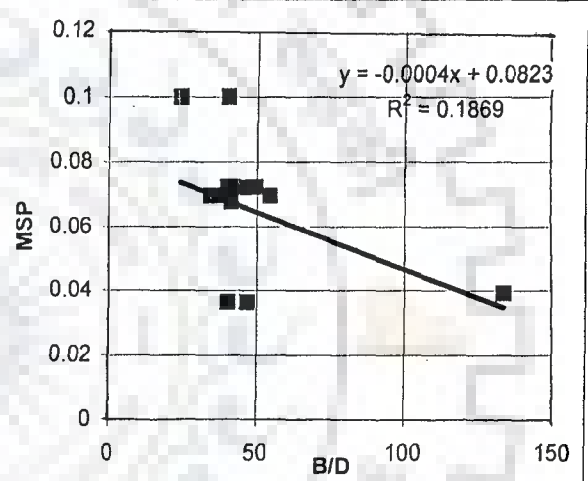


FIG. 6.23d Variation of MSP with B/D ratio for Run-58

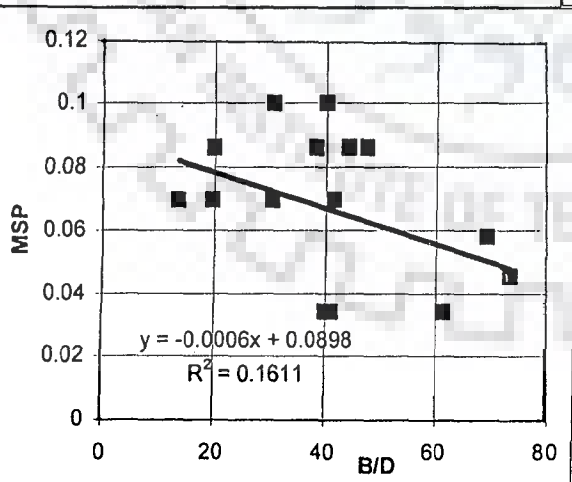


FIG. 6.23e Variation of MSP with B/D ratio for Run-59

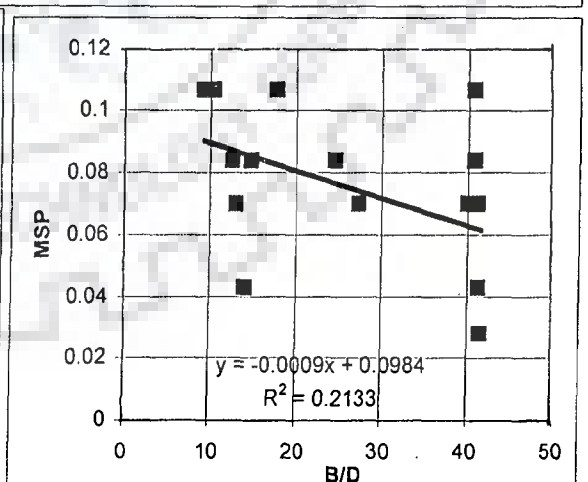


FIG. 6.23f Variation of MSP with B/D ratio for Run-60

FIG. 6.23;a,b,c,d,e,f: VARIATION OF 'MSP' WITH B/D RATIO FOR LAB. DATA

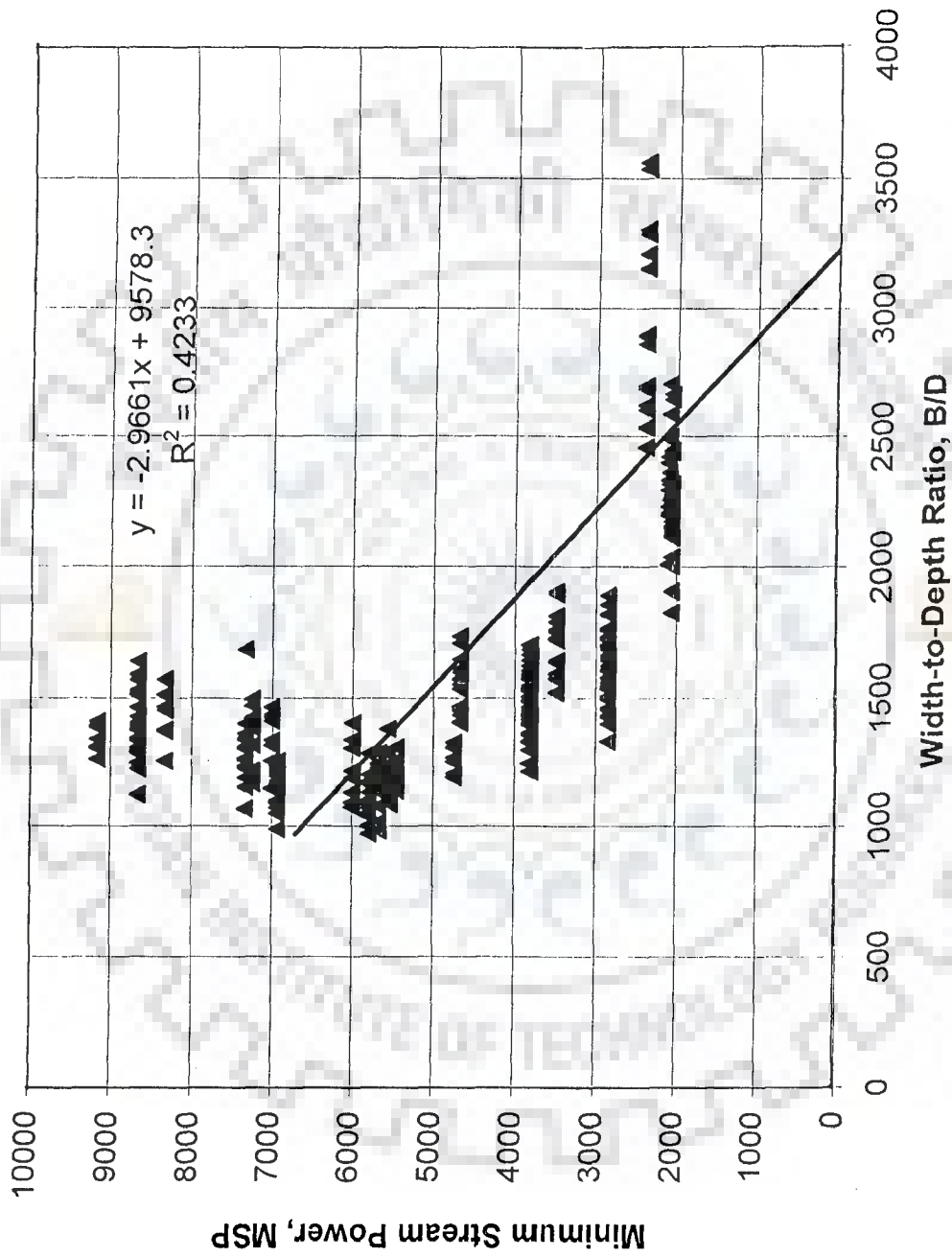


FIG. 6.24: VARIATION OF 'MSP' WITH B/D RATIO FOR MODEL STUDY OF A PARTICULAR STRETCH OF THE BRAHMAPUTRA RIVER

and Fig. 6.25 show the variation of MSP with B/D ratio for the model experiments and field data, respectively. From these above figures, it clearly emerges that energy expenditure process has a profound bearing on enhancement of braid bar formation. From the afore-said graphical plots, it has become evident that one of the root causes of braid bar formations can be attributed to energy loss mechanism, which is confirmation of research findings of Parker (1976) and Sharma (1995). However, Parker (1976) and Sharma (1995) did not carry out investigations on theoretical based concept of minimum energy dissipation rate.

6.4.1.3 Variation of MFF

Furthermore, in this work an assessment of maximum friction factor, MFF, hypothesis was undertaken, adopting the same sets of laboratory and field data. Figs. 6.26 to Fig.6.35 vividly depict the general trend of variation of MFF with B/D ratio for the laboratory based experiments, conducted in phase-I. Similarly, Fig. 6.36 and 6.37 show the variation of MFF for the model experiments and field data, respectively. With the exception of the field data, these figures exhibit by and large encouraging trend when friction factor values register a rising behavior with increasing B/D ratio. From the above-mentioned graphical plots, it can be surmised that with intensification of braiding, flow resistance channel assumes higher values. This behavior is in closed conformity with the maximum friction factor concept, as was enunciated by Davis and Sutherland (1980). However, some of the plots of maximum friction factor (MFF) versus B/D ratio have also displayed departure from the aforementioned trend. Perhaps this deviation can

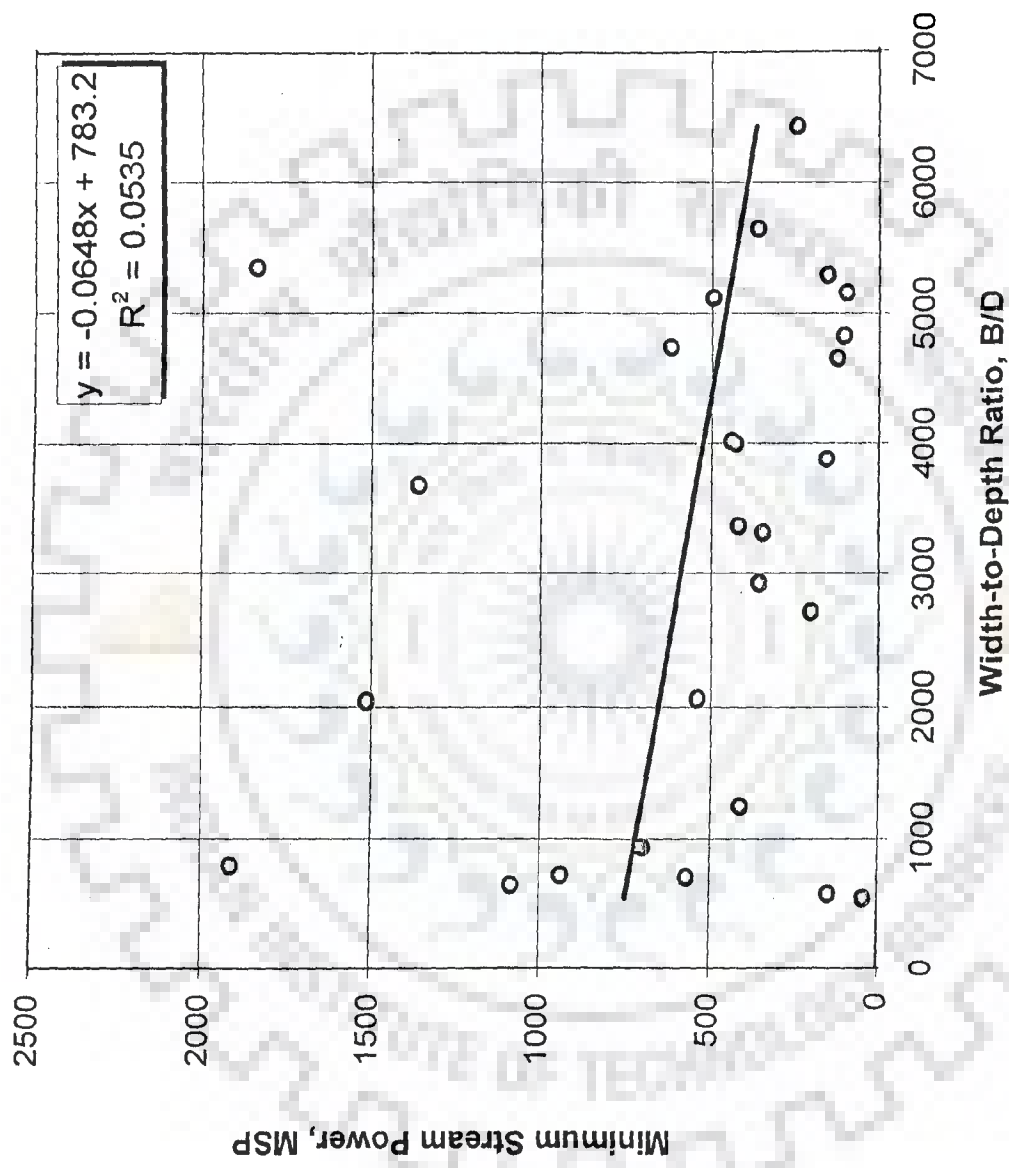


FIG. 6.25: VARIATION OF 'MSP' WITH B/D RATIO FOR FIELD DATA

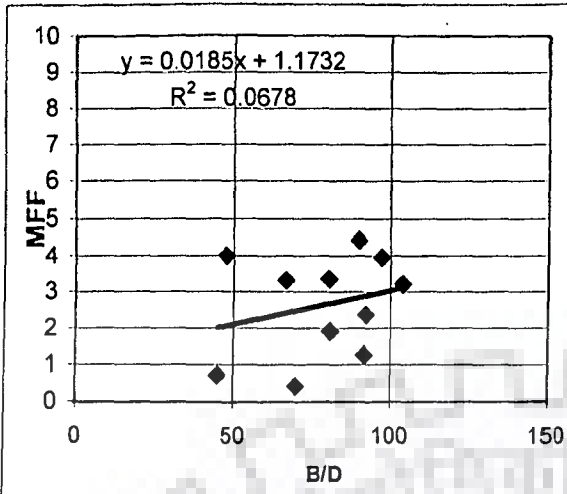


Fig 6.26a Plot of MFF against B/D ratio for Run-1

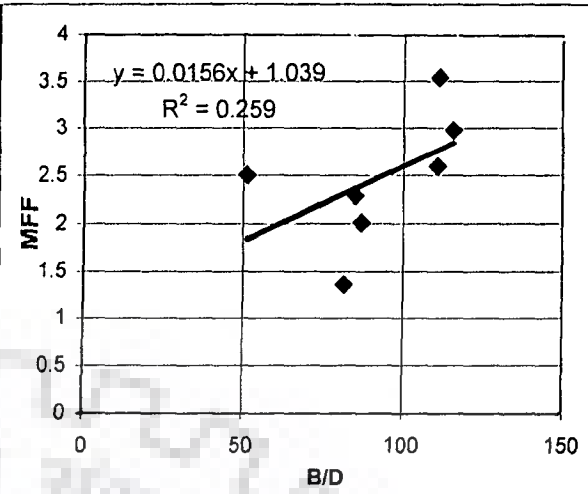


FIG. 6.26b Plot of MFF against B/D ratio for Run-2

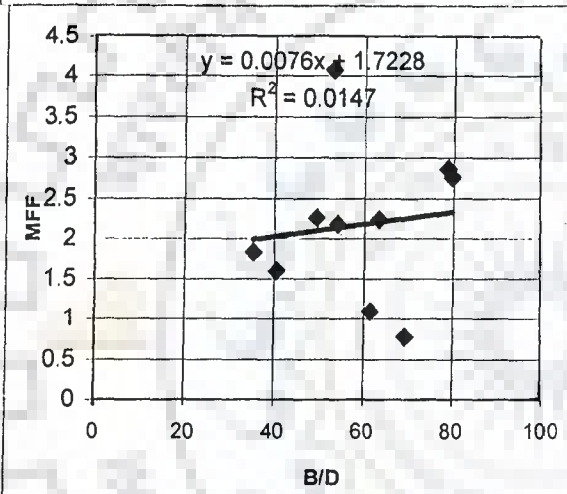


FIG. 6.26c Plot of MFF against B/D ratio for Run-3

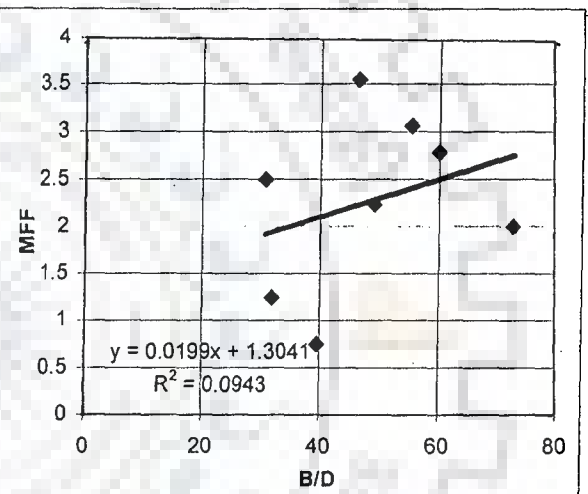


FIG 6.26d Plot of MFF against B/D for Run-4

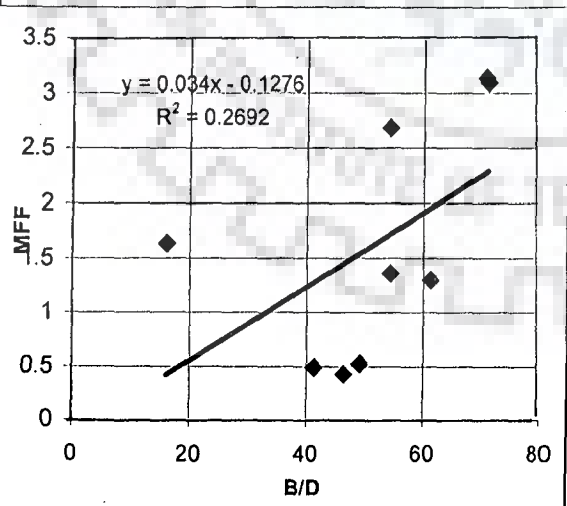


FIG 6.26e Plot of MFF against B/D ratio for Run-5

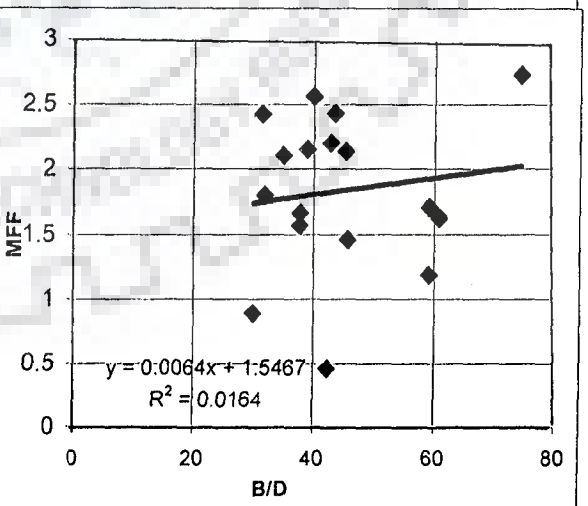


FIG. 6.26f Plot of MFF against B/D ratio for Run-6

FIG. 6.26.a,b,c,d,e,f:PLOT OF 'MFF' AGAINST B/D RATIO FOR LAB. DATA

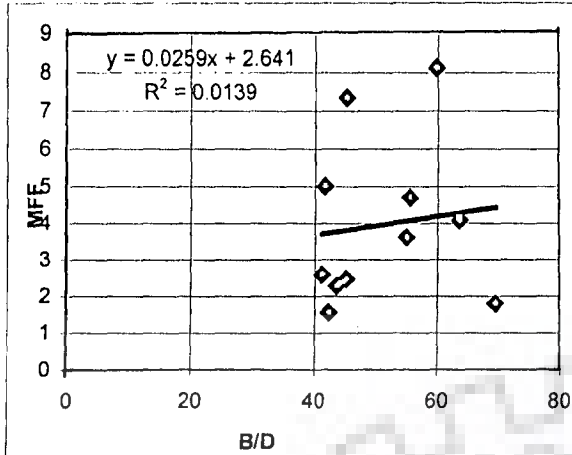


FIG. 6.27a Plot of MFF against B/D ratio for Run-7

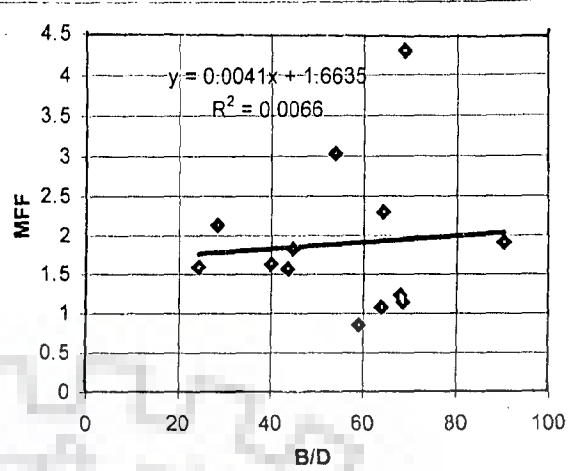


FIG. 6.27b Plot of MFF against B/D ratio for Run-8

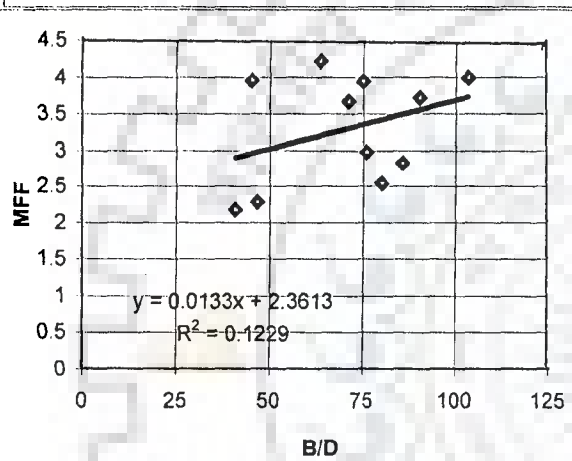


FIG. 6.27c Plot of MFF against B/D ratio for Run-9

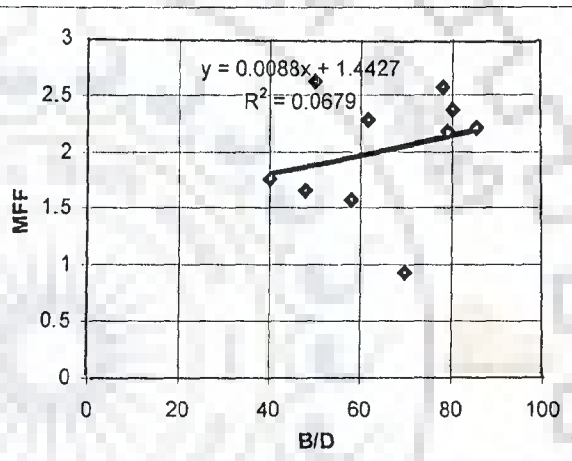


FIG. 6.27d Plot of MFF against B/D ratio for Run-10

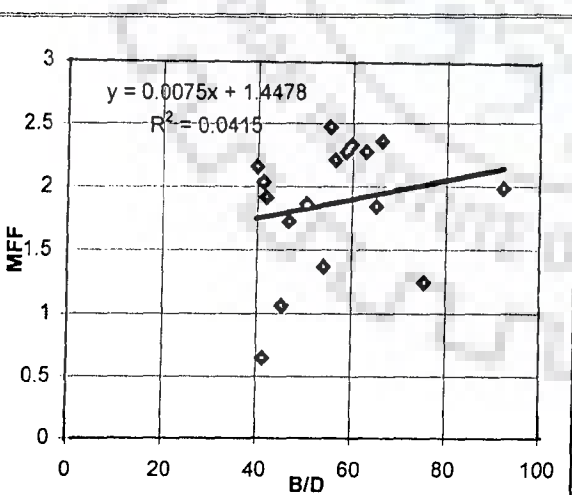


FIG. 6.27e Plot of MFF against B/D ratio for Run-11

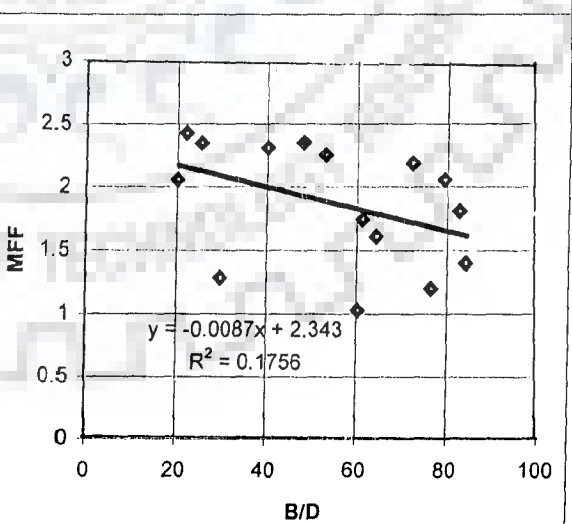


FIG. 6.27f Plot of MFF against B/D ratio for Run-12

FIG. 6.27.a,b,c,d,e,f; PLOT OF 'MFF' AGAINST B/D RATIO FOR LAB. DATA

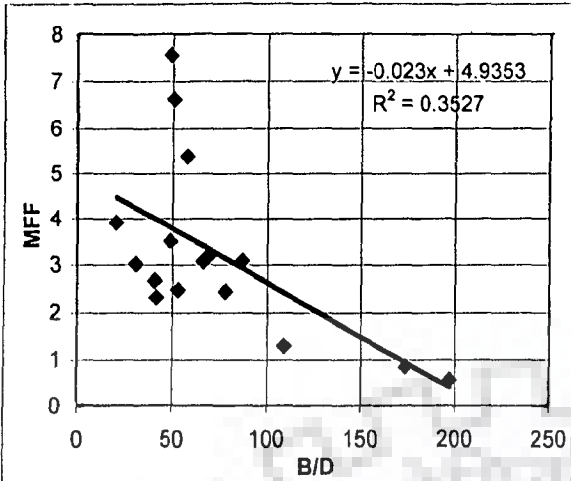


FIG.6.28a Plot of MFF against B/D ratio for Run-13

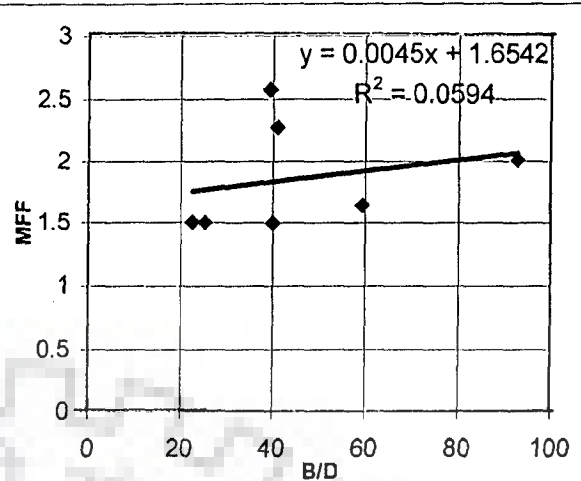


FIG.6.28b Plot of MFF against B/D ratio for Run-14

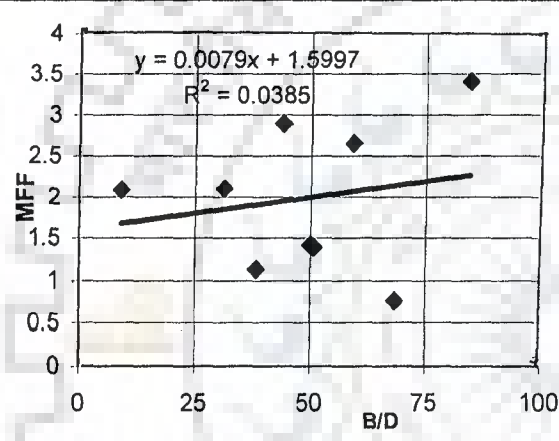


FIG.6.28c Plot of MFF against B/D ratio for Run-15

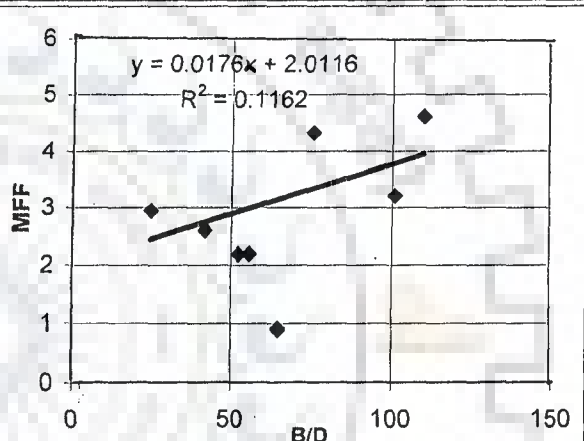


FIG.6.28d Plot of MFF against B/D ratio for Run-16

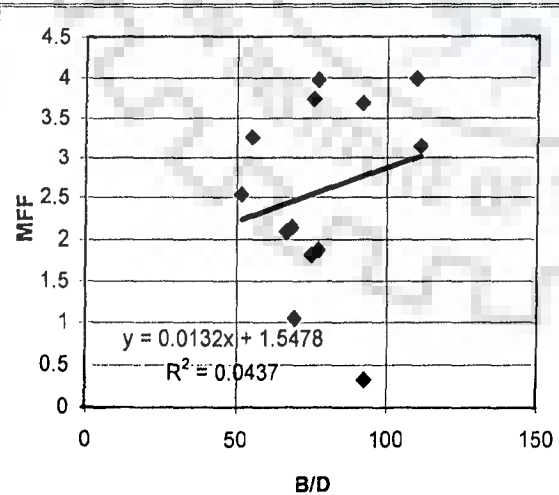


FIG.6.28e Plot of MFF against B/D ratio for Run-17

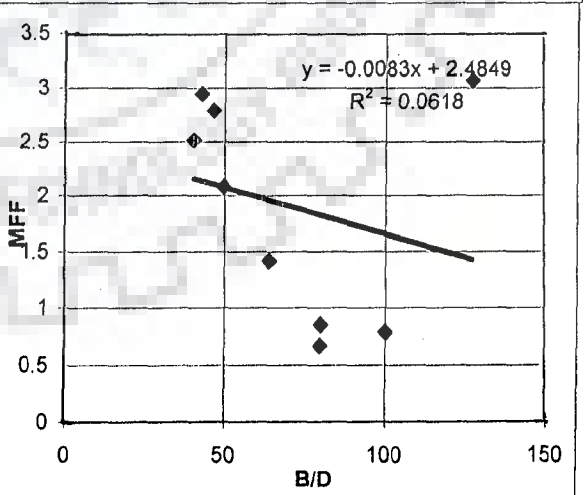


FIG.6.28e Plot of MFF against B/D ratio for Run-18

FIG. 6.28.a,b,c,d,e,f PLOT OF 'MFF' AGAINST B/D RATIO FOR LAB. DATA

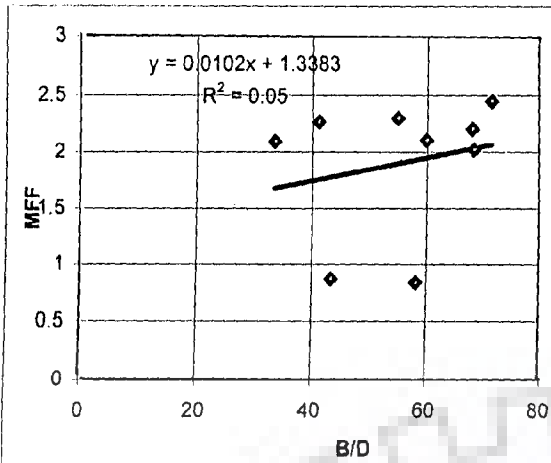


FIG. 6.29a Plot of MFF against B/D ratio for Run-19

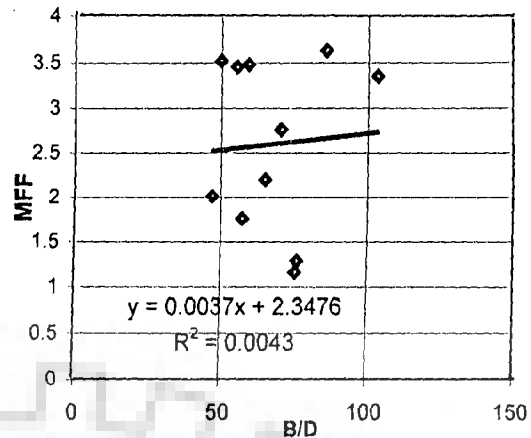


FIG. 6.29b Plot of MFF against B/D ratio for Run-20

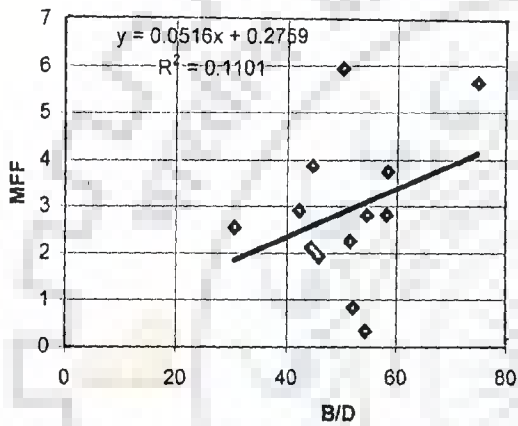


FIG. 6.29c Plot of MFF against B/D ratio for Run-21

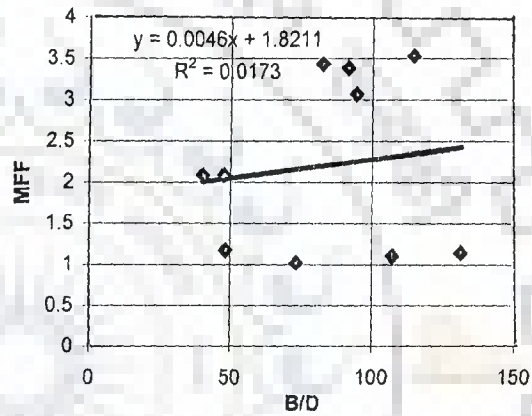


FIG. 6.29d Plot of MFF against B/D ratio for Run-22

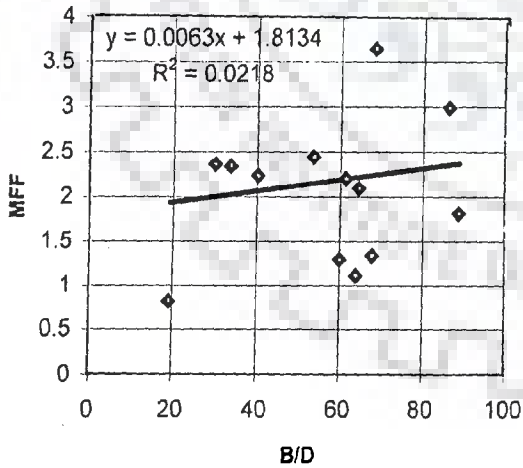


FIG. 6.29e Plot of MFF against B/D ratio for Run-23

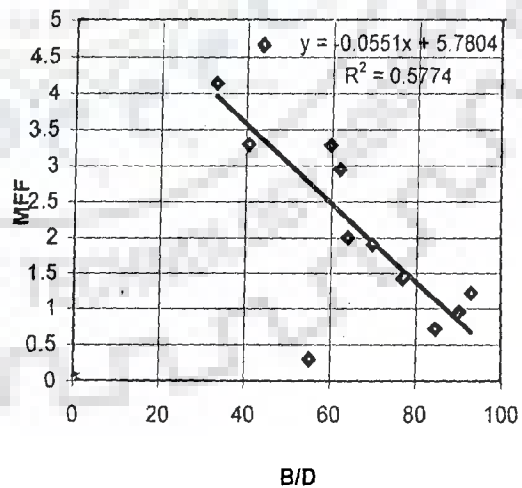


FIG. 6.29f Plot of MFF against B/D ratio for Run-24

Fig. 6.29 a,b,c,d,e,f; PLOT OF 'MFF' AGAINST B/D RATIO FOR LAB. DATA

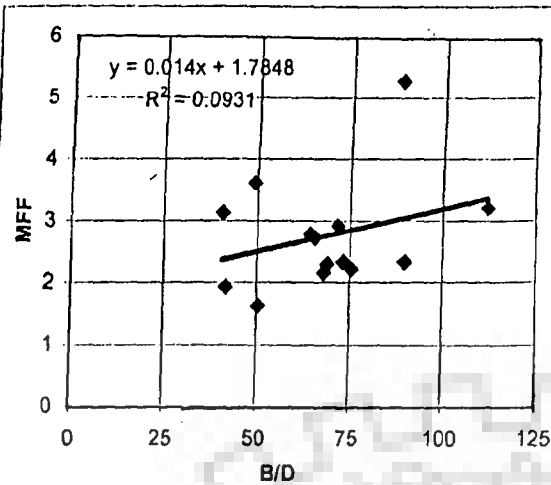


FIG. 6.30a Plot of MFF against B/D ratio for Run-25

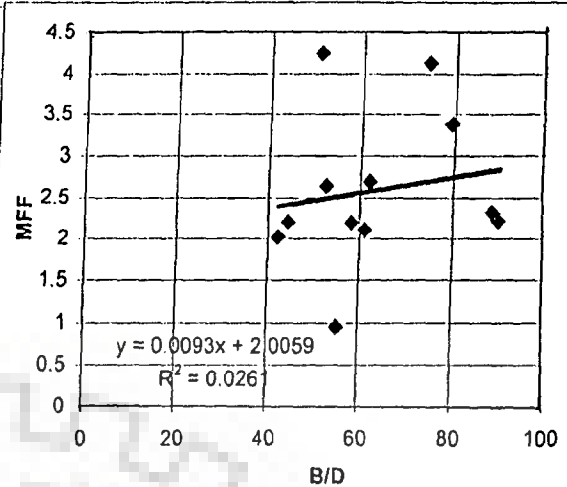


FIG. 6.30b Plot of MFF against B/D ratio for Run-26

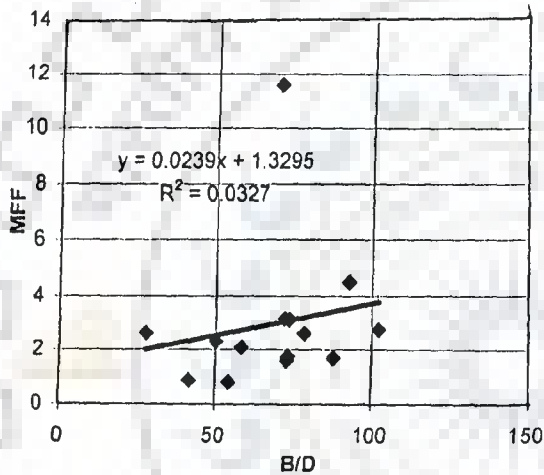


FIG. 6.30c Plot of MFF against B/D ratio for Run-27

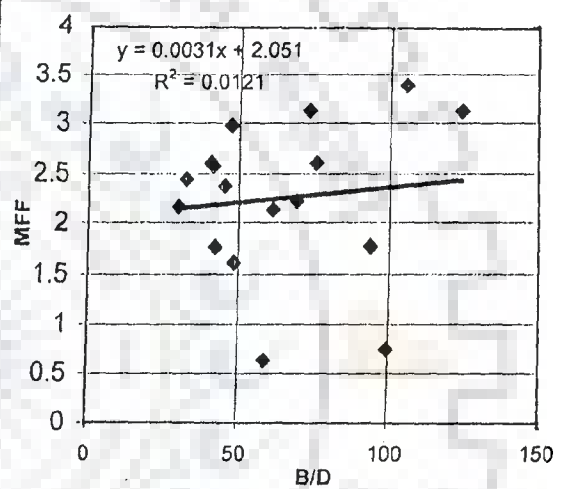


FIG. 6.30d Plot of MFF against B/D ratio for Run-28

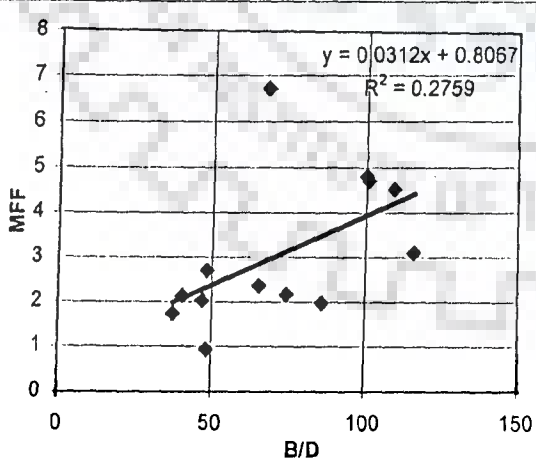


FIG. 6.30e Plot of MFF against B/D ratio for Run-29

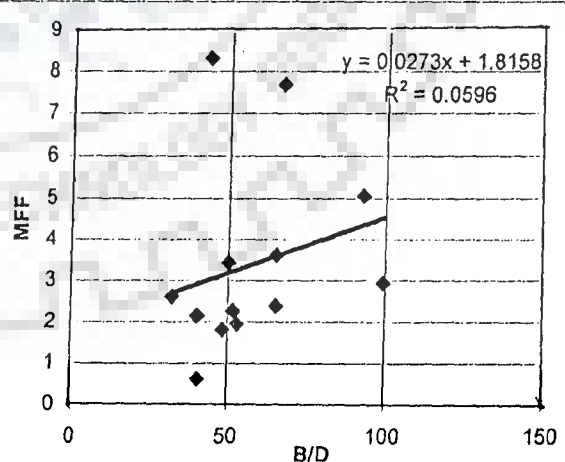


FIG. 6.30f Plot of MFF against B/D ratio for Run-30

FIG. 6.30 a,b,c,d,e,f: PLOT OF 'MFF' AGAINST B/D RATIO FOR LAB. DATA

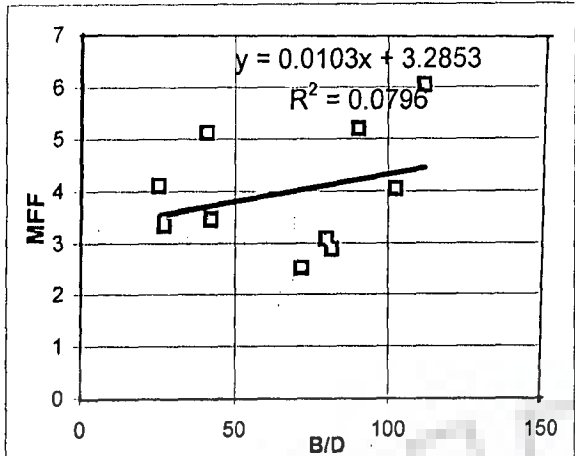


FIG. 6.31a Plot of MFF against B/D ratio for Run-31

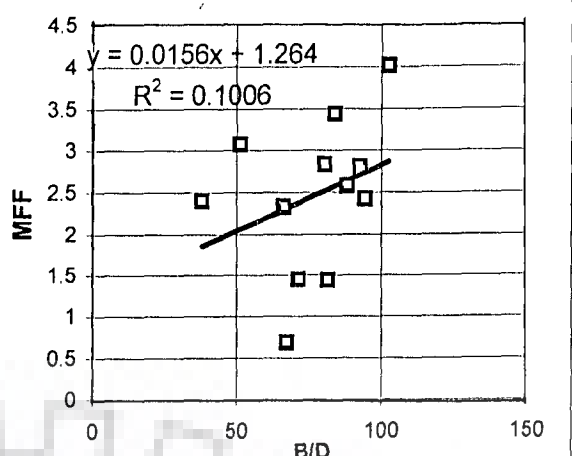


FIG. 6.31b Plot of MFF against B/D ratio for Run-32

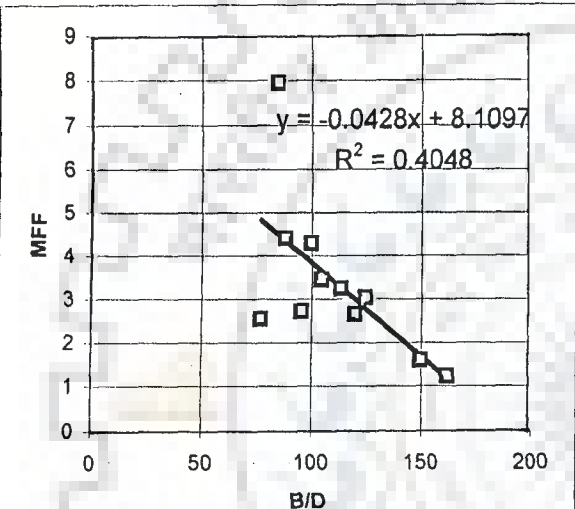


FIG. 6.31c Plot of MFF against B/D ratio for Run-33

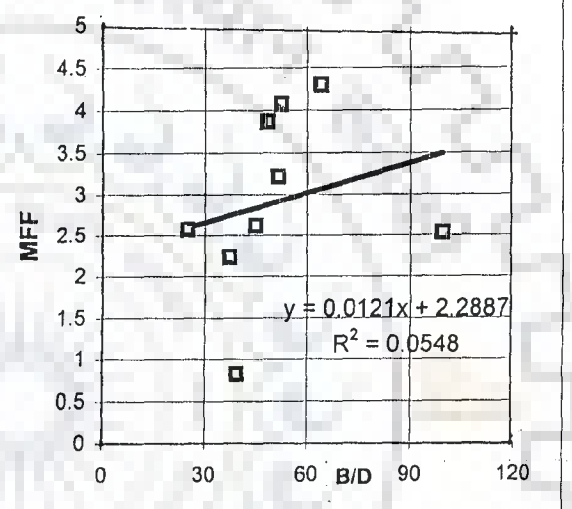


FIG. 6.31d Plot of MFF against B/D ratio for Run-34

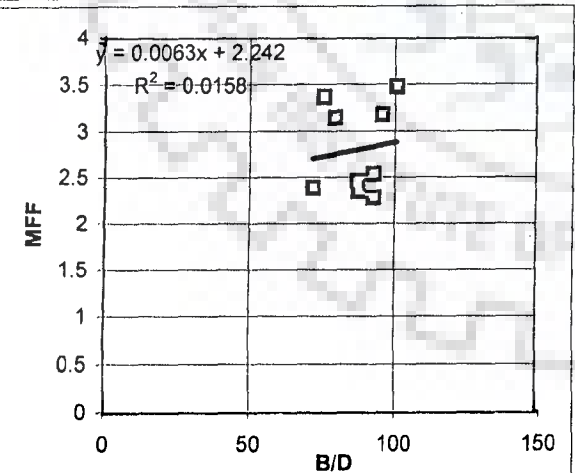


FIG. 6.31e Plot of MFF against B/D ratio for Run-35

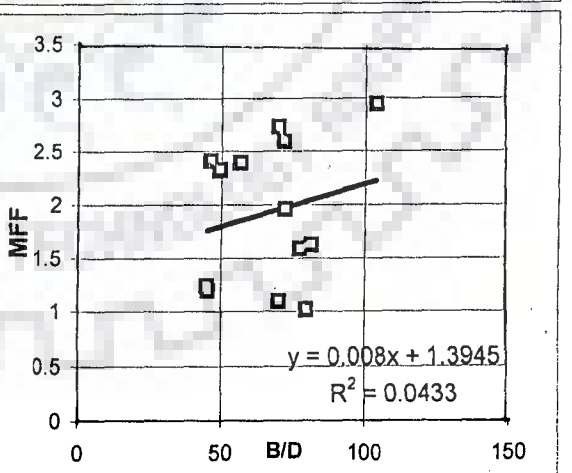


FIG. 6.31f Plot of MFF against B/D ratio for Run-36

FIG. 6.31 a,b,c,d,e,f; PLOT OF 'MFF' AGAINST B/D RATIO FOR LAB. DATA

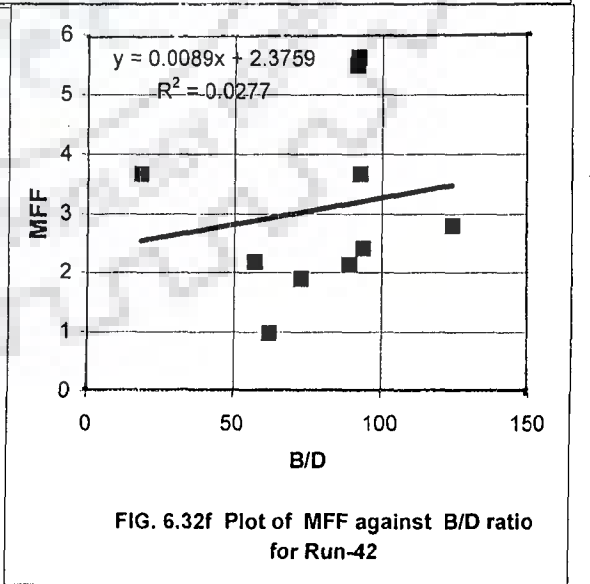
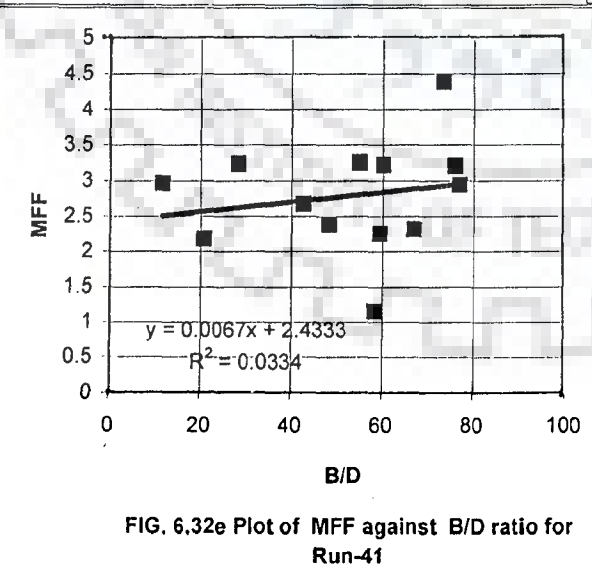
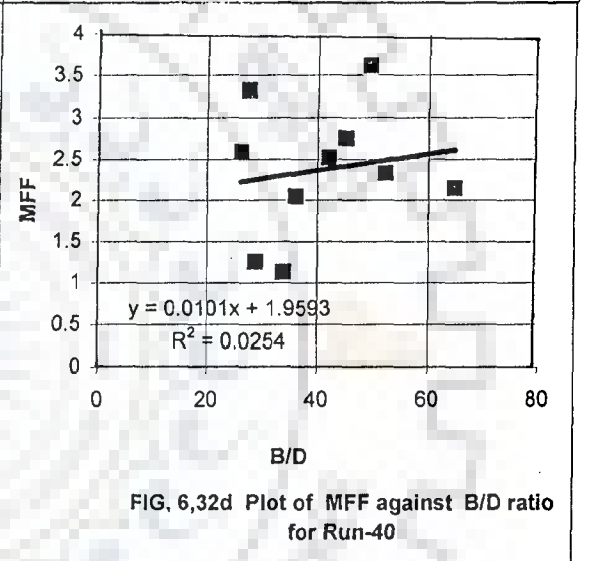
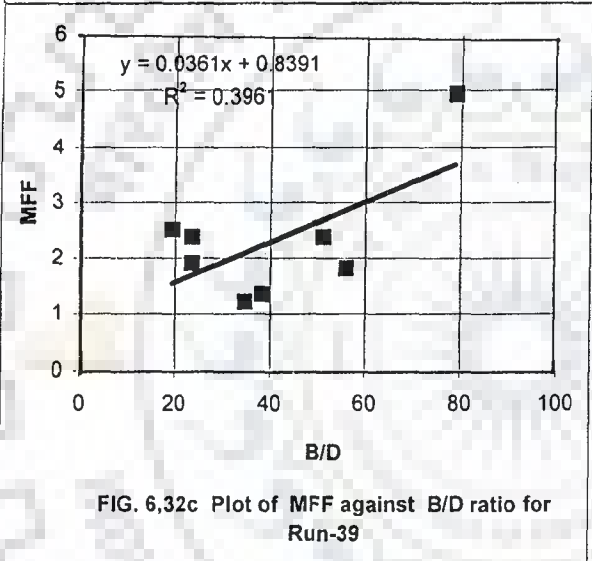
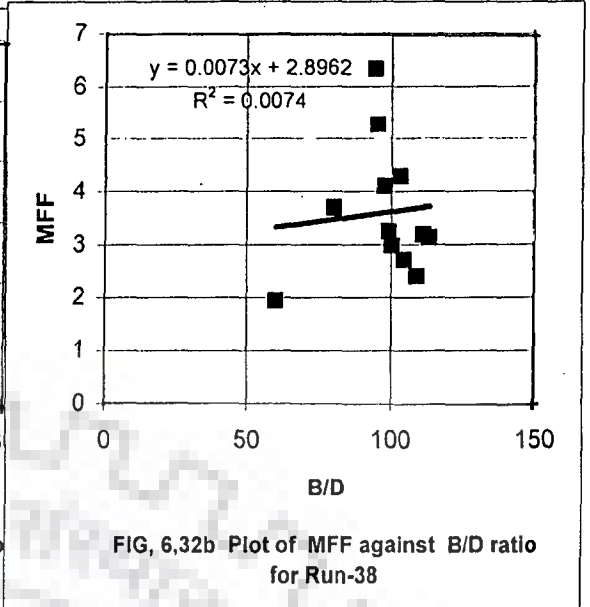
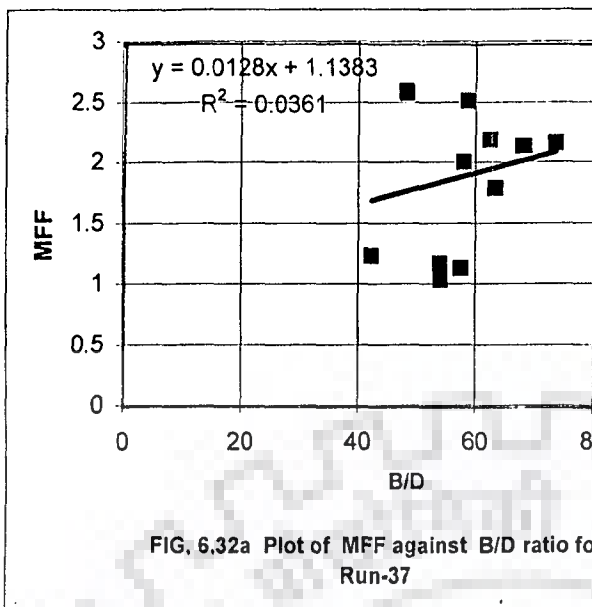


FIG. 6.32.a,b,c,d,e,f PLOT OF 'MFF' AGAINST B/D RATIO FOR LAB. DATA

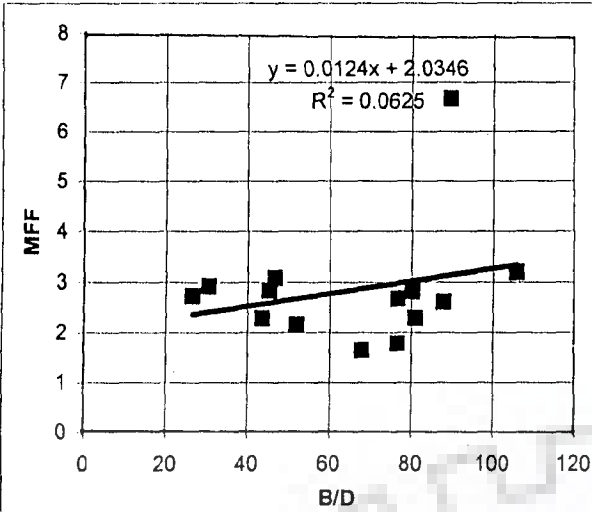


FIG. 6.33a Plot of MFF against B/D ratio for Run-43

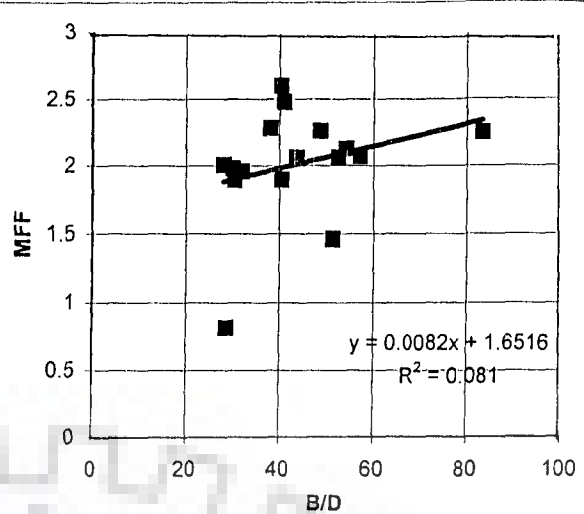


FIG. 6.33b Plot of MFF against B/D ratio for Run-44

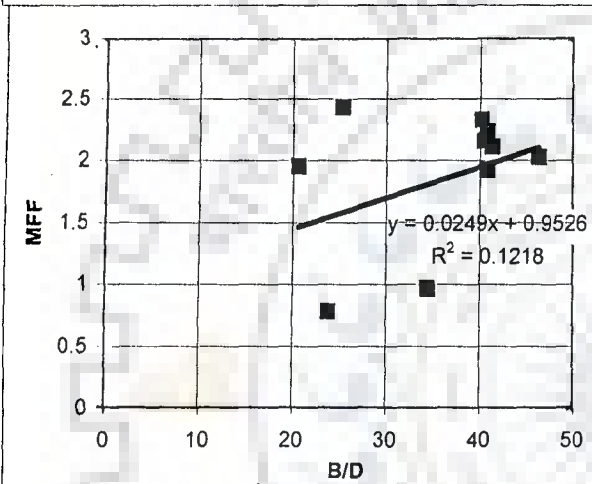


FIG. 6.33c Plot of MFF against B/D ratio for Run-45

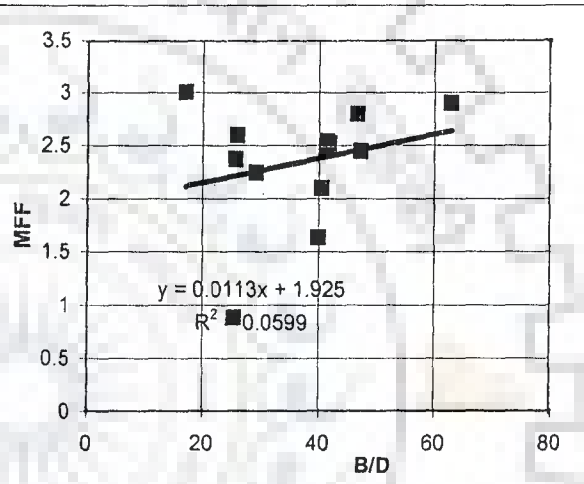


FIG. 6.33d Plot of MFF against B/D ratio for Run-46

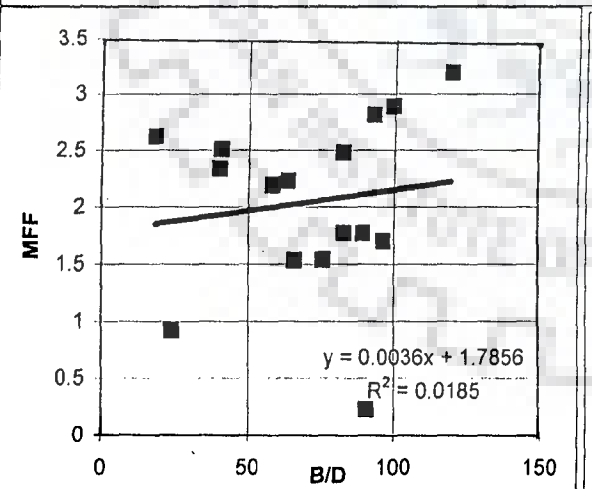


FIG. 6.33e Plot of MFF against B/D ratio for Run-47

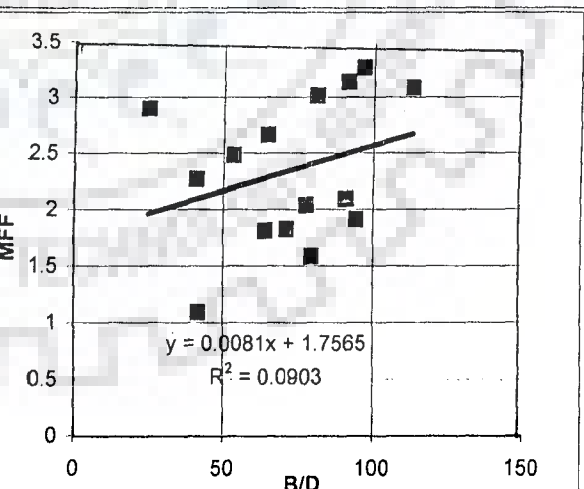


FIG. 6.33f Plot of MFF against B/D ratio for Run-48

FIG.6.33 a,b,c,d,e,f: PLOT OF 'MFF' AGAINST B/D RATIO FOR LAB. DATA

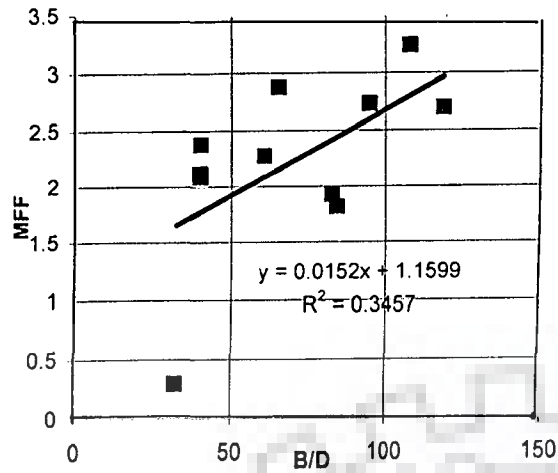


FIG. 6.34a Plot MFF against B/D ratio for Run-49

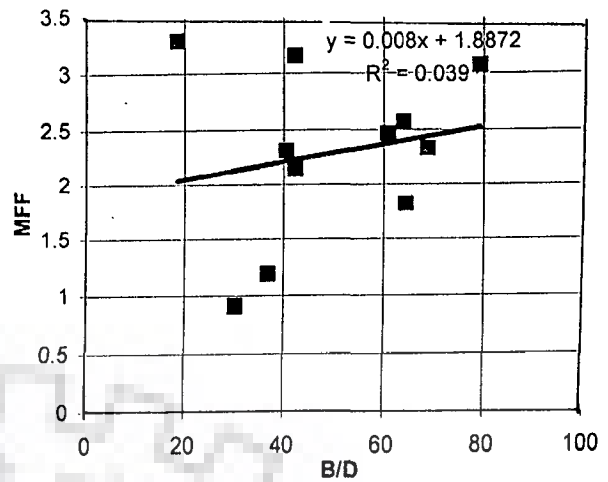


FIG. 6.34b Plot MFF against B/D ratio for Run-50

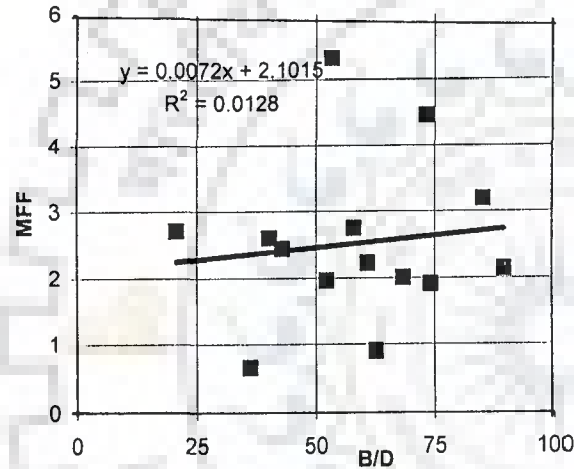


FIG. 6.34c Plot MFF against B/D ratio for Run-51

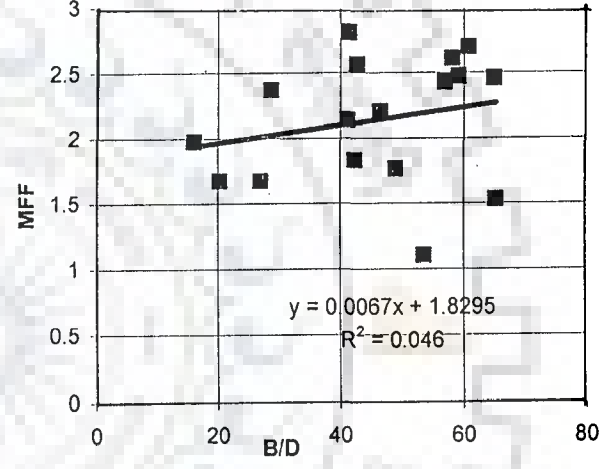


FIG. 6.34d Plot MFF against B/D ratio for Run-52

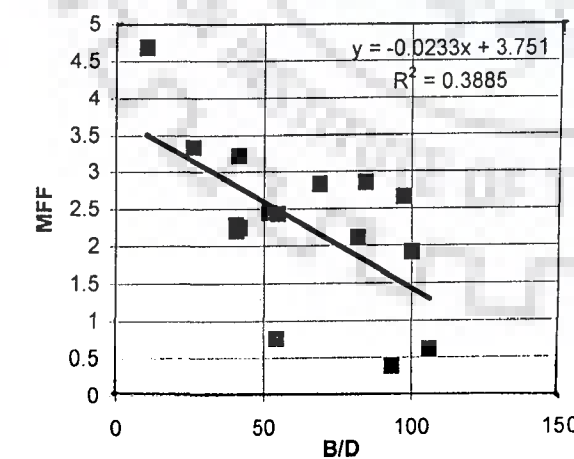


FIG. 6.34e Plot MFF against B/D ratio for Run-53

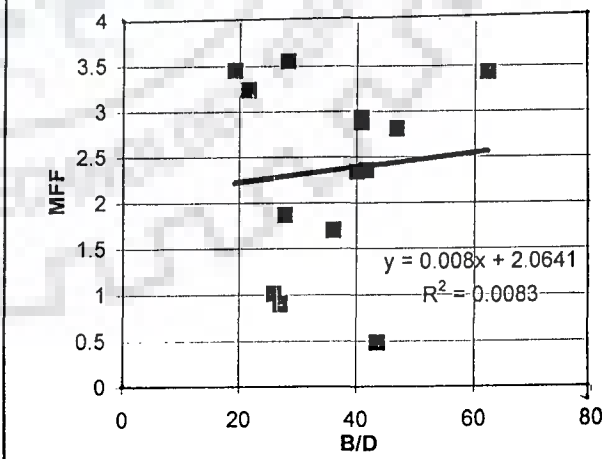


FIG. 6.34f Plot MFF against B/D ratio for Run-54

FIG. 6.34 a,b,c,d,e,f; PLOT OF 'MFF' AGAINST B/D RATIO FOR LAB. DATA

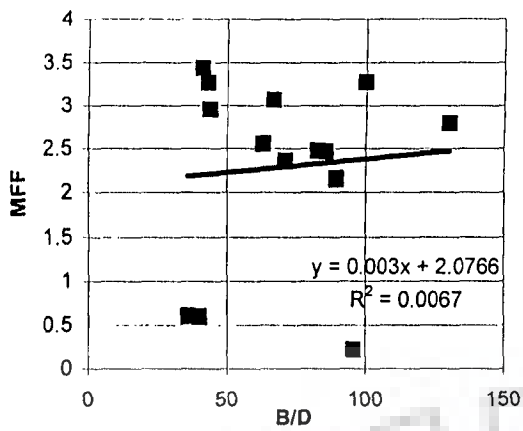


FIG. 6.35a Plot of MFF against B/D ratio for Run-55

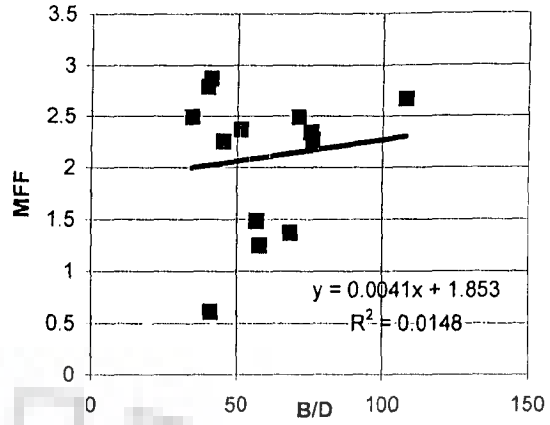


FIG. 6.35b Plot of MFF against B/D ratio for Run-56

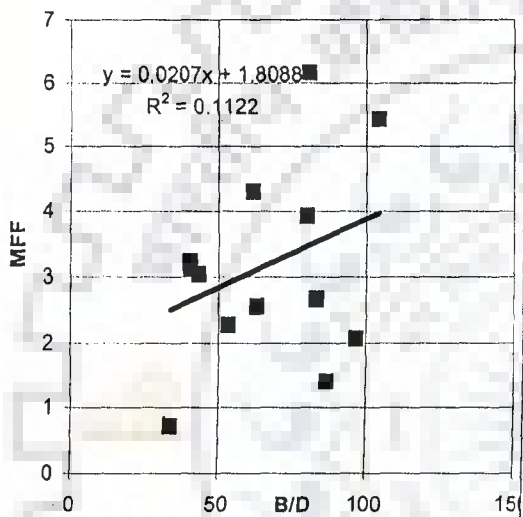


FIG. 6.35c Plot of MFF against B/D ratio for Run-57

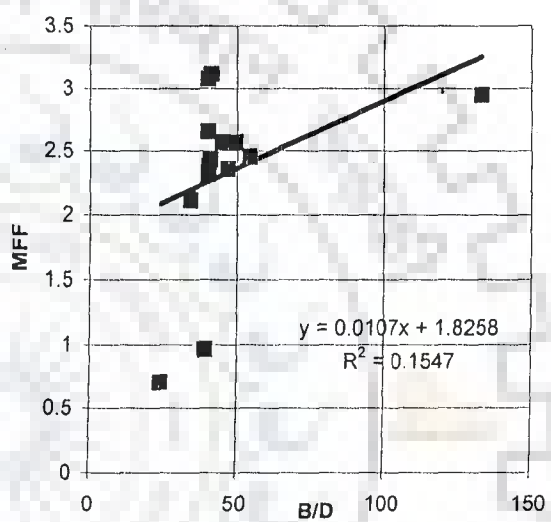


FIG. 6.35d Plot of MFF against B/D ratio for Run-58

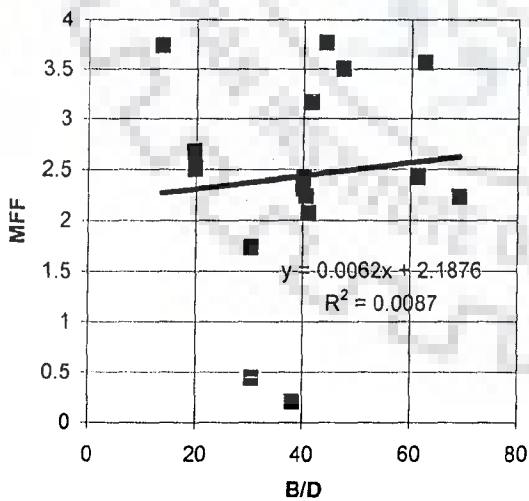


FIG. 6.35e Plot of MFF against B/D ratio for Run-59

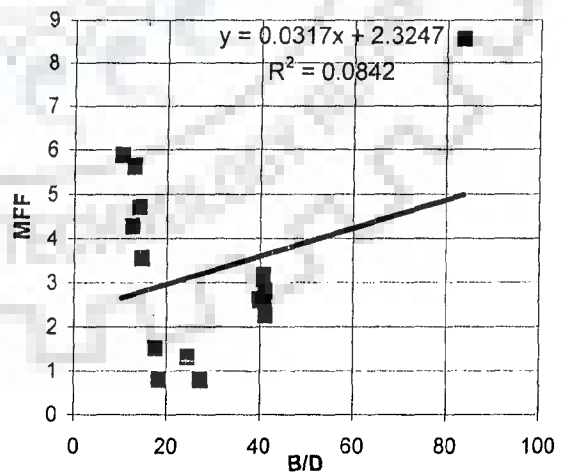


FIG. 6.35f Plot of MFF against B/D ratio for Run-60

FIG. 6.35 a,b,c,d,e,f: PLOT OF 'MFF' AGAINST B/D RATIO FOR LAB. DATA

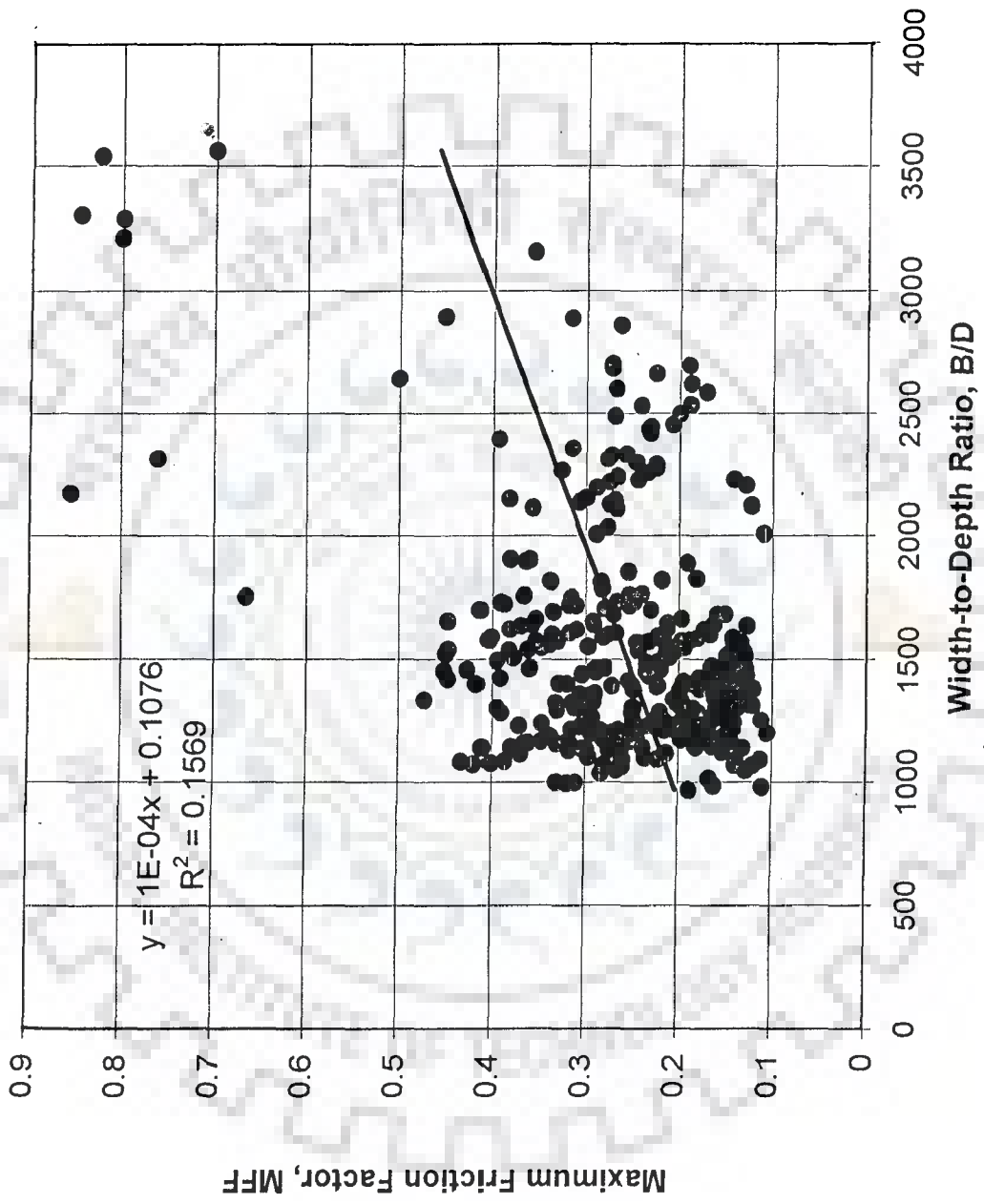


FIG. 6.36: VARIATION OF 'MFF' WITH B/D RATIO FOR MODEL STUDY OF A PARTICULAR STRETCH OF THE BRAHMAPUTRA RIVER

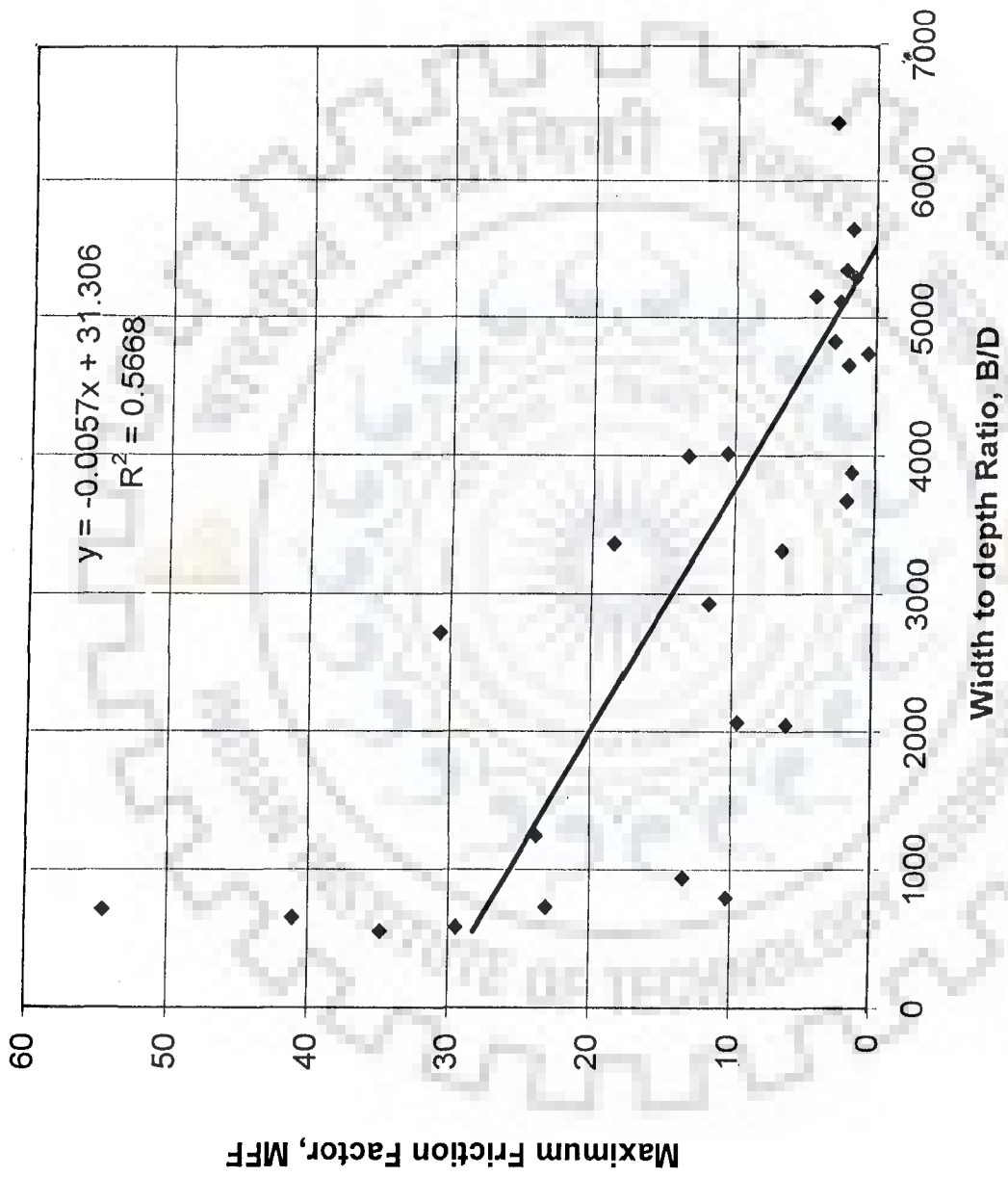


FIG .6.37: VARIATION OF 'MFF' WITH B/D RATIO FOR FIELD DATA

be ascribed to the basic empiricism of the approach or the uncertainties inherent in the data.

6.4.2 Entropy Based Approach

Formulations given by Deng and Singh (1999) based on the principle of maximum entropy have been adopted here to analyse the data from the present laboratory experiments of phase-I, model experiments of phase-II, and field data. As channel pattern coefficient (CPC) depends on Manning's n , two type of plots have been prepared. Figs. 6.38, 6.39 and 6.40 indicate the variation of CPC with calibrated Manning's n for the laboratory experiments of phase-I, model experiments and field data. It can be seen that the Fig. 6.40 does not indicate any definite trend due to scattered points. Figs. 6.41, 6.42 and 6.43 indicate the variation of CPC with constant Manning's n , based on eq. (5.3) for the lab experiments of phase-I, model experiments of phase II and field data of Brahmaputra River.

Values of stability criteria, channel pattern coefficient, different morphological coefficient and m values have been given in the Tables 6.1a and 6.1b for field data and laboratory data of phase-I respectively. Table 6.2a summarizes the range of parameters based on the analysis of laboratory experiments, model experiments and field data. Table 6.2b presents the ranges of values of different morphological parameters reported in the literature.

From the Figs. 6.38 to 6.43, one can observe that CPC increases with B/D with the exception of Fig.6.40. From the values reported in Table 6.2b, one can observe that the ranges of the stability criteria and channel pattern coefficients fairly match with

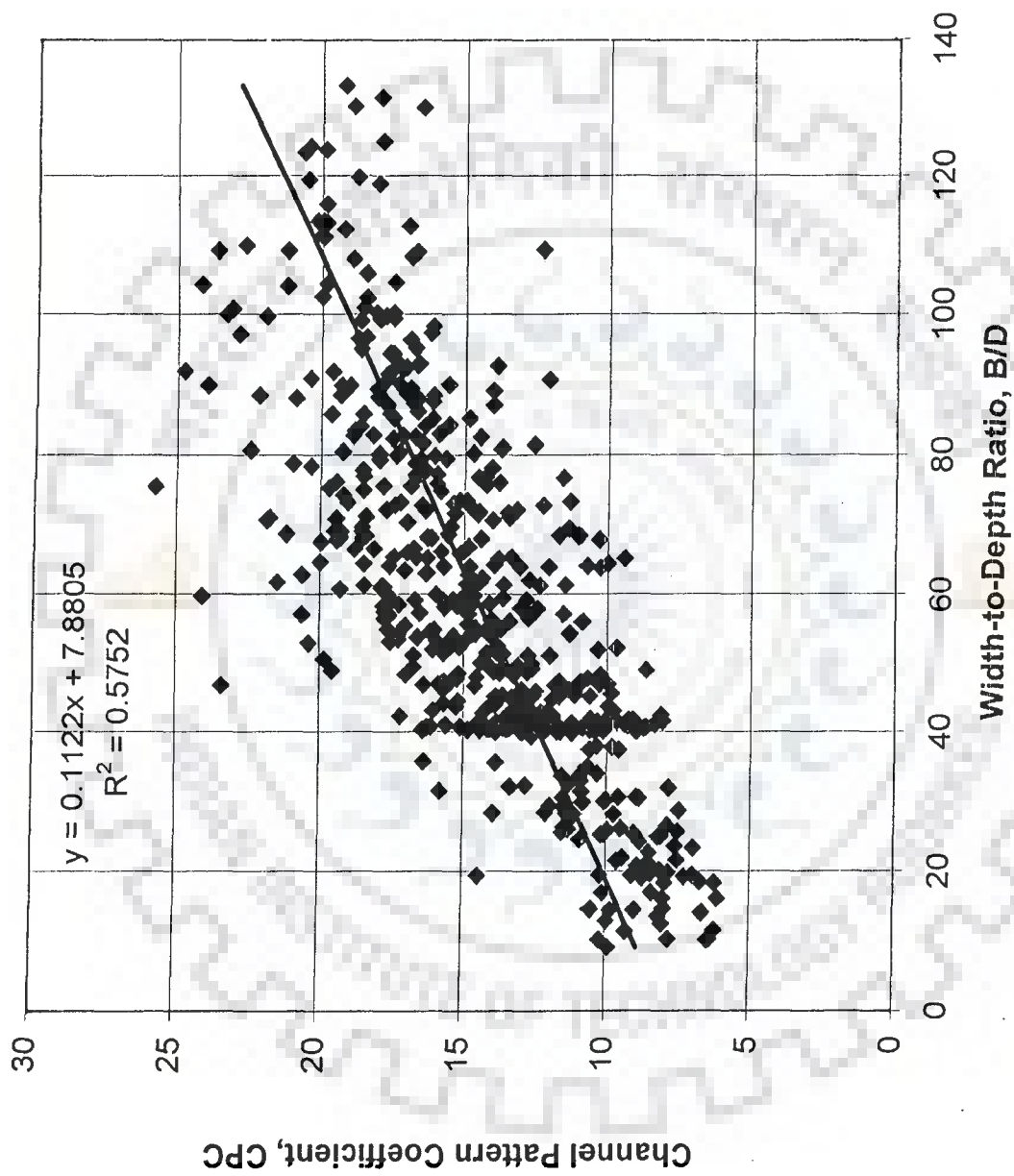


FIG. 6.38: PLOT OF CHANNEL PATTERN COEFFICIENT (CPC) AGAINST B/D RATIO FOR LABORATORY EXPERIMENTAL DATA

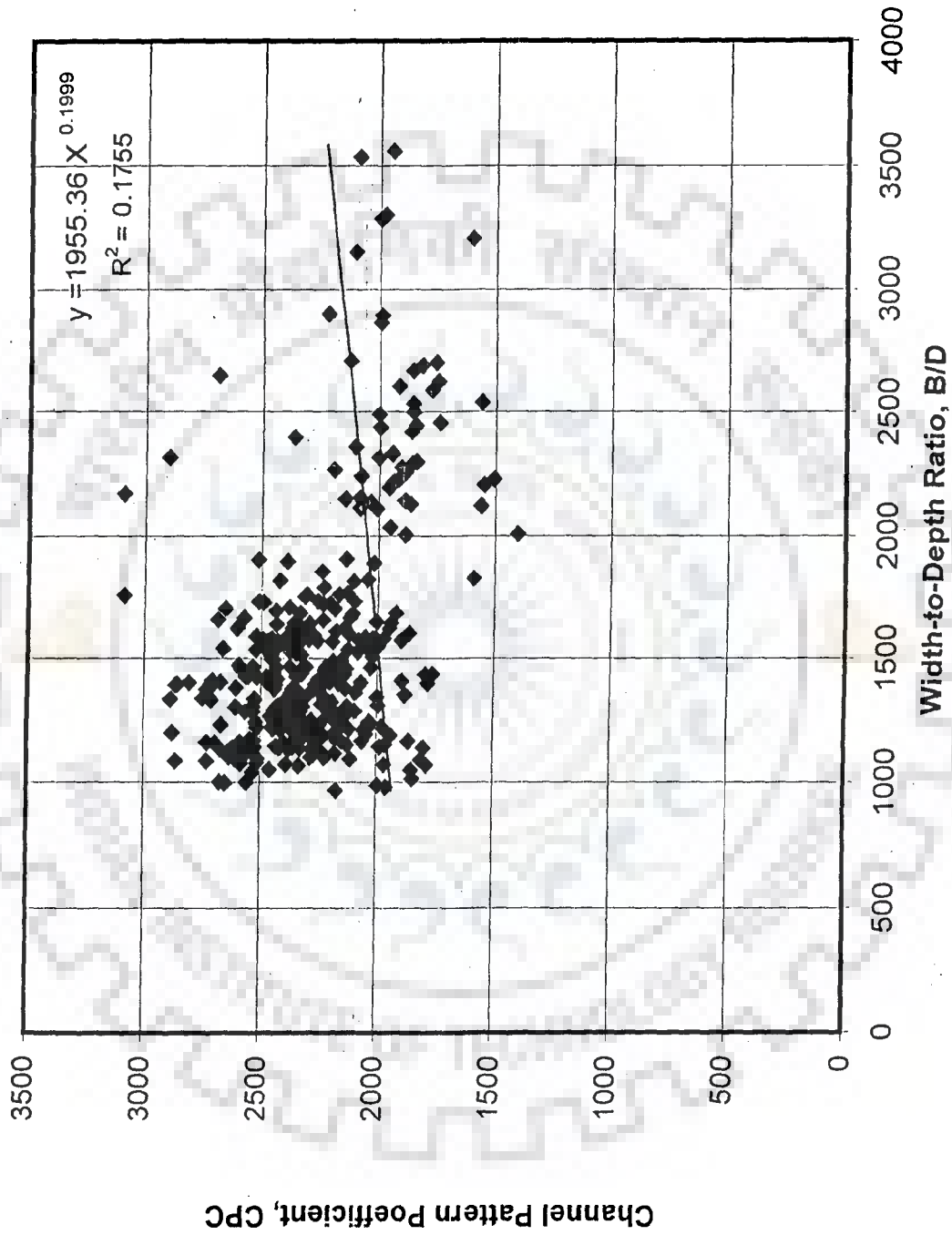


FIG. 6.39: VARIATION OF CHANNEL PATTERN COEFFICIENT (CPC) WITH B/D RATIO FOR MODEL STUDY OF A STRETCH IN THE BRAHMAPUTRA RIVER

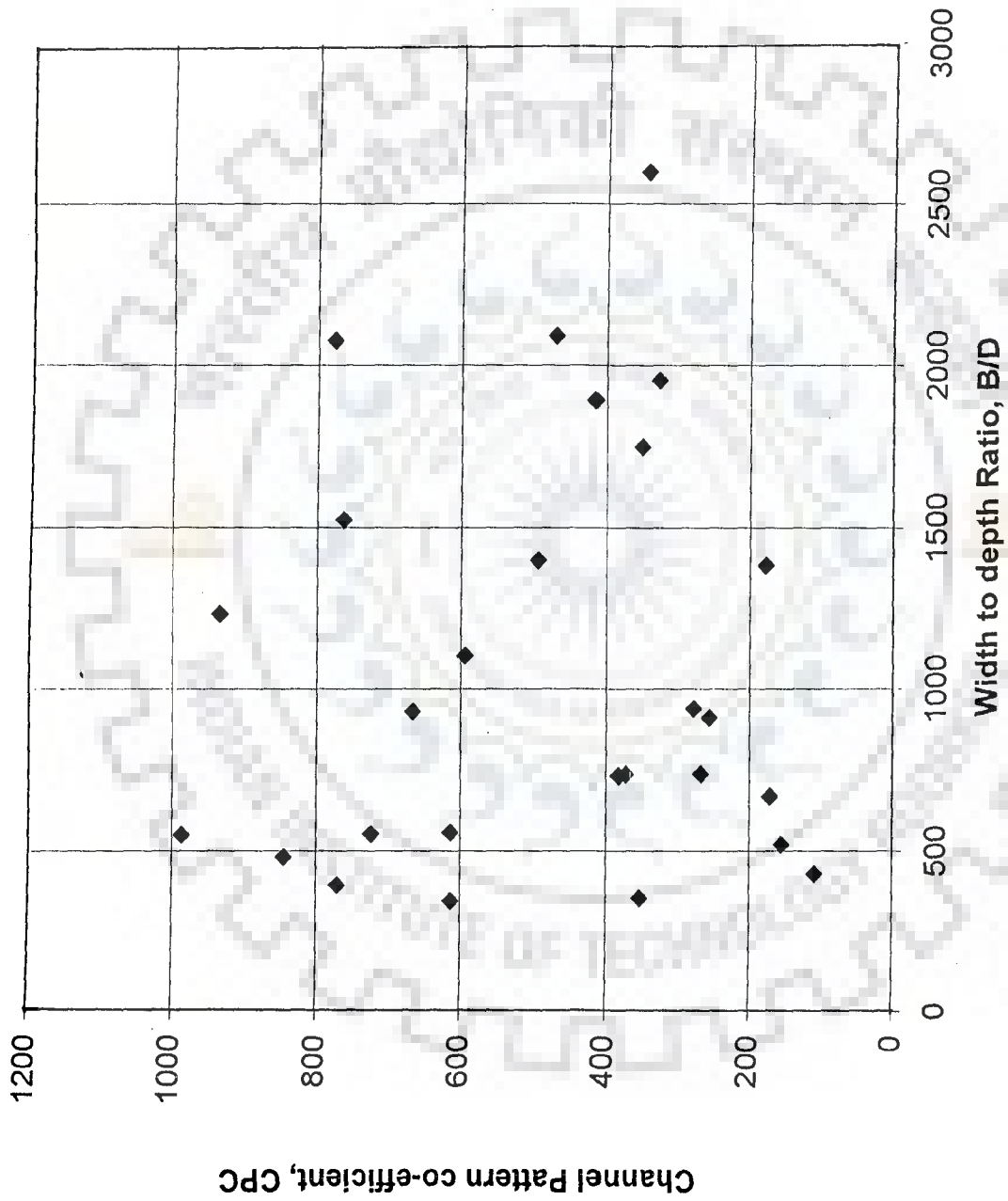


FIG. 6.40: PLOT OF 'CPC' AGAINST B/D RATIO FOR FIELD DATA OF BRAHMAPUTRA RIVER.

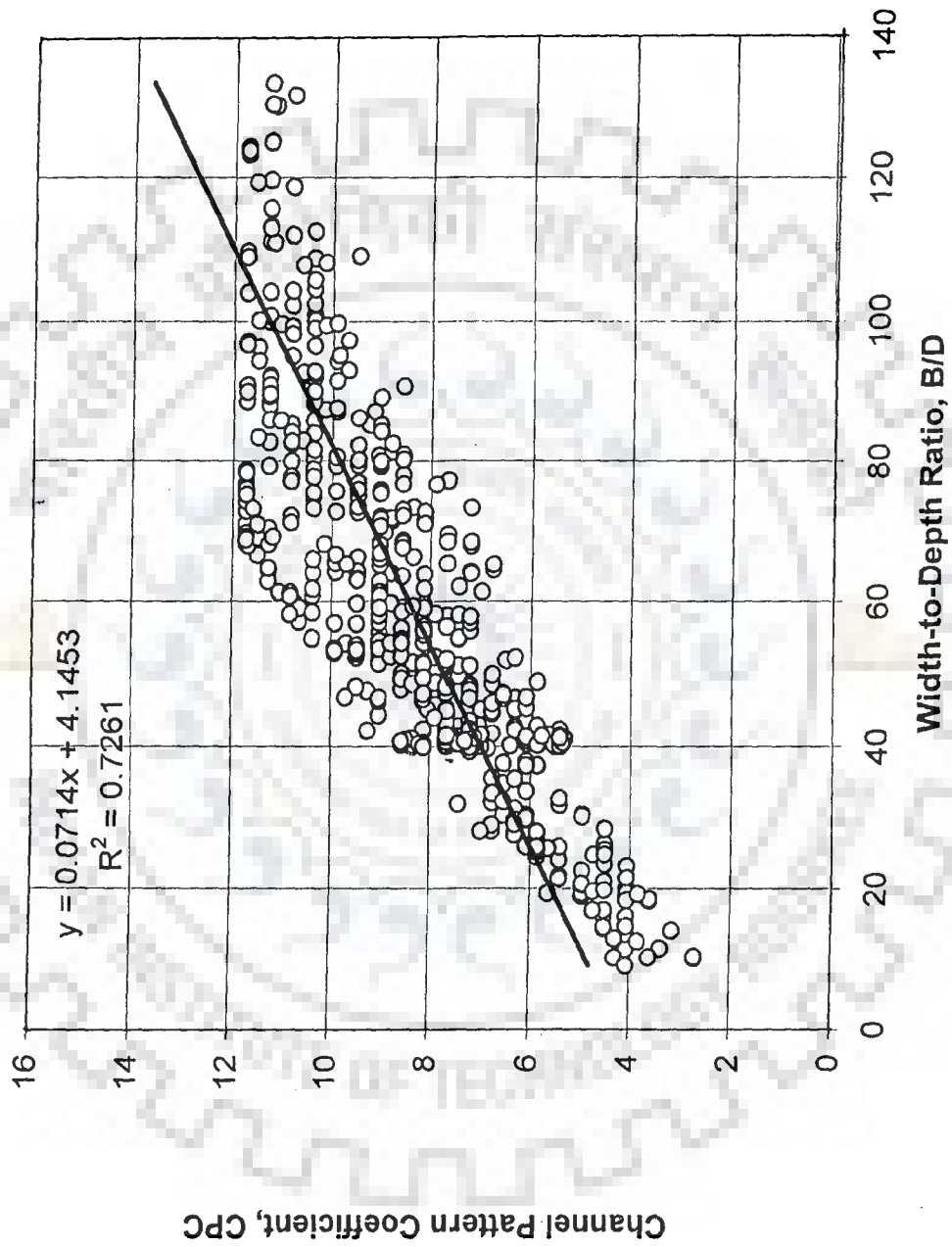


FIG. 6.41: VARIATION OF CHANNEL PATTERN COEFFICIENT, CPC VS B/D RATIO BASED ON CONSTANT 'n' FOR LABORATORY DATA

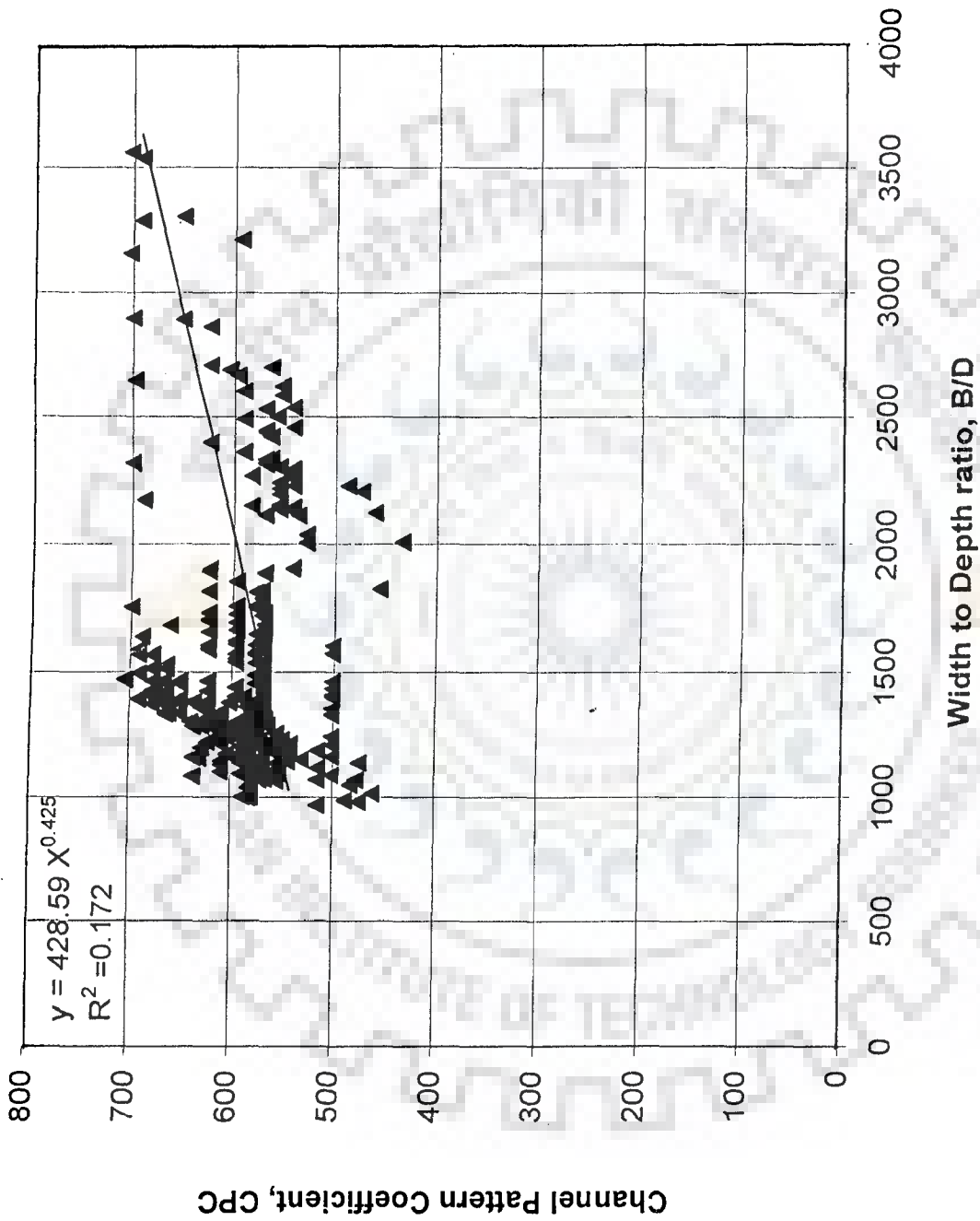


FIG. 6.42: VARIATION OF CHANNEL PATTERN COEFFICIENT (CPC) BASED ON CONSTANT 'n' WITH B/D RATIO FOR MODEL STUDY OF A STRETCH IN THE BRAHMAPUTRA RIVER

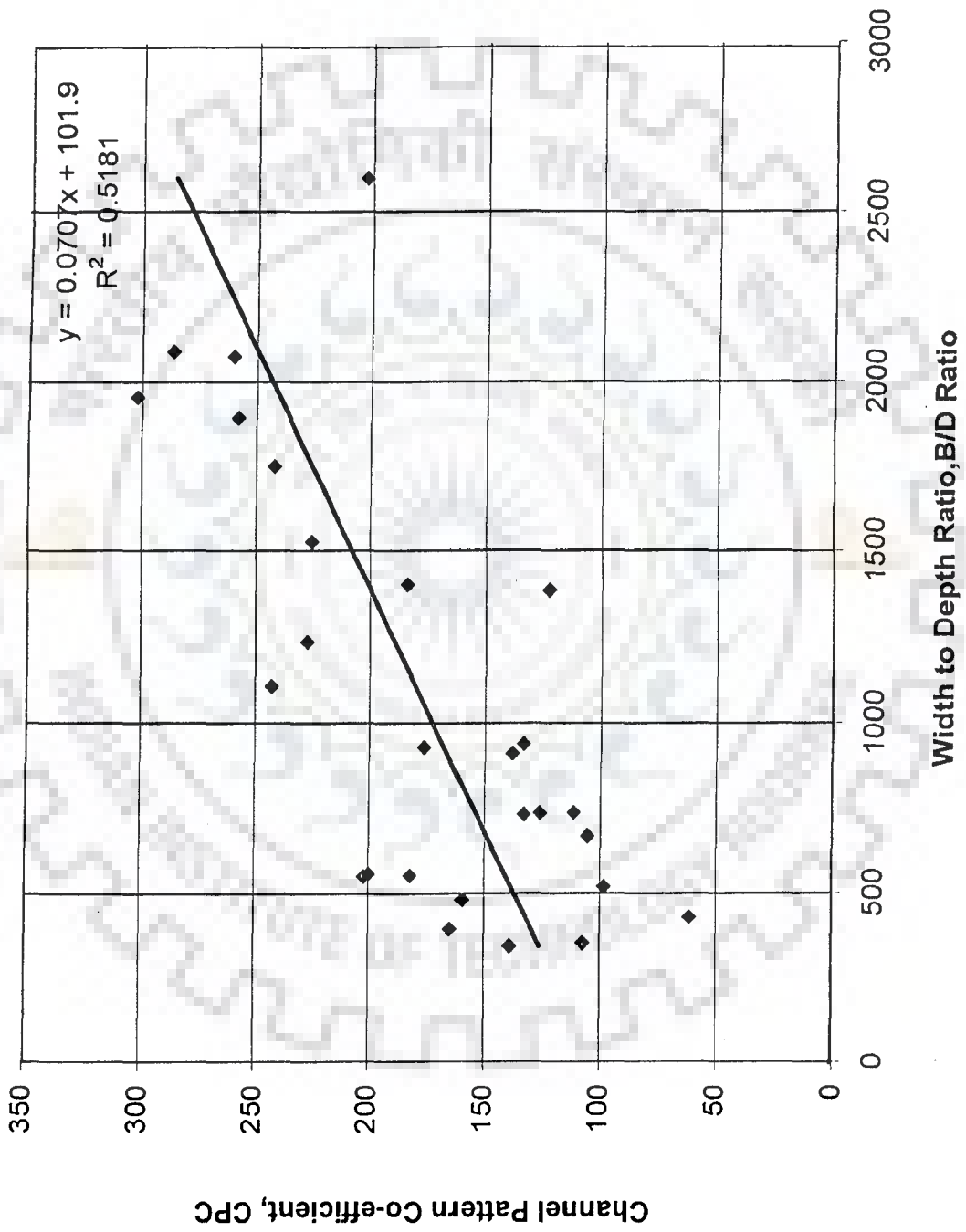


FIG. 6.43: VARIATION OF CPC VS B/D BASED ON CONSTANT 'n' FOR FIELD DATA

**Table 6.1a: DIFFERENT MORPHOLOGICAL PARAMETERS (ξ_0 , S_{cr} & ξ_p)
FOR FIELD DATA OF THE BRAHMAPUTRA RIVER**

C/S	Year	ξ_0 (eq.6.18)	Slope S	S_{cr} (eq.6.25)	ξ_B (eq.6.22)	m	ξ_p (eq.6.26)	ξ_p (eq.6.24)
	1988	32,06932	7,67E-05	0,17741572	3,8609431	7,7218862	353,00553	352,4633
	89	42,04429	7,73E-05	0,14885229	4,5356176	9,0712353	614,5226	613,5786
	90	42,90275	7,3E-05	0,17225074	5,5198788	11,039758	724,4166	723,3038
	91	41,34989	8,15E-05	0,19140358	6,1867037	12,373407	987,30663	985,79
	92	38,90382	7,55E-05	0,21016568	6,2500902	12,50018	845,50231	844,2035
J# 0-1	93	28,84571	2,23E-05	0,2928764	4,3655259	8,7310518	614,06752	613,1243
A-A	94	31,45514	9,04E-06	0,35753756	4,8665695	9,733139	771,51784	770,3327
	95	72,80234	7,57E-05	0,12754877	8,0266299	16,05326	667,39064	666,3655
	97	108,2494	9,41E-05	0,08234423	8,5908314	17,181663	494,33248	493,5731
	1988	110,6906	7,67E-05	0,09699201	10,270653	20,541306	764,39259	763,2184
	89	78,35206	7,99E-05	0,0955474	6,2713752	12,54275	594,99065	594,0767
	90	144,1762	7,49E-05	0,07972919	11,542004	23,084009	777,4232	776,229
	91	131,7257	7,98E-05	0,05853516	7,0006657	14,001331	415,90343	415,2646
	92	121,1393	7,85E-05	0,05775436	6,088337	12,176674	177,73205	177,459
J# 6-1	93	63,99262	7,54E-05	0,11883732	6,1124917	12,224983	372,77085	372,1982
B-B	94	66,53823	7,47E-05	0,10424791	5,4561232	10,912246	268,21327	267,8013
	95	195,0429	5,88E-05	0,05315607	9,839828	19,679656	344,08501	343,5565
	97	89,36497	4,47E-05	0,13610965	9,9599253	19,919851	935,66931	934,232
	1988	62,52891	7,59E-05	0,11816991	5,8858832	11,771766	382,73883	382,1509
	89	48,72128	2,44E-05	0,12518182	3,1925013	6,3850025	155,0485	154,8103
	90	129,6088	2,49E-05	0,06218754	5,2498998	10,4998	327,84851	327,3449
	91	140,9739	9,25E-05	0,05523292	7,4745283	14,949057	470,28025	469,5579
	92	124,1675	1,73E-05	0,08112378	6,2160762	12,432152	351,24378	350,7042
J#13-1	93	61,42906	2,53E-05	0,11223814	3,8962232	7,7924465	171,00657	170,7439
C-C	94	76,86709	2,25E-05	0,11101547	5,0870239	10,174048	256,42494	256,031
	95	80,10621	2,65E-05	0,11179233	5,7035157	11,407031	278,5612	278,1333
	97	46,46145	0,00011	0,09619922	3,3293712	6,6587424	108,49352	108,3269

Table 6.1b: DIFFERENT MORPHOLOGICAL PARAMETERS (ξ_0 , S_{cr} & ξ_p)

OF LABORATORY EXPERIMENTAL DATA

RUN	ξ_0 (eq.6.18)	m	ξ_B (eq.6.22)	ξ_D (eq.6.23)	S_{cr} (eq.6.25)	S (Slope)	ξ_p (eq.6.26)	Manning's n	ξ_p eq(6.24)	B/D
RN1	17,5497	3,377	1,68849	0,0818899	0,0590244	0,00944	22,827	0,02607	22,86216	97,12644
RN2	16,5543	2,819	1,409463	0,0766089	0,0608693	0,00591	14,8172	0,01948	14,83999	85,15704
RN3	14,2361	2,705	1,352334	0,0865685	0,0646431	0,00816	20,9403	0,02291	20,97256	78,78788
RN4	14,0191	2,433	1,216326	0,0816883	0,0621961	0,00723	14,7754	0,01871	14,79817	72,65239
RN5	12,8304	2,56	1,280245	0,0924781	0,0733991	0,00645	21,7264	0,02421	21,75986	71,0084
RN6	10,9943	2,272	1,135919	0,0993456	0,0771325	0,00726	17,5457	0,02421	17,57269	56,97674
RN7	12,6475	2,657	1,328422	0,096246	0,0700158	0,0096	17,0112	0,02685	17,03739	63,55634
RN8	16,47	2,721	1,360597	0,0751431	0,054514	0,00864	17,2748	0,01821	17,30139	90,05764
RN9	14,4721	2,912	1,456066	0,0896271	0,0639861	0,01014	18,4664	0,02614	18,49483	75
RN10	15,7799	2,726	1,363147	0,0785311	0,0531315	0,01193	17,4384	0,01963	17,46526	85,2071
RN11	12,3195	2,281	1,140646	0,0889144	0,0671262	0,00777	14,8134	0,0202	14,83617	62,89308
RN12	13,3674	2,42	1,209929	0,0853588	0,0655092	0,00714	17,6691	0,02002	17,69631	72,18045
RN13	16,5587	3,036	1,517768	0,0806166	0,0604305	0,00784	17,6797	0,02283	17,7069	87,05036
RN14	8,48328	1,566	0,78321	0,099533	0,0768355	0,00721	10,1285	0,01674	10,1441	40,04167
RN15	16,4174	2,96	1,480175	0,0799105	0,0541352	0,01205	20,3479	0,02194	20,37917	90,86022
RN16	10,9126	2,077	1,038539	0,0940683	0,0729276	0,00706	14,8147	0,02021	14,83748	55,71031
RN17	14,851	2,972	1,485768	0,0885703	0,0695739	0,00669	18,4716	0,02615	18,50007	76,96335
RN18	10,2014	2,052	1,025894	0,0997761	0,0761011	0,00778	10,9817	0,02202	10,99859	46,66667
RN19	12,2826	2,294	1,146838	0,0895169	0,0687252	0,00725	19,3977	0,02054	19,42754	67,89575
RN20	19,7009	3,503	1,75141	0,0748192	0,0607872	0,00542	21,1576	0,02327	21,1902	109,0323
RN21	10,6892	2,168	1,083762	0,0989095	0,0739567	0,00848	16,1157	0,02293	16,1405	54,57026
RN22	17,9466	3,205	1,602537	0,0772338	0,0581269	0,00758	17,4793	0,02245	17,50621	94,34698
RN23	16,6203	3,011	1,505427	0,0798648	0,0612251	0,00708	16,6106	0,0223	16,6362	86,13281
RN24	12,5923	2,258	1,128818	0,0863626	0,0673312	0,00666	18,523	0,01905	18,54367	69,69072
RN25	16,5985	3,449	1,724308	0,0878499	0,0652644	0,00859	22,140	0,02994	22,17433	88,46154
RN26	15,9876	2,797	1,398296	0,0788887	0,0582624	0,00821	19,3122	0,02029	19,34195	88,48168
RN27	18,947	3,262	1,630815	0,0740471	0,0594829	0,00562	18,4096	0,02129	18,43793	102,3091
RN28	22,2894	3,781	1,890535	0,0697243	0,0521512	0,00753	20,5858	0,02233	20,61743	123,3577
RN29	19,7009	3,779	1,88931	0,0788498	0,0598262	0,00751	23,5902	0,02739	23,62644	109,0323
RN30	21,119	3,45	1,724753	0,0690582	0,0499375	0,0086	16,948	0,02005	16,97404	112,5532
RN31	15,6391	2,898	1,448885	0,0826556	0,0591118	0,00968	16,0209	0,02272	16,04556	79,84032
RN32	16,5432	2,978	1,489131	0,079635	0,0572477	0,00932	18,0033	0,02195	18,03104	88,16667
RN33	18,3488	3,539	1,769251	0,0808982	0,0581385	0,00954	21,8922	0,02677	21,92592	99,7093
RN34	18,3917	3,132	1,566223	0,0741783	0,0525434	0,00964	17,957	0,02051	17,98315	99,31034
RN35	17,4139	3,008	1,503826	0,0761693	0,0539647	0,00972	17,256	0,02058	17,274	92,80702
RN36	13,7065	2,565	1,282716	0,0866826	0,0626742	0,00934	15,421	0,02178	15,44104	69,75801
RN37	14,1827	2,495	1,247579	0,082177	0,0591477	0,00926	15,1274	0,01938	15,15067	73,5
RN38	20,7068	3,587	1,793679	0,0723696	0,0517185	0,00928	19,9194	0,02254	19,95002	113,2246
RN39	11,7526	2,069	1,034355	0,0871009	0,0628653	0,00926	10,8512	0,0177	10,86794	56,01751
RN40	14,6717	2,399	1,199476	0,0773045	0,0553388	0,00918	13,7684	0,01683	13,78962	76,03448
RN41	16,5985	2,76	1,379792	0,0752879	0,0532535	0,00966	16,0763	0,01852	16,10103	88,46154
RN42	16,8091	3,548	1,774108	0,0884764	0,0618774	0,0112	24,7211	0,03117	24,75911	91,91176
RN43	16,1071	2,753	1,376583	0,0774598	0,0549345	0,00968	13,690	0,01938	13,70658	80,9417
RN44	11,1932	2,118	1,058987	0,0929564	0,0663644	0,01003	14,8115	0,0202	14,83432	57,14286
RN45	8,4701	1,717	0,858642	0,1062402	0,0758282	0,01051	12,3251	0,02046	12,34404	40,75599
RN46	11,4992	2,329	1,1643	0,096621	0,0711508	0,00902	20,5881	0,02369	20,61982	62,87726
RN47	16,3522	2,662	1,331106	0,074545	0,0552043	0,00786	16,8738	0,01758	16,89973	89,41345
RN48	20,6694	3,57	1,784824	0,0722527	0,0518766	0,00909	19,8181	0,02237	19,84863	113,0199
RN49	21,9942	3,605	1,802431	0,0683636	0,0493506	0,00865	18,0085	0,0206	18,03618	118,7629
RN50	11,4222	2,221	1,110615	0,0941442	0,0666066	0,01054	17,8323	0,02164	17,85971	60,87457
RN51	13,2783	2,416	1,208158	0,0858446	0,0618555	0,00939	19,0218	0,02018	19,05104	73,22506
RN52	10,9553	1,932	0,965816	0,0891084	0,0661169	0,00826	8,6387	0,01717	8,65193	48,98551
RN53	18,2122	2,926	1,462855	0,071451	0,0506889	0,00935	17,4857	0,018	17,51259	100,1926
RN54	13,8445	2,511	1,255679	0,0845622	0,0591715	0,01061	16,4304	0,02046	16,45566	72,78195
RN55	12,1914	2,333	1,166692	0,0912641	0,0660665	0,00945	16,2543	0,02158	16,27927	63,18052
RN56	13,7551	2,499	1,249707	0,0848313	0,0597455	0,01033	19,4246	0,02047	19,45445	76,12613
RN57	15,3444	3,376	1,687907	0,0936368	0,0684275	0,00949	22,4121	0,03259	22,44662	80,66667
RN58	10,8189	2,112	1,056039	0,0959864	0,0697024	0,00946	14,5544	0,02125	14,57681	54,36747
RN58	24,3713	3,965	1,982287	0,0658948	0,0449585	0,01093	19,1865	0,02131	19,21603	133,2623
RN59	13,0027	2,373	1,186421	0,0865691	0,0624077	0,00939	11,4406	0,0201	11,4582	61,37359
RN60	9,51229	1,744	0,872191	0,0956313	0,0729483	0,00751	8,05852	0,01744	8,070913	41,49856

**Table 6.2a: RANGES OF VALUES OF DIFFERENT MORPHOLOGICAL
PARAMETERS FOR PRESENT STUDY**

Present study	Morphological coefficient, ζ_0	Channel pattern coefficient, ζ_p	Stability criteria, S_{cr}
Field data	28.85-195.04	108.49 -987.31	0.053-0.35
Lab. data	8.475-24.37	8.0587-24.7211	0.04496-0.078
Model data	54.24-182.83	433.62-704.6477	0.06433-0.1657

Deng and Singh (1999) demarcated the following ranges of threshold values for different channel pattern,

i.e. $S_{cr} < 0.07$ for Wandering river (multi-channel pattern)

$0.07 < S_{cr} < 0.1$ for Anabranched River (multi-channel pattern)

and >0.10 for single channel pattern including meandering and straight rivers

Based on the analysis of many natural rivers, they got following values of stability criteria, channel pattern coefficient and other morphological parameters for different streams, as shown in Table 6.2b.

**Table 6.2b: RANGES OF VALUES OF DIFFERENT MORPHOLOGICAL
PARAMETERS OF DIFFERENT RIVERS (Deng and Singh, 1999)**

Description	Morphological coefficient, ζ_0	Channel pattern coefficient, ζ_p	Stability criteria, S_{cr}	Remarks
General ranges of values from reported data	24 - 182		0.028 - 0.064	Wandering pattern
	11- 144		0.079 - 0.095	Anabranched pattern
	3.5 - 23		0.1134 - 0.338	Single channel
Brahmaputra river (Bangladesh)	89		0.068	Multi-channel Pattern
Laohahe river	96.8	87.6	0.05	Multi-channel
	13	11.1	0.144	Single channel
Yellow river - Huayankou-Gao	150		0.034	Wandering pattern
Hanjiang-Taipindian-X	62		0.057	Multi-channel pattern
Ohau river (New Zealand)	123		0.028	Wardering rivers
Yangtze-maanshan	115		0.088	Anabranched rivers
Warta (Poland Reach)	48		0.079	Anabranched rivers
Alwin (U.K. Reach)	11		0.084	Anabranched rivers
Songhua (Harbin)	23		0.154	Single channel
Wei (Huaxian)	16		0.146	Single channel
Mississippi (USA Rea.)	7.4		0.338	Single channel
Yellow river (Aishan Reach)	12.11 - 37.20	15.56 - 18.3	0.083 - 0.139	Anabranched- single channel
Yellow river (Luokou Reach)	5.99 - 15.67	13.8 - 15.83	0.111 - 0.232	Single channel
Yellow river (Lijin Reach)	17.36 - 40.01	17.23 - 24.36	0.083 - 0.122	Anabranched Pattern

values yielded from the present study. As the braided river has a lower value of stability criteria, the same is justified with respect to the Brahmaputra river.

6.5 GENERAL REMARKS

With respect to extremal hypotheses testing, it will be appropriate to mention here that in almost all the figures, scatter of data exists. As the experimental runs lasted for 20 to 24 hrs, it is possible that the channel conditions might not have reached a dynamic equilibrium. This may possibly be attributed as one of the important parameters behind the scatter of data points. However, from most of the figures, despite the persistence of scatter, one may judge the general trend of variation and it is needless to say that the stream power attenuates with an enhancement in the braiding characteristics in general resulting in dissipation of flow energy. This is analogous to the statement that the friction factor, which is an indicator of energy expenditure, plays an important role in the occurrence of braiding with an increase in its value.

With respect to application of maximum entropy principle, it is apparent here that entropy based models explain the braiding characteristics in a more rational manner, which perhaps has not been observed with the use of different braiding indicators, despite certain overlap, which also occurs in these ranges. Despite the existence of the braided conditions, very few values of braided river based stability criteria exceeds 0.1 in the present analyses. It is noted that Deng and Singh (1999) suggested that value of stability criteria is greater than 0.1 for single-channel pattern including meandering and straight rivers.

CONCLUSIONS AND SCOPE FOR FUTURE WORK

7.1 CONCLUSIONS

Based on the present study the following conclusions are drawn

1. A set of 60 laboratory experiments was performed on mobile bed to study the evolution of braiding patterns. The braiding phenomenon was observed to be dependent on flow as well as sediment inputs. It was also seen to be dependent on the extent of initial sinuosity inherent in the channel. The channel sinuosity displayed an ascending trend in the initial period of the run and dropped afterwards. From the analysis, it could be seen that channel sinuosity varied with channel slope. This behaviour was found similar to that reported by Schumm and Khan (1972).
2. Width to depth ratio followed an increasing trend as one proceeded downstream along the experimental laboratory flume. However, the same was not observed in the case of shear stress with the exception of the bar tops. With the losses occurring in the braided rivers, the flow energy indicated a declining trend and the intensity of braiding has registered an increase with progressive decline of channel hydraulic efficiency.

3. A braiding indicator must show a consistent variation with B/D ratio. However, this was found absent in case of many braiding indicators. The best-fit correlations between braiding indices and B/D ratio have seldom exceeded a value beyond 0.75.
4. Plots in respect of slope to Froude number ratio versus width to depth ratio were examined to check whether the data related to braided streams fall in the zone corresponding to braiding. In this respect demarcation criteria proposed in the literature have been found to work reasonably well.
5. In the laboratory based model experiments, velocity head being very small, the variation of specific energy with B/D ratio could be seen to reflect useful relation. However, this should not be considered as an aid to explain braiding phenomenon.
6. Based on the hypothetical patterns of river channel form, conditions were created having increasing braiding tendency. Indices of Howard et al. (1970), were tested against such patterns. The indices were found to increase with B/D ratio. However, the same was not found valid based on the analysis of complicated channel networks.
7. As the braiding phenomenon might depend on fluid flow, channel and sediment properties, the use of composite indicators were considered by combining different variables. These indicators showed some pattern with B/D ratio. Thus, the uses of composite indicators were also feasible in the characterisation of braided streams.

8. Certain resistance relationships were evaluated using the field data from the Brahmaputra river in Bangladesh. It was observed that the use of constant value of Manning's rugosity coefficient might lead to erroneous representation of the flow resistance in rivers with braided configuration.
9. Using a generalised friction formula, new expressions for the Manning's rugosity coefficient have been derived. These expressions are of general nature and can be converted into functional forms of many available relationships.
10. A new functional form of the variation of Manning's rugosity coefficient was also developed. The utility of this functional form has been shown with respect to the analysis of field as well as laboratory data.
11. Use of various extremal hypotheses was also examined. It has been observed that minimum energy dissipation rate (MEDR) varies inversely with B/D ratio. With a decrease in MEDR, B/D ratio was found to exhibit an increasing trend. The same also was found true in case of minimum stream power (MSP). The above trend of variation was reflective of enhanced energy loss process and hydraulic inefficiency of channel associated with intensified braiding configuration.
12. Considering that another school of thought in explaining channel processes is the approach of maximum friction factor (MFF), as proposed by New Zealand based research workers, the variation of MFF with B/D ratio was also studied. In general, it was observed that with an increase in MFF, B/D ratio also increased, which could be a vindication of the general observation reported earlier in para 11 above.

13. Stability of channel patterns was also assessed using entropy-based indicators. Analysis of laboratory based experiments indicated the similar values of channel pattern coefficient, as indicated in the literature.
14. Even with the use of entropy-based approach, some of the data related to braiding were found to lie in the meandering zone.
15. Effect of using different expressions of Manning's rugosity coefficient was also apparent in channel pattern coefficients. Nevertheless, channel pattern coefficients showed an increasing trend with B/D ratio.
16. Using the parameters of resistance relationships, a plot between these resistance parameters and B/D ratio revealed an interesting trend exhibiting a very good correlation (Figs.5.5 and 5.6).

7.2 FUTURE WORK

Three types of data were used in the present analysis. The conclusions reported in this work are based on the general trend obtained from the majority of cases. It is desirable that experiments can be conducted for longer duration in order to ascertain the equilibrium conditions. In certain plots related to field data, trends have not been as per expectations. Thus, it may be also necessary to collect additional field data. Scale effects in the model and prototype may also influence the results. Construction of models with different levels of scale exaggeration may be done to assess the role of scale effects on the reported conclusions.

REFERENCES

1. Ackers, P. (1964), "Experiments on Small Streams in Alluvium," *Journal of the Hydraulics Division, Proceedings of the American Society of Civil Engineers (ASCE)*, Vol. 90, No. HY 4, pp. 1-37.
2. Ackers, P. and Charlton, F. G. (1970a), "Meander Geometry Arising from Varying Flows," *Journal of Hydrology*, Vol. 11, pp.230-252.
3. Ackers, P. and White, W. R. (1973), "Sediment Transport: New Approach and Analysis," *Journal of the Hydraulics Division, proceedings of the ASCE*, Vol. 99, No. HY 11, pp. 2041-2060.
4. Ackers, P. and Charlton, F.G. (1970b), "The Slope and Resistance of Small Meandering Channels," *proceedings of the institution of Civil Engineers*, Vol. 47, Supplementary paper 7362-5, pp. 349-370.
5. Amorocho, J. and Espiledora, B (1973), "Entropy in the Assessment of Uncertainty of Hydrologic Systems and Models," *Water Resources Research*, Vol.9, No.6.
6. Alam, Z. U. and Kennedy, J. F. (1969), "Friction Factors for Flow in Sand-Bed Channels," *Journal of the Hydraulics Division, ASCE*, Vol. 95, No. HY 6.
7. Allen, J.R.L. (1965), "A Review of the Origin and Characteristics of Recent Alluvial Sediments," *Sedimentology*, Vol. 5. pp. 89-191.
8. Antropovskiy, V.I. (1972), "Critical Relations of Type of Channel Processes," *Soviet Hydrology*, Vol. 11, pp. 371-381.
9. Ashmore, P.E. (1982) "Laboratory Modelling of Gravel Braided Stream Morphology," *Earth Surface Processes*, Vol.7, pp.201-225.
10. Ashmore, P.E. and Parker, G. (1983), "Confluence Scour in Coarse Braided Streams," *Water Resources Research*, Vol. 19, pp.392-402.
11. Ashmore, P.E. (1988), "Bed Load Transport in Braided Gravel-Bed Stream Models," *Earth Surfaces Processes and Landforms*. Vol. 13, pp. 677-695.

12. Ashmore, P.E. (1991), "How do Gravel Bed Rivers Braid," *Canadian Journal of Earth Sciences*, Vol.28, pp. 326-341.
13. Ashmore, P.E. (1991a), "Channel Morphology and Bedload Pulses in Braided, Gravel-bed Streams," *Geografiska Annaler*, Vol.73A, pp.37-52.
14. Ashworth, P.J., Ferguson, R. and Powell, M. (1992) "Bedload Load Transport and Sorting in Braided Channels," In: Bill, P., Hey, R.D., Thorne, C.R. and Tacconi, P. (Eds.) 'Dynamics of gravel bed rivers'. Wiley and Sons, pp. 497-513.
15. Ashworth, P.J., (1996), "Mild-Channel Bar Growth and its Relationship to Local Flow Strength and Direction," *Earth Surface. Processes Landforms*, Vol. 21, pp.103-124.
16. Aziz, N. M. and Prasad, S.N. (1985), " Sediment Transport in Shallow Flows," *Journal of the Hydraulics Engineering*, ASCE, Vol. 111, No. 10, pp. 1327-1343.
17. Babarutsi, S. Ganoulis and Chu, V. H. (1989), "Experimental Investigation of Shallow Re-circulating Flows," *Journal of Hydraulics Division*, ASCE Vol. 115, No. 7, pp. 906-924.
18. Bathurst, J.C., and Thorne C.R. and Hey, R. D. (1979), "Secondary Flow and Stress at River Bends," *Journal of the Hydraulics Divisions Proceedings of the American Society of Civil Engineers*, Vol. 105, No. HY10, pp.1278-1295.
19. Basak, B.C. (1992), "Design of Open-channel Transitions," Ph.D. Thesis, Civil Engineering Department, University of Roorkee, India.
20. Beltaos, S. (2001), "Hydraulic Roughness of Breakup Ice Jams," *Journal of the Hydraulics. Division*, ASCE, Vol. 127, No 8, pp. 650-656.
21. Best, J.L. (1986), "The Morphology of River Channel Confluences," *Progress in Physical Geography*, Vol. 10, pp.157-174.
22. Best, J.L. (1988), "Sediment Transport and Bed Morphology at River Channel Confluences," *Sedimentology*, Vol.35, pp.481-498.
23. Best, J.L. and Roy, A.G (1991), "Mixing-Layer Distortion at the Confluence of Channels of Different Depth," *Nature*, Vol. 350, pp. 411-413.
24. Bluck, B.J. (1979), "Structure of Coarse Grained Braided Alluvium," *Transactions of the Royal Society of Edinburgh*, Vol. 70, pp.29-46.

25. Bharat Singh, (1961), "Bed Load Transport in Channels," JIP (India), Vol. 18, No. 2.
26. Brice, J.C. (1960), "Index for Description of Channel Braiding," Bulletin of the Geological Society of America, Vol.71, and pp.1833.
27. Brice, J.C. (1964), "Channel Patterns and Terraces of the Loup Rivers in Nebraska", U.S Geological Survey professional Paper, 422-D.
28. Bristow, C.S (1987a), "Brahmaputra River: Channel Migration and Deposition." In: Ethridge F.G., Flores, R.M. and Harvey, M.D. (Eds.) Recent development of Sedimentology. Soc. of Eco. Pale. and Mine. Special. Publication. Vol.39, pp. 63-74
29. Bristow, C.S. (1987b), "Sedimentology of Large Braided Rivers Ancient and Modern," Ph.D. thesis, University of Leeds, U.K.
30. Bristow, C.S. (1993), "Sedimentary Structures Exposed in Bar Tops in the Brahmaputra River, Bangladesh," A chapter in 'Braided Rivers' by Best, J.L and Bristow, C.S. (Eds. 1993), Geological Society, London, Special. Publication No.75, pp.277-289.
31. Bristow, C.S. and Best, J.L (1993), "Braided Rivers: Perspectives and Problems," A chapter in 'Braided rivers' by Best, J.L and Bristow, C.S. (Eds. 1993), Geological Society, London, Special. Publication, No. 75. pp. 1-11.
32. Bristow, C.S., Best J.L. and Roy, A.G. (1993), "Morphology and facies models of channel confluences," In PUIGDEFABREGAS and TOMAS (Eds.) Alluvial Sedimentation, Special Publications of the International Association of Sedimentologists, Vol.17, pp.91-100.
33. Burkham, D.E. and Dawdy, D. R.. (1976), " Resistance Equation for Alluvial Channel Flow," Journal of the Hydraulics Division, ASCE, Vol. 102, No. HY10, pp.1479-1489.
34. Bridge, J.S., Smith, N.D., Trent, F., Gabel, S.L. and Bernstein, P. (1986), "Sedimentology and Morphology of a Low Sinuosity Rivers, Calamus River Nebraska Sand Hills," Sedimentology Vol. 33, pp.851-870.

35. Callander, R.A. (1969), "Instability and River Channels," *Journal of Fluid Mechanics*, Vol.36, Part 3, pp.465-480.
36. Carson, M.A. (1984), "The Meandering – Braided River Threshold: A Reappraisal," *Journal of Hydrology*, Vol. 73, pp.315-334.
37. Chang, H.H., (1979a), "Minimum Stream Power and River Channel Patterns," *Journal of Hydrology*, Vol.41, pp. 303-327.
38. Chang, H.H., (1979b), "Geometry of Rivers in Regime," *Journal of the Hydraulics Division, ASCE*, Vol.105 (HY6), pp.691-706.
39. Chang, H.H., (1980b), "Geometry of Gravel Stream," *Journal of the Hydraulics Division, ASCE*, Vol. 106, No. HY9, pp1443-1456.
40. Chao-Lin Chiu and Hsin-Chi Lin and Kazumasa Mizumura (1976), "Simulation of Hydraulic Processes in Open channels," *Journal of the Hydraulics Division, ASCE*, Vol. 102, No. HY2, pp.185-206.
41. Cheetham, G.H. (1979), "Flow Competence in Relation Channel Form and Braiding," *Geological Society of America Bulletin*, Vol.90, pp.877-886.
42. Church, M. (1967), "Observations of Turbulent Diffusion in a Natural Channel," *Canadian Journal of Earth Science*, Vol.4, pp.855-872
43. Coleman, J.M. (1969), "Brahmaputra River: Channel Process and Sedimentation," *Sedimentary Geology*, Vol.3, pp.129-239.
44. Colombini, M., Seminara, G. and Tubino, M. (1987), "Finite Amplitude Alternate Bars," *Journal of Fluid Mechanics*. Vol. 181, pp. 213-232.
45. Cowan, E.J. (1991), "The Large Scale Architecture of the Fluvial Wastewater Canyon Member," *Morrison Formation (Jurassic) San Juan Basin, New Mexico*, In: Miall, A.D. and Tyler, N. (eds.) *The three dimensional facies architecture of terrigenous clastic sediments, and its implications for hydrocarbon discovery and recovery. Society of Economic paleontologists and mineralogists concepts in sedimentology and Paleontology*, Vol. 3, pp. 80-93.
46. Davies, T.R.H., and A.J. Sutherland, (1980), "Resistance to Flow Past Deformable Boundaries," *Earth Surface Processes*, Vol. 5, pp.175-179.
47. Davies, T.R.H. and Sutherland, A.J. (1983), "External Hypotheses for River Behaviour," *Water Resources Research*, Vol. 19, pp.141-48.

48. Dury, G.H. (1966a), "The Concept of Grad," In Dury, G.H. (Ed.). *Essays in Geomorphology*, London, Heinemann, pp.211-234.
49. Deng, Z.Q. and Zhang, K.Q. (1994), "Morphologic Equations Based on the Principle of Maximum Entropy," *International Journal of Sediment Research*, Vol.9, No.1, pp. 131-461.
50. Deng, Z.Q. and Singh, V.P. (1999), "Mechanism and Conditions for Change in Channel Pattern", *Journal of Hydraulic Research*, Vol. 37, No.4, pp.465-478.
51. Einstein, H.A. (1950), "The Bed Load Function of Sediment Transportation in Open Channel Flow," USDA, Tech. Bull. No. 1026, September. Also see closure to the Paper " Fluid Resistance of Composite Roughness," *Trans. AGU*, Vol. 31, No.4, Aug. 1950.
52. Einstein, H.A. and Barbarossa, N. L. (1952), "River Channel Roughness," *Transactions American Society for Civil Engineers*, Vol.117, pp.1121-1132.
53. Engelund, F. (1966,67), "Hydraulic Resistance of Alluvial Streams," *Journal of Hydraulics Division. Proceedings of the ASCE*, Vol. 92, No. HY 2, March and also see closure to the Paper *Journal of the Hydraulics Division, Proceedings of the ASCE*, Vol.93, No.HY4, July.
54. Engelund, F. and Skovgaard, O. (1973), "On the Origin of Meandering and Braiding in Alluvial Streams," *Journal of Fluid Mechanics*, Vol.57, Part 2,pp.289-302.
55. Ervine, D. A. (2000), "Two Dimensional Solution for Straight and Meandering Overbank Flows," *Journal of the Hydraulic Engineering, ASCE*, Vol. 126, No. 9, pp. 653-669.
56. Fahnstock, R.K. (1963), "Morphology and Hydrology of a Glacial Stream," U.S. Geological Survey, Professional Paper, 422A.
57. Ferguson, R.I (1981), "Channel Form and Channel Changes," In 'British Rivers' by Lewin, J. (Editor), Allen and Unwin, London, pp.90-125.
58. Ferguson, R.I. (1993), "Understanding Braiding Processes in Gravel-Bed Rivers: Progress and Unsolved Problems," In Best, J.L. and Bristow, C.S. (Eds.). *Braided rivers*, Geological Society, London, Special. Publication 75, pp.73-88.
59. "Friction Factors in Open Channels: Progress Report of Task Force on Friction Factors in Open Channels," (1963) *Journal of the Hydraulic Division, ASCE*, Vol.89 (2), pp. 97-143.

60. Fujita, Y. (1989), "Bar and Channel Formation in Braided Streams," In Ikeda, S. and Parker, G. (Eds) River Meandering,. American Geophysical Union, Water Resources Monographs, Vol.12, pp. 417-462.
61. Friend, P.F. and Sinha, R. (1993), "Braiding and Meandering Parameters," A chapter in 'Braided Rivers' by Best, J.L. and Bristow, C.S. (Eds. 1993), Geological Society, London, Special. Publication. No.75, pp.105-111.
62. Garde, R.J. (1959), "Total Sediment Transport in Alluvial Channels," Ph.D Thesis, CSU.
63. Garde R,J. and Ranga Raju K.G. (1966), "Resistance Relationships for Alluvial Channel Flow," Journal of the Hydraulics Division, proceedings of ASCE, Vol. 92, No. HY- 4.
64. Garde, R.J. and Ranga Raju, K.G. (2000), "Mechanics of Sediment Transportation and Alluvial Stream Problems," New Age international (P) limited, Publishers 4835/24, Ansari Road, Daryaganj, New Delhi, India.
65. Gorycki, M.A. (1973), "Hydraulic Drag; A Meander-Initiating Mechanism," Bulletin of the Geological Society of America, Vol. 84, pp.175-86.
66. Graf, W. H. (1971), "Hydraulics of Sediment Transport in Open Channels," McGraw Hill Book Company New York.
67. Griffith, G.A. (1984), "Extremal Hypotheses for River Regime," An illusion of Progress. Water Resources Research, Vol. 20, No. 1, pp.113-118.
68. Griffiths, G. A. (1989), "Form Resistance in Gravel Channels with Mobile Beds," Journal of the Hydraulics Engineering, ASCE, Vol.115, No.3, pp. 341-355.
69. Griffiths, G.A. (1993), "Sediment Translation Waves in Braided Gravel-Bed Rivers," Journal of Hydraulic Division, ASCE, Vol. 119, No. 8, pp. 924-937.
70. Goswami, D.C. (1985), "Brahmaputra River, Assam, India: Physiography, Basin Denundation, and Channel Aggradation," Water Resources Research, 21(7), pp. 959-978.
71. Gupta, A. and Dutta, A (1989), "The Auranga: Description of a Tropical Monsoon River," Zeischrift fiir Geomorphologie, Vol. 33, pp. 73-92.

72. Hager, W.H.(1989) Discussion of "Non Circular Sewer Design," *Journal of the Environmental Engineering, ASCE*, Vol.115, No.1, pp.274-276.
73. Hager, W.H. (2001), "Gauckler and the GMS Formula," *Journal of the Hydraulics Engineering, ASCE*, Vol. 127, No.8, pp. 694-701.
74. Henderson, F.M. (1961), "Stability of Alluvial Channels," *Journal of the Hydraulics Division, Proceedings of the ASCE*, Vol. 87, pp.109-138.
75. Hong, L. B. and Davies, T.R.H. (1979), "A Study of Streams Braiding," *Geological Society of America Bulletin*, Vol. 79, pp.391-394.
76. Howard, A.D., Keeth, M.E. and Vincent, L.C. (1970), "Topological and Geometrical Properties of Braided Streams," *Water Resources Research*, Vol.6, pp. 1674-1688.
77. Ilo, C.G. (1975), "Resistance to Flow in Alluvial Channels," *Journal of the Hydraulics Division, ASCE*, Vol. 101, No. HY6, pp.665-679.
78. Jansen, P. Ph., Bendegom, L.Van, Berg, J.Van Den, Vries, M. De and Zansen, A. (1979), "Principles of River Engineering," Pitman Publishing Limited London Sanfrancisco Melbourne 39, Paker Street, London WC2B 5PB.
79. Jaynes, E.T. (1957), "Information Theory and Statistical Mechanics," I, *Physics Review*, Vol.106, pp.620-630.
80. Jarrett, R. D. (1984), "Hydraulics of High-Gradient Streams," *Journal of the Hydraulic Engineering, ASCE*, Vol.110, No.11, pp.1519-1539.
81. Keulegan, G.H. (1938), "Laws of Turbulent Flow in Open Channel," U.S. Deptt. of commerces NBS. Vol. 21.
82. Karcz, I. (1971), "Development of a Meandering Thalweg in a Straight, Erodible Laboratory Channel," *Journal. of Geology*, Vol.79, pp.234-240.
83. Karim, M. F. and Kennedy, J.F. (1987), "Velocity and Sediment-Concentration Profiles in River Flows," *Journal of the Hydraulics Engineering, ASCE*, Vol. 113, No. HY2, pp. 159-177.
84. Kirkgoz, M. S. (1989),"Turbulent Velocity Profiles for Smooth and Rough Open Channel Flow," *Journal of the Hydraulics Engineering, ASCE*, Vol. 115, No. HY11, pp. 1543-1561.

85. Knight, D.W and Macdonald, J.A. (1979), "Open Channel Flow With Varying Bed Roughness," Journal of the Hydraulics Division, Proceedings of the ASCE, Vol. 105, No. HY9, pp.1167-1183.
86. Kouwen, N. and Unny, T.E. (1973), "Flexible Roughness in Open Channels," Journal of the Hydraulics Division, ASCE, Vol. 99, No. HY5, pp.713-728.
87. Krigstrom, A. (1962) "Geomorphological Studies of Sandur Plains and Their Braided Rivers in Iceland," Geografiska Annaler, Vol.44, pp.328-346.
88. Krishnappan, B. G. (1985), "Modeling of Unsteady Flows in Alluvial Stream," Journal of the Hydraulics Engineering, ASCE, Vol. 111, No. 2, pp. 257-266.
89. Lane, E.W. (1957), "A Study of the Shape of Channels Formed by the Natural Streams Flowing in Erodible Material," U.S Army Corps Engg. Div., Missouri River, M.R.D. Sediment. Ser. No. 9, pp.106.
90. Lacey, G. (1930), "Stable Channels in Alluvium," Min. Proc. ICE (London), Vol. 229.
91. Lau, Y.L. (1983), " Suspended Sediment Effect on Flow Resistance," Journal of the Hydraulics Division, ASCE, Vol. 109, No. 5, pp.757-763.
92. Leopold, L. B. and Wolman, M.G. (1957), "River Channel Patterns: Braided Meandering and Straight," United States, Geological Survey Professional Paper 282-B, pp.35-85.
93. Leopold, L.B. and Wolman, M.G. (1957), "River Channel Patterns," A Chapter In 'Rivers and River Terraces', By Dury, G.H. (Ed.1970), Published By Macmillan and Co. Ltd., Little Essex Street London, pp.197-237.
94. Leopold, L.B. and Wolman, M.G. and Miller, J.P. (1964), "Fluvial Processes in Geomorphology," San Francisco, W.H. Freeman.
95. Lyn, D. A. (1993), "Turbulence Measurements in Open-Channel Flows Over Artificial Bed Forms," Journal of the Hydraulic Engineering, ASCE, Vol. 119, No. 3, pp. 306-326.
96. Maddock, T. (1973), "A Role of Sediment Transport in Alluvial Channels," Journal of the Hydraulics Division, ASCE, Vol. 99, No.HY11, pp.1915-1931.
97. Myers, W.R.C., (1982), "Flow Resistance in Wide Rectangular Channels," Journal of the Hydraulics Division, ASCE, Vol. 108, No. HY.4, pp. 471- 482.

98. Miall, A.D. (1977), "A Review of the Braided River Depositional Environment," *Earth Science Reviews*, Vol.13, pp.1-62.
99. Miller, J.P. (1958), "High Mountain Streams; Effects of Geology on Channel Characteristics and Bed Material," *New Mexico State Bureau of Mines and Mineral Resources, Memoir 4*.
100. Modi, P.N. and Seth, S.M., (1982) "Hydraulics and Fluid Mechanics," *Standard Book House 1705 A, New Sarak, Delhi, India*.
101. Mosley, M.P. (1976), "An Experimental Study of Channel Confluence's," *Journal of Geology*, Vol. 84, pp. 535-562.
102. Mosley, M. P. (1981), "Semi-Determinate Hydraulic Geometry of River Channel, South Island New Zealand," *Earth Surface Processes and Landforms*, Vol.6 pp.127-137.
103. Mosley M.P. (1982a), "Scour Depths in Branch Channel Confluences, Ohio River, Orago, New Zealand," *Transactions, the Institutions of Professional Engineers New Zealand Vol.9*, pp17-24.
104. Mosley, M.P. (1982b), "Analysis of the Effect of Changing Discharge on Channel Morphology and Instream Uses in a Braided River, Oahu river, New Zealand," *Water Resources Research*, Vol.8, pp.800-812.
105. "Morphological Dynamics of the Brahmaputra-Jamuna River," (1997), Prepared by: Environment and GIS Support Project for Water Sector Planning, Delft Hydraulics, Sponsored by Royal Netherlands Government.
106. Nagabushanaiah, H.S., (1967), "Meandering of Rivers," *Bulletin of the International Association of Scientific Hydrology*, Vol.12, pp.28-43.
107. Ore, H.T. (1964), "Some Criteria for Recognition of Braided Stream Deposits," *Wyoming Univ. Geology contr.*, pp. 1-14.
108. Parker, G. (1976), "On the Cause and Characteristic Scales of Meandering and Braiding in Rivers," *Journal of Fluid Mechanics*, Vol. 76, pp.459-480.
109. Parker, G. and Peterson, A. W. (1980), "Bar Resistance of Gravel-Bed Streams," *Journal of the Hydraulics Division, Proceeding of the, ASCE*, Vol. 106, No. 10, pp. 1559-1575.
110. Patra, K.C. and Kar, S.K. (2000), "Flow Interaction of Meandering River with Flood Plains," *Journal of the Hydraulics Engineering, ASCE*, Vol. 126, No.8, pp. 593-604.

111. Phillips, J. D. (1990), "The Instability of Hydraulic Geometry," *Water Resources Research*, Vol. 26, No.4, pp. 739-744.
112. Preston, J. H. (1954), "The Determination of Turbulent Skin Friction by Means of Pitot Tubes," *Journal of the Royal Aeronautical Society*. London, England, Vol. 58, pp. 109-121.
113. Ranga Raju, K.G. (1970), "Resistance Relationship for Alluvial Stream," *La Houille Blanche*, No.1.
114. "Report. Model Studies for Siting Bridge Across River Brahmaputra at Bogibil, Assam," U.P. Irrigation Research Institute, Roorkee, 1999.
115. Richards K. (Ed.1982), "Rivers: Forms and Process in Alluvial Channels," Published by Methuen and Co. Ltd., 11 New Fetter Lane, London.
116. Richardson, W.R. and Thorne, C.R., (2001), "Multiple Thread Flow and Channel Bifurcation in a Braided River: Brahmaputra-Jamuna River," *Bangladesh: Geomorphology*, Vol. 38, No. (3-4), pp.185-196.
117. Robertson-Rintoul, M.S.E. and Richards, K.S. (1993), "Braided-Channel Pattern and Palaeohydrology using an index of total sinuosity," A chapter in 'Braided rivers' by Best, J.L and Bristow, C.S. (Eds. 1993), Geological Society, London, Special. Publication, No. 75. pp. 113-118.
118. Rijn, L.C. V. (1984), "Sediment Transport Part III Bed Forms and Alluvial Roughness," *Journal of Hydraulic Engineering*, ASCE, Vol. 110, No. HY.12, pp. 1733-1752.
119. Roy, A.G. and Roy, R. (1988), "Changes in Channel Size at River Confluences with Coarse Bed Material," *Earth Surface Processes and Landforms*, Vol. 13, pp.77-84.
120. Rust, B.R. (1978a), "A Classification of Alluvial Channel Systems," In: MIALL, A.D. (Ed) *Fluvial Sedimentology*. Canadian Society of Petroleum Geologists Memoirs, Vol. 5, pp. 187-198.
121. Rust, B.R. (1978b), "Depositional Models for Braided Alluvium," In: MIALL, A.D. (Ed) *Fluvial Sedimentology*. Canadian Society of Petroleum Geologists Memoirs, Vol. 5, pp. 605-626.
122. Schumm, S.A. and Khan, H.R. (1972), "Experimental Study of Channel Patterns," *Geological Society of America Bulletin*, Vol. 83, pp.1755-1770.
123. Scumm, S.A. (1963), "Sinuosity of Alluvial Rivers on the Great Plains," *Geological Society of America Bulletin*, Vol.74, pp.1089-1100.

124. Senturk, H.A. (1978), "Resistance to Flow in Sand Bed Channels," *Journal of the Hydraulics Division, ASCE*, Vol. 104, No. HY3, pp. 421-436.
125. Seminara, G., Tubino, M. (1989), "Alternate Bar and Meandering: Free Forced and Mixed Interactions," In: Ikeda, S., Parker, G.(Eds), *River Meandering, Water Resources Monogr.*, Vol. 12, AGU, Washington, DC, pp.267-320.
126. Sharma, Nayan (1995), "Modeling of Braided Alluvial Channels," Ph.D. Thesis, WRDTC, University of Roorkee, India.
127. Shu-Guang Li. et al. (1992), "Stochastic Theory for Irregular Stream Modeling Part I: Flow Resistance," *Journal of the Hydraulic Engineering, ASCE*, Vol. 118. No. 8, pp. 1079-1090.
128. Singh V.P and Fiorentino, M. (1992), "Entropy and Energy Dissipation in Water Resources," (Eds.), Kluwer Academic Publishers. P.O. Box 17, 3300 A.A Dordrecht, The Netherlands.
129. Singh V.P (1996), "Kinematic Wave Modelling in Water Resources, Surface Water Hydrology," A wiley-Inter science Publications, JOHN WILEY AND SOSNS, INC. NEW YORK.
130. Smith, N.D. (1970), "The Braided Stream Depositional Environment," Comparison of the Platte river with some Silurian Clastic Rocks, North central Appalacians, *Geological Society of America Bulletin*, Vol.81, pp.2993-3014.
131. Smith, N.D. (1974), "Sedimentology and Bar Formation in the Upper Kicking Horse River, A Braided Out Wash Stream," *Journal of Geology*, Vol.82, pp.205-223.
132. Song, T. and Graf, W.H. (1996), "Velocity and Turbulence Distribution in Unsteady Open-Channel Flows," *Journal of the Hydraulics Engineering, ASCE*, Vol. 122, No. 3, pp. 141-154.
133. Sturm, T. W. and Sadiq, A. (1996), "Water Surface Profiles in Compound Channel with Multiple Critical Depths," *Journal of the Hydraulics Engineering, ASCE*, Vol. 122, No.12, pp. 703-709.
134. Sumer, B.M. and Kozakiewicz, Fredsoe, J. and Deigaard, R. (1996), "Velocity and Concentration Profiles in Sheet-Flow Layer of Movable Bed," *Journal of the Hydraulics Engineering, ASCE*, Vol. 122, No. 10, pp. 549-558.

135. Thorne, C.R., Russel, A.P.G. and Alam, M.K. (1993), "Planform Pattern and Channel Evolution of the Brahmaputra River, Bangladesh," A chapter in 'Braided Rivers' by Best, J.L. and Bristow, C.S. (eds.1993), Geological. Society London, Special Publication, No.75, pp.257-276.
136. Thompson, S.M. and Camphell, P.L. (1979), "Hydraulics of a Large Channel Paved with Boulders," *Journal of Hydraulic Research*, Vol. 17, No.4.
137. Tubino, M. (1991), "Growth of Alternate Bars in Unsteady Flow," *Water Resources Research*, Vol. 27, pp.37-52.
138. Valentine, E.M., Benson I. A., Nalluri, C. and Bathurst, J.C.(2001) "Regime Theory and the Stability of Straight Channels with Bankful and Overbank Flow," *Journal of Hydraulic Research* Vol. 39, pp. 258-268.
139. Vedula, S. and Achanta, R.R. (1985), "Bed Shear from Velocity Profiles: A New Approach," *Journal of the Hydraulics Engineering, ASCE*, Vol. 111, No.1, pp. 131-143.
140. Wang, S. and White, W.R. (1993)," Alluvial Resistance in Transition Regime," *Journal of the Hydraulics Engineering, ASCE*, Vol. 119, No. 6, pp. 725-741.
141. White, W.R., Bettes, R. and Paris, E. (1982), "Analytical Approach to River Regime," *Journal of the Hydraulics Division, ASCE*, Vol.108, No. HY10, pp. 1179-1192.
142. Willis, J.C. (1983), "Flow Resistance in Large Test Channel," *Journal of the Hydraulics Engineering, ASCE*, Vol.109, No.12, pp. 1755-1770.
143. Yang, C.T. and Song, C.C.S. (1979), "Velocity Profiles and Minimum Stream Power," *Journal of the Hydraulics Engineering, ASCE*, Vol. 105, No. 8, pp. 981-998.
144. Yang, C.T., Song C.C.S. and, M.J. Woldenberg, (1981),"Hydraulic Geometry and Minimum Rate of Energy Dissipation," *Water Resources Research*, Vol.17 No.4, pp.1014-1018.
145. Yang, C. T. , Albert Molinas and Bausheng, Wu (1996), "Sediment Transport in the Yellow River," *Journal of the Hydraulics Engineering, ASCE*, Vol. 122, No. 5, pp. 237-244.
146. Yen, C.L. (1973), "Shape Effects on Resistance in Flood-Plane Channels," *Journal of the Hydraulics Engineering, ASCE*, Vol. 99, No. HY1, pp. 219-238.
147. Yen, C. L. (1992),"Aggradation-Degradation Process in Alluvial Channels," *Journal of the Hydraulics Engineering, ASCE*, Vol. 118, No. 12, pp. 1651-1669.

APPENDIX



BRAHMAPUTRA RIVER UNDER STUDY

For the present research work, the field data of a stretch of the Brahmaputra River in Bangladesh have been adopted for undertaking analyses. The river originates from Man Sarovar of Tibet (on the North Slope of the Himalayas) and flows eastward for about 700 miles before it turns towards south into the Indian province of Assam. The river then takes a sharp bend towards west and flows for about 400 miles until it reaches the border of Bangladesh at Dhubri where its bed elevation is 28.4m. It flows over the alluvial soils in the territory of Bangladesh up to Daulatdia-ArichaBaruria where it confluences with the Ganges and continues its flow up to the Bay of Bengal. Elevation at origin in the Kailash Range of south China is 5300 m and elevation at Guwahati is 50.5m. Total length of the river 2897 km of which 1625 km in Tibet, 918 km in India and remaining length 354 km is in Bangladesh up to Bay of Bengal.

The Brahmaputra is one of the largest and biggest sand bed braided rivers in the world. It's channel width varies from 5 to 20 km. This river has been ranked 5th in discharge, 11th in drainage area, 3rd in sediment discharge in the world (Thorne et al., 1993). Mean flow of the river is 12200 m³/s and drainage area is 666000 sq. km. Basin area of the river 50.5% in China, 33.6% in India, 8.1% in Bangladesh and 7.8% in Bhutan. Dominant discharge of the river is 38000 m³/s and bankfull discharge is 65000 m³/s. The study reach length is about 160 km. from Bahadurabad to Daulatdia-ArichaBaruria for general study. For scale model study of experimental programme Phase-II, the study stretch is confined between Bahadurabad ghat and Bhangabadhu-

Jamuna bridge site. The river has braid plains up to 20 km. and carries 500 million tonnes sediments annually. In 1988 flood, the peak discharge was 100000 cumecs (100 year return period). In some places, width to depth ratio is greater than 700 at bank full flow. The slope of the river at Gorge section is 4-17 m/km, at Pasighat 27cm/ km, at Guwahati 10cm/km and in Bangladesh around 1 m / 12.5 km - 13 km.

The Brahmaputra River has developed with metastable islands and notable reaches, mobile sandbars, shifting anabranches due to severe bank erosion. In the study reach the river is braided, with numerous small bars and fewer large islands, locally called chars, which divide the flow into sub-channels called anabranches. It's braid bars are highly unstable and their size, shape and position change radically between each seasonal high flow but islands are relatively stable. Coleman, (1969) had given a brief description of large braided Brahmaputra River and its channel process and sedimentation. During maximum flood period, some of the bedforms attain gigantic size with heights upto 50 ft., and migrate downstream at rates as high as 2000 ft/24 hrs. The Brahmaputra river adopts peaks late July and early August like 65500 m³/s but Ganges peak flow is in late August and early September like 51625 cumecs. Sometimes Brahmaputra river creates late peak, coincides with Ganges peak, causes catastrophic flooding which is extensive and damaging. The Ganges and the Brahmaputra rivers combined have formed one of the largest deltas in the world, comprising some 23000 sq. miles. Having large drainage area and charged with sediment, transporting 13000000 tons of suspended sediment/day. The Brahmaputra followed a route some 60 miles to east of its present course only 200 years ago. The Brahmaputra river displays a braided pattern in plan view, and short term channel migration is quite drastic, with rates of movement as

high as 2600 ft a year being common. The combined Bengal Basin rivers deliver some 10000000000 tones of suspended sediment load a year to the Bay of Bengal. Most of sediment brought to the Bay by passes the bar and continues on into deeper water through a canyon called the Swatch of No Ground. This in deep water a subaqueous delta is being formed that dwarfs the subaerial delta, one of the largest in the world.

The bed load consists predominantly of silt and fine sand. The sediments within Bangladesh part consist of fine sands and silts, with little clay matrix. Brahmaputra's sediments are not only deposited in millions of tons but are also highly susceptible to erosion when flow conditions change. As the river, Brahmaputra is heavily charged with sediment, rates of deposition and erosion are quite high. Scour depth of the river is up to 50m. The constant shifting of the thalweg adds to the magnitude and complexity of deposition and erosion patterns.



Plate A2.1a: INITIAL CONDITION OF RUN - 1 HAVING NON-SEDIMENT FEEDING CONDITION AND OBLIQUE FLOW (OF) AT AN ANGLE 40° , SLOPE (S_0) = 0.01

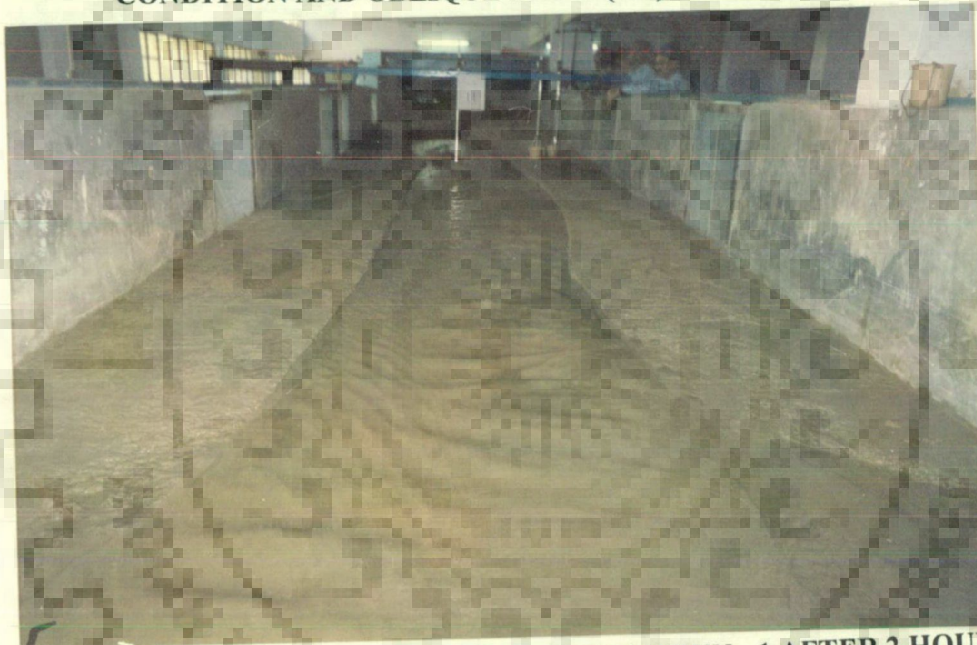


Plate A2.1b: MEANDERING FORMATION OF RUN - 1 AFTER 2 HOURS OF RUNNING



Plate A2.1c: BAR DEVELOPMENT OF RUN - 1 AFTER 20 HOURS OF RUNNING



Plate A2.2a: INITIAL CONDITION OF RUN - 10 HAVING NON-SEDIMENT FEEDING CONDITION AND INITIAL SINUOSITY $P_c = 1.10$, OF = 0^0 , SLOPE (S_0) = 0.02



Plate A2.2b: EMERGING OF BARS OF RUN - 10 AFTER 12 HOURS OF RUNNING



Plate A2.2c: BRAIDING CONDITION WITH MULTIPLE CHANNEL OF RUN - 10 AFTER 20 HOURS OF RUNNING



Plate A2.3a: MEANDERING CONDITION OF RUN - 23 AFTER 1 HOUR HAVING NON-SEDIMENT FEEDING CONDITION WITH OBLIQUE FLOW (OF) = 60° , $S_0 = 0.02$

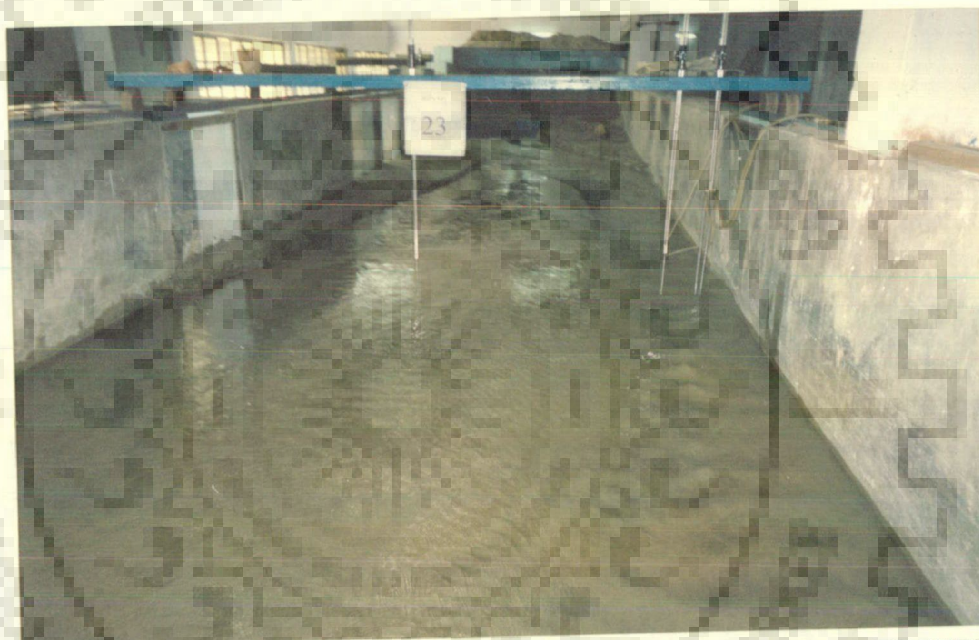


Plate A2.3b: PLAN FORM OF RUN - 23 AFTER 8 HOURS OF RUNNING EXPERIMENT

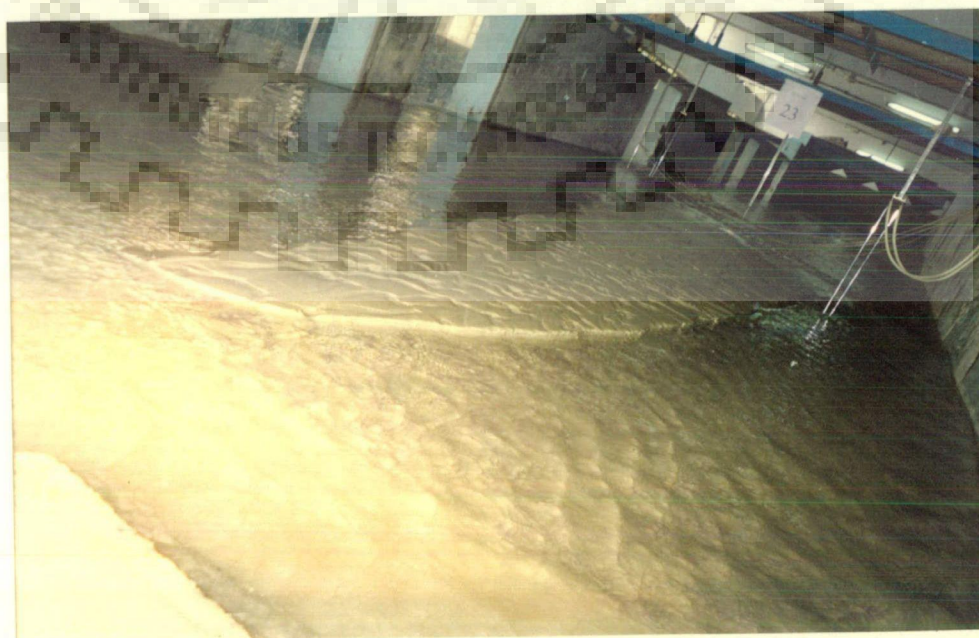


Plate A2.3c: BRAIDING CONDITION WITH ISLAND OF RUN - 23 AFTER 10 HOURS OF RUNNING



Plate A2.4a: INITIAL CONDITION OF RUN - 26 HAVING NON-SEDIMENT FEEDING CONDITION AND OBLIQUE FLOW (OF) AT AN ANGLE 20° , SLOPE (S_0) = 0.03 $P_C=0$



Plate A2.4b: BEGINNING OF MEANDERING OF RUN - 26 AFTER 2 HOURS OF RUNNING

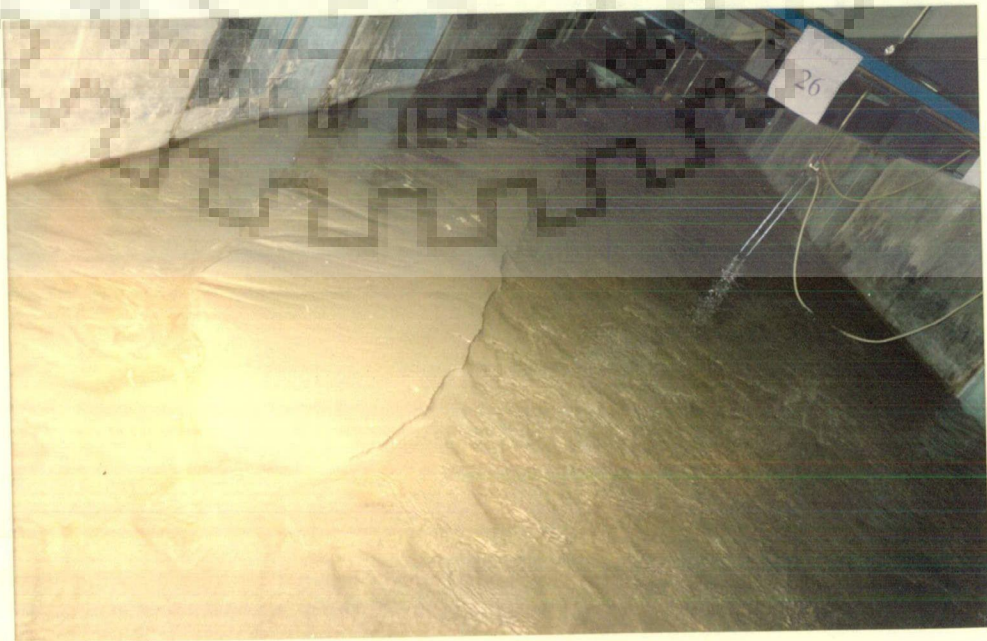


Plate A2.4c : SHOWING BAR OR CHAR FORMATION AFTER 20 HOURS OF RUNNING



**Plate A2.5a: INITIAL CONDITION OF RUN - 29 HAVING NON-SEDIMENT FEEDING
CONDITION WITH INITIAL SINUOSITY $P_c=1.05$ AND OBLIQUE FLOW = 0° , $S_0=0.03$**



Plate A2.5b: MEANDERING PLAN FORM OF RUN-29 AFTER 1/2 HOURS OF RUNNING



Plate A2.5c: BRAIDING CONDITION WITH BARS AFTER 16 HOURS OF RUNNING



Plate A2.6a: INITIAL CONDITION OF RUN - 30 HAVING NON-SEDIMENT FEEDING CONDITION WITH INITIAL SINUOSITY $P_c=1.10$ AND OBLIQUE FLOW = 0^0 , $S_0 = 0.03$



Plate A2.6b: DEVELOPMENT OF BARS AFTER 8 HOURS OF RUNNING



Plate A2.6c: SHOWING BAR OR CHAR FORMATION AFTER 16 HOURS OF RUNNING



Plate A2.7a: INITIAL CONDITION OF RUN - 35 HAVING SEDIMENT FEEDING CONDITION WITH INITIAL SINUOSITY $P_C=1.10$ AND OBLIQUE FLOW = 0° , $S_0 = 0.01$



Plate A2.7b: MULTIPLE CHANNEL WITH BARS OF RUN - 35 AFTER 14 HOURS



Plate A2.7c: BRAIDING CONDITION WITH ISLANDS OF RUN-35 AFTER 20 HRS

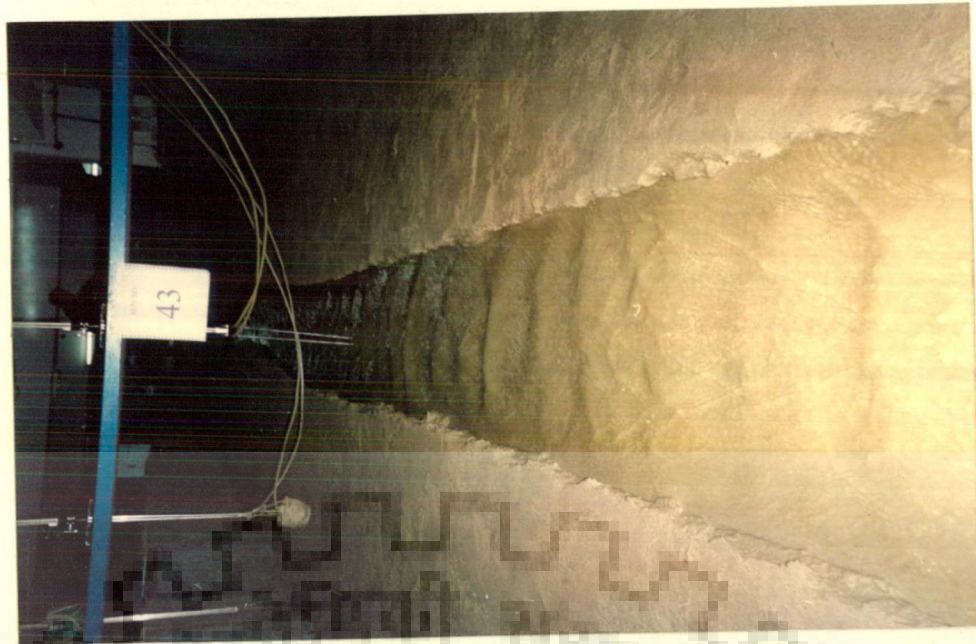


Plate A2.8a: INITIAL CONDITION OF RUN -43 HAVING SEDIMENT FEEDING CONDITION WITH OBLIQUE FLOW AT AN ANGLE 60° , $P_c=0.0$ AND $S_0=0.03$

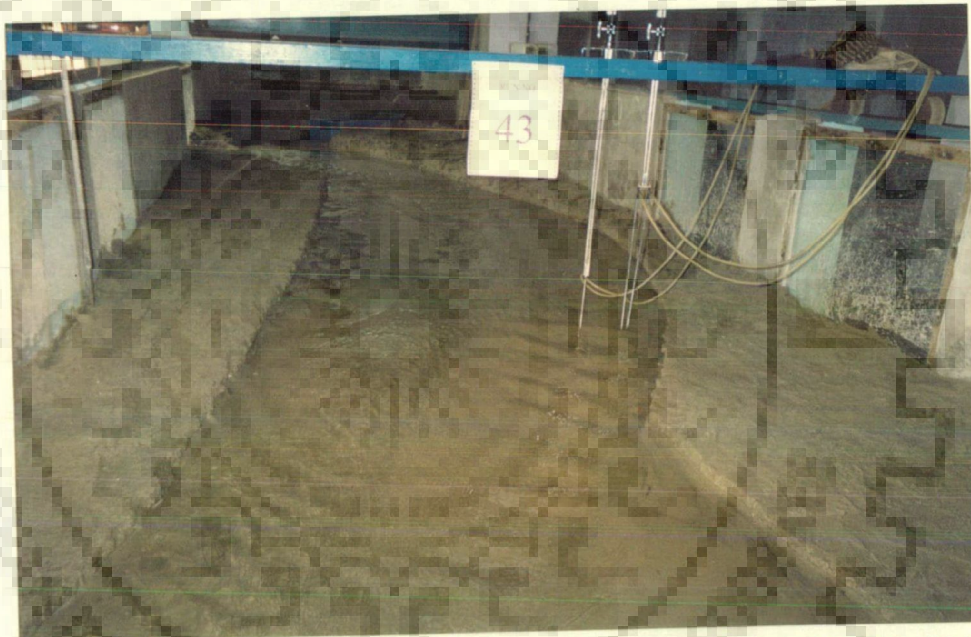


Plate A2.8b: MEANDERING CONDITION OF RUN - 43 AFTER 1/2 HOURS OF RUNNING



Plate A2.8c: BARS WITH MULTI CHANNEL FORMATION OF RUN-43 AFTER 16 HOURS



Plate A2.9a: INITIAL CONDITION OF RUN - 47 HAVING SEDIMENT FEEDING CONDITION WITH OBLIQUE FLOW AT AN ANGLE 40° , $P_C=0.0$ AND $S_0=0.01$



Plate A2.9b: BAR FORMATION OF RUN - 47 AFTER 12 HOURS OF RUNNING



Plate A2.9c: BRAIDING CONDITION WITH MULTI CHANNEL OF RUN - 47 AFTER 20 HOURS OF RUNNING



Plate A2.10a: INITIAL CONDITION OF RUN - 48 HAVING SEDIMENT FEEDING CONDITION WITH OBLIQUE FLOW AT AN ANGLE 60° , $P_c=0.0$ AND $S_0=0.01$



Plate A2.10b: MEANDERING PLANFORM OF RUN - 48 AFTER 1.5 HOURS OF RUNNING



Plate A2.10c: BRAIDED BAR WITH MULTI CHANNEL FORMATION OF RUN - 48 AFTER 20 HOURS



Plate A2.11a: INITIAL CONDITION OF RUN - 51 HAVING SEDIMENT FEEDING CONDITION WITH OBLIQUE FLOW AT AN ANGLE 20° , $P_c=0.0$ AND $S_0=0.02$



Plate A2.11b: PLANFORM OF RUN - 51 AFTER 12 HOURS OF RUNNING



Plate A2.11c: MULTI CHANNEL WITH BRAID BAR. FORMATION OF RUN - 51 AFTER 18 HOURS



Plate A2.12a: INITIAL CONDITION OF RUN - 59 HAVING SEDIMENT FEEDING
CONDITION WITH INITIAL SINUOSITY $P_c=1.05$ OBLIQUE FLOW 0° AND $S_0=0.02$

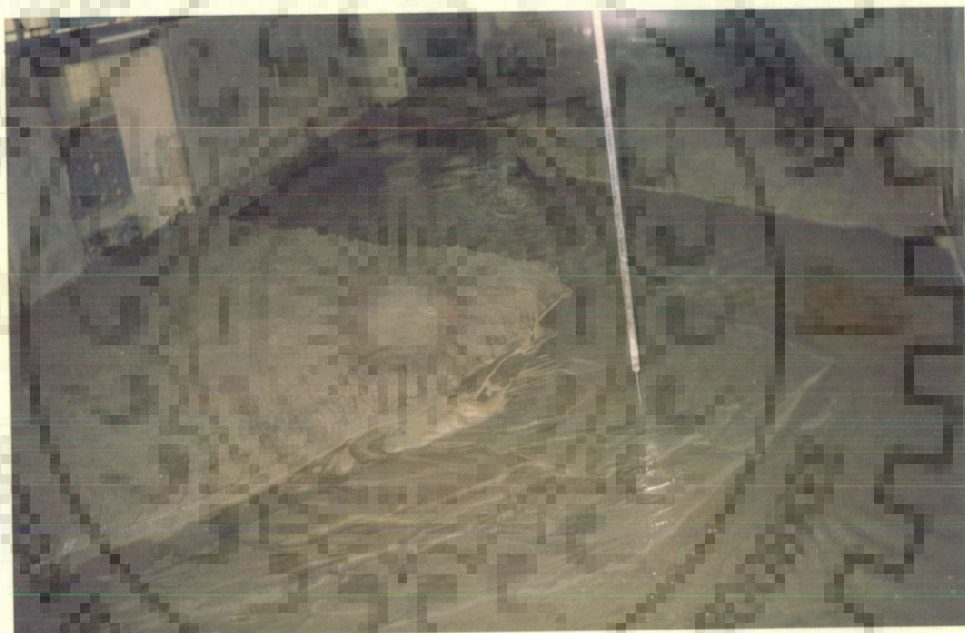


Plate A2.12b: MEANDERING PLANFORM OF RUN - 59 AFTER 3 HOURS OF RUNNING



Plate A2.12c: MULTI CHANNEL PATTERN OF RUN - 59 AFTER 16 HOURS OF RUNNING

Table A2.1 DATA OF STUDY REACH OF THE BRAHMAPUTRA RIVER

C/S	Year	Q (m ³ /s)	A (m ²)	B (m)	W (m)	D (m)	R=A/(W+2D)	S
	1988	9040	16287.36	6405.5	2392.12	6.808755	6.77	0.0000773
	89	24600	35716.41	6362	4464.72	7.999698	7.97	0.0000777
	90	12760	29802.4	5323	4060	7.340493	7.31	0.0000734
	91	13220	36927.828	5330	4509	8.189804	8.16	0.0000819
	92	7465	26261.992	5249	3556	7.385262	7.35	0.000076
J# 0-1	93	6546.67	28094.03	5276	3101	9.059668	9.01	0.00002249
A-A	94	4738.33	34262.594	5140	3670	9.335857	9.29	0.000009098
	95	5416	16635.918	5276	3932	4.230905	4.22	0.000076
	97	5723	12034.06	6057	4105	2.931562	2.93	0.0000942
	1988	5460	16626.91	11100	5035	3.302266	3.3	0.0000768
	89	18900	26617.11	10050	5421	4.91	4.9	0.0000801
	90	5710	16260.13	11185	5809	2.799127	2.8	0.0000749
	91	17000	17559.171	11185	5763	3.04688	3.04	0.00008
	92	4600	5432.288	11187	2742	1.981141	1.9751	0.0000788
J# 6-1	93	4726.67	10744.54	11185	2814	3.818244	3.81	0.0000756
B-B	94	4614	8395.524	11175	2489	3.373051	3.36	0.0000751
	95	4160	7870.03	11185	4523	1.740002	1.7351	0.000059
	97	4536	20893.2	11187	5078	4.114455	4.11	0.00004479
	1988	5790	12067.128	16300	2972.88	4.05907	4.05	0.0000761
	89	6390	9282.95	16376	2197	4.225284	4.21	0.0000245
	90	24800	23290.62	16377	6745	3.45302	3.45	0.00002498
	91	19900	19572.002	16376	6396.05	3.060014	3.06	0.0000925
	92	8915.72	16717.33	16376	5406	3.092366	3.09	0.00001733
J#13-1	93	4926	8280.8	16376	2355	3.516263	3.51	0.0000254
C-C	94	4688.75	10473.823	16376	3089	3.390684	3.38	0.0000226
	95	3680	9462.88	16374	2981	3.174398	3.17	0.0000265
	97	4500	4393.506	16376	1373	3.199932	3.1949	0.00011

Table A2.2 BASIC DATA OF LABORATORY EXPERIMENTAL RUN-43

Oblique Flow direction = 60°					Sediment Feeding condition				Initial Slope S=0.03			
Xi	Yi	WL	Z	D _i	A _i (cm ²)	W (cm)	B (cm)	Vx(.6D) cm/s	S	Time	Q Litre/s	Q _s (gm/min)
7m	10	17,5	25	-7,5	0	90	100		0,03	1.5 hrs	4	385
	30	17,5	22,4	-4,9	0							
	50	17,5	21,6	-4,1	0							
	70	17,5	19,9	-2,4	0							
	90	17,5	15,4	2,1	11			45				
	110	17,5	15	2,5	46			50				
	130	17,5	17,02	0,48	29,8							
	150	17,5	16,9	0,6	10,8							
	170	17,5	20,4	-2,9	6							
	190	17,5	21,2	-3,7	0							
	210	17,5	20,9	-3,4	0							
	230	17,5	22	-4,5	0							
	250	17,5	22,1	-4,6	0							
					103,6							
9m	10	15	18,9	-3,9	0	93	104			1.5 hrs		
	30	15	18,4	-3,4	0							
	50	15	17,6	-2,6	0							
	70	15	16,2	-1,2	0							
	90	15	15,6	-0,6	6							
	110	15	13,2	1,8	12							
	130	15	13,3	1,7	35							
	150	15	13,9	1,1	28							
	170	15	14,1	0,9	20			33				
	190	15	12,4	2,6	35			30				
	210	15	19,8	-4,8	26							
	230	15	20,6	-5,6	0							
	250	15	20,4	-5,4	0							
				0	162							
11m	10	14	14,4	-0,4	0	100	110			1.5 hrs		
	30	14	14,6	-0,6	0							
	50	14	12,6	1,4	8							
	70	14	11,9	2,1	35							
	90	14	11,4	2,6	47							
	110	14	10,1	3,9	65							
	130	14	12,1	1,9	58							
	150	14	12,4	1,6	35							
	170	14	12,9	1,1	27			40				
	190	14	13,4	0,6	17			42				
	210	14	13,6	0,4	10							
	230	14	17,8	-3,8	0							
	250	14	19	-5	0					1.5 hrs		
				0	302							

1000 litre = 1 m³

Xi	Yi	WL	Z	D _i	A _i (cm ²)	W (cm)	B (cm)	Vx(.6D)	S	Time	Q L/s	Q _s (gm/min)
13m	10	11,5	12	-0,5	0	105	115		.02	1.5 hrs	4 lps	385
	30	11,5	11,7	-0,2	0							
	50	11,5	11,6	-0,1	0							
	70	11,5	10,1	1,4	13							
	90	11,5	7,4	4,1	55							
	110	11,5	8,6	2,9	70							
	130	11,5	9,6	1,9	48			45				
	150	11,5	10,4	1,1	30			41				
	170	11,5	8,1	3,4	45							
	190	11,5	9,6	1,9	53							
	210	11,5	9	2,5	44							
	230	11,5	13,2	-1,7	8							
	250	11,5	14,9	-3,4	0					1.5 hrs		
					366							
16m	10	7,3	-0,1	7,4	74	230	235	40		1.5 hrs		
	30	7,3	4,9	2,4	98			38				
	50	7,3	5,4	1,9	43							
	70	7,3	5,1	2,2	41							
	90	7,3	6,2	1,1	33							
	110	7,3	6,8	0,5	16							
	130	7,3	6,2	1,1	16							
	150	7,3	7	0,3	14							
	170	7,3	7,4	-0,1	2							
	190	7,3	8,1	-0,8	0							
	210	7,3	7,1	0,2	0							
	230	7,3	7,3	0	2							
	250	7,3	7,1	0,2	2							
				0	341							
18m	10	5	2,4	2,6	26	230	238	45		1.5 hrs		
	30	5	4,3	0,7	33			42				
	50	5	4,9	0,1	8							
	70	5	8,2	-3,2	0							
	90	5	6,9	-1,9	0							
	110	5	5,4	-0,4	0							
	130	5	5	0	0							
	150	5	4,6	0,4	4							
	170	5	2,4	2,6	30							
	190	5	1,1	3,9	65			30				
	210	5	2,9	2,1	60			32				
	230	5	2,3	2,7	48							
	250	5	2	3	57					1.5 hrs		
					331							
7m	10	17,8	24	-6,2	0	145			0,012	5 hrs	4 lps	385
	30	17,8	15,5	2,3	0			31,8674				
	50	17,8	15,1	2,7	50			45,06731				
	70	17,8	15,8	2	47			55,19596				
	90	17,8	16,2	1,6	36			52,8461				
	110	17,8	16,3	1,5	31			39,02944				

Xi	Yi'	WL	Z	D _i	A _i (cm ²)	W (cm)	B(cm)	Vx(.6D)	S	Time	Q L/s	Q _s (gm/min)
7m	130	17,8	17,3	0,5	20			0	.012		4 lps	385
	150	17,8	17,5	0,3	8			0				
	170	17,8	16,6	1,2	15			0				
	190	17,8	20,7	-2,9	0			0				
	210	17,8	21,1	-3,3	0			0				
	230	17,8	22	-4,2	0			0				
	250	17,8	22	-4,2	0			0				
				0	207			0				
9m	10	15,3	10,7	4,6	46	180		0		5 hrs		
	30	15,3	11,4	3,9	85			45,06731				
	50	15,3	14	1,3	52			50,38678				
	70	15,3	15,2	0,1	14			39,02944				
	90	15,3	15,5	-0,2	0			31,8674				
	110	15,3	15,2	0,1	0			0				
	130	15,3	15	0,3	4			0				
	150	15,3	14,5	0,8	11			0				
	170	15,3	14,4	0,9	17			0				
	190	15,3	14,5	0,8	17			0				
	210	15,3	21,1	-5,8	0			0				
	230	15,3	20	-4,7	0			0				
	250	15,3	20,5	-5,2	0			0				
				0	246			0				
11m	10	13,3	14	-0,7	0	170		0		5 hrs		
	30	13,3	11	2,3	16			0				
	50	13,3	11,4	1,9	42			0				
	70	13,3	11,9	1,4	33			0				
	90	13,3	12,4	0,9	23			0				
	110	13,3	12,6	0,7	16			55,19596				
	130	13,3	12,9	0,4	11			50,38678				
	150	13,3	12,8	0,5	9			45,06731				
	170	13,3	12	1,3	18			31,8674				
	190	13,3	11,5	1,8	31			0				
	210	13,3	12,2	1,1	29			0				
	230	13,3	12,2	1,1	22			0				
	250	13,3	10	3,3	44			0				
				0	294			0				
13m	10	11,5	12	-0,5	0	190	200	0		5 hrs		
	30	11,5	12	-0,5	0			0				
	50	11,5	12,2	-0,7	0			0				
	70	11,5	9	2,5	18			0				
	90	11,5	9,8	1,7	42			31,8674				
	110	11,5	8,4	3,1	48			0				
	130	11,5	11,7	-0,2	29			0				
	150	11,5	11,8	-0,3	-5			0				
	170	11,5	7,9	3,6	33			0				
	190	11,5	6,5	5	86			0				
	210	11,5	7,46	4,04	90,4			0				
	230	11,5	10,1	1,4	54,4			67,60096				

Xi	Yi	WL	Z	D _i	A _i (cm ²)	W (cm)	B(cm)	Vx(.6D)	S	Time	Q	Q _s
13m	250	11,5	9,5	2	34			71,25767	.012	5 hrs		
				0	20			0				
				0	449,8							
16m	10	8,3	3,7	4,6	46	230	240	39,02944				
	30	8,3	3,6	4,7	93			39,02944				
	50	8,3	3,4	4,9	96			0				
	70	8,3	4,6	3,7	86			0				
	90	8,3	5,1	3,2	69			0				
	110	8,3	7,2	1,1	43			39,02944				
	130	8,3	8,6	-0,3	8			39,02944				
	150	8,3	9,3	-1	0			0				
	170	8,3	9,9	-1,6	0			0				
	190	8,3	10,5	-2,2	0			0				
	210	8,3	8	0,3	3			0				
	230	8,3	6,3	2	23			42,15661				
	250	8,3	7	1,3	33			45,06731		5 hrs		
				0	500			0				
18m	10	6,6	2,7	3,9	78,2	260	260	42,15661				
	30	6,6	2,68	3,92	80,2			39,02944				
	50	6,6	2,5	4,1	67			0				
	70	6,6	4	2,6	53			0				
	90	6,6	3,9	2,7	64			0				
	110	6,6	2,9	3,7	39			0				
	130	6,6	6,4	0,2	4			0				
	150	6,6	7,2	-0,6	0			0				
	170	6,6	7,95	-1,35	0			0				
	190	6,6	6,2	0,4	10			0				
	210	6,6	6	0,6	30			0				
	230	6,6	4,2	2,4	51			45,06731				
	250	6,6	3,9	2,7	27			45,06731		5 hrs		
					503,4							
7m	10	16,8	25,6	-8,8	0	120	130		0,011	10 hrs	4 lps	385
	30	16,8	14,4	2,4	0							
	50	16,8	14,1	2,7	51							
	70	16,8	16,6	0,2	29							
	90	16,8	17,6	-0,8	0							
	110	16,8	17,9	-1,1	0							
	130	16,8	17,9	-1,1	0							
	150	16,8	14,8	2	9							
	170	16,8	15,1	1,7	37			35,62884				
	190	16,8	12,4	4,4	61			47,8011				
	210	16,8	14,8	2	64			45,06731				
	230	16,8	12,2	4,6	66			42,15661				
	250	16,8	14,6	2,2	68			39,02944				
				0	385			0				
9m	10	15	12	3	30	125	135	0		10 hrs		
	30	15	15,2	-0,2	28			0				
	50	15	15,3	-0,3	0			0				

Xi	Yi	WL	Z	D _i	A _i (cm ²)	W (cm)	B(cm)	Vx(.6D)	S	Time	Q L/s	Q _s (gm/min)
9m	70	15	15,6	-0,6	0			0	.011		4 lps	385
	90	15	15,4	-0,4	0			0				
	110	15	10,1	4,9	45			39,02944				
	130	15	11	4	89			45,06731				
	150	15	12,9	2,1	61			59,61845				
	170	15	11	4	61			55,19596				
	190	15	11,4	3,6	76			39,02944				
	210	15	19,1	-4,1	0			31,8674				
	230	15	20,7	-5,7	0			0				
	250	15	20,2	-5,2	0			0				
				0	390							
11m	10	12,8	9,9	2,9	29	135	145	0		10 hrs		
	30	12,8	10,2	2,6	55			0				
	50	12,8	10,4	2,4	50			0				
	70	12,8	10,2	2,6	50			52,8461				
	90	12,8	10,6	2,2	48			55,19596				
	110	12,8	10	2,8	50			59,61845				
	130	12,8	9,8	3	58			57,44977				
	150	12,8	10,8	2	50			0				
	170	12,8	13,8	-1	10			0				
	190	12,8	12,9	-0,1	0			0				
	210	12,8	13,1	-0,3	0			0				
	230	12,8	14,2	-1,4	0			0				
	250	12,8	14,6	-1,8	0			0				
					0	400			0			
13m	10	10,5	6,6	3,9	39	100	110	63,7348		10 hrs		385
	30	10,5	3,1	7,4	113			59,61845				
	50	10,5	4,6	5,9	133			55,19596				
	70	10,5	4,5	6	119			39,02944				
	90	10,5	7,6	2,9	89			0				
	110	10,5	12,1	-1,6	13			0				
	130	10,5	12,4	-1,9	-35			0				
	150	10,5	10,9	-0,4	-23			0				
	170	10,5	10,9	-0,4	-8			0				
	190	10,5	10,6	-0,1	-5			0				
	210	10,5	11,2	-0,7	-8			0				
	230	10,5	11,9	-1,4	-21			0				
	250	10,5	10,2	0,3	3			0				
					0	409		377	0			
				0	0							
16m	10	8,3	2,8	5,5	55	110	120	50,38678		10 hrs		
	30	8,3	4,6	3,7	92			47,8011				
	50	8,3	4,65	3,65	73,5			45,06731				
	70	8,3	7,2	1,1	47,5			0				
	90	8,3	4,6	3,7	48			0				
	110	8,3	7	1,3	50			0				
	130	8,3	7,2	1,1	24			0				
	150	8,3	8,6	-0,3	8			0				

Xi	Yi	WL	Z	D _i	A _i (cm ²)	W (cm)	B(cm)	Vx(.6D)	S	Time	Q L/s	Q _s (gm/min)
16m	170	8,3	8,9	-0,6	0			0	.011	10 hrs	4	385
	190	8,3	10,6	-2,3	0			0				
	210	8,3	9,3	-1	0			0				
	230	8,3	9,2	-0,9	0			0				
	250	8,3	9,1	-0,8	0			0				
				0	398			0				
18m	10	6,7	3,7	3	30	130	140	45,06731		10 hrs		
	30	6,7	3,2	3,5	65			42,15661				
	50	6,7	4,3	2,4	59			39,02944				
	70	6,7	3,5	3,2	56			31,8674				
	90	6,7	5,4	1,3	45			0				
	110	6,7	5,9	0,8	0							
	130	6,7	5,6	1,1	19							
	150	6,7	6,2	0,5	16							
	170	6,7	6,6	0,1	6							
	190	6,7	7,3	-0,6	0							
	210	6,7	6,4	0,3	0							
	230	6,7	5,9	0,8	11							
	250	6,7	6,6	0,1	9							
					316							
7m	10	16,8	24,3	-7,5	0	130	140		0,01	13 hrs	4 lps	385 gm
	30	16,8	12,8	4	0							
	50	16,8	13,4	3,4	74							
	70	16,8	17,3	-0,5	29							
	90	16,8	17,1	-0,3	0							
	110	16,8	17,9	-1,1	0							
	130	16,8	17,4	-0,6	0							
	150	16,8	14,6	2,2	16							
	170	16,8	13,2	3,6	58			39,02944				
	190	16,8	12,4	4,4	80			39,02944				
	210	16,8	15,1	1,7	61			39,02944				
	230	16,8	13,9	2,9	46			42,15661				
	250	16,8	13,1	3,7	66			42,15661				
				0	37			0				
				0	467			0				
9m	10	14,8	15	-0,2	0	155	165	0		13 hrs		
	30	14,8	15	-0,2	0			0				
	50	14,8	14,9	-0,1	0			0				
	70	14,8	14,9	-0,1	0			0				
	90	14,8	11,4	3,4	33			0				
	110	14,8	12,7	2,1	55			0				
	130	14,8	10,8	4	61			0				
	150	14,8	9,4	5,4	94			45,06731				
	170	14,8	10,8	4	94			47,8011				
	190	14,8	10,4	4,4	84			42,15661				
	210	14,8	10,9	3,9	83			0				
	230	14,8	20	-5,2	0			0				
	250	14,8	20	-5,2	0			0				

Xi	Yi	WL	Z	D _i	A _i (cm ²)	W (cm)	B(cm)	Vx(.6D)	S	Time	Q L/s	Q _s (gm/min)
9m					504				.01		4	385
11m	10	12,6	10,2	2,4	24	210	220	0		13 hrs		
	30	12,6	10,9	1,7	41			0				
	50	12,6	7,2	5,4	71			27,59798				
	70	12,6	6,4	6,2	116			31,8674				
	90	12,6	9,2	3,4	96			35,62884				
	110	12,6	8,5	4,1	75			39,02944				
	130	12,6	9,9	2,7	68			39,02944				
	150	12,6	10,8	1,8	45			35,62884				
	170	12,6	12,1	0,5	23			0				
	190	12,6	11,6	1	15			0				
	210	12,6	13,1	-0,5	5			0				
	230	12,6	13,6	-1	0			0				
	250	12,6	14,5	-1,9	0			0				
				0	579			0				
13m	10	9,9	5,6	4,3	43	130	140	42,15661		13 hrs		
	30	9,9	5,6	4,3	86			40,93442				
	50	9,9	7,2	2,7	70			39,02944				
	70	9,9	6,6	3,3	60			31,8674				
	90	9,9	7,1	2,8	61			0				
	110	9,9	6,5	3,4	62			0				
	130	9,9	9,8	0,1	35			0				
	150	9,9	10,5	-0,6	0			0				
	170	9,9	11,6	-1,7	0			0				
	190	9,9	11,4	-1,5	0			0				
	210	9,9	11,1	-1,2	0			0				
	230	9,9	10	-0,1	0			0				
	250	9,9	9,8	0,1	0			0				
				0	417			0				
16m	10	8,2	3,4	4,8	48	115	125	55,19596		13 hrs		
	30	8,2	3,9	4,3	91			52,8461				
	50	8,2	5,4	2,8	71			0				
	70	8,2	4,5	3,7	65			0				
	90	8,2	7,1	1,1	48			0				
	110	8,2	8,4	-0,2	9			0				
	130	8,2	8,6	-0,4	0			0				
	150	8,2	6,2	2	16			0				
	170	8,2	8,1	0,1	21			0				
	190	8,2	10,6	-2,4	0			0				
	210	8,2	9,6	-1,4	0			0				
	230	8,2	5,5	2,7	13			0				
	250	8,2	8,9	-0,7	20			0				
				0	402			0				
18m	10	6,6	3,2	3,4	34	133	142	45,06731		13 hrs		
	30	6,6	2,5	4,1	75			42,15661				
	50	6,6	3,3	3,3	74			39,02944				
	70	6,6	4,1	2,5	58							
	90	6,6	6,1	0,5	30							

Xi	Yi	WL	Z	D _i	A _i (cm ²)	W (cm)	B(cm)	Vx(.6D)	S	Time	Q L/s	Q _s (gm/min)
18m	110	6,6	5,8	0,8	13				.01	13hrs	4	385
	130	6,6	6,8	-0,2	6							
	150	6,6	6,8	-0,2	0							
	170	6,6	7,5	-0,9	0							
	190	6,6	7,2	-0,6	0							
	210	6,6	6,6	0	0							
	230	6,6	4,1	2,5	25							
	250	6,6	6,2	0,4	29							
					0	344						
7m	10	15,7	20,6	-4,9	0	140	150		0,01	16 hrs	4 lps	385
	30	15,7	12	3,7	37							
	50	15,7	16,4	-0,7	30							
	70	15,7	16,6	-0,9	0							
	90	15,7	16,8	-1,1	0							
	110	15,7	16,9	-1,2	0							
	130	15,7	13,2	2,5	13			27,59798				
	150	15,7	13,1	2,6	51			31,8674				
	170	15,7	13,25	2,45	50,5			31,8674				
	190	15,7	11,1	4,6	70,5			31,8674				
	210	15,7	14,4	1,3	59			35,62884				
	230	15,7	11	4,7	60			35,62884				
	250	15,7	14,2	1,5	62			35,62884				
					0	433			0			
9m	10	14,4	10,3	4,1	41	190	200	0		16 hrs	16	
	30	14,4	10,4	4	81			0				
	50	14,4	14,1	0,3	43			0				
	70	14,4	14,2	0,2	5			0				
	90	14,4	12,6	1,8	20			0				
	110	14,4	11,5	2,9	47			0				
	130	14,4	10,2	4,2	71			0				
	150	14,4	14,5	-0,1	41			31,8674				
	170	14,4	14,5	-0,1	-2			31,8674				
	190	14,4	13,6	0,8	7			35,62884				
	210	14,4	13,1	1,3	21			31,8674				
	230	14,4	13,4	1	23			0				
	250	14,4	20	-5,6	0			0				
					0	398						
11m	10	12,7	6,6	6,1	61	215	225	0		16 hrs	16	
	30	12,7	7,8	4,9	110			0				
	50	12,7	6,9	5,8	107			0				
	70	12,7	9,1	3,6	94			0				
	90	12,7	9,4	3,3	69			39,02944				
	110	12,7	12,1	0,6	39			42,15661				
	130	12,7	10,6	2,1	27			39,02944				
	150	12,7	10,2	2,5	46			31,8674				
	170	12,7	12,2	0,5	30			31,8674				
	190	12,7	13,8	-1,1	0			0				
210	12,7	13,8	-1,1	0			0					

Xi	Yi	WL	Z	D _i	A _i (cm ²)	W (cm)	B(cm)	Vx(.6D)	S	Time	Q L/s	Q _s (gm/min)
11m	230	12,7	13,8	-1,1	0			0	.01	16 hrs	4	385
	250	12,7	13,6	-0,9	0			0				
				0	583			0				
13m	10	10	5	5	50	190	200	31,8674		16 hrs		
	30	10	6,9	3,1	81			39,02944				
	50	10	7,2	2,8	59			35,62884				
	70	10	7,5	2,5	53			35,62884				
	90	10	7,8	2,2	47			33,42281				
	110	10	7,6	2,4	46			31,8674				
	130	10	8,6	1,4	38			31,8674				
	150	10	10,6	-0,6	8			0				
	170	10	9	1	4			0				
	190	10	8,8	1,2	22			0				
	210	10	8,5	1,5	27			0				
	230	10	10,4	-0,4	11			0				
	250	10	10,9	-0,9	0			0				
				0	446			0				
16m	10	8,3	3,4	4,9	49	145	155	45,06731		16 hrs		
	30	8,3	4,4	3,9	88			42,15661				
	50	8,3	4,77	3,53	74,3			39,02944				
	70	8,3	5,23	3,07	66			31,8674				
	90	8,3	7	1,3	43,7			0				
	110	8,3	8,6	-0,3	10			0				
	130	8,3	8,6	-0,3	0			0				
	150	8,3	7	1,3	10			0				
	170	8,3	8,2	0,1	14			0				
	190	8,3	10,6	-2,3	0			0				
	210	8,3	8,8	-0,5	0			0				
	230	8,3	6	2,3	18			0				
	250	8,3	8	0,3	26			0				
				0	399			0				
18m	10	6,5	3	3,5	35	190	200	45,06731		16 hrs		
	30	6,5	2,1	4,4	79			42,15661				
	50	6,5	3,6	2,9	73			39,02944				
	70	6,5	4,4	2,1	50			0				
	90	6,5	6,8	-0,3	18			0				
	110	6,5	6,8	-0,3	0			0				
	130	6,5	6,6	-0,1	0			0				
	150	6,5	6,3	0,2	1			0				
	170	6,5	7,3	-0,8	0			0				
	190	6,5	7,9	-1,4	0			0				
	210	6,5	3	3,5	0			0				
	230	6,5	4,1	2,4	59			0				
	250	6,5	4,2	2,3	47			31,8674		16 hrs		
					362							
7m	10	15,3	10	5,3	53	140	150		0,01	20hrs	4 lps	385 gm
	30	15,3	17,5	-2,2	31							
	50	15,3	17	-1,7	0							

Xi	Yi	WL	Z	D _i	A _i (cm ²)	W (cm)	B (cm)	Vx(.6D)	S	Time	Q L/s	Q _s (gm/min)
	70	15,3	17	-1,7	0				.01	20hrs	4	385
	90	15,3	17	-1,7	0							
	110	15,3	17,7	-2,4	0							
	130	15,3	13,9	1,4	0			27,59798				
	150	15,3	13	2,3	37			31,8674				
	170	15,3	10,9	4,4	67			31,8674				
	190	15,3	11,4	3,9	83			31,8674				
	210	15,3	12,7	2,6	65			35,62884				
	230	15,3	12,7	2,6	52			35,62884				
	250	15,3	11,4	3,9	65			35,62884				
				0	453			0				
9m	10	14,4	14,5	-0,1	0	175	185	0				
	30	14,4	15	-0,6	0			0				
	50	14,4	15,1	-0,7	0			0				
	70	14,4	12,7	1,7	10			0				
	90	14,4	10	4,4	61			0				
	110	14,4	12,35	2,05	64,5			0				
	130	14,4	12,5	1,9	39,5			0				
	150	14,4	11,9	2,5	44			31,8674				
	170	14,4	10,2	4,2	67			31,8674				
	190	14,4	13,2	1,2	54			35,62884				
	210	14,4	12,7	1,7	29			31,8674				
	230	14,4	13,1	1,3	30			0				
	250	14,4	20,7	-6,3	0			0				
				0	399							
11m	10	12,2	10,5	1,7	17	220	230	0		20hrs		
	30	12,2	9,5	2,7	44			0				
	50	12,2	9,6	2,6	53			0				
	70	12,2	10	2,2	48			0				
	90	12,2	9	3,2	54			39,02944				
	110	12,2	8,8	3,4	66			42,15661				
	130	12,2	10	2,2	56			39,02944				
	150	12,2	10,7	1,5	37			31,8674				
	170	12,2	11,4	0,8	23			31,8674				
	190	12,2	11,5	0,7	15			0				
	210	12,2	13,5	-1,3	0			0				
	230	12,2	14,9	-2,7	0			0				
	250	12,2	14,2	-2	0			0				
				0	413			0				
13m	10	10	6,1	3,9	39	190	200	31,8674		20hrs		
	30	10	5,8	4,2	81			39,02944				
	50	10	6,7	3,3	75			35,62884				
	70	10	8,1	1,9	52			35,62884				
	90	10	8,45	1,55	34,5			33,42281				
	110	10	7	3	45,5			31,8674				
	130	10	8,25	1,75	47,5			31,8674				
	150	10	8,5	1,5	32,5			0				
	170	10	10,8	-0,8	0			0				

Xi	Yi	WL	Z	D _i	A _i (cm ²)	W (cm)	B (cm)	Vx(.6D)	S	Time	Q L/s	Q _s (gm/min)
	190	10	11,4	-1,4	0			0		20 hrs	4	385
	210	10	11,3	-1,3	0			0				
	230	10	7,2	2,8	15			0				
	250	10	8	2	48			0				
				0	470	470		0				
16m	10	8,5	3,4	5,1	51	145	155	45,06731		20hrs		
	30	8,5	4,4	4,1	92			42,15661				
	50	8,5	4,8	3,7	78			39,02944				
	70	8,5	4,8	3,7	74			31,8674				
	90	8,5	7	1,5	52			0				
	110	8,5	8,6	-0,1	14			0				
	130	8,5	8,6	-0,1	0			0				
	150	8,5	8	0,5	4			0				
	170	8,5	7,7	0,8	13			0				
	190	8,5	10,6	-2,1	0			0				
	210	8,5	8,8	-0,3	0			0				
	230	8,5	5,5	3	27			0				
	250	8,5	7	1,5	45			0				
				0	450			0				
18m	10	6,5	2,5	4	40	160	170	45,06731		20hrs		
	30	6,5	3,1	3,4	74			42,15661				
	50	6,5	3,3	3,2	66			39,02944				
	70	6,5	4,4	2,1	53							
	90	6,5	6,8	-0,3	18							
	110	6,5	6,8	-0,3	0							
	130	6,5	5	1,5	12							
	150	6,5	4,5	2	35							
	170	6,5	7,3	-0,8	12							
	190	6,5	7,9	-1,4	0							
	210	6,5	5	1,5	0							
	230	6,5	4,55	1,95	34,5							
	250	6,5	5,2	1,3	32,5							
					377				0,01		4 lps	385

Table A2.3 SAMPLE DATA OF LABORATORY EXPERIMENTS PHASE - I

RUN	Q _s (kg/min)	Q (m ³ /s)	A (m ²)	W (m)	B (m)	S (slope)	Running Time (Hrs)	C/S	Manning's 'n'
RN1	0,7	0,005	0,06	2	2,1	0,00979	4	16	0,024216
	0,7	0,005	0,05	2,01	2,11	0,00979	6	16	0,017872
	0,7	0,005	0,0607	1,7	1,8	0,0097	18	9	0,027176
	0,7	0,005	0,065	2,6	2,6	0,0097	18	11	0,023287
	0,7	0,005	0,0696	2,6	2,6	0,0097	18	16	0,026074
	0,7	0,005	0,05885	2,33	2,43	0,00863	24	13	0,019991
	0,7	0,005	0,06577	2,3	2,4	0,00863	24	16	0,024216
	0,7	0,005	0,0752	2,6	2,6	0,00863	24	11	0,02795
RN2	0,21	0,0035	0,05657	1,56	1,66	0,00793	13	11	0,032954
	0,21	0,0035	0,04935	2,05	2,15	0,0061	13	11	0,019477
	0,21	0,0035	0,04733	2,03	2,13	0,006	18	11	0,018143
	0,21	0,0035	0,05273	1,6	1,7	0,006	18	13	0,02516
RN3	0,665	0,0075	0,0756	2,5	2,6	0,01	24	16	0,020746
	0,665	0,0075	0,06675	1,9	2	0,01	24	7	0,020076
	0,665	0,0075	0,0913	2,2	2,3	0,00844	13	13	0,028179
	0,665	0,0075	0,0858	2,6	2,7	0,00844	13	16	0,02291
	0,665	0,0075	0,06933	1,85	1,95	0,00854	15	11	0,020073
	0,665	0,0075	0,0596	1,35	1,45	0,00854	15	16	0,018946
RN4	0,42	0,0056	0,0667	2	2,1	0,0075	18	16	0,022527
	0,42	0,0056	0,0698	1,8	1,9	0,0075	13	13	0,025904
	0,42	0,0056	0,0607	2,1	2,2	0,0075	13	13	0,018706
	0,42	0,0056	0,0587	1,7	1,8	0,0075	13	16	0,020195
	0,42	0,0056	0,0451	1,2	1,3	0,008	4	13	0,016721
RN5	0,7	0,0075	0,0503	0,9	1	0,0083	13	16	0,017798
	0,7	0,0075	0,0596	1,8	1,9	0,0083	13	18	0,015701
	0,7	0,0075	0,0852	2,15	2,25	0,00669	24	11	0,022713
	0,7	0,0075	0,0956	2,6	2,6	0,00669	24	13	0,02438
	0,7	0,0075	0,0952	2,6	2,6	0,00669	24	16	0,024212
	0,7	0,0075	0,0653	2	2,1	0,00669	24	18	0,015341
RN6	0,8162	0,0065	0,0636	1,65	1,75	0,0076	24	11	0,020341
	0,8162	0,0065	0,0696	1,5	1,6	0,0076	24	13	0,02495
	0,8162	0,0065	0,0664	1,7	1,8	0,0076	24	16	0,021436
	0,8162	0,0065	0,0774	2,1	2,2	0,0076	24	18	0,024206
	0,8162	0,0065	0,0638	1,7	1,8	0,00753	18	16	0,019985
	0,8162	0,0065	0,0624	1,4	1,5	0,00753	18	13	0,021652
	0,8162	0,0065	0,0557	1,45	1,55	0,00753	18	11	0,017622
	0,8162	0,0065	0,0602	1,45	1,55	0,00753	18	9	0,020004
	0,8162	0,0065	0,0848	2,2	2,3	0,00838	14	16	0,028693
	0,8162	0,0065	0,0641	2	2,1	0,00838	11	13	0,019216
	0,8162	0,0065	0,053	1,6	1,7	0,00846	10	11	0,016221
	0,8162	0,0065	0,0594	1,95	2,05	0,00846	10	16	0,017304
	0,8162	0,0065	0,061	1,9	2	0,00769	4,5	16	0,017518
RN7	0,392	0,0043	0,0738	2,1	2,2	0,01	24	18	0,038811
	0,392	0,0043	0,0568	1,9	2	0,01	24	16	0,026852

1000gm = 1 kg

RUN	Q _s (kg/min)	Q (m ³ /s)	A (m ²)	W (m)	B (m)	S (slope)	Time (Hrs)	C/S	Manning's 'n'
RN7	0,392	0,0043	0,0584	1,8	1,9	0,01	24	13	0,029071
	0,392	0,0043	0,0418	1,35	1,45	0,01	24	11	0,020043
	0,392	0,0043	0,0434	1,4	1,5	0,01	24	9	0,020847
	0,392	0,0043	0,0416	1,7	1,8	0,01	24	7	0,017239
	0,392	0,0043	0,041	1,3	1,4	0,01153	6	13	0,021334
	0,392	0,0043	0,0496	1,65	1,75	0,01153	6	16	0,02519
RN8	0,5831	0,007	0,0694	2,5	2,6	0,0089	14	16	0,018206
	0,5831	0,007	0,0743	2	2,1	0,00923	14	7	0,023873
	0,5831	0,007	0,0688	2,1	2,2	0,00923	14	11	0,020407
	0,5831	0,007	0,05073	1,8	1,9	0,00923	14	16	0,013611
	0,5831	0,007	0,0594	1,2	1,3	0,0073	17	11	0,019974
	0,5831	0,007	0,06	1,55	1,65	0,0073	17	13	0,017478
	0,5831	0,007	0,0647	1,7	1,8	0,00715	22	11	0,018503
	0,5831	0,007	0,0584	2	2,1	0,00715	22	13	0,014138
	0,5831	0,007	0,0693	1,4	1,5	0,00715	22	16	0,023232
RN9	0,455	0,0045	0,05269	2	2,1	0,0105	25	16	0,022493
	0,455	0,0045	0,0588	2,1	2,2	0,0105	25	13	0,026136
	0,455	0,0045	0,063	1,5	1,6	0,0105	25	11	0,036012
	0,455	0,0045	0,0532	1,55	1,65	0,0105	25	9	0,026779
	0,455	0,0045	0,0551	1,4	1,5	0,0112	15	13	0,031145
	0,455	0,0045	0,0419	1,4	1,5	0,0112	15	16	0,019901
	0,455	0,0045	0,0401	1,28	1,38	0,01115	20	13	0,019514
	0,455	0,0045	0,0622	1,4	1,5	0,01115	20	16	0,03786
RN10	1,05	0,0075	0,0536	1,6	1,7	0,0123	5	11	0,017267
	1,05	0,0075	0,0676	2,4	2,5	0,0123	5	13	0,019631
	1,05	0,0075	0,0671	2,3	2,4	0,0119	15	11	0,019597
	1,05	0,0075	0,065	2	2,1	0,0119	15	13	0,020306
	1,05	0,0075	0,06	1,55	1,65	0,0119	15	16	0,020827
	1,05	0,0075	0,072	2,4	2,5	0,0109	22	14	0,020508
	1,05	0,0075	0,074	2,4	2,5	0,0109	22	16	0,021456
RN11	0,8169	0,006	0,0636	2	2,1	0,0081	4	16	0,020204
	0,8169	0,006	0,0636	1,95	2,05	0,0081	4	18	0,020526
	0,8169	0,006	0,0616	1,9	2	0,00846	13	13	0,020228
	0,8169	0,006	0,0538	1,5	1,6	0,00846	13	16	0,018732
	0,8169	0,006	0,0654	1,9	2	0,00769	13	18	0,02128
	0,8169	0,006	0,058	1,52	1,62	0,00769	16	7	0,020035
	0,8169	0,006	0,053	2	2,1	0,0769	16	9	0,046098
	0,8169	0,006	0,0548	1,6	1,7	0,0769	16	13	0,055962
	0,8169	0,006	0,0374	1,7	1,8	0,0769	16	16	0,028745
	0,8169	0,006	0,0666	2,1	2,2	0,00769	16	18	0,020599
	0,8169	0,006	0,0583	1,55	1,65	0,0073	22	16	0,019454
	0,8169	0,006	0,0641	1,9	2	0,0073	22	13	0,02006
	0,8169	0,006	0,0678	2,5	2,6	0,0073	22	11	0,018509
	0,8169	0,006	0,0614	2	2,1	0,0073	22	9	0,0181
RN12	1,05	0,0075	0,0666	1,3	1,4	0,0074	22	18	0,021582
	1,05	0,0075	0,0656	1,2	1,3	0,0074	22	16	0,022031
	1,05	0,0075	0,0798	2,4	2,5	0,0074	22	13	0,020022
	1,05	0,0075	0,0669	1,2	1,3	0,0074	22	7	0,022738

RUN	Q _s (kg/min)	Q (m ³ /s)	A (m ²)	W (m)	B (m)	S (slope)	Time (Hrs)	C/S	Manning's 'n'
RN12	1,05	0,0075	0,06	1,1	1,2	0,0075	17	18	0,020157
	1,05	0,0075	0,0756	2,5	2,6	0,0075	17	13	0,017966
	1,05	0,0075	0,072	1,7	1,8	0,00753	13	18	0,021111
	1,05	0,0075	0,0788	2,5	2,6	0,00753	13	16	0,019277
	1,05	0,0075	0,0752	1,9	2	0,00753	13	7	0,021186
	1,05	0,0075	0,0686	2,1	2,2	0,0075	10	16	0,017087
	1,05	0,0075	0,0755	2	2,1	0,0075	10	13	0,020621
	1,05	0,0075	0,0652	2	2,1	0,009	4,5	16	0,017749
RN13	0,4669	0,004	0,0556	2,2	2,3	0,00808	20	16	0,022834
	0,4669	0,004	0,0676	1,85	1,95	0,00808	20	13	0,03512
	0,4669	0,004	0,045	1,35	1,45	0,00809	20	7	0,021865
	0,4669	0,004	0,0516	1,85	1,95	0,00846	15	16	0,023049
	0,4669	0,004	0,0526	1,9	2	0,00846	15	13	0,023395
	0,4669	0,004	0,0404	2,1	2,2	0,00846	15	13	0,014197
	0,4669	0,004	0,042	1,32	1,42	0,00846	12	16	0,020247
	0,4669	0,004	0,0462	1,9	2	0,00961	6	16	0,020132
	0,4669	0,004	0,0396	1,1	1,2	0,0109	19	13	0,023274
	0,4669	0,004	0,0462	1,5	1,6	0,0109	4	16	0,024851
	0,4669	0,004	0,0404	0,9	1	0,0109	4	11	0,026932
	0,4669	0,004	0,0564	1,8	1,9	0,011	4	9	0,030951
	0,4669	0,004	0,0626	1,75	1,85	0,011	4	7	0,03738
RN14	0,665	0,0075	0,06	1,55	1,65	0,00769	24	16	0,016743
	0,665	0,0075	0,0636	1,1	1,2	0,00769	24	13	0,022411
	0,665	0,0075	0,065	1,6	1,7	0,01076	9	13	0,022145
	0,665	0,0075	0,0624	1,6	1,7	0,01076	9	12	0,020715
RN15	0,42	0,0075	0,0677	1,7	1,8	0,0123	20	7	0,024396
	0,42	0,0075	0,0659	1,7	1,8	0,0123	20	9	0,023343
	0,42	0,0075	0,0676	2	2,1	0,0123	20	11	0,022202
	0,42	0,0075	0,0641	1,3	1,4	0,01239	24	13	0,026249
	0,42	0,0075	0,0422	1,7	1,8	0,1239	24	13	0,03562
	0,42	0,0075	0,0744	2,6	2,7	0,0124	17	18	0,021944
RN16	0,21	0,0035	0,0573	1,8	1,9	0,008	20	18	0,030962
	0,21	0,0035	0,0404	1,3	1,4	0,008	20	16	0,021312
	0,21	0,0035	0,0524	2,3	2,4	0,008	20	9	0,022884
	0,21	0,007	0,0718	2	2,1	0,0074	16	13	0,020207
	0,21	0,007	0,0686	1,3	1,4	0,0074	16	16	0,024257
	0,21	0,009	0,0842	2,1	2,2	0,007946	12	16	0,020529
RN17	0,525	0,0035	0,0562	2,5	2,6	0,006923	20	9	0,022656
	0,525	0,0035	0,0576	2,3	2,4	0,006923	20	11	0,024892
	0,525	0,0035	0,0616	2,6	2,6	0,006923	20	13	0,025714
	0,525	0,0035	0,0573	2,1	2,2	0,006923	20	16	0,026148
	0,525	0,0035	0,0495	1,65	1,75	0,006923	20	18	0,023902
	0,525	0,007	0,0746	2,4	2,5	0,006769	16	11	0,018359
	0,525	0,007	0,0776	2	2,1	0,006769	16	16	0,021956
	0,525	0,01	0,0976	2,55	2,6	0,0073	12	9	0,020006
	0,525	0,01	0,099	2,6	2,6	0,0073	12	13	0,020232
	0,525	0,007	0,0707	2,3	2,4	0,00738	8	18	0,018024
RN18	0,5831	0,0035	0,0458	1,4	1,5	0,00823	20	13	0,025377

RUN	Q _s (kg/min)	Q (m ³ /s)	A (m ²)	W (m)	B (m)	S (slope)	Time (Hrs)	C/S	Manning's 'n'
RN18	0,5831	0,0035	0,042	1,4	1,5	0,00823	20	16	0,02202
	0,5831	0,007	0,0674	1,65	1,75	0,00846	16	11	0,021913
	0,5831	0,007	0,0651	1,8	1,9	0,00846	16	13	0,019632
	0,5831	0,01	0,0826	2,3	2,4	0,00738	12	11	0,016303
RN19	0,56	0,01	0,0988	2,59	2,6	0,00754	15	13	0,020544
	0,56	0,01	0,0963	2,3	2,4	0,00754	15	16	0,021211
	0,56	0,01	0,0946	2,38	2,48	0,00754	15	18	0,020165
	0,56	0,007	0,0654	1,48	1,58	0,00692	10	9	0,020135
	0,56	0,007	0,0743	2,25	2,35	0,00692	10	11	0,019206
	0,56	0,007	0,0703	1,7	1,8	0,00692	10	13	0,020853
	0,56	0,007	0,0809	2,4	2,5	0,00692	10	16	0,021218
RN20	0,7	0,0035	0,0547	1,65	1,75	0,005538	25	9	0,025188
	0,7	0,0035	0,0498	1,7	1,8	0,005548	25	11	0,021213
	0,7	0,0035	0,0617	2,3	2,4	0,005548	25	13	0,024964
	0,7	0,0035	0,062	2,6	2,6	0,005548	25	16	0,023267
	0,7	0,01	0,0985	2,15	2,25	0,00576	15	7	0,020055
	0,7	0,01	0,0972	2,36	2,46	0,00576	15	13	0,018526
	0,7	0,009	0,0941	2,36	2,46	0,00615	10	13	0,020166
	0,7	0,009	0,0888	2,5	2,6	0,00615	10	16	0,01768
RN21	0,7	0,007	0,0664	1,85	1,95	0,0089	8	19	0,020452
	0,7	0,007	0,0733	2	2,1	0,0089	8	16	0,022926
	0,7	0,01	0,0995	2,05	2,15	0,00769	12	13	0,024253
	0,7	0,007	0,0689	1,75	1,85	0,00707	16	13	0,020039
	0,7	0,007	0,0688	1,45	1,55	0,00707	16	16	0,02237
	0,7	0,007	0,0668	1,75	1,85	0,00707	16	18	0,019048
	0,7	0,0035	0,0525	1,75	1,85	0,00707	20	18	0,025652
	0,7	0,0035	0,0504	1,5	1,6	0,00707	20	16	0,02638
	0,7	0,0035	0,0468	1,65	1,75	0,00707	20	13	0,022026
RN22	0,42	0,0035	0,0513	2,2	2,3	0,0078	20	16	0,022447
	0,42	0,0035	0,0564	1,7	1,8	0,0078	20	13	0,03086
	0,7	0,01	0,085	1,85	1,95	0,008	12	13	0,020344
	0,7	0,01	0,088	2,05	2,15	0,008	12	16	0,020229
RN23	0,35	0,0035	0,0536	2,1	2,2	0,0073	25	9	0,024049
	0,35	0,0035	0,0512	2,1	2,2	0,0073	25	11	0,022297
	0,35	0,0035	0,0488	1,5	1,6	0,0073	25	13	0,025426
	0,35	0,0035	0,0529	1,9	2	0,0073	25	16	0,02507
	0,7	0,007	0,0656	1,4	1,5	0,00732	20	13	0,021502
	0,7	0,007	0,0747	2	2,1	0,00732	20	16	0,021448
	0,7	0,007	0,0669	1,5	1,6	0,00732	20	7	0,021318
	1,30004	0,01	0,0969	2,5	2,6	0,00733	15	13	0,020058
	1,30004	0,01	0,0979	2,45	2,55	0,00733	15	16	0,02066
	0,7	0,007	0,0654	1,62	1,72	0,008076	8	11	0,020608
	0,7	0,007	0,0705	2,5	2,6	0,008076	8	16	0,017799
RN24	0,28	0,0035	0,0543	1,8	1,9	0,00576	25	11	0,024048
	0,28	0,0035	0,0587	1,6	1,7	0,00576	25	13	0,029386
	0,28	0,0035	0,0524	1,8	1,9	0,00576	25	16	0,022679
	1,05	0,01	0,088	2,6	2,6	0,00692	15	11	0,016222
	1,05	0,01	0,097	2,6	2,6	0,00692	15	13	0,019047

RUN	Q _s (kg/min)	Q (m ³ /s)	A (m ²)	W (m)	B (m)	S (slope)	Time (Hrs)	C/S	Manning's 'n'
RN24	0,7	0,007	0,0596	2,35	2,45	0,00846	10	9	0,014358
	0,7	0,0035	0,0438	1,2	1,3	0,00923	5	11	0,027401
	0,7	0,0035	0,0417	1,3	1,4	0,00923	5	13	0,024109
RN25	0,56	0,0035	0,0514	2,4	2,5	0,008846	22	16	0,02268
	0,56	0,0035	0,0598	2,3	2,4	0,008846	22	13	0,029935
	0,56	0,007	0,0752	2,6	2,6	0,008866	18	13	0,020235
	0,56	0,007	0,0754	2,2	2,3	0,008866	18	16	0,022589
	0,56	0,007	0,0722	2,3	2,4	0,008866	18	18	0,020451
	0,77	0,01	0,0942	2,55	2,6	0,008866	15	16	0,020796
	0,77	0,01	0,0918	2,5	2,6	0,008866	15	13	0,02018
	0,35	0,007	0,0711	1,7	1,8	0,00923	10	13	0,024533
	0,35	0,007	0,0739	2,2	2,3	0,00923	10	16	0,022297
	0,35	0,007	0,07	2,3	2,4	0,00923	10	18	0,019828
RN26	0,6531	0,0035	0,0504	2	2,1	0,00823	20	13	0,023794
	0,6531	0,0035	0,04385	1,65	1,75	0,00823	20	16	0,021351
	0,6531	0,007	0,0724	1,95	2,05	0,00848	16	13	0,022275
	0,6531	0,007	0,0686	2	2,1	0,00848	16	16	0,020069
	1,05	0,01	0,0943	2,4	2,5	0,00769	12	13	0,020153
	1,05	0,01	0,09	2	2,1	0,00769	12	16	0,02089
	0,35	0,007	0,0764	2,6	2,6	0,00846	8	16	0,02029
	0,35	0,007	0,0752	2,6	2,6	0,00846	8	18	0,019767
RN27	0,6762	0,0035	0,0563	2,4	2,5	0,005769	20	16	0,021294
	0,6762	0,0035	0,0555	2	2,1	0,005769	20	18	0,023354
	0,8862	0,007	0,0703	1,4	1,5	0,006615	16	16	0,022871
	0,8862	0,007	0,0862	2,6	2,6	0,006615	16	13	0,021898
	0,8862	0,01	0,0928	2,6	2,6	0,006615	12	16	0,017312
	0,8862	0,01	0,0988	2,4	2,5	0,006615	12	13	0,020182
	0,6762	0,007	0,0711	2,5	2,6	0,007308	8	13	0,01717
	0,6762	0,007	0,072	1,9	2	0,007308	8	16	0,020822
	0,6762	0,0035	0,0466	1,85	1,95	0,00892	4	16	0,022866
RN28	0,7	0,0035	0,0444	1,45	1,55	0,00769	25	9	0,02282
	0,7	0,0035	0,0494	1,9	2	0,00769	25	11	0,022986
	0,7	0,0035	0,0548	2,6	2,6	0,00769	25	13	0,02233
	0,7	0,0035	0,0548	1,8	1,9	0,00769	25	16	0,028209
	0,7	0,007	0,0711	1,7	1,8	0,00769	20	16	0,022393
	0,7	0,007	0,07	1,78	1,88	0,00769	20	18	0,021227
	0,7	0,01	0,094	2,4	2,5	0,007846	15	16	0,02025
	0,7	0,01	0,0978	2,6	2,6	0,007846	15	9	0,020558
	0,7	0,007	0,0608	1,35	1,45	0,00812	10	11	0,020446
	0,7	0,007	0,0648	1,45	1,55	0,00812	10	13	0,021748
	0,7	0,007	0,0618	1,6	1,7	0,0109	10	16	0,021989
	0,7	0,007	0,07	2,3	2,4	0,0109	6	16	0,021548
	0,7	0,007	0,0533	1,1	1,2	0,0109	6	13	0,021517
RN29	0,28	0,0035	0,062	2,6	2,6	0,00769	25	13	0,027393
	0,28	0,0035	0,054	2,5	2,6	0,00769	25	16	0,022351
	0,28	0,0035	0,0625	2,5	2,6	0,00769	25	18	0,028467
	0,28	0,0035	0,062	2,5	2,6	0,00769	25	18	0,028091
	0,28	0,007	0,074	2,2	2,3	0,008	20	13	0,020805

RUN	Q _s (kg/min)	Q (m ³ /s)	A (m ²)	W(m)	B (m)	S (slope)	Time (Hrs)	C/S	Manning's 'n'
RN29	0,91	0,007	0,0728	2,5	2,6	0,008	20	16	0,01868
	0,91	0,01	0,091	2,6	2,6	0,0095	15	18	0,020087
	0,91	0,01	0,0912	2,1	2,2	0,0095	15	13	0,023031
	0,91	0,01	0,08	1,8	1,9	0,0095	15	16	0,020412
	0,91	0,0035	0,0534	1,9	2	0,013076	3	18	0,034077
RN30	0,525	0,0035	0,045	1,5	1,6	0,0088	20	13	0,024441
	0,525	0,0035	0,047	2,3	2,4	0,0088	20	16	0,020049
	0,525	0,007	0,0618	1,58	1,68	0,009	16	9	0,020133
	0,525	0,007	0,0616	1,57	1,67	0,009	16	13	0,020104
	0,525	0,007	0,0662	1,85	1,95	0,009	16	16	0,020465
	0,91	0,007	0,0708	2,15	2,25	0,009	16	18	0,020815
	1,05	0,01	0,0848	1,65	1,75	0,009	12	13	0,023012
	1,05	0,01	0,0833	2,1	2,2	0,009	12	16	0,019319
	1,05	0,01	0,0792	1,5	1,6	0,01	4	13	0,02295
	1,05	0,01	0,0817	2,1	2,2	0,01	4	16	0,019725
RN31	0,455	0,004	0,0452	1,8	1,9	0,01	24	9	0,020497
	0,455	0,004	0,0463	1,4	1,5	0,01	24	13	0,024915
	0,455	0,004	0,0501	2	2,1	0,01	24	16	0,022724
	0,455	0,004	0,0438	2,4	2,5	0,016	12	11	0,020478
	0,455	0,004	0,0445	1,35	1,45	0,016	12	13	0,030193
	0,455	0,004	0,0393	1	1,1	0,0138	5	11	0,027329
	0,455	0,004	0,0516	2,3	2,4	0,0138	5	16	0,025638
RN 32	0,665	0,005	0,0555	2,1	2,2	0,0095	24	16	0,020341
	0,665	0,005	0,0606	2,4	2,5	0,0095	24	11	0,021603
	0,665	0,005	0,0572	2,3	2,4	0,0095	24	9	0,020178
	0,665	0,005	0,0602	2,2	2,3	0,009	21	18	0,021983
	0,665	0,005	0,06	2,3	2,4	0,0096	21	16	0,02195
	0,665	0,005	0,0532	1,65	1,75	0,009	21	11	0,021474
	0,665	0,005	0,063	2,3	2,4	0,009	21	9	0,023037
	0,665	0,005	0,0605	2	2,1	0,0099	12	13	0,024687
	0,665	0,005	0,0532	1,95	2,05	0,0099	12	16	0,020293
RN33	0,56	0,004	0,0522	2,5	2,6	0,0095	20	16	0,020551
	0,56	0,004	0,0504	2,19	2,29	0,0095	20	13	0,021112
	0,56	0,004	0,0601	2,3	2,4	0,0095	20	9	0,02737
	0,56	0,004	0,047	1,9	2	0,0095	20	7	0,020591
	0,56	0,004	0,0552	2,5	2,6	0,0098	16	9	0,022896
	0,56	0,004	0,0602	2,45	2,55	0,0098	16	16	0,026772
	0,56	0,004	0,0544	2,6	2,6	0,01	12	16	0,022012
	0,56	0,004	0,0552	2,4	2,5	0,01	12	11	0,023743
RN34	0,56	0,005	0,058	2,4	2,5	0,0099	24	13	0,020511
	0,56	0,005	0,056	1,7	1,8	0,0099	13	13	0,024054
	0,56	0,005	0,0596	1,7	1,8	0,0099	13	16	0,026644
	0,56	0,005	0,05	1,5	1,6	0,01	7	13	0,021677
	0,56	0,005	0,0441	1,05	1,15	0,01	7	16	0,021812
	0,56	0,005	0,0452	1,3	1,4	0,01	7	16	0,020039
RN35	0,63	0,005	0,058	2,25	2,35	0,009	20	24	0,020379
	0,63	0,005	0,057	2,3	2,4	0,009	20	16	0,019526
	0,63	0,005	0,061	2,2	2,3	0,0097	13	16	0,023324

RUN	Q _s (kg/min)	Q (m ³ /s)	A (m ²)	W (m)	B (m)	S (slope)	Time (Hrs)	C/S	Manning's 'n'
RN35	0,63	0,005	0,0553	2,2	2,3	0,0097	13	13	0,019837
	0,63	0,005	0,0529	1,95	2,05	0,01	9	13	0,020206
	0,63	0,005	0,057	2,3	2,4	0,01	9	16	0,020582
RN36	0,28	0,005	0,0558	2	2,1	0,0095	20	16	0,021166
	0,28	0,005	0,05	1,9	2	0,0095	20	13	0,018243
	0,28	0,005	0,0562	1,98	2,08	0,0097	15	13	0,021778
	0,28	0,005	0,048	1,35	1,45	0,0097	15	16	0,021285
	0,28	0,005	0,0511	1,7	1,8	0,0097	15	18	0,020484
	0,28	0,005	0,0467	1,95	2,05	0,0099	12	13	0,016368
	0,49	0,005	0,0487	1,35	1,45	0,0099	12	16	0,022017
	0,49	0,005	0,0488	1,5	1,6	0,0099	12	18	0,020727
	0,49	0,005	0,0584	1,75	1,85	0,01	10	16	0,02544
RN37	0,21	0,006	0,0599	1,7	1,8	0,0094	22	13	0,021814
	0,21	0,006	0,0577	1,55	1,65	0,0094	22	16	0,021705
	0,21	0,006	0,0598	1,7	1,8	0,0094	22	18	0,021754
	0,56	0,006	0,061	1,6	1,7	0,0094	22	11	0,023321
	0,56	0,006	0,06	2,1	2,2	0,0096	18	11	0,019378
	0,56	0,006	0,0588	2	2,1	0,0096	18	13	0,019329
	0,56	0,006	0,0537	1,35	1,45	0,0096	18	16	0,021191
	0,56	0,006	0,0578	1,8	1,9	0,009846	8	13	0,020325
RN38	0,56	0,004	0,05	2,5	2,6	0,0095	16	9	0,019137
	0,56	0,004	0,0552	2,5	2,6	0,0095	16	11	0,022543
	0,56	0,004	0,0528	2,3	2,4	0,0095	16	13	0,022096
	0,56	0,004	0,0554	2,48	2,58	0,0095	16	16	0,022795
	0,56	0,004	0,055	2,1	2,2	0,0095	16	7	0,025049
	0,56	0,004	0,0486	2,3	2,4	0,0098	13	11	0,019567
	0,56	0,004	0,0506	2,3	2,4	0,0098	13	13	0,020917
	0,56	0,004	0,0534	2,3	2,4	0,01	9	13	0,023098
RN39	0,49	0,005	0,05	1,6	1,7	0,0097	20	13	0,020521
	0,49	0,005	0,0457	1,6	1,7	0,0097	20	16	0,017703
	0,49	0,005	0,0416	0,9	1	0,01	10	13	0,02163
	0,49	0,005	0,0473	1	1,1	0,01	10	11	0,025097
	0,49	0,005	0,0423	1	1,1	0,01	10	16	0,020961
RN40	0,3969	0,0065	0,073	1,9	2	0,0095	17	13	0,026152
	0,3969	0,0065	0,058	2,1	2,2	0,0095	17	16	0,016827
	0,3969	0,0065	0,0609	1,6	1,7	0,0096	9	13	0,021696
	0,3969	0,0065	0,064	1,7	1,8	0,0096	9	16	0,022682
	0,3969	0,0065	0,062	1,1	1,2	0,01	5	13	0,028307
	0,3969	0,0065	0,0551	1,2	1,3	0,01	5	16	0,022295
	0,3969	0,0065	0,0615	1,3	1,4	0,01	5	11	0,025444
RN41	0,63	0,006	0,0484	0,75	0,85	0,008985	20	3	0,023841
	0,63	0,006	0,0599	1,3	1,4	0,008985	20	13	0,025033
	0,63	0,006	0,0602	1,6	1,7	0,008985	20	16	0,022312
	0,63	0,006	0,0598	2,3	2,4	0,009952	15	13	0,018522
	0,63	0,006	0,0588	2,3	2,4	0,009523	15	16	0,01762
	0,63	0,006	0,0658	1,9	2	0,009946	10	13	0,024445
	0,63	0,006	0,0586	2,4	2,5	0,009946	10	16	0,017426
	0,63	0,006	0,0598	2	2,1	0,009946	10	18	0,020228

RUN	Q _s (kg/min)	Q (m ³ /s)	A (m ²)	W (m)	B (m)	S (slope)	Time (Hrs)	C/S	Manning's 'n'
RN41	0,63	0,006	0,0566	2	2,1	0,01	8	13	0,018526
	0,63	0,006	0,0576	1,85	1,95	0,01	8	16	0,020023
RN42	0,49	0,0045	0,044	0,9	1	0,01	20	9	0,026294
	0,49	0,0045	0,0445	1,8	1,9	0,01	20	13	0,017757
	0,49	0,0045	0,0448	1,6	1,7	0,01	20	16	0,019329
	0,49	0,0045	0,068	2,5	2,6	0,01153	10	13	0,031167
	0,49	0,0045	0,0473	2,48	2,58	0,01153	10	16	0,017182
	0,49	0,0045	0,0546	2,6	2,6	0,01153	10	18	0,021138
	0,49	0,0045	0,0449	2	2,1	0,01215	5	13	0,01858
RN43	0,385	0,004	0,0399	1,75	1,85	0,01	20	9	0,016986
	0,385	0,004	0,047	1,9	2	0,01	20	13	0,021126
	0,385	0,004	0,045	1,45	1,55	0,01	20	16	0,023276
	0,385	0,004	0,0377	1,6	1,7	0,01	20	18	0,016369
	0,385	0,004	0,0433	1,4	1,5	0,01	16	7	0,022326
	0,385	0,004	0,0398	1,9	2	0,01	16	9	0,016054
	0,385	0,004	0,0446	1,9	2	0,01	16	13	0,019376
	0,385	0,004	0,0399	1,44	1,54	0,01	16	16	0,019189
	0,385	0,004	0,0377	1	1,1	0,0104	10	13	0,022181
	0,385	0,004	0,0398	1,1	1,2	0,0104	10	16	0,02292
	0,385	0,004	0,045	1,9	2	0,012	5	13	0,02154
	0,385	0,004	0,05	2,3	2,4	0,012	5	16	0,022694
RN44	0,7	0,008	0,0687	1,9	2	0,00985	20	13	0,019584
	0,7	0,008	0,0715	1,7	1,8	0,00985	20	16	0,02238
	0,7	0,008	0,078	2,55	2,6	0,00985	20	18	0,020071
	0,7	0,008	0,0704	1,7	1,8	0,0099	17	11	0,021875
	0,7	0,008	0,0702	1,85	1,95	0,0099	17	13	0,020679
	0,7	0,008	0,0696	1,35	1,45	0,0099	17	16	0,024597
	0,7	0,008	0,0631	1,6	1,7	0,0105	9	11	0,019538
	0,7	0,008	0,0605	1,35	1,45	0,0105	9	13	0,02018
	0,7	0,008	0,07	2	2,1	0,0105	9	16	0,0202
	0,7	0,008	0,06	1,3	1,4	0,0107	7	9	0,020545
	0,7	0,008	0,0662	1,7	1,8	0,0107	7	13	0,020564
	0,7	0,008	0,07	1,95	2,05	0,0107	7	16	0,020715
	0,7	0,008	0,0621	1,1	1,2	0,0107	7	11	0,023853
RN45	0,63	0,0085	0,0667	1,3	1,4	0,0098	18	11	0,021967
	0,63	0,0085	0,0719	1,7	1,8	0,0098	18	13	0,021202
	0,63	0,0085	0,0698	1,68	1,78	0,0098	18	16	0,020344
	0,63	0,0085	0,069	1	1,1	0,01	19	11	0,026992
	0,63	0,0085	0,0619	1	1,1	0,01	19	13	0,022713
	0,63	0,0085	0,0709	1,7	1,8	0,01	19	16	0,020933
	0,63	0,0085	0,0668	1,65	1,75	0,0112	5	11	0,020463
	0,63	0,0085	0,05867	1,1	1,2	0,0112	5	13	0,020965
	0,63	0,0085	0,0659	1,65	1,75	0,0112	5	16	0,020014
RN46	0,28	0,004	0,0389	1	1,1	0,0082	20	11	0,020721
	0,28	0,004	0,044	1,35	1,45	0,0082	20	13	0,021219
	0,28	0,004	0,0445	1,45	1,55	0,0082	20	16	0,020695
	0,28	0,007	0,0588	1	1,1	0,00923	16	11	0,024412
	0,28	0,007	0,0651	1,64	1,74	0,00923	16	13	0,021705

RUN	Q _s (kg/min)	Q (m ³ /s)	A (m ²)	W (m)	B (m)	S (slope)	Time (Hrs)	C/S	Manning's 'n'
RN46	0,28	0,007	0,0603	1,25	1,35	0,00923	16	16	0,022485
	0,28	0,01	0,08	1,8	1,9	0,0094	12	11	0,020304
	0,28	0,01	0,077	1,5	1,6	0,0094	12	13	0,021256
	0,28	0,01	0,0994	2,5	2,6	0,0094	12	16	0,023687
	0,28	0,007	0,0694	1,8	1,9	0,0095	8	16	0,023105
RN47	0,42	0,0035	0,0349	0,8	0,9	0,0077	20	7	0,021803
	0,42	0,0035	0,0461	1,95	2,05	0,0077	20	11	0,020186
	0,42	0,0035	0,0549	2,56	2,6	0,0077	20	13	0,022637
	0,42	0,0035	0,0497	2,15	2,25	0,0077	20	16	0,021478
	0,42	0,0035	0,0509	2,25	2,35	0,0077	20	18	0,021701
	0,42	0,007	0,0699	2,5	2,6	0,0081	16	13	0,017576
	0,42	0,007	0,0639	2,2	2,3	0,0081	16	16	0,016437
	0,42	0,01	0,086	1,86	1,96	0,0087	12	9	0,021554
	0,42	0,01	0,0887	1,9	2	0,0087	12	11	0,022383
	0,42	0,01	0,0802	2,3	2,4	0,0087	12	13	0,016862
	0,42	0,01	0,0904	2,3	2,4	0,0087	12	16	0,020535
	0,42	0,007	0,0666	2,35	2,45	0,0088	8	13	0,017592
	0,42	0,007	0,0675	2,55	2,6	0,0088	8	16	0,017074
RN48	0,42	0,004	0,0548	2,3	2,4	0,0093	20	7	0,023248
	0,42	0,004	0,0553	2,5	2,6	0,0093	20	9	0,022371
	0,42	0,004	0,0399	1,6	1,7	0,0093	20	13	0,017332
	0,42	0,004	0,0399	1,28	1,38	0,0093	20	16	0,019887
	0,42	0,004	0,0399	1	1,1	0,0093	20	18	0,022992
	0,42	0,007	0,0689	2,55	2,6	0,0093	16	13	0,018158
	0,42	0,007	0,0668	1,4	1,5	0,0093	16	16	0,024961
	0,42	0,007	0,068	2,3	2,4	0,0093	16	18	0,018974
	0,42	0,01	0,0966	2,5	2,6	0,0094	12	13	0,022599
	0,42	0,01	0,0904	2,2	2,3	0,0094	12	16	0,021942
	0,42	0,004	0,0529	2,2	2,3	0,0095	6	9	0,022804
	0,42	0,004	0,0555	1,7	1,8	0,0095	6	11	0,029023
RN49	0,35	0,0035	0,0512	2,35	2,45	0,008846	24	11	0,022842
	0,35	0,0035	0,0442	1,7	1,8	0,008846	24	13	0,022012
	0,35	0,0035	0,0485	2,4	2,5	0,008846	24	16	0,020602
	0,35	0,007	0,0698	2,4	2,5	0,00846	20	13	0,018391
	0,35	0,007	0,0685	2,4	2,5	0,00846	20	16	0,017829
	0,35	0,01	0,0854	1,85	1,95	0,008	13	11	0,0205
	0,35	0,01	0,0896	1,9	2	0,008	13	13	0,02182
	0,35	0,01	0,085	1,85	1,95	0,008	13	16	0,020344
RN50	0,63	0,0035	0,03499	1,19	1,29	0,01	20	13	0,019869
	0,63	0,0035	0,0345	0,8	0,9	0,01	20	16	0,024393
	0,63	0,007	0,0659	1,3	1,4	0,01	16	11	0,026425
	0,63	0,01	0,0869	2,3	2,4	0,011	12	16	0,021638
	0,63	0,01	0,0766	1,8	1,9	0,011	12	13	0,020458
	0,63	0,01	0,0764	1,8	1,9	0,011	12	16	0,02037
	0,63	0,007	0,0688	2,5	2,6	0,0098	8	13	0,018832
	0,63	0,007	0,0606	1,6	1,7	0,0098	8	16	0,020191
	0,63	0,0035	0,0349	1,5	1,6	0,01	5	13	0,017155
	0,63	0,0035	0,04	1,6	1,7	0,01	5	16	0,020624

RUN	Q _s (kg/min)	Q (m ³ /s)	A (m ²)	W (m)	B (m)	S (slope)	Time (Hrs)	C/S	Manning's 'n'
RN51	0,546	0,00375	0,03938	1,3	1,4	0,00931	20	13	0,020577
	0,546	0,00375	0,0375	1,4	1,5	0,00931	20	16	0,01815
	0,546	0,00375	0,0442	1,6	1,7	0,00913	20	18	0,021677
	0,546	0,007	0,0582	1,1	1,2	0,00946	16	13	0,023096
	0,546	0,007	0,0653	1,62	1,72	0,00946	16	16	0,022248
	0,546	0,01	0,0909	2,2	2,3	0,00973	12	13	0,022527
	0,546	0,01	0,0902	2,57	2,6	0,00973	12	16	0,020183
	0,546	0,007	0,0657	2	2,1	0,0098	8	13	0,020095
	0,546	0,007	0,0698	2,5	2,6	0,0098	8	16	0,019286
	0,546	0,00375	0,0374	1,6	1,7	0,011	4	13	0,018073
	0,546	0,00375	0,047	2	2,1	0,011	4	16	0,022878
RN52	0,63	0,0035	0,0347	0,9	1	0,00871	20	9	0,021538
	0,63	0,0035	0,0345	1,3	1,4	0,00871	20	11	0,01717
	0,63	0,0035	0,0349	1	1,1	0,00871	20	13	0,02047
	0,63	0,0035	0,0345	1,5	1,6	0,00871	20	16	0,01571
	0,63	0,0035	0,034	1,2	1,3	0,00871	20	18	0,017603
	0,63	0,007	0,0702	0,9	1	0,008769	16	9	0,033202
	0,63	0,007	0,0698	1,7	1,8	0,008769	16	11	0,023201
	0,63	0,007	0,0692	1	1,1	0,008769	16	13	0,030834
	0,63	0,007	0,0677	1,7	1,8	0,00769	16	16	0,020668
	0,63	0,01	0,0862	2	2,1	0,00967	12	11	0,021827
	0,63	0,01	0,0832	1,85	1,95	0,00967	12	13	0,021597
	0,63	0,01	0,0948	2,4	2,5	0,00967	12	16	0,022797
	0,63	0,007	0,0688	2	2,1	0,01	8	13	0,021898
	0,63	0,007	0,0676	2	2,1	0,01	8	16	0,021273
RN53	0,392	0,00375	0,04751	2,15	2,25	0,009523	20	7	0,020693
	0,392	0,00375	0,0475	2	2,1	0,009523	20	13	0,021662
	0,392	0,00375	0,0375	1,25	1,35	0,009523	20	16	0,019674
	0,392	0,00375	0,0375	1,23	1,33	0,009523	20	18	0,019867
	0,392	0,0065	0,0648	2,3	2,4	0,0096	16	7	0,019173
	0,392	0,0065	0,0649	2,55	2,6	0,0096	16	13	0,017998
	0,392	0,0065	0,0627	1,8	1,9	0,0096	16	16	0,021175
	0,392	0,01	0,0983	2,6	2,6	0,00986	12	13	0,023241
	0,392	0,01	0,08	1,8	1,9	0,00986	12	16	0,020795
	0,392	0,007	0,0647	1,3	1,4	0,01	8	11	0,02565
	0,392	0,007	0,0699	1,7	1,8	0,01	8	13	0,024835
	0,392	0,007	0,066	1,9	2	0,01	8	16	0,021114
	0,392	0,007	0,0616	0,8	0,9	0,01	8	9	0,030515
RN54	0,56	0,00375	0,0375	1,25	1,35	0,009976	20	9	0,020137
	0,56	0,00375	0,0371	1,22	1,32	0,009976	20	13	0,020079
	0,56	0,00375	0,0374	0,9	1	0,009976	20	16	0,024275
	0,56	0,00375	0,0375	0,85	0,95	0,009976	20	18	0,025155
	0,56	0,007	0,0667	1,65	1,75	0,01	16	13	0,023421
	0,56	0,007	0,0665	2,2	2,3	0,011	16	16	0,020457
	0,56	0,01	0,0848	1,55	1,65	0,0115	12	13	0,02698
	0,56	0,01	0,0854	2	2,1	0,0115	12	16	0,023442
	0,56	0,007	0,0804	1,25	1,35	0,01115	8	13	0,039295
	0,56	0,007	0,0684	1	1,1	0,01115	8	16	0,034133

RUN	Q _s (kg/min)	Q (m ³ /s)	A (m ²)	W (m)	B (m)	S (slope)	Time (Hrs)	C/S	Manning's 'n'
RN54	0,56	0,007	0,0643	1,62	1,72	0,01115	8	18	0,023552
RN55	0,7	0,0035	0,048	2,5	2,6	0,009846	20	13	0,020809
	0,7	0,0035	0,0485	2,2	2,3	0,009846	25	16	0,022985
	0,7	0,007	0,0698	2,1	2,2	0,009846	20	13	0,021584
	0,7	0,007	0,07	2,5	2,6	0,009846	20	16	0,019423
	0,7	0,007	0,0698	2,5	2,6	0,009846	20	18	0,019332
	0,7	0,01	0,0918	2,55	2,6	0,009923	15	13	0,021085
	0,7	0,01	0,0917	2,55	2,6	0,009923	15	16	0,021047
	0,7	0,007	0,07	2,45	2,55	0,011	10	13	0,020796
	0,7	0,007	0,0726	2,2	2,3	0,011	10	16	0,02364
	0,7	0,007	0,0696	2,4	2,5	0,011	10	18	0,020872
	0,7	0,007	0,0658	1,7	1,8	0,011	10	11	0,023593
	0,7	0,0035	0,035	0,6	0,7	0,015	5	13	0,035255
	0,7	0,0035	0,0346	0,6	0,7	0,015	5	16	0,034629
RN56	0,35	0,004	0,0456	1,8	1,9	0,00962	25	11	0,020398
	0,35	0,004	0,04009	1,35	1,45	0,00962	25	13	0,019731
	0,35	0,004	0,05013	1,42	1,52	0,00962	25	16	0,027595
	0,35	0,007	0,063	1,8	1,9	0,01062	20	11	0,020844
	0,35	0,007	0,065	1,05	1,15	0,01062	20	13	0,029952
	0,35	0,007	0,064	1,6	1,7	0,01062	20	16	0,022982
	0,35	0,01	0,0888	2,6	2,6	0,010692	15	13	0,020468
	0,35	0,01	0,0898	2,6	2,6	0,010692	15	16	0,020849
	0,35	0,01	0,0863	1,88	1,98	0,010692	15	11	0,023877
	0,35	0,004	0,0468	2,25	2,35	0,011923	5	16	0,020564
RN57	0,56	0,0035	0,06	2,2	2,3	0,0098	20	11	0,032591
	0,56	0,0035	0,05	2	2,1	0,0098	20	13	0,025625
	0,56	0,0035	0,06	2,5	2,6	0,0098	20	16	0,030038
	0,56	0,007	0,0856	2,3	2,4	0,00984	16	11	0,02852
	0,56	0,007	0,0699	2,1	2,2	0,00984	16	13	0,021628
	0,56	0,007	0,0699	2,6	2,7	0,00984	16	16	0,018892
	0,56	0,01	0,0896	1,9	2	0,010823	12	11	0,02538
	0,56	0,01	0,0826	2,1	2,2	0,010823	12	13	0,020894
	0,56	0,01	0,0888	1,9	2	0,010823	12	16	0,025011
	0,56	0,007	0,0673	1,65	1,75	0,010923	8	13	0,024839
	0,56	0,007	0,0666	1,7	1,8	0,010923	8	16	0,02398
RN58	0,35	0,00375	0,042	1,3	1,4	0,00968	20	7	0,023316
	0,35	0,00375	0,0375	1,23	1,33	0,00968	20	11	0,02003
	0,35	0,00375	0,0389	1,35	1,45	0,00968	20	13	0,020099
	0,35	0,007	0,0699	1,7	1,8	0,00968	20	16	0,024434
	0,35	0,007	0,0664	1,9	2	0,00993	16	13	0,02125
	0,35	0,007	0,0625	1,6	1,7	0,00993	16	16	0,021378
	0,35	0,007	0,0618	1,58	1,68	0,00993	16	18	0,021148
	0,35	0,01	0,082	1,82	1,92	0,01	12	9	0,02166
	0,35	0,007	0,0642	1,7	1,8	0,010308	8	13	0,021936
	0,35	0,007	0,0636	1,6	1,7	0,010308	8	16	0,022411
	0,35	0,007	0,0654	1,8	1,9	0,010308	8	18	0,021835
	0,35	0,0035	0,0469	2,5	2,6	0,01115	4	16	0,02131
RN59	0,63	0,0035	0,0359	1,2	1,3	0,0098	20	11	0,020409

RUN	Q _s (kg/min)	Q (m ³ /s)	A (m ²)	W (m)	B (m)	S (slope)	Time (Hrs)	C/S	Manning's 'n'
RN59	0,63	0,0035	0,0339	1,18	1,28	0,0098	20	13	0,018773
	0,63	0,0035	0,03915	1,55	1,65	0,0098	20	16	0,020099
	0,63	0,0035	0,0349	1,19	1,29	0,0098	20	18	0,019587
	0,63	0,007	0,0595	0,9	1	0,009962	16	11	0,027275
	0,63	0,007	0,056	1,05	1,15	0,009962	16	13	0,022852
	0,63	0,007	0,0696	1,7	1,8	0,009962	16	16	0,024613
	0,63	0,01	0,081	1,8	1,9	0,01	12	13	0,021372
	0,63	0,01	0,089	2,48	2,58	0,01	12	16	0,020469
	0,63	0,007	0,0503	1	1,1	0,0123	8	11	0,021947
	0,63	0,007	0,0684	1,8	1,9	0,0123	8	13	0,025672
	0,63	0,007	0,0694	1,75	1,85	0,0123	8	16	0,026746
	0,63	0,0035	0,0349	1,6	1,7	0,013	4	16	0,018782
RN60	0,63	0,007	0,0694	0,95	1,05	0,01	20	11	0,033931
	0,63	0,007	0,0638	1,6	1,7	0,01	20	13	0,022188
	0,63	0,007	0,064	1,6	1,7	0,01	20	16	0,022301
	0,63	0,007	0,0606	1,58	1,68	0,01	20	18	0,020552
	0,63	0,0035	0,0395	1,28	1,38	0,008	25	13	0,020735
	0,63	0,0035	0,0347	1,2	1,3	0,008	25	16	0,017443
	0,63	0,01	0,0874	0,95	1,05	0,01066	15	11	0,035209
	0,63	0,01	0,088	0,9	1	0,01066	15	13	0,036442
	0,63	0,01	0,0886	1,9	2	0,01066	15	16	0,02473
	0,63	0,007	0,0574	0,85	0,95	0,012	10	11	0,029088
	0,63	0,007	0,055	0,9	1	0,012	10	13	0,026428
	0,63	0,007	0,0644	1,62	1,72	0,012	10	16	0,024496
	0,63	0,0035	0,0347	0,7	0,8	0,0123	5	13	0,029265
	0,63	0,0035	0,0349	1,2	1,3	0,0123	5	16	0,021832



Table A2.4 DATA OF MODEL STUDY OF THE BRAHMAPUTRA RIVER (PHASE-II)

RUN	Q (cm ³ /s)	Q(m ³ /s)	A (m ²)	W (cm)	W (m)	B (m)	S	S	Manning's 'n'
	Model	Prototype	Prototype	Model	Prototype	Prototype	Model	Prototype	
MR1	1461,5	24802,5	42000	148	8880	12000	0,0029	9,667E-05	0,046879
	1461,5	24802,5	42720	153	9180	15300	0,0029	9,667E-05	0,047171
	1461,5	24802,5	43320	145	8700	13380	0,0029	9,667E-05	0,050036
	1461,5	24802,5	42000	171	10260	13140	0,0029	9,667E-05	0,042582
	1461,5	24802,5	44520	149	8940	14400	0,0029	9,667E-05	0,051427
	1461,5	24802,5	43440	147	8820	15540	0,0029	9,667E-05	0,049811
	1461,5	24802,5	41880	160	9600	15540	0,0029	9,667E-05	0,044297
	1461,5	24802,5	44880	140	8400	15480	0,0029	9,667E-05	0,054326
	2240	38014,1	78600	164	9840	12600	0,002754	9,179E-05	0,079071
	2240	38014,1	78000	157	9420	12600	0,002754	9,179E-05	0,080364
	2240	38014,1	75840	159	9540	12660	0,002754	9,179E-05	0,07605
	2240	38014,1	75600	168	10080	13200	0,002754	9,179E-05	0,072931
	2240	38014,1	76200	180	10800	11100	0,002754	9,179E-05	0,070585
	2240	38014,1	76320	175	10500	13800	0,002754	9,179E-05	0,072108
	2240	38014,1	76320	173	10380	12660	0,002754	9,179E-05	0,072661
	2240	38014,1	72240	171	10260	12780	0,002754	9,179E-05	0,066821
	3000	50911,7	90600	174	10440	12600	0,002754	9,179E-05	0,071918
	3000	50911,7	90000	167	10020	12600	0,002754	9,179E-05	0,073094
	3000	50911,7	87840	169	10140	12660	0,002754	9,179E-05	0,069643
	3000	50911,7	87600	178	10680	13200	0,002754	9,179E-05	0,066976
	3000	50911,7	88200	190	11400	11100	0,002754	9,179E-05	0,064867
	3000	50911,7	88320	185	11100	13800	0,002754	9,179E-05	0,066177
	3000	50911,7	88320	183	10980	12660	0,002754	9,179E-05	0,066657
	3000	50911,7	84240	181	10860	12780	0,002754	9,179E-05	0,062059
	3860	65506,4	116760	192	11520	12300	0,00275	9,167E-05	0,07983
	3860	65506,4	119400	190	11400	14700	0,00275	9,167E-05	0,083438
	3860	65506,4	114600	179	10740	13920	0,00275	9,167E-05	0,081075
	3860	65506,4	117000	193	11580	12000	0,00275	9,167E-05	0,079828
	3860	65506,4	121560	185	11100	14640	0,00275	9,167E-05	0,087503
	3860	65506,4	120000	185	11100	12240	0,00275	9,167E-05	0,08564
	3860	65506,4	124560	178	10680	12540	0,00275	9,167E-05	0,093492
	3860	65506,4	121200	172	10320	12840	0,00275	9,167E-05	0,091386
	4714	79999,2	120240	201	12060	12300	0,00275	9,167E-05	0,066587
	4714	79999,2	126000	195	11700	14400	0,00275	9,167E-05	0,073448
	4714	79999,2	123360	195	11700	13740	0,00275	9,167E-05	0,070903
	4714	79999,2	121200	198	11880	11760	0,00275	9,167E-05	0,068153
	4714	79999,2	108000	207	12420	14640	0,00275	9,167E-05	0,054606
	4714	79999,2	117000	195	11700	12240	0,00275	9,167E-05	0,06492
	4714	79999,2	117600	205	12300	12540	0,00275	9,167E-05	0,063335
	4714	79999,2	114000	199	11940	12840	0,00275	9,167E-05	0,061338
	5893	100008	168000	260	15600	13500	0,0025	8,333E-05	0,074715
	5893	100008	159960	255	15300	14400	0,0025	8,333E-05	0,069749
	5893	100008	154560	254	15240	13920	0,0025	8,333E-05	0,066044
	5893	100008	154680	256	15360	13800	0,0025	8,333E-05	0,065785

1000 cm³ = 1 litre

RUN	Q (cm ³ /s)	Q(m ³ /s)	A (m ²)	W (cm)	W (m)	B (m)	S	S	Manning's 'n'
MR1	5893	100008	151560	260	15600	14700	0,0025	8,333E-05	0,062937
	5893	100008	154440	260	15600	14400	0,0025	8,333E-05	0,064942
	5893	100008	151920	260	15600	15300	0,0025	8,333E-05	0,063186
	5893	100008	153240	260	15600	14400	0,0025	8,333E-05	0,064104
MR2	1461,5	24802,5	51360	160	9600	12300	0,0025	8,333E-05	0,057781
	1461,5	24802,5	52440	155	9300	12000	0,0025	8,333E-05	0,061096
	1461,5	24802,5	54240	163	9780	12300	0,0025	8,333E-05	0,062502
	1461,5	24802,5	49440	170	10200	10800	0,0025	8,333E-05	0,052084
	1461,5	24802,5	67800	161	9660	15240	0,0025	8,333E-05	0,091389
	1461,5	24802,5	49320	166	9960	13200	0,0025	8,333E-05	0,052702
	1461,5	24802,5	51000	165	9900	12600	0,0025	8,333E-05	0,055951
	1461,5	24802,5	53760	160	9600	12000	0,0025	8,333E-05	0,062349
	2240	38014,1	85200	194	11640	12600	0,002246	7,488E-05	0,073053
	2240	38014,1	85440	178	10680	12600	0,002246	7,488E-05	0,077718
	2240	38014,1	87360	185	11100	12660	0,002246	7,488E-05	0,078608
	2240	38014,1	88800	190	11400	13200	0,002246	7,488E-05	0,079358
	2240	38014,1	88800	195	11700	11100	0,002246	7,488E-05	0,078
	2240	38014,1	85560	179	10740	13800	0,002246	7,488E-05	0,077611
	2240	38014,1	84000	183	10980	12660	0,002246	7,488E-05	0,07417
	2240	38014,1	87480	183	10980	12780	0,002246	7,488E-05	0,079359
	3000	50911,7	91560	204	12240	12600	0,002246	7,488E-05	0,059475
	3000	50911,7	91800	188	11280	12600	0,002246	7,488E-05	0,063068
	3000	50911,7	93720	195	11700	12660	0,002246	7,488E-05	0,063713
	3000	50911,7	95160	200	12000	13200	0,002246	7,488E-05	0,064261
	3000	50911,7	95160	205	12300	11100	0,002246	7,488E-05	0,063215
	3000	50911,7	91920	189	11340	13800	0,002246	7,488E-05	0,062983
	3000	50911,7	90360	193	11580	12660	0,002246	7,488E-05	0,060366
	3000	50911,7	93840	193	11580	12780	0,002246	7,488E-05	0,064288
	3860	65506,4	107520	185	11100	12480	0,00255	0,000085	0,068684
	3860	65506,4	114000	192	11520	12180	0,00255	0,000085	0,07387
	3860	65506,4	112800	182	10920	12060	0,00255	0,000085	0,075205
	3860	65506,4	108600	190	11400	11100	0,00255	0,000085	0,06861
	3860	65506,4	100800	174	10440	13320	0,00255	0,000085	0,064248
	3860	65506,4	112800	183	10980	13260	0,00255	0,000085	0,074932
	3860	65506,4	110400	185	11100	12780	0,00255	0,000085	0,071775
	3860	65506,4	112200	180	10800	12240	0,00255	0,000085	0,075089
	4714	79999,2	119160	190	11400	12480	0,0026	8,667E-05	0,06621
	4714	79999,2	125280	200	12000	12180	0,0026	8,667E-05	0,069559
	4714	79999,2	119520	189	11340	12060	0,0026	8,667E-05	0,066777
	4714	79999,2	120360	197	11820	11100	0,0026	8,667E-05	0,065725
	4714	79999,2	117960	185	11100	13320	0,0026	8,667E-05	0,066267
	4714	79999,2	122760	190	11400	13260	0,0026	8,667E-05	0,069575
	4714	79999,2	121800	194	11640	12780	0,0026	8,667E-05	0,067727
	4714	79999,2	123360	184	11040	12240	0,0026	8,667E-05	0,071653
	5893	100008	160560	255	15300	13500	0,0026	8,667E-05	0,071576
	5893	100008	160200	238	14280	12600	0,0026	8,667E-05	0,074655
	5893	100008	165960	252	15120	14100	0,0026	8,667E-05	0,076227
	5893	100008	165960	245	14700	13800	0,0026	8,667E-05	0,077668

RUN	Q (cm ³ /s)	Q(m ³ /s)	A (m ²)	W (cm)	W (m)	B (m)	S	S	Manning's 'n'
MR2	5893	100008	165960	260	15600	14700	0,0026	8,667E-05	0,07466
	5893	100008	171960	260	15600	14700	0,0026	8,667E-05	0,07921
	5893	100008	170160	260	15600	15000	0,0026	8,667E-05	0,077834
	5893	100008	166680	260	15600	15000	0,0026	8,667E-05	0,0752
MR3	1461,5	24802,5	56640	179	10740	12000	0,0025	8,333E-05	0,06312
	1461,5	24802,5	60600	184	11040	12300	0,0025	8,333E-05	0,069359
	1461,5	24802,5	59760	175	10500	12900	0,0025	8,333E-05	0,070064
	1461,5	24802,5	57120	198	11880	10200	0,0025	8,333E-05	0,059857
	1461,5	24802,5	61200	175	10500	15420	0,0025	8,333E-05	0,072899
	1461,5	24802,5	59280	173	10380	12300	0,0025	8,333E-05	0,069659
	1461,5	24802,5	57360	185	11100	12600	0,0025	8,333E-05	0,063064
	1461,5	24802,5	59760	177	10620	11880	0,0025	8,333E-05	0,069536
	2240	38014,1	91560	189	11340	12600	0,002246	7,488E-05	0,083803
	2240	38014,1	91800	173	10380	12600	0,002246	7,488E-05	0,089265
	2240	38014,1	93720	180	10800	12660	0,002246	7,488E-05	0,089993
	2240	38014,1	95160	185	11100	13200	0,002246	7,488E-05	0,090642
	2240	38014,1	95160	190	11400	11100	0,002246	7,488E-05	0,08905
	2240	38014,1	91920	174	10440	15480	0,002246	7,488E-05	0,089118
	2240	38014,1	90360	178	10680	12660	0,002246	7,488E-05	0,085315
	2240	38014,1	93840	178	10680	12780	0,002246	7,488E-05	0,090857
	3000	50911,7	103560	194	11640	12600	0,002246	7,488E-05	0,075499
	3000	50911,7	103800	178	10680	12600	0,002246	7,488E-05	0,080251
	3000	50911,7	105720	185	11100	12660	0,002246	7,488E-05	0,080645
	3000	50911,7	107160	190	11400	13200	0,002246	7,488E-05	0,081035
	3000	50911,7	107160	195	11700	11100	0,002246	7,488E-05	0,079648
	3000	50911,7	103920	179	10740	13800	0,002246	7,488E-05	0,080107
	3000	50911,7	102360	183	10980	12660	0,002246	7,488E-05	0,076976
	3000	50911,7	105840	183	10980	12780	0,002246	7,488E-05	0,081384
	3860	65506,4	121920	174	10440	12600	0,0026	8,667E-05	0,089054
	3860	65506,4	120360	189	11340	12900	0,0026	8,667E-05	0,082508
	3860	65506,4	123960	180	10800	13080	0,0026	8,667E-05	0,089512
	3860	65506,4	116760	182	10920	10500	0,0026	8,667E-05	0,08043
	3860	65506,4	110760	170	10200	12900	0,0026	8,667E-05	0,077078
	3860	65506,4	116640	179	10740	12600	0,0026	8,667E-05	0,081183
	3860	65506,4	117960	180	10800	12660	0,0026	8,667E-05	0,082414
	3860	65506,4	115920	179	10740	12240	0,0026	8,667E-05	0,080351
	4714	79999,2	127560	210	12600	12720	0,00275	9,167E-05	0,071367
	4714	79999,2	120960	212	12720	12960	0,00275	9,167E-05	0,064913
	4714	79999,2	119760	215	12900	13020	0,00275	9,167E-05	0,06325
	4714	79999,2	126120	213	12780	10560	0,00275	9,167E-05	0,069373
	4714	79999,2	127560	195	11700	12960	0,00275	9,167E-05	0,074969
	4714	79999,2	123720	200	12000	12660	0,00275	9,167E-05	0,07006
	4714	79999,2	122520	202	12120	12780	0,00275	9,167E-05	0,068477
	4714	79999,2	135480	196	11760	12300	0,00275	9,167E-05	0,082599
	5893	100008	154080	255	15300	13500	0,0026	8,667E-05	0,066829
	5893	100008	157560	256	15360	13800	0,0026	8,667E-05	0,069181
	5893	100008	157560	254	15240	14400	0,0026	8,667E-05	0,069543
	5893	100008	156600	255	15300	14100	0,0026	8,667E-05	0,068659

RUN	Q (cm ³ /s)	Q(m ³ /s)	A (m ²)	W (cm)	W (m)	B (m)	S	S	Manning's 'n'
MR3	5893	100008	154200	255	15300	14760	0,0026	8,667E-05	0,066915
	5893	100008	154560	260	15600	15000	0,0026	8,667E-05	0,066314
	5893	100008	154200	260	15600	15000	0,0026	8,667E-05	0,066057
	5893	100008	157560	250	15000	15000	0,0026	8,667E-05	0,070281
MR4	1461,5	24802,5	57600	167	10020	11700	0,0025	8,333E-05	0,067979
	1461,5	24802,5	60000	159	9540	12000	0,0025	8,333E-05	0,075177
	1461,5	24802,5	55440	155	9300	12600	0,0025	8,333E-05	0,067029
	1461,5	24802,5	54600	165	9900	10080	0,0025	8,333E-05	0,062684
	1461,5	24802,5	62160	155	9300	15480	0,0025	8,333E-05	0,081101
	1461,5	24802,5	55800	155	9300	12900	0,0025	8,333E-05	0,067755
	1461,5	24802,5	57000	165	9900	12300	0,0025	8,333E-05	0,067341
	1461,5	24802,5	54240	155	9300	11700	0,0025	8,333E-05	0,064629
	2240	38014,1	91560	199	11940	12600	0,002246	7,488E-05	0,080979
	2240	38014,1	91800	183	10980	12600	0,002246	7,488E-05	0,085993
	2240	38014,1	93720	190	11400	12660	0,002246	7,488E-05	0,086817
	2240	38014,1	95160	195	11700	13200	0,002246	7,488E-05	0,087525
	2240	38014,1	95160	200	12000	11100	0,002246	7,488E-05	0,086064
	2240	38014,1	91920	184	11040	13800	0,002246	7,488E-05	0,085869
	2240	38014,1	90360	188	11280	12660	0,002246	7,488E-05	0,082271
	2240	38014,1	93840	188	11280	12780	0,002246	7,488E-05	0,087616
	3000	50911,7	103560	199	11940	12600	0,002246	7,488E-05	0,074232
	3000	50911,7	103800	183	10980	12600	0,002246	7,488E-05	0,078788
	3000	50911,7	105720	190	11400	12660	0,002246	7,488E-05	0,079229
	3000	50911,7	107160	195	11700	13200	0,002246	7,488E-05	0,079648
	3000	50911,7	107160	200	12000	11100	0,002246	7,488E-05	0,078319
	3000	50911,7	103920	184	11040	13800	0,002246	7,488E-05	0,078654
	3000	50911,7	102360	188	11280	12660	0,002246	7,488E-05	0,075609
	3000	50911,7	105840	188	11280	12780	0,002246	7,488E-05	0,079939
	3860	65506,4	115560	195	11700	12000	0,0025	8,333E-05	0,074405
	3860	65506,4	120480	205	12300	12300	0,0025	8,333E-05	0,076781
	3860	65506,4	123960	197	11820	12720	0,0025	8,333E-05	0,082668
	3860	65506,4	115560	209	12540	10500	0,0025	8,333E-05	0,070716
	3860	65506,4	119760	190	11400	12900	0,0025	8,333E-05	0,079954
	3860	65506,4	120840	192	11520	13080	0,0025	8,333E-05	0,080596
	3860	65506,4	118920	200	12000	12960	0,0025	8,333E-05	0,076375
	3860	65506,4	119160	192	11520	12180	0,0025	8,333E-05	0,078739
	4714	79999,2	131400	208	12480	12120	0,0026	8,667E-05	0,073373
	4714	79999,2	132960	215	12900	12420	0,0026	8,667E-05	0,073201
	4714	79999,2	132840	210	12600	12780	0,0026	8,667E-05	0,074243
	4714	79999,2	131880	216	12960	10680	0,0026	8,667E-05	0,071991
	4714	79999,2	136800	201	12060	12960	0,0026	8,667E-05	0,080268
	4714	79999,2	133560	208	12480	13140	0,0026	8,667E-05	0,075393
	4714	79999,2	133320	211	12660	13020	0,0026	8,667E-05	0,074455
	4714	79999,2	133560	200	12000	12240	0,0026	8,667E-05	0,077383
	5893	100008	165360	260	15600	13200	0,0026	8,667E-05	0,074211
	5893	100008	161160	260	15600	13500	0,0026	8,667E-05	0,071098
	5893	100008	164760	257	15420	13800	0,0026	8,667E-05	0,074334
	5893	100008	162360	254	15240	13800	0,0026	8,667E-05	0,073108

RUN	Q (cm ³ /s)	Q(m ³ /s)	A (m ²)	W (cm)	W (m)	B (m)	S	S	Manning's 'n'
MR4	5893	100008	154560	268	16080	14700	0,0026	8,667E-05	0,064991
	5893	100008	159480	278	16680	15000	0,0026	8,667E-05	0,066825
	5893	100008	158880	275	16500	15300	0,0026	8,667E-05	0,066888
	5893	100008	155160	278	16680	15240	0,0026	8,667E-05	0,063837
MR5	1461,5	24802,5	51960	168	10080	12480	0,00255	0,000085	0,057596
	1461,5	24802,5	55920	173	10380	12000	0,00255	0,000085	0,063835
	1461,5	24802,5	53280	169	10140	13080	0,00255	0,000085	0,059818
	1461,5	24802,5	53040	185	11100	9600	0,00255	0,000085	0,055901
	1461,5	24802,5	59400	172	10320	13800	0,00255	0,000085	0,070862
	1461,5	24802,5	52920	163	9780	12600	0,00255	0,000085	0,060585
	1461,5	24802,5	54360	173	10380	12000	0,00255	0,000085	0,060896
	1461,5	24802,5	54120	161	9660	12300	0,00255	0,000085	0,06341
	2240	38014,1	91560	204	12240	12600	0,002246	7,488E-05	0,079653
	2240	38014,1	91800	188	11280	12600	0,002246	7,488E-05	0,084466
	2240	38014,1	93720	195	11700	12660	0,002246	7,488E-05	0,08533
	2240	38014,1	95160	200	12000	13200	0,002246	7,488E-05	0,086064
	2240	38014,1	95160	205	12300	11100	0,002246	7,488E-05	0,084663
	2240	38014,1	91920	189	11340	13800	0,002246	7,488E-05	0,084352
	2240	38014,1	90360	193	11580	12660	0,002246	7,488E-05	0,080848
	2240	38014,1	93840	193	11580	12780	0,002246	7,488E-05	0,086101
	3000	50911,7	97200	204	12240	12600	0,002246	7,488E-05	0,065702
	3000	50911,7	97440	188	11280	12600	0,002246	7,488E-05	0,069653
	3000	50911,7	99360	195	11700	12660	0,002246	7,488E-05	0,070227
	3000	50911,7	100800	200	12000	13200	0,002246	7,488E-05	0,07073
	3000	50911,7	100800	205	12300	11100	0,002246	7,488E-05	0,069579
	3000	50911,7	97560	189	11340	13800	0,002246	7,488E-05	0,069551
	3000	50911,7	96000	193	11580	12660	0,002246	7,488E-05	0,066772
	3000	50911,7	99480	193	11580	12780	0,002246	7,488E-05	0,070852
	3860	65506,4	115560	183	10980	12600	0,0026	8,667E-05	0,078771
	3860	65506,4	121080	192	11520	12900	0,0026	8,667E-05	0,082465
	3860	65506,4	119040	185	11100	13320	0,0026	8,667E-05	0,082166
	3860	65506,4	116280	193	11580	10200	0,0026	8,667E-05	0,076826
	3860	65506,4	113760	175	10500	13920	0,0026	8,667E-05	0,07905
	3860	65506,4	121200	179	10740	12900	0,0026	8,667E-05	0,086537
	3860	65506,4	118680	183	10980	12300	0,0026	8,667E-05	0,082344
	3860	65506,4	120000	192	11520	12600	0,0026	8,667E-05	0,081243
	4714	79999,2	137760	206	12360	12720	0,0026	8,667E-05	0,079893
	4714	79999,2	137160	216	12960	12960	0,0026	8,667E-05	0,076856
	4714	79999,2	140760	206	12360	13380	0,0026	8,667E-05	0,082812
	4714	79999,2	138360	211	12660	10800	0,0026	8,667E-05	0,079202
	4714	79999,2	138360	191	11460	13980	0,0026	8,667E-05	0,084617
	4714	79999,2	137160	201	12060	12960	0,0026	8,667E-05	0,08062
	4714	79999,2	134760	199	11940	12420	0,0026	8,667E-05	0,078806
	4714	79999,2	135960	192	11520	12660	0,0026	8,667E-05	0,081903
	5893	100008	160560	250	15000	13500	0,00275	9,167E-05	0,074587
	5893	100008	160320	254	15240	13800	0,00275	9,167E-05	0,07362
	5893	100008	171120	260	15600	14700	0,00275	9,167E-05	0,080801
	5893	100008	168120	258	15480	14160	0,00275	9,167E-05	0,078859

RUN	Q (cm ³ /s)	Q(m ³ /s)	A (m ²)	W (cm)	W (m)	B (m)	S	S	Manning's 'n'
MR5	5893	100008	167400	260	15600	14880	0,00275	9,167E-05	0,077896
	5893	100008	165840	260	15600	15000	0,00275	9,167E-05	0,076691
	5893	100008	171000	260	15600	15300	0,00275	9,167E-05	0,080707
	5893	100008	171360	260	15600	15300	0,00275	9,167E-05	0,080999
MR6	1461,5	24802,5	48720	174	10440	12240	0,002899	9,662E-05	0,053887
	1461,5	24802,5	48000	173	10380	12480	0,002899	9,662E-05	0,052769
	1461,5	24802,5	48360	165	9900	12000	0,002899	9,662E-05	0,05514
	1461,5	24802,5	48240	160	9600	13080	0,002899	9,662E-05	0,056048
	1461,5	24802,5	48000	185	11100	15300	0,002899	9,662E-05	0,050466
	1461,5	24802,5	48600	168	10080	13800	0,002899	9,662E-05	0,054934
	1461,5	24802,5	48960	164	9840	12600	0,002899	9,662E-05	0,056513
	1461,5	24802,5	48120	184	11040	14400	0,002899	9,662E-05	0,050859
	2240	38014,1	78600	179	10740	12600	0,002754	9,179E-05	0,074603
	2240	38014,1	79200	172	10320	12600	0,002754	9,179E-05	0,077584
	2240	38014,1	80760	174	10440	12660	0,002754	9,179E-05	0,079533
	2240	38014,1	83880	183	10980	13200	0,002754	9,179E-05	0,081923
	2240	38014,1	82560	195	11700	11100	0,002754	9,179E-05	0,076488
	2240	38014,1	82560	190	11400	13800	0,002754	9,179E-05	0,07782
	2240	38014,1	79800	188	11280	12660	0,002754	9,179E-05	0,074054
	2240	38014,1	81360	186	11160	12780	0,002754	9,179E-05	0,077027
	3000	50911,7	90600	184	11040	12600	0,002754	9,179E-05	0,069297
	3000	50911,7	91200	177	10620	12600	0,002754	9,179E-05	0,071892
	3000	50911,7	92760	179	10740	12660	0,002754	9,179E-05	0,073402
	3000	50911,7	95880	188	11280	13200	0,002754	9,179E-05	0,075072
	3000	50911,7	94560	200	12000	11100	0,002754	9,179E-05	0,070402
	3000	50911,7	94560	195	11700	13800	0,002754	9,179E-05	0,071597
	3000	50911,7	91800	193	11580	12660	0,002754	9,179E-05	0,068619
	3000	50911,7	93360	191	11460	12780	0,002754	9,179E-05	0,071063
	3860	65506,4	127080	186	11160	12720	0,002536	8,454E-05	0,09016
	3860	65506,4	124680	188	11280	12900	0,002536	8,454E-05	0,086724
	3860	65506,4	127320	190	11400	12960	0,002536	8,454E-05	0,089175
	3860	65506,4	126960	193	11580	13500	0,002536	8,454E-05	0,087837
	3860	65506,4	126600	207	12420	11400	0,002536	8,454E-05	0,083448
	3860	65506,4	130800	188	11280	13920	0,002536	8,454E-05	0,093928
	3860	65506,4	133320	187	11220	12900	0,002536	8,454E-05	0,097305
	3860	65506,4	132960	195	11700	12900	0,002536	8,454E-05	0,094211
	4714	79999,2	151320	211	12660	13080	0,002174	7,246E-05	0,084068
	4714	79999,2	152520	198	11880	12840	0,002174	7,246E-05	0,088855
	4714	79999,2	152640	205	12300	12900	0,002174	7,246E-05	0,086943
	4714	79999,2	150240	210	12600	13500	0,002174	7,246E-05	0,083334
	4714	79999,2	151080	214	12840	11400	0,002174	7,246E-05	0,083064
	4714	79999,2	155760	200	12000	14100	0,002174	7,246E-05	0,091409
	4714	79999,2	159000	205	12300	12900	0,002174	7,246E-05	0,093059
	4714	79999,2	158280	203	12180	13020	0,002174	7,246E-05	0,092961
	5893	100008	176640	250	15000	13500	0,002101	7,005E-05	0,076436
	5893	100008	160560	255	15300	13800	0,002101	7,005E-05	0,064348
	5893	100008	159600	260	15600	14700	0,002101	7,005E-05	0,062891
	5893	100008	164280	260	15600	13200	0,002101	7,005E-05	0,065993

RUN	Q (cm ³ /s)	Q(m ³ /s)	A (m ²)	W (cm)	W (m)	B (m)	S	S	Manning's 'n'
MR6	5893	100008	171840	260	15600	14700	0,002101	7,005E-05	0,071129
	5893	100008	164520	260	15600	14880	0,002101	7,005E-05	0,066154
	5893	100008	159720	260	15600	15000	0,002101	7,005E-05	0,06297
	5893	100008	160920	260	15600	14700	0,002101	7,005E-05	0,06376
MR7	1461,5	24802,5	52800	186	11160	12240	0,002536	8,454E-05	0,055132
	1461,5	24802,5	54240	169	10140	12480	0,002536	8,454E-05	0,061457
	1461,5	24802,5	55200	173	10380	12000	0,002536	8,454E-05	0,062303
	1461,5	24802,5	55560	167	10020	13080	0,002536	8,454E-05	0,064478
	1461,5	24802,5	54000	189	11340	10500	0,002536	8,454E-05	0,05663
	1461,5	24802,5	55080	180	10800	13800	0,002536	8,454E-05	0,060461
	1461,5	24802,5	55200	169	10140	12600	0,002536	8,454E-05	0,06328
	1461,5	24802,5	54000	182	10920	12360	0,002536	8,454E-05	0,05807
	2240	38014,1	79560	199	11940	12600	0,002246	7,488E-05	0,064082
	2240	38014,1	79800	183	10980	12600	0,002246	7,488E-05	0,068096
	2240	38014,1	81720	190	11400	12660	0,002246	7,488E-05	0,069101
	2240	38014,1	83160	195	11700	13200	0,002246	7,488E-05	0,069923
	2240	38014,1	83160	200	12000	11100	0,002246	7,488E-05	0,068755
	2240	38014,1	83760	184	11040	13800	0,002246	7,488E-05	0,073551
	2240	38014,1	78360	188	11280	12660	0,002246	7,488E-05	0,064888
	2240	38014,1	81840	188	11280	12780	0,002246	7,488E-05	0,069759
	3000	50911,7	91560	199	11940	12600	0,002246	7,488E-05	0,060464
	3000	50911,7	91800	183	10980	12600	0,002246	7,488E-05	0,064208
	3000	50911,7	93720	190	11400	12660	0,002246	7,488E-05	0,064823
	3000	50911,7	95160	195	11700	13200	0,002246	7,488E-05	0,065352
	3000	50911,7	95160	200	12000	11100	0,002246	7,488E-05	0,064261
	3000	50911,7	95760	184	11040	13800	0,002246	7,488E-05	0,068639
	3000	50911,7	90360	188	11280	12660	0,002246	7,488E-05	0,061429
	3000	50911,7	93840	188	11280	12780	0,002246	7,488E-05	0,06542
	3860	65506,4	115560	198	11880	12720	0,002174	7,246E-05	0,068355
	3860	65506,4	122160	188	11280	12900	0,002174	7,246E-05	0,077606
	3860	65506,4	119520	192	11520	12960	0,002174	7,246E-05	0,073794
	3860	65506,4	123480	193	11580	13500	0,002174	7,246E-05	0,077643
	3860	65506,4	119640	208	12480	11400	0,002174	7,246E-05	0,070089
	3860	65506,4	123480	193	11580	13920	0,002174	7,246E-05	0,077643
	3860	65506,4	120960	188	11280	12900	0,002174	7,246E-05	0,076341
	3860	65506,4	118440	203	12180	12900	0,002174	7,246E-05	0,070046
	4714	79999,2	135360	221	13260	13080	0,002174	7,246E-05	0,06771
	4714	79999,2	148680	203	12180	12840	0,002174	7,246E-05	0,083763
	4714	79999,2	139080	211	12660	12900	0,002174	7,246E-05	0,073051
	4714	79999,2	152640	208	12480	13500	0,002174	7,246E-05	0,086108
	4714	79999,2	139200	218	13080	11400	0,002174	7,246E-05	0,071586
	4714	79999,2	151560	208	12480	14100	0,002174	7,246E-05	0,085096
	4714	79999,2	139320	211	12660	12900	0,002174	7,246E-05	0,073261
	4714	79999,2	140160	215	12900	13020	0,002174	7,246E-05	0,07308
	5893	100008	166680	250	15000	13500	0,002174	7,246E-05	0,070579
	5893	100008	160320	255	15300	13800	0,002174	7,246E-05	0,065285
	5893	100008	163080	260	15600	14820	0,002174	7,246E-05	0,066307
	5893	100008	165720	244	14640	13200	0,002174	7,246E-05	0,071041
	5893	100008	159120	260	15600	14100	0,002174	7,246E-05	0,063646
	5893	100008	164160	260	15600	15000	0,002174	7,246E-05	0,06704
	5893	100008	165360	260	15600	15600	0,002174	7,246E-05	0,067858
	5893	100008	159480	260	15600	15300	0,002174	7,246E-05	0,063887

DESIGN AND CONSTRUCTION OF EXPERIMENTAL SET-UP

1.0 INTRODUCTION

To conduct the planform changes or similar experiments on a model of large braided river, different data set from the field have been collected. It is seen that width of the river of the study reach varies around from 5 km to 16 km and depth of flow varies from 5 m to 50 m at bankfull stage. In the River Engineering laboratory of WRDTC 2.6 m wide, 1.4 m deep, and 22.5 m long channel including upstream stilling basin and downstream small sump has been constructed. The schematic diagram of the experimental set-up is shown in the Fig.3.5.

2.0 DESIGN CRITERIA

To design the experimental set-up, the following criteria have been followed:

2.1 Wall Construction

A 25 cm thick boundary walls has been constructed by first class brick which is provided with reinforcement. Total bed area of the flume is made up of 30 cm thick R.C.C. casting mixed with water tightening material. Six windows are provided in each side wall to observe the flow condition. Each window was closed by 12 mm thick fibreglass of 1m x 1.4 m size. Middle stage construction procedure of the laboratory flume has been presented in the Plate A3.1a .

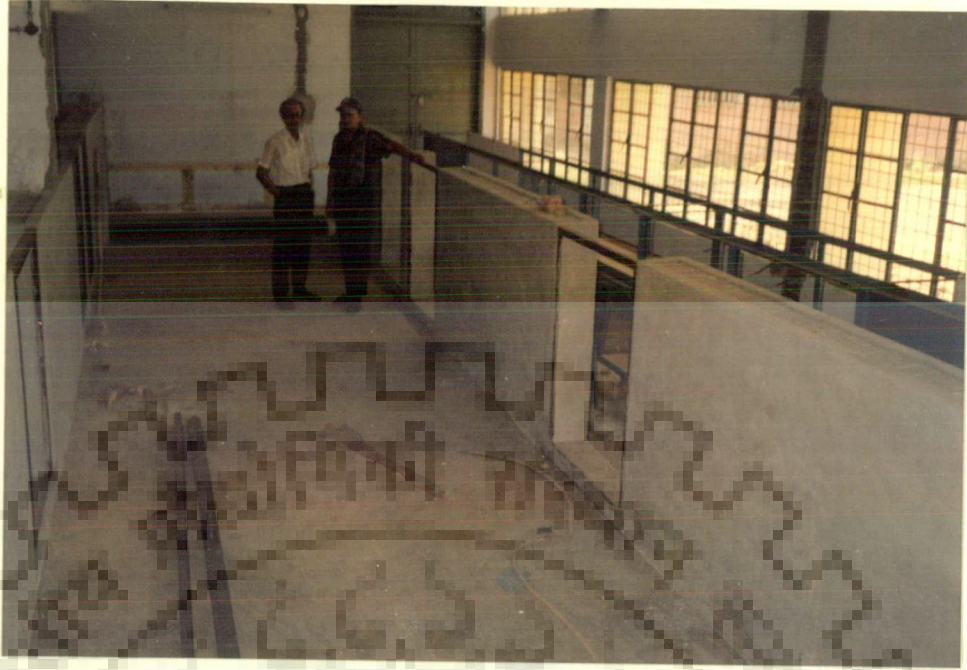


**Plate A3.1a: MIDDLE STAGE CONSTRUCTION OF EXPERIMENTAL SET-UP OR FLUME
IN R. E. LAB, WRDTC**



**Plate A3.1b: CONSTRUCTION OF WATER STORAGE TANK OUT SIDE THE
BUILDING**

2.2 Pump and Water Reservoir Tank Selection

For the operation of experiments in the above mentioned laboratory channel, two submersible pumps of 15 HP capacity were installed. Another centrifugal pump of 10-HP was installed at the downstream of the flume to supply the water in case of lean flow. The water reservoir of size 12.5m*2m*2m was constructed to supply the maximum flow in the channel. The construction procedure of under ground water reservation tank at initial stage has been shown in the Plate A3.1 b .

2.3 Sediment Feeder and Sediment Collector

A sediment feeder has been installed at upstream of the channel. It contains four chambers to feed the sediment either manually or mechanically in to the channel with flowing water as shown in Fig. 3.6b.

The sediment collector consists of fine nets has been fixed in the tail box at the downstream of the channel, as shown in Fig. 3.6c. The collector traps the fine sand also.

2.4 Tail Gate

A movable tail gate of size 2.6mx1.4mx2.5cm has been fixed at the end of the constructed channel through which the depth of the flow is controlled (Fig. 3.6d).

2.5 Wooden Transitional Channel

The wooden transition channel of size 1m*0.3m*3cm is also constructed (Fig. 3.6a). This transition has been used to transmit the water from stilling basin to sand experimental initial channel with different flow directions.

3.0 GENERAL SAFETY AND MAINTENANCE

For controlling the experimental runs to precision, the following safety measures have been taken care of.

1. The water reservoir tank is to be kept filled during experimental run and the drain cock should be closed properly.
2. Before starting the pump, the electric supply, mating flanges should be properly checked.
3. At the start pump and flow control valves is opened slightly to allow gentle circulation, which relieves air from system.
4. The channel may be levelled approximately with the aid of a spirit level.
5. After use, the water was always allowed to drain down into reservoir tank. The reservoir was emptied at regular intervals so as to flush out sand and then refilled with fresh, clean water added with correct proportion of rust inhibitor.
6. Pump service is to be under taken periodically. All moving parts, jack, inlet tank supporting fulcrum, jack hinge point and trunnions gear boxes, etc should be lubricated using light engineering oils, or general purpose grease as necessary.
7. Due precaution should be taken for poisoning from toxic materials, injury from handling large or heavy components, injury from rotating components, burns from components at high temperatures and injury from corrosive liquids.

INSTRUMENTS

1.0 ACOUSTIC DOPPLER VELOCIMETER (ADV)

The Acoustic Doppler Velocimeter (ADV) is a versatile, high-precision instrument that measures all three flow velocity components. The measurements are insensitive to water quality, which allows for a wide range of applications. ADVs is used in laboratories, wave basins, rivers, estuaries and oceanographic research.

The ADV uses acoustic sensing techniques to measure flow in a remote sampling volume. The measured flow is practically undisturbed by the presence of the probe. Data are available at an output rate of 25 Hz. The 3-D velocity range is ± 2.5 m/s, and the velocity output has no zero-offset.

The instrument consists of three modules: the measuring probe, the conditioning module and the processing module. The measurement probe is attached to the waterproof conditioning module, which contains low-noise electronic circuit. The housing and cable attachment are rugged and can be deployed up to 30 m in the standard configuration.

The ADV Lab is designed for use with a desktop PC in a laboratory settings. It is very simple to set up and operate, the data are stored directly in to computer, and the power is supplied from the PC. The standard unit is delivered with a 5 cm down-looking sensor mounted on a rigid 40 cm stem. The standard cable length leading to the PC is 10 meters. Analog outputs for use with a secondary data acquisition system is optional.

The down-looking probe (standard for all systems) cannot measure the velocity in the upper 5 cm of the water column. If the main interest is to measure the surface layer or to measure under structures, an up-looking probe may be very useful. The side-looking probe is primarily used in wave flumes.

In very shallow water (minimum 2 cm) a 2D side-looking probe measures the two horizontal components. A full set of data collection, data conversion and diagnostic software is included with all ADVs. The software displays the real time and time filtered velocity, echo amplitude, the standard deviation of velocity, and correlation - a quality parameter.

2.0 PRESTON TUBE

A Preston tube of 6.35 mm outer diameter, made of brass was used for the measurement of skin shear on the sand bed. A static pressure tube was provided at the same level as that of the Preston tube. The movable carriage on which the assembly is along the flume width. The combination could tilt a vertical plane and be clamped in any position. At each section, a number of readings were taken across the width. The temperature of water was recorded and the discharge was measured. The process was repeated for a number of depths and slopes.

Preston (1954), has developed a simple technique for estimating the local shear in smooth boundaries using a Pitot tube in contact with the surface. He has demonstrated

that a unique relation exists between $\frac{\tau_0 d_p^2}{4\rho v^2}$ and $\frac{(P_t - P_0)^2 d_p^2}{4\rho v^2}$ for smooth boundaries.

Here d_p is the outer diameter of the Preston tube, τ_0 the boundary shear stress and $(P_t - P_0)$

is the Preston tube reading, ρ and ν are the mass density and kinematic viscosity of the fluid respectively.

The use of a Pitot tube at the wall has been suggested for measuring the shear stresses at the wall. Close to a smooth wall is the laminar sub-layer. The velocity distribution for the laminar sub-layer close to a smooth wall can be given by may be represented by

$$\frac{u_y}{u_*} = \frac{yu_*}{\nu} \quad (\text{A4.1})$$

where, u_y is the velocity at a distance y , and $u_* = \sqrt{\tau_0/\rho}$ is the frictional velocity.

A circular Pitot tube with an outside diameter d_p resting on the bed reads

the total pressure p_t , measured relative to the static pressure p_0 , where $(p_t - p_0)$ depends on the independent variables ρ , ν , τ_0 and d_p . Functional grouping yielded a relation of the form by Preston in 1954 (Graf, 1971)

$$\frac{p_t - p_0}{\rho \nu^2} d_p^2 = fct \left(\frac{\tau_0 d_p^2}{\rho \nu^2} \right) \quad (\text{A4.2})$$

Actual observations for four different pitot tubes could well be represented by

$$\log \frac{\tau_0 d_p^2}{4 \rho \nu^2} = 2.604 + \frac{7}{8} \log \frac{(p_t - p_0)}{4 \rho \nu^2} d_p^2 \quad (\text{A4.3})$$

The pressure shear relationship originally developed for closed conduits has been extended to open channel flows by earlier researchers with considerable success (Graf, 1971). Using the Preston-tube technique, it became possible to check indirect determinations against the direct measurement.

3.0 PITOT TUBE:

A pitot tube is a instrument to determine the velocity of flow at a point in a pipe or stream. The liquid in pitot tube rises due to the pressure exerted by the flowing liquid. Pitot tube consists of one limb having two holes, which registers static head and velocity pressure head, related by the following equation.

$$H+h = H + u^2/2g \quad (A4.4)$$

Form eq. (A4.4) one can find out the velocity of flow as below:

$$u = \sqrt{2gh} \quad (A4.5)$$

In which u = velocity of flow; and h = Depth of flow.

4.0 POINTER GAUGE

It is made of 1 meter long vertical steel rectangular bar that is fixed in a rectangular steel base. It can be smoothly moved through the base in upward and downward direction. Pointer gauge is graduated in millimeter. One sharp niddle, of 6 inches long is fitted at the bottom end of the gauge.

5.0 V-NOTCH

A 90° V-notch has been made of steel plate, is fixed in the channel system. The size of the V-notch is 1m wide and 50 cm deep. The V-notch has been calibrated with test runs and got its discharge coefficient C_d equal to 0.59.

LIST OF RESEARCH PAPERS PUBLISHED / COMMUNICATED

1. **Abdullah, M.**, Sharma, N. and Ojha, C.S.P. " Performance Evaluation of Certain Braiding Indicators Using Data of a Reach of the Brahmaputra River in Bangladesh" Journal of Indian Water Resources Society, Vol. 19(5), No.3, pp. 21-27, July 1999. (Published)
2. **Abdullah, M.**, Sharma, N. and Ojha, C.S.P."Appraisal of Manning's Resistance Relationship in a Typical Stretch of the River Brahmaputra in Bangladesh", Water Resources Research (communicated, 2001)